8-15-2019 12:00 PM

The Role of Defective Macrophage Efferocytosis During Early Atherosclerosis in Humans

Charles Yin
The University of Western Ontario

Supervisor
Heit, Bryan
The University of Western Ontario

Graduate Program in Microbiology and Immunology
A thesis submitted in partial fulfillment of the requirements for the degree in Doctor of Philosophy

Abstract

Atherosclerosis is a chronic inflammatory disease characterized by thickening of the arterial wall from accumulation of lipoproteins and immune cells within the vessel intima, forming a lipid-rich plaque. Macrophages play a central role in atherosclerosis progression through phagocytic removal of apoptotic cells in a process termed efferocytosis. With disease progression however, macrophage efferocytosis becomes defective and uncleared apoptotic cells undergo secondary necrosis and form a necrotic core that increases the risk of plaque rupture. Despite the importance of defective efferocytosis in atherosclerosis, little is known about how efferocytosis becomes impaired. The aim of this thesis was to characterize mechanisms regulating efferocytic clearance of apoptotic cells and to identify potential mechanisms that contribute to impaired efferocytosis in atherosclerosis. Using a combination of mass spectrometry and microscopy-based efferocytosis uptake assays, we identified Rab17 as a regulator of apoptotic cargo trafficking to the recycling endosomes. Disruption of Rab17 function using a dominant-negative mutant resulted in mis-trafficking of apoptotic cargo away from recycling endosomes and into the MHC class II loading compartment. We then examined the gene expression profile of macrophages from the aortas of patients undergoing open heart surgery to identify potential mechanisms driving defective efferocytosis. We found over 3,000 differentially-expressed protein-coding genes in these macrophages, with particular enrichment in pathways involved in cholesterol handling, efferocytosis and efferosome maturation. Interestingly, we observed upregulation of the hematopoietic transcription factor GATA2, which has been shown by genetic linkage studies to be associated with coronary artery disease. By perturbing GATA2 expression in oxLDL-treated THP-1 human macrophages, we found that oxLDL-induced impairment in efferocytosis and efferosome maturation is dependent on GATA2. Our findings indicate that exposure to pro-atherogenic conditions induces upregulation of GATA2 expression, which specifically impairs efferocytic uptake of apoptotic cells and efferosome maturation. Our data shed new light on the process of macrophage efferosome maturation and how this process is impaired in atherosclerosis. We are also the first to describe a role for GATA2 in mediating oxLDL-induced impairment in efferocytosis. Therefore, GATA2 and other processes involved in dysregulation of efferosome maturation may be suitable therapeutic targets in human atherosclerotic disease.

Lay Abstract

Atherosclerosis is a disease of the blood vessels involving the accumulation of cholesterol and cells of the immune system within the vessel wall. This results in the formation of an atherosclerotic plaque, which grows over time and may eventually rupture and cause a number of complications, including heart attack and stroke. A type of immune cell called macrophages can migrate into the atherosclerotic plaque and remove dying cells and debris from within the plaque in a process called 'efferocytosis'. Macrophage efferocytosis helps limit the growth of the plaque. However, over time efferocytosis within the plaque becomes defective, and macrophages are no longer able to limit plaque growth leading to faster disease progression. In this thesis, we studied macrophages isolated from atherosclerotic plaques in human patients to understand how efferocytosis becomes defective in atherosclerosis. We first identified a new regulator of efferocytosis called Rab17, which helps the macrophage properly break down the dead cells and debris it takes up during efferocytosis. We then found that certain genes and pathways related to efferocytosis were dysregulated in the macrophages from patients. These included pathways related to how the macrophage processes excess cholesterol and how macrophages deal with the dead cells they take up. Finally, we identified a transcription factor (protein that regulates gene expression) that was associated with defective efferocytosis called GATA2. We found that an increase in the amount of GATA2 in the cell seemed to be required for macrophages to develop defective efferocytosis. Taken together, these results advance our understanding of atherosclerosis and uncovers a role for GATA2 in the development of atherosclerotic disease.

Keywords

Macrophages, atherosclerosis, defective efferocytosis, efferosome maturation, gene expression profiling, Rab17, GATA2

Co-Authorship Statement

The studies described in **Chapters 3-5** were performed by Charles Yin in the laboratory of Dr. Bryan Heit. Dr. Bryan Heit contributed to experimental design, data collection, data interpretation and manuscript preparation throughout. The contributions of others in these studies are described below.

Chapter 3

Sections of this chapter (**Figures 3.2** to **3.8**) were adapted from: "Rab 17 mediates differential antigen sorting following efferocytosis and phagocytosis" by **Charles Yin**, Yohan Kim, Dean Argintaru and Bryan Heit. *Cell Death and Disease* 2016;7:e2529. Text and images were reproduced with permission from SpringerNature (see **Appendix H** for permissions and http://creativecommons.org/licenses/by/4.0/ for a copy of the Creative Commons license).

Additionally, other sections of this chapter (**Figures 3.9** to **3.11**) were adapted from: "Rab17 mediates intermixing of phagocytosed apoptotic cells with recycling endosomes" by **Charles Yin**, Dean Argintaru and Bryan Heit. *Small GTPases* 2019;10(3):218-226. and Taylor & Francis, respectively (see **Appendix I** for permissions).

YK conducted the live-cell Rab5 and Rab7 tracking experiments and performed the mass spectrometry on isolated phagosomes and efferosomes. DA assisted with collection of data for the live-cell Rab17 tracking experiments. The manuscripts were written by CY and BH. All authors read, edited, and approved of the final manuscripts.

Chapter 4

Data from this chapter are being prepared as part of a manuscript as: "Overexpression of GATA2 by intima-infiltrating macrophages drives early atheroma formation" by **Charles Yin**, Angela M. Vrieze, James Akingbasote, Emily N. Pawlak, Rajesh A. Jacob, Jonathan Hu, Neha Sharma, Garth Blackler, Jimmy D. Dikeakos, Lillian Barra, A. Dave Nagpal and Bryan Heit.

ADN obtained all surgical aortic punch specimens. AMV assisted with conducting RT-PCR experiments. Caroline O'Neil from the Robarts Molecular Pathology facility performed all

histological staining with the exception of anti-CD163 immunofluorescence staining. David Carter and Jenn Biltcliffe performed the whole transcriptome microarray.

Chapter 5

Data from this chapter are being prepared as part of a manuscript as: "Overexpression of GATA2 by intima-infiltrating macrophages drives early atheroma formation" by **Charles Yin**, Angela M. Vrieze, James Akingbasote, Emily N. Pawlak, Rajesh A. Jacob, Jonathan Hu, Neha Sharma, Garth Blackler, Jimmy D. Dikeakos, Lillian Barra, A. Dave Nagpal and Bryan Heit.

JH and NS assisted in the creation of the pLVX-IRES-ZsGreen1 GATA2 and pGFP-C-shLenti constructs and in experiments examining macrophage efferocytic and phagocytic capacity. ENP, RAJ and JDD designed and produced the lentiviral vectors. JA and LB performed the aortic punch peptide citrullination immunohistochemistry and assisted with all other peptide citrullination experiments. GB and LB handled all animals and assisted with obtaining mouse aorta for *Gata2* RT-PCR experiments.

Acknowledgments

I would like to express my gratitude to the many individuals who have provided their guidance, support and solidarity throughout the course of my PhD. Without them, this journey would have been all the more difficult, if not altogether impossible.

I would first like to acknowledge my supervisor, Dr. Bryan Heit, for his unwavering support during the time I spent as a trainee in his laboratory. It was an honour and pleasure to train as the first PhD student in the Heit laboratory and to learn and grow as a scientist under Dr. Heit's mentorship. Thank you for believing in me and in the bold vision we developed together for the direction of this thesis. And thank you for providing guidance when I needed it and the freedom to pursue both new scientific directions and opportunities outside the lab. You have been a role model and source of inspiration for me as a scientist and for that I am truly grateful.

I would also like to thank my supervisory committee members Dr. Rob Hegele and Dr. Lakshman Gunaratnam for your guidance and advice on my thesis and especially for the many valuable discussions we have had throughout the years. Thank you as well for your advice on my career and clinical development as part of my MD/PhD mentorship committee. I would especially like to acknowledge and thank my collaborator and unofficial co-supervisor Dr. Dave Nagpal, who has also been a part of my MD/PhD mentorship committee and served as a role model for me as a clinician. Thank you for taking the time to mentor me in the clinic and operating room and especially for your support for my scientific endeavours.

This thesis would not have been possible without the contributions of many outstanding collaborators that have helped advanced our science and bring the thesis to the next level. I would first like thank to Caroline O'Neil for her patient assistance with operating the laser capture microscope and doing much of our slide staining. Thanks are also due to Jenn Biltcliffe and especially David Carter for their much-needed help in our RNA experiments and microarray analysis. Thanks as well to Dr. Ted Tweedie for his assistance with interpreting our aortic punch stains and staging of the atheromas. Thank you to Dr. Jimmy Dikeakos and members of his lab Drs. Emily Pawlak and Rajesh Jacob for their help in producing our lentiviral vectors. Finally, I need to thank Dr. Lillian Barra and members of her lab Dr. James

Akingbasote and Garth Blackler for not only contributing to our peptide citrullination work but for pushing me to be a more careful and rigorous scientist.

I have had the privilege of getting to know many amazing friends and colleagues in the course of my degree. Thank you to everyone that I have had the pleasure to get to know during my time in the lab: Ron Flannagan, Amanda Evans, Jack Blackburn, Dean Argintaru, Sara Ndombele, Ryan Yip, Darius Lau, Kyle Taruc, Janakan Somasundaram, Caroline Banas, Elaine Liu, Adam Tepperman, Ushra Khan, Josh Yu, Neha Sharma, Jonathan Hu, Ryan LaPenna, Tara Tasnim, Austin Lam, Maria Aboutaka and David Zheng. I would like to give special mention our indefatigable lab technician Angela Vrieze, for not only being the lab member I have worked alongside for the longest and known the best but for the many conversations and laughs we've shared along the way.

Being a clinician-scientist trainee had its own unique challenges and obstacles to overcome. I am grateful for a supremely supportive program director in Dr. Jim Lewis, who I could always count on to speak up in the best interests of myself and my colleagues in the MD/PhD program. I would also like to thank our program administrator Stacey Bastien for helping me navigate the twists and turns of my training so far and Schulich graduate studies manager Janelle Pritchard for taking an interest in my work and for her many words of encouragement over the years. I would also be remiss here to not thank Leslea Ernewein for the many times she has had to help me with the administrative side of the clinical aspect of my research.

Finally—and most importantly—I would like to express my gratitude towards my family and friends for their endless love and support during the ups and downs of my PhD. To my parents, Jing and Don, I would like to say thank you for always being there and rooting for me in the background. While I haven't said it nearly enough, I am grateful for your support. To my friends James Han and Angela Huynh, who are going through their own PhD journeys alongside me, I thank you for the words we've shared through the years, about science and about life. For helping me keep sane outside of research, I thank my dog Copper and my guinea pigs Hershey, KitKat, Peanut and Waldo. Lastly, I would like to say thank you to my partner Emily for sharing in my life and the privilege of sharing in yours. Your love and support through the entirety of this adventure is more than I had the right to expect. Thank you for always being there for me at the end of the day.

Table of Contents

List of Abbreviations

AA	arachidonic acid
ABCA1	ATP-binding cassette transporter member 1
ABCG1	ATP-binding cassette family G member 1
ACAT1	acyl coenzyme A:cholesterol acyltransferase 1
ACTA2	actin alpha 2, smooth muscle
AMC	anti-modified citrulline
AML	acute myeloid leukemia
ApoB	apolipoprotein B
Ask-1	apoptosis signal-regulating kinase
ATF-1	activating transcription factor 1
ATP	adenosine triphosphate
AUP	animal use protocol
β2M	β_2-microglobulin
BAI1	brain angiogenesis inhibitor 1
Bax	Bcl-3-associated X
CABG	coronary artery bypass graft
CDS	consensus coding sequences
CETP	cholesteryl ester transfer protein
CHIP	clonal hematopoiesis of indeterminant potential
CHOP	C/EBP-homologous protein
CLIP	class II-associated invariant chain-associated peptide
CML	chronic myeloid leukemia
CoA	coenzyme A
Crk	adaptor molecule crk
CRP	C-reactive protein
CVD	cardiovascular disease
DAMP	damage-associated molecular pattern
DC	dendritic cell
DHA	docosahexaenoic acid
DN	dominant negative

Drp	dynamin related protein 1
ECM	extracellular matrix
EDV	efferosome-derived vesicle
ELMO	engulfment and cell motility protein 1
EPA	eicosapentaenoic acid
ER	endoplasmic reticulum
Fak	focal adhesion kinase
FBS	fetal bovine serum
FDR	false discovery rate
FFPE	formalin-fixed, paraffin imbedded
FRET	fluorescence resonance energy transfer
GAP	GTPase-activating protein
GEF	guanine nucleotide exchange factor
GFP	green fluorescent protein
GILT	γ-interferon-inducible lysosomal thiol reductase
Glut1	glucose transporter 1
GO	gene ontology
GPCR	G-protein-coupled receptor
GSEA	gene set enrichment analysis
GTPase	guanosine triphosphatases
GWAS	genome-wide association study
H&E	hematoxylin and eosin
HA	hemorrhage-associated
HAT	histone acetyltransferase
HDL	high-density lipoprotein
HMT	histone methyltransferase
HO-1	hemeoxygenase 1
HOPS	homotypic fusion and protein sorting
HSREB	Health Sciences Research Ethics Board
ICAM-1	intercellular adhesion molecule 1
Ii	invariant chain
IL	interleukin

ITIM	immunoreceptor tyrosine-based inhibitory motif
KEGG	Kyoto Encyclopedia of Genes and Genomes
LAL	lysosomal acid lipase
LCM	laser capture microdissection
LFA-1	lymophocyte function-associated antigen 1
LILRβ	leukocyte immunoglobulin like receptor B subfamily
lncRNA	long non-coding RNA
LOX	lipoxygenase
LOX-1	lectin-like low-density oxidized lipoprotein receptor 1
Lp(a)	lipoprotein (a)
LPS	lipopolysaccharide
LRP1	lipoprotein receptor-related protein 1
LXR	liver X receptor
lysoPC	lysophosphatidylcholine
MβCD	methyl-β-cyclodextran
MACCE	major adverse cardiovascular and cerebrovascular events
MFG-E8	milk fat globule-EGF-factor 8
MHC	major histocompatibility complex
MMP	matrix metalloproteinase
mmLDL	minimally-modified lipoproteins
MOI	multiplicity of infection
moLDL	modified low-density lipoproteins
MSigDB	Molecular Signatures Database
NADPH	nicotinamide adenine dinucleotide phosphate
NBT	nitroblue tetrazolium
NCEH	neutral cholesterol ester hydrolase
NF-κB	nuclear factor kappa-light-chain-enhancer of activated B cells
NLRP3	Nod-like receptor pyrin containing domain
NOX	NADPH-oxidase complex
NPC1	Niemann-Pick disease, type C1
NPC2	Niemann-Pick disease, type C2
LAP	LC3-associated phagocytosis

LI-COR	CLx Imaging Systems
LXR	liver X receptor
ORPL1	oxysterol-binding protein-related protein 1
oxLDL	oxidized low-density lipoprotein
PAD	protein arginine deaminase
PAMP	pathogen-associated molecular pattern
pAPC	professional antigen presenting cell
PCA	principal component analysis
PDAY	Pathological Determinants of Atherosclerosis in Youth
PFA	paraformaldehyde
PI3K	phosphoinositide 3-kinase
PI3P	phosphoinoside 3-phosphate
PPAR	peroxisome proliferator-activated receptor
PC	phosphatidylcholine
PE	phosphatidylethanolamine
PM	plasma membrane
PMA	phorbol 12-myristate-13-acetate
PS	phosphatidylserine
RAGE	receptor for advanced glycation end products
PCSK9	proprotein converatase subtilisn/kexin type 9
RAR	retinoic acid receptor
RE	recycling endosome
REP	Rab escort protein
RFP	red fluorescent protein
RILP	Rab7-interacting lysosomal protein
RMA	Robust Multi-array Average
ROCK	Rho-associated protein kinase
ROI	region of interest
RXR	retinoid X receptor
S1P	sphingosine-1-phosphate
S1PR	sphingosine-1-phosphate receptor
SIRPα	signal regulatory protein α

SENP1	sentrin-specific protease 1
SFK	Src-family kinase
SHP	Src homology region 2 domain-containing phosphatase
SLE	systemic lupus erythematous
SOCS3	suppressor of cytokine signaling 3
SPM	specialized pro-resolving mediator
SykI	Syk inhibitor
STAT3	signal transducer and activator of transcription 3
TAM	Tyro3, Axl and MerTK
Tet2	Tet methylcytosine dioxygenase 2
TfR	transferrin receptor
TIFF	tagged image file format
TG2	transglutaminase 2
TIM	T-cell immunoglobulin and mucin domain
TLR	Toll-like receptor
TULP1	tubby-like protein 1
TUNEL	transferase-mediated dUTP nick end-labeling
UCP2	uncoupling protein 2
UPR	unfolded protein response
UTP	uridine triphosphate
VAMP	vesicle-associated membrane protein
v-ATPase	vacuolar-adenosine triphosphatase
VCAM	vascular cell adhesion molecule 1
VLA-4	very late antigen 4
VSMC	vascular smooth muscle cell

List of Tables

List of Figures

List of Appendices

Chapter 1

1 Introduction

1.1 Efferocytosis and regulation of tissue homeostasis

1.1.1 Overview of efferocytosis

The removal of dying and dead cells *in situ* is essential in multicellular organisms for proper growth during embryogenesis and early development, and for maintenance of tissue homeostasis in adults.[1,2] Cells that are senescent, damaged or have otherwise received an appropriate signal undergo a form of programmed cell death termed "apoptosis".[1,3] Apoptosis involves a series of tightly regulated processes mediated by sequential activation of caspase enzymes that result in degradation of cellular compartments and packaging of cellular contents in plasma membrane-contained vesicles known as apoptotic bodies.[2,4] Apoptotic bodies must be efficiently removed in order to safely dispose of their contents and to avoid secondary necrosis, a process whereby uncleared apoptotic bodies leak their contents, which include a number of pro-inflammatory damage-associated molecular patterns (DAMPs), into the extracellular milieu and instigate a pathological inflammatory response.[5,6]

Apoptotic bodies are removed by other cells through phagocytic uptake and intracellular degradation of the apoptotic contents.[1] This process of phagocytic removal of apoptotic cells is known as "efferocytosis".[1,2] Efferocytosis is a highly conserved physiological process that is crucial for the maintenance of tissue homeostasis, play a role in organogenesis, tissue remodeling (e.g. bone growth, involution of mammary glands, etc.), tissue repair following injury, and, in certain species, during organ or limb regeneration.[7–9] Efferocytosis is a highly efficient process. Under normal conditions, uncleared apoptotic cells are rarely detectable *in vivo*, even in tissues undergoing high rates of cellular turnover such as the tonsils and thymus.[10]

The importance of efferocytosis in tissue homeostasis is underscored by fact that defective apoptotic cell clearance appears to be a central feature of several inflammatory and autoimmune diseases, including systematic lupus erythematosus and atherosclerosis.[10–12]

1.1.2 Types of efferocytes in the body

In higher mammals, including humans, dying cells within tissues are removed by either cells that are specially adapted for efferocytosis or by neighbouring cells for which efferocytosis is not a primary function depending on the specific tissue in question and the circumstances of cellular death.[13,14] The professional phagocytes for which efferocytic removal of apoptotic cells is a primary function include macrophages and dendritic cells, of which macrophages in particular are thought to carry out the majority of efferocytosis across a diverse range of tissues within the body.[3] However, many other cell types have been observed to possess limited efferocytic capacity and usually function to remove neighbouring apoptotic cells under specific circumstances.[13] These so-called non-professional phagocytes include epithelial cells, endothelial cells and fibroblasts.[15–17] Non-professional phagocytes are less efficient at apoptotic cell clearance, internalize apoptotic cells at a slower rate and lack the capacity to clear multiple apoptotic cells in rapid succession.[18]

In certain immune-privileged sites where circulating immune cells cannot access, non-professional phagocytes play an essential role in apoptotic cell clearance.[19,20] One example of this is within the eye, where specialized epithelial cells known as retinal pigment epithelial cells efferocytose membrane-bound, rhodopsin-containing disc structures shed on a daily basis by photoreceptor cells.[21] Mutations in efferocytic receptors involved in this process results in the development of retinitis pigmentosa, a progressive degenerative disease characterized by loss of photoreceptor cells and resultant visual impairment and loss.[22] Another example of the role non-professional phagocytes within an immune-privileged site is the clearance of apoptotic germ cells that arise in the process of spermatogenesis by Sertoli cells within the testes.[20] The presence of non-professional phagocytes within these tissues highlights the importance of apoptotic cell clearance across all tissues in the body.[13]

1.1.3 Recognition and uptake of apoptotic cells

1.1.3.1 Find-me signals

Efferocytosis proceeds through a number of distinct stages, the first of which involves migration of an efferocyte to the apoptotic cell.[23,24] Similar to the migration of immune cells towards pathogens and sites of infection, migration of efferocytes to apoptotic cells is dependent on a number of soluble chemoattractants, called "find-me" signals, that guide efferocyte migration in a concentration-dependent fashion.[24] To date, four distinct find-me signals have been identifying: extracellular adenosine triphosphate (ATP) and uridine triphosphate (UTP), fractalkine (CX_3CL1), lysophosphatidylcholine (lysoPC) and sphingosine-1-phosphate (S1P).[23] These signals are generated following activation of executioner caspases that cleave a variety of structural components of the apoptotic cell.[23,25]

The release of the extracellular nucleotides ATP and UTP occurs early in the execution phase of apoptosis.[26] Caspase 3/7-mediated cleavage of pannexin-1 on the apoptotic cell surface leads to the opening of pannexin channels and release of cytosolic nucleotides into the extracellular environment.[27] Macrophages and other phagocytes recognize ATP and UTP in the environment through the G-protein-coupled receptor (GPCR) P2Y2. P2Y2 activation promotes myeloid cell vascular adhesion and motility, and genetic deletion of P2Y2 in mice delays the kinetics of apoptotic cell clearance in these animals.[26]

Another find-me signal that is released relatively early on during apoptosis is fractalkine/CX_3CL1.[28] Fractalkine is an atypical chemokine that initially exists in a membrane-bound form and is cleaved to a soluble form through the activity of the metal metalloproteinases ADAM10 and ADAM17.[29] Fractalkine is recognized by the receptor CX_3CR1.[28] Truman *et al.* found that soluble fractalkine is released by apoptotic Burkitt lymphoma cells and stimulated macrophage chemotaxis.[28] In addition to acting as a find-me signal for apoptotic cells, the CX_3CL1-CX_3CR1 signaling axis also appears to play an important role in promoting monocyte cell survival.[30] Absence of either ligand or receptor results in decreased numbers of circulating monocytes in knockout mice and treatment of human monocytes *ex vivo* with fractalkine extended their survival.[31,32]

The other two known find-me signals, LysoPC and S1P, accumulate to physiologically-relevant levels only later in apoptosis (4-12 hrs following induction).[23] LysoPC was first described as a lymphocyte chemoattractant by Hoffman *et al.* in 1982.[33] Caspase-mediated activation of phospholipase A_2 drives the production of lysoPC from phosphatidylcholine found on plasma membranes.[34] Peter *et al.* demonstrated that monocytes and macrophages recognize lysoPC using the GPCR G2A, and that knocking down G2A expression in macrophages inhibited cell migration in the presence of lysoPC.[35] S1P is a lipid signal mediator with a diverse range of biological functions.[23] During the process of apoptosis, S1P is generated by the activity of S1P kinase 2, which has been shown to be a target of caspase 1.[36] S1P is recognized by five GPCR's on a range of lymphocytes (S1PR1-S1PR5) and activation of these receptor drive lymphocyte migration under a variety of circumstances, including mediating migration of monocytes and macrophages in response to S1P release from apoptotic cells.[24]

1.1.3.2 Eat-me signals

Following migration of a phagocyte to the apoptotic cell through the action of find-me signals, the next step in efferocytosis is recognition of the apoptotic cell by the phagocyte.[2] This is achieved through recognition by the phagocyte of specific ligands on the surface of the apoptotic cells, called "eat-me" signals.[23,37] A number of eat-me signals have now been identified, including exposure of phosphatidylserine (PS) on the outer leaflet of the plasma membrane, alterations in the glycosylation patterns on the apoptotic cell surface, changes in ICAM-1 epitopes on the cell surface, and exposure of the endoplasmic protein calreticulin on the cell surface.[2,5]

Of these, PS exposure on the plasma membrane outer leaflet has been by far the most recognized and well-understood eat-me signal.[38] In healthy cells, PS is sequestered on the cytoplasmic face of the plasma membrane through the activity of membrane flippases that actively shuttle PS from the outer leaflet to the inner leaflet.[5,38] Segawa *et al.* were able to demonstrate that caspase 3/7-mediated cleavage of the ATP-dependent flippase enzyme ATP11C is required for PS exposure during apoptosis.[39] In contrast, scramblase enzymes mediate movement of PS to the outer leaflet and Suzuki *et al.* showed caspase 3/7-mediated cleavage of the scramblase Xkr8 led to its constitutive enzymatic activity and drove PS

exposure.[40] In a series of experiments using camptothecin- or anti-Fas-induced apoptosis of Jurkat T cells, Borisenko *et al.* demonstrated that the amount of PS exposed on the cell surface increased by >280-fold following induction of apoptosis and that a minimum threshold of an 8-fold increase in PS levels on the cell outer surface was required before macrophage-mediated efferocytosis would occur.[41] In addition, it is also thought that a fraction of exposed PS becomes oxidized or otherwise modified and that this may increase its affinity towards certain efferocytic receptors.[38]

Despite the requirement for significant PS exposure before efferocytosis can occur, healthy cells possess an additional means of safeguarding themselves against inappropriate efferocytosis in the form of so-called "don't eat-me" signals that inhibit phagocytosis.[1,23] To date, just two such signals have been identified: CD47 and the recently recognized β_2-microglobulin (B2M) component of the major histocompatibility complex (MHC) class I molecule.[42,43] CD47 is a surface protein that belongs to the immunoglobulin superfamily and interacts *in cis* with integrins and plays a role in immune cell migration and proliferation.[44] In the context of efferocytosis, CD47 is recognized by the surface glycoprotein SIRPα expressed on the surface of phagocytes and the CD47-SIRPα signaling axis serves to inhibit phagocytosis of the CD47-expressing cell through phosphorylation of immunoreceptor tyrosine-based inhibitory motifs (ITIMs) on the cytoplasmic tail of SIRPα, which leads to the recruitment of the phosphatases SHP1 and SHP2.[45,46] The activity of these phosphatase inhibits the accumulation of myosin II during phagocytic cup formation to inhibit phagocytosis.[46] More recently, Barkal *et al.* described the expression of β2M on the surface of a range of human cancer cell lines and found that the level of β2M expression correlated with the degree of protection against macrophage-mediated phagocytosis.[43] The authors found that β2M was recognized by the inhibitory receptor LILRB1 expressed on the surface of macrophages and β2M-LILRB1 signaling was sufficient to inhibit phagocytosis.[43]

1.1.3.3 Efferocytic receptors

Exposed eat-me signals on the surface of apoptotic cells are recognized by efferocytic receptors expressed on the surface of efferocytes, either directly or through bridging molecules that opsonize the apoptotic cell.[3,46] Curiously, although there are only a few

recognized eat-me signals, these signals can be recognized by a wide range of efferocytic receptors and opsonins.[1,3] The majority of efferocytic receptors function by binding to PS, either directly or through one or more opsonins. Among the efferocytic receptors that are capable of binding directly to PS are: member of the TIM family of receptors (including TIM-1, TIM-3 and TIM-4), brain angiogenesis inhibitor 1 (BAI1), Stabilin-2, members of the CD300 family of receptors and the receptor for advanced glycation end products (RAGE).[47–51] Opsonin-dependent efferocytosis receptors include integrin $\alpha_V\beta_3$, the TAM family of receptors, which includes three members: Tyro-3, Axl and Mer, and integrin $\alpha_X\beta_2$, which was recently described by our lab to participate in efferocytosis.[52–54] The other eat-me signals also have corresponding efferocytic receptors. Modified ICAM3 is recognized by CD14 on the phagocyte surface, calreticulin is recognized by low density lipoprotein receptor-related protein 1 (LRP1; CD91) with the complement molecule C1q acting as a bridging opsonin, while modified phospholipids, including oxidized PS, can be recognized to a limited extent by the class B scavenger receptor CD36.[55–57]

Several bridging opsonins that recognize PS have been identified and work in concert with efferocytic receptors that do not directly recognize PS to mediate recognition of apoptotic cells.[58] Hanayama *et al.* identified that the secreted glycoprotein milk fat globule-EGF-factor 8 (MFG-E8) could bind to PS on the surface of apoptotic cells.[59] The same group later found that in mice lacking MFG-E8, apoptotic lymphocytes in the spleen and lymph nodes were not efficiently cleared and the mice went on to develop autoimmune glomerulonephritis, underscoring the importance of this MFG-E8 in efferocytosis *in vivo*.[60] MFG-E8 is recognized by integrin $\alpha_V\beta_3$ and mediates $\alpha_V\beta_3$-dependent recognition of apoptotic cells.[38] Two other opsonins, the vitamin K-dependent proteins Gas6 and protein S, are recognized by the TAM family of efferocytic receptors and mediate TAM receptor-dependent apoptotic cell recognition.[53,58] Protein S is produced by a wide variety of tissues across the body and is found as a circulating factor in the blood.[53] In addition to its role in efferocytosis, protein S also plays an important role as a cofactor for protein C in the inactivation of factors Va and VIIIa in the extrinsic pathway of the coagulation cascade.[53] Gas6 is primarily produced by endothelial cells, vascular smooth muscle cells and in the bone marrow.[53] Members of the TAM family have different affinities for each of these opsonins, with Gas6 preferentially binding to Axl and protein S binding preferentially to

Tyro-3 and MerTK.[53] Two other potential opsonins that have been recently proposed to function cooperatively with the TAM family of receptors are the signaling proteins tubby and tubby-like protein 1 (TULP1), both of which are preferentially recognized by MerTK.[61] Mice lacking either tubby or TULP1 have significantly impaired efferocytosis within the retina and develop a number of vision disorders as a result.[62,63] Finally, our lab has recently identified a soluble form of the transmembrane glycoprotein CD93 (solCD93) as an opsonin that mediates integrin $\alpha_X\beta_2$-dependent efferocytosis.[54] A summary of find-me signals, eat-me/don't eat me signals and their cognate receptors and opsonins is presented in **Table 1.1**.

Table 1.1 List of find-me, eat-me and don't eat me along with their cognate opsonins and/or receptors.

Signal	Opsonin	Receptor
Find-me signals		
ATP/UTP	-	P2Y2
Fractalkine (CX_3CL1)	-	CX_3CR1
LysoPC	-	G2A
S1P	-	S1PR1-5
Eat-me signals		
PS	-	TIM-1, -3, -4
PS	-	BAI1
PS	-	Stabilin-2
PS	-	CD300A/B/F
PS	-	RAGE
PS	Gas6, Protein S, Tubby, TULP1	TAM family (Tyro-3, Axl, MerTK)
PS	MFG-E8	$\alpha_V\beta_3$
PS	solCD93	$\alpha_X\beta_2$
Modified phospholipids	-	CD36
Modified ICAM3	-	CD14
Calreticulin	C1q	LRP1 (CD91)
Don't eat-me signals		
CD47	-	SIRPα
B2M	-	LILRB1

1.1.4 Apoptotic cell internalization

Following recognition of the apoptotic cell, it is subsequently internalized by the efferocyte for degradation and clearance.[64] The process of apoptotic cell uptake is complex and there are probably multiple signaling pathways utilized by different efferocytic receptors. Peter Henson and others have suggested that the process of apoptotic cell uptake occurs through two distinct steps: binding of the apoptotic cell to the efferocyte and subsequently its uptake into the efferocyte in what has been termed the "tether-and-tickle" process.[1,23,65] Tethering holds the apoptotic cell in place while the phagocyte forms an invagination within their plasma membrane called a "phagocytic cup" to mediate the engulfment of the apoptotic cell.[66] Certain efferocytic receptors are able to mediate both apoptotic cell binding and uptake, while others, including CD14 and TIM4, are able to tether apoptotic cells but do not initiate their uptake.[1] Indeed, it is believed that many efferocytic receptors that recognize and tether apoptotic cells require cooperative binding and signaling through integrins and other canonical phagocytic receptors to mediate apoptotic cell internalization.[67,68] One example of this is the efferocytic receptor TIM-4, which utilizes β1 integrins as coreceptors in order to induce the necessary signal to initiate apoptotic cell internalization.[69]

A complete discussion of the signaling pathways used by efferocytic receptors is beyond the scope of this thesis, but has been reviewed in detail by Elliot *et al.*, Freeman *et al.* and others.[46,58] However, signaling from efferocytic receptors appear to converge on the activation of several Rho guanosine triphosphatases (GTPases): Rac1, Cdc42 and RhoA, that drive formation of the phagocytic cup required to engulf and then internalize the target apoptotic cell.[37] Rac1 in its active state is a crucial mediator of actin polymerization via the Scar/WAVE complex, which is required for formation of membrane extrusion and the phagocytic cup.[70] Signaling from efferocytic receptors activate Rac1 through recruitment of several guanine nucleotide exchange factors (GEFs), in particular the Dock180-Elmo complex which is crucial for apoptotic cell uptake and highly evolutionarily conserved.[37] A number of other factors have also been found to participate in this process and drive Rac1 activation. Among these is CrkII, a member of the Crk family of adaptor proteins that are known to associate with Dock180.[71] While a direct physical association between

Dock180 and CrkII appears not to be required for internalization of apoptotic cells, deletion of the CrkII homologue in *C. elegans* was sufficient to abrogate efferocytosis.[72] An illustration of efferocytic receptor crosstalk and convergence at Rac1-Dock180-Elmo complex is presented in **Figure 1.1**.

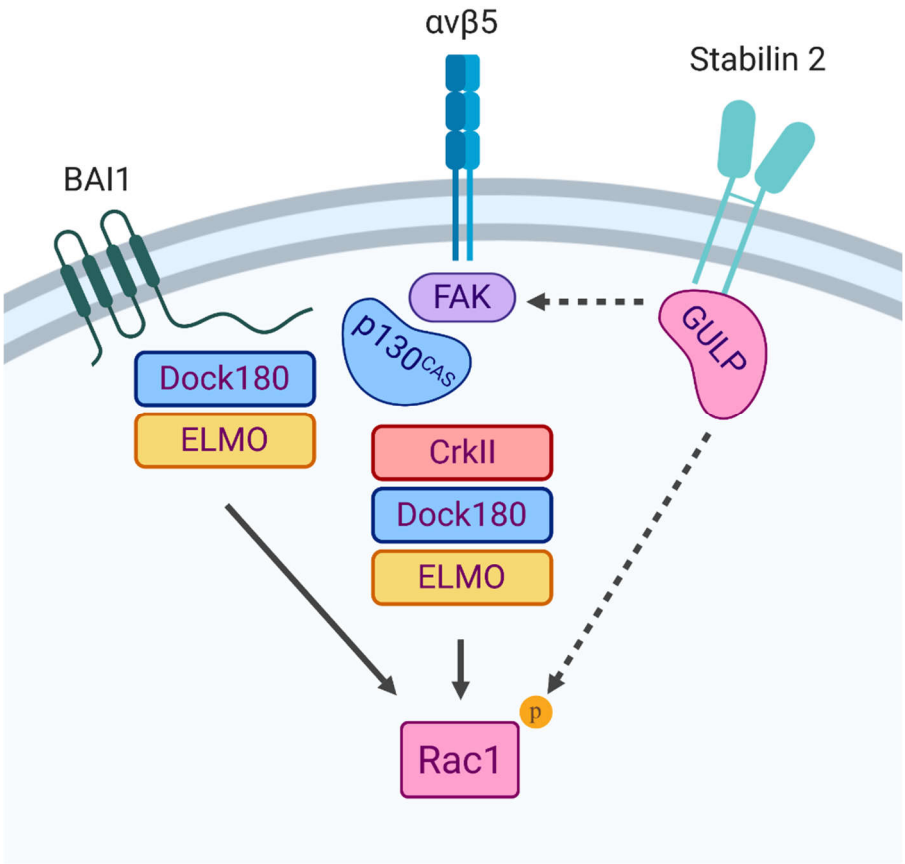

Figure 1.1 Convergence of efferocytic receptor signaling onto Rac1 activation.

Efferocytic receptors (BAI1, integrin αVβ5, stabilin-2) utilize distinct signaling pathways that convergence on the activation of the Rho-GTPase Rac1. Activation of BAI1 results in recruitment of the Dock180-Elmo GEF complex, which directly activates Rac1. Signaling from integrin αVβ5 recruits focal adhesion kinase (Fak), which recruits the CrkII-Dock180-Elmo complex using the scaffold protein p130Cas as a mediator. Stabilin-2 signaling recruits the adaptor protein Gulp1, which is thought to mediate direct activation of Rac1 or enable cooperative signaling with integrin αVβ5 to drive Rac1 activation. Figure adapted from Penberthy & Ravichandran.[37]

Rac1 activity is antagonized by RhoA, which activates the Rac1 GTPase-activating proteins (GAPs) p190Rho-GAP and FilGAP to drive Rac1 inactivation.[73] The contribution of RhoA to efferocytosis has been somewhat controversial since it plays different roles during phagocytic cup formation and phagocytic cup closure.[70] While impairment of RhoA function results in impaired apoptotic cell clearance, there is evidence that its activity is required for phagocytic cup closure and internalization of the apoptotic cell.[74,75] Indeed, it has been demonstrated that RhoA signaling through Rho-associated protein kinase (ROCK) drives activation of myosin II, which is crucial for actin contraction and functions to pull the engulfed apoptotic cell into the efferocyte.[76] Using fluorescence resonance energy transfer (FRET)-based biosensors to examine the spatiotemporal dynamics of Rac1 and RhoA activation, Kim *et al.* found that the ratio of Rac1/RhoA appeared to play a role in determining whether apoptotic materials were internalized by the efferocyte, with the authors suggesting that this served as an additional mechanism to prevent inappropriate efferocytosis.[77]

1.1.5 Efferosome maturation

Following closure of the phagocytic cup, the apoptotic cell is fully contained within a plasma membrane-derived vacuole, which then undergoes scission from the cell surface membrane to form an efferosome.[70] The efferosome then undergoes a series of highly regulated biochemical modifications to efficiently degrade the internalized apoptotic cell in a remodeling process called efferosome maturation.[64,70] Efferosome maturation is characterized both by sequential fusion with early and then late endosomes along with progressive acidification of the efferosomal lumen in order to drive the breakdown of apoptotic cargo.[64] The regulation of efferosome maturation is complex but the most well-defined mechanism driving this process is the sequential recruitment of the small GTPases Rab5 and Rab7 to the efferosome surface (see **Figure 1.2**).[64]

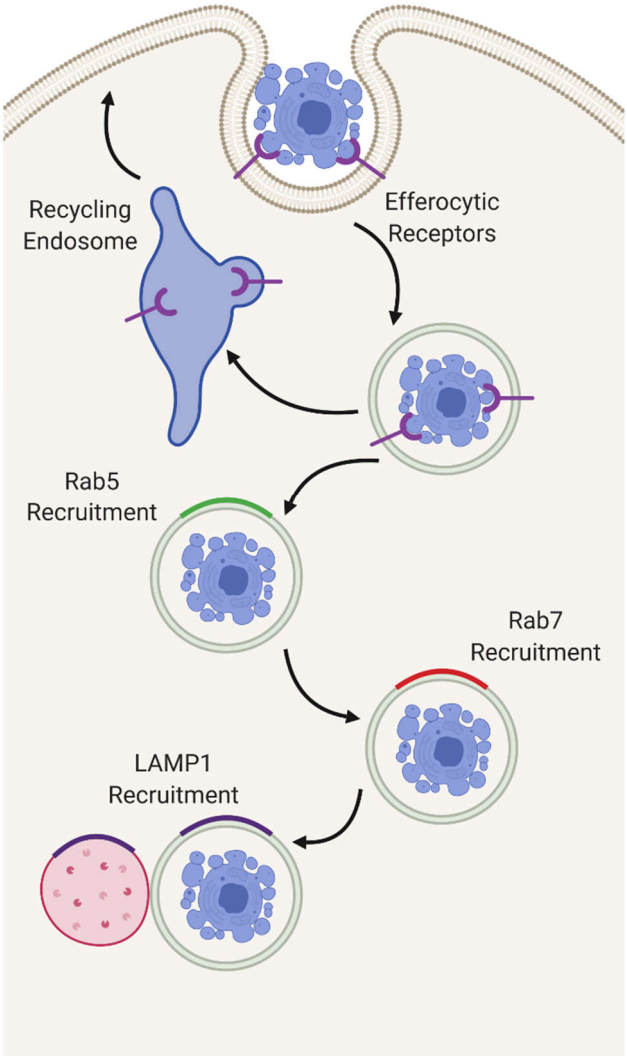

Figure 1.2 Sequential recruitment of the small GTPases Rab5 and Rab7 to the efferosome surface regulates efferosome maturation.

Following apoptotic cell recruitment, Rab5 is recruited to the surface of the nascent efferosome, where it drives fusion between the efferosome and early endosomes to form the early efferosome. Fusion with early endosomes also mediates recycling of efferocytic receptors to the cell surface. Rab5 is then replaced on the efferosome surface by Rab7, marking the transition to the late efferosome. The late efferosome undergoes acidification and fusion with lysosomes, acquiring the lysosomal marker LAMP-1 as a result. Figure adapted from Kinchen & Ravichandran.[64]

One of the earliest maturation events following apoptotic cell internalization is recruitment of Rab5 to the nascent efferosome, a process that is driven by the Rab5 GEF Gapex-5.[78] Initially, activated Rab5 recruits another GEF, Rabex-5, which is thought to further recruit Rab5 and stabilize Rab5 on the surface of the efferosome.[79] A series of Rab5 effectors are also recruited to the early efferosome, including: EEA-1, Vps-34 and Mon1a/b.[79] EEA-1 mediates fusion between the efferosome and early endosomes, which mediates trafficking to the recycling endosome and receptor recycling back to the cell surface.[80] Vps-34 functions as a phosphoinositide 3-kinase (PI3K) and mediates formation of phosphoinositide 3-phosphate (PI3P), which functions to both enhance Rab5 recruitment and mediate Rab7 recruitment to the efferosome downstream of Rab5 activation.[81] Mon1a/b displaces Rabex-5 and shuts down the Rab5 recruitment loop and also functions in complex with the vacuolar trafficking protein Ccz1 to recruit the tethering homotypic fusion and protein sorting (HOPS) complex.[82,83] The Vps-39 subunit of HOPS complex possesses Rab7 GEF activity and this complex mediates the transition between Rab5 and Rab7 on the efferosome surface.[83]

Replacement of Rab5 by Rab7 marks the transition from the early efferosome to the late efferosome.[64,83,84] Rab7 effectors have crucial roles in driving remodeling events that result in apoptotic cell degradation. These mediators include Rab7-interacting lysosomal protein (RILP) and oxysterol-binding protein-related protein 1 (ORPL1), which together interact with the dynein/dynactin motor complex to drive trafficking of late efferosome along microtubules to the perinuclear region of the efferocyte.[85–87] This movement is necessary for efficient fusion between late efferosomes and lysosomes, and the delivery of degradative lysosomal hydrolases into the efferosomal lumen.[87,88] RILP further recruits V1G1, a subunit of the vacuolar ATPase (v-ATPase), which mediates v-ATPase assembly on the efferosome surface and drives efferosomal acidification and activation of lysosomal hydrolases to complete degradation of apoptotic cargo.[89]

1.1.6 Cellular consequences of efferocytosis

The hallmark of efferocytosis is the lack of an inflammatory response.[1,2] Indeed, efferocytosis is considered to be either immunologically silent—meaning that efferocytes do not produce pro-inflammatory factors nor do they present apoptotic cell-derived

antigens or initiate an immunological response—or actively anti-inflammatory.[1] Additionally, the efferocyte must effectively deal with the added metabolic stress of internalizing an entire apoptotic cell and the contents thereof.[1,90] In macrophages, efferocytosis leads to further reinforcement of a tissue remodeling/repair state. This is achieved through a positive feedback loop whereby engagement of efferocytic receptors drives the upregulation of the expression of both efferocytic receptors and certain opsonins.[91]

Efferocytosis has a well-documented role in restraining the generation of inflammation.[92] Many of the receptors involved in efferocyte recruitment and apoptotic cell recognition themselves have been shown to suppress inflammation.[58,92] For example, signaling from the fractalkine receptor CX_3CR1 simultaneously induces production of proinflammatory cytokines while enhancing expression of both pro-survival signals such as the anti-apoptotic protein Bcl-2 and anti-oxidant factors such as hemeoxygenase-1 (HO-1).[32,93] In addition, almost every PS receptor has been shown to exhibit some degree of anti-inflammatory activity. Signaling through both TIM-3 and MerTK have been shown to inhibit nuclear factor kappa-light-chain-enhancer of activated B cells (NF-κB)-mediated expression of pro-inflammatory genes.[94,95] Engulfment of apoptotic cells leads to activation of several nuclear factor family transcription factors in the efferocyte.[96,97] Activation of these transcription factors play a role in generation of an anti-inflammatory state through increasing the expression of several anti-inflammatory cytokines. Activation of liver X receptor (LXR)-α/β and peroxisome proliferator-activated receptor (PPAR)-δ downstream of apoptotic cell internalization drive the expression of TGF-β and IL-10.[96,98]

Internalization of apoptotic cells imposes a significant metabolic load upon efferocytes, which must adapt accordingly to deal with this stress.[1,90] Activation of LXR-α/β, in addition to dampening inflammation, also leads to upregulation of ATP-binding cassette transporter member 1 (ABCA1), which is a major transporter responsible for cholesterol efflux from the cell.[99] Upregulation of ABCA1 (and the related cholesterol transporter ABCG1) has also been shown by Yvan-Charvet *et al.* to protect against excessive production of superoxides as a result of nicotinamide adenine dinucleotide phosphate (NADPH) oxidase 2 activation in response to apoptotic cell internalization.[100] In addition

to cholesterol efflux and anti-oxidant activity, efferocytes are able to cope with cholesterol and lipid accumulation, which have been shown to exert a pro-apoptotic effect, through cell survival signaling through the PI3K/Akt axis and activation of anti-apoptotic proteins such as Bcl-2.[101] Finally, due to the intake of excess carbohydrates and lipids from efferocytosis, mitochondrial function in efferocytes has been shown to be altered post-apoptotic cell internalization. Park *et al.* demonstrated that mitochondrial membrane potential decreased post-efferocytosis in manner dependent on the mitochondrial membrane protein mitochondrial uncoupling protein 2 (Ucp2).[102] More recently, Wang *et al.* demonstrated that dynamin related protein 1 (Drp1)-mediated mitochondrial fission in response to apoptotic cell internalization was required for increasing intracellular calcium levels, which the authors found to be required for efficient continuous uptake of multiple apoptotic cells by professional phagocytes.[103] Similarly, Morioka *et al.* found that expression of glucose transporter 1 (Glut-1) was upregulated following efferocytosis and helped drive metabolic reprogramming of the efferocyte towards being glycolysis-dominant.[104] This transition was found by the authors to also be required for continuous efferocytosis.[104]

1.2 Atherosclerosis and the role of macrophages

1.2.1 Atherosclerosis

Atherosclerosis is characterized by thickening of the arterial intima as a result of the accumulation of modified lipoproteins and immune cells beneath the vessel endothelium.[105] The result of this accumulation is the formation of a lipid-rich plaque overlaid by a fibrotic cap, referred to interchangeably as an "atherosclerotic lesion" or "atheroma".[106,107] Atheromas cause stenosis of the arterial lumen, resulting in the constriction of blood flow to vital organs.[105] Significantly, atheroma growth over time can result in weakening of the fibrotic cap and increased risk of plaque rupture.[108] Rupture of the plaque results in the formation of a thrombus overlying the plaque. Within the coronary arteries, thrombus formation over a ruptured plaque may result in the occlusion of a vessel and a subsequent myocardial infarction. The thrombus can also break off from the inciting

plaque, travel through arteries and potentially lodge in the circulation, resulting in serious complications including ischemic stroke and critical limb ischemia.[105,109] (See **Figure 1.3** for a summary of atherosclerotic plaque development). Atherosclerosis is the most common cause of cardiovascular disease (CVD) such as coronary heart disease and cerebrovascular disease, which together form the leading cause of death in Canada—accounting for over 30% of all-cause mortality in the 2013 national census.[110]

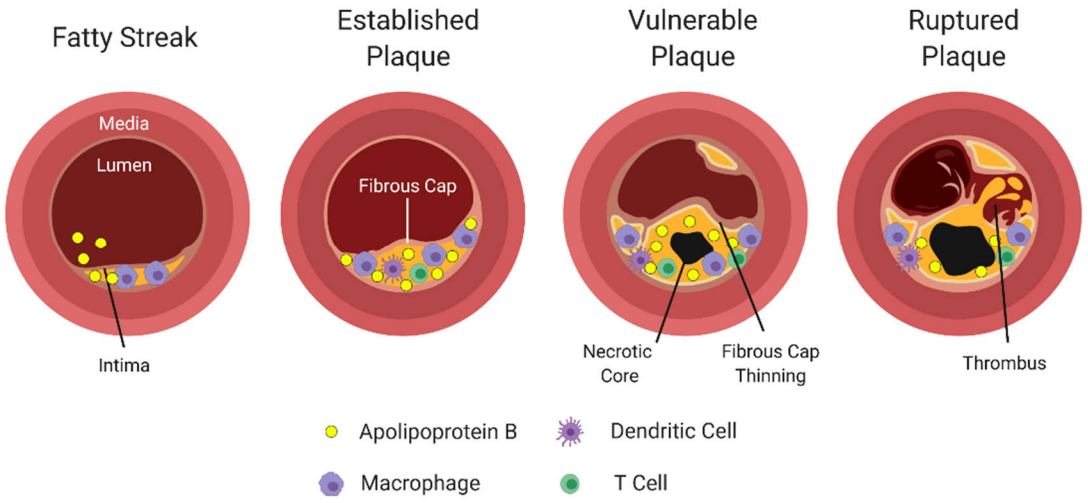

Figure 1.3 Pathogenesis and progression of atherosclerosis.

Stages of atherosclerotic plaque progression. Lesions begin as pre-atherosclerotic fatty streaks characterized by accumulation of ApoB-containing lipoproteins and a number of immune cell types within the arterial intima. Next, proliferation of endothelial cells and smooth muscle cells of the artery results in the formation of a fibrous cap that overlies the lesion, leading to the formation of the established atherosclerotic lesion. Cell death and generation of chronic inflammation within the lesion results in the formation of a necrotic core and the thinning of the fibrous cap, increasing the risk of plaque rupture and forming a vulnerable plaque. Finally, disruption of fibrous cap integrity through either endothelial erosion or fibrous cap fissure results in the exposure of lesion contents to the circulation and the formation of a thrombus. Figure adapted from Moore & Tabas.[111]

Atherosclerosis is a prevalent disease and is found almost ubiquitously in individuals living in post-industrial nations.[109,112] The influential Pathological Determinants of Atherosclerosis in Youth (PDAY) study has reported that among 2,876 U.S. subjects aged 15-34, lesions were identified in all of the aortas and more than half of the coronary arteries of the youngest age group (15-19 years) and that lesions increased in both prevalence and extent with increasing age.[112] The risk factors for atherosclerosis align closely with those identified for development of coronary artery disease by the Framingham Heart Study.[113] The most important risk factor for atherosclerosis development and progression was age, with older individuals possessing a greater lesion extent and more lesions that are considered to be vulnerable and prone to rupture and causing serious complications.[112,113] Other risk factors for atherosclerosis include: male sex, race (Southeast Asians are particularly prone to developing significant atherosclerotic disease), smoking and the components of metabolic syndrome (abdominal obesity, insulin resistance, hypertension and high triglycerides/low high-density lipoprotein [HDL] levels).[113] Atherosclerosis has a clear genetic component as well, with certain monogenic disorders such as familial hypercholesterolemia raising the risk of significant atherosclerotic disease significantly and a multitude of allelic variants linked to increased risk of atherosclerosis.[114]

Atherosclerosis is a complex and multi-faceted disease with a number of factors that contribute to its pathogenesis.[105,115] The initiating event in atherosclerosis is thought to be the retention of apolipoprotein B (ApoB)-containing lipoproteins, in particular modified low-density lipoproteins (moLDLs) and lipoprotein remnant particles in the arterial intima.[116] Regions of the arterial tree with disturbed laminar flow (e.g. where a single vessel branches into multiple vessels) are particularly prone to lipoprotein accumulation.[117] Damage to the vessel endothelium, for example resulting from decreased nitric oxide bioavailability and increased adhesion molecule expression on the endothelium as a result of smoking, is a further potentiating factor for lipoprotein accumulation and plaque formation.[118] Disturbed or damaged endothelium upregulates cell surface adhesion molecules.[118–120] These receptors promote infiltration of circulating immune cells, especially macrophages and T lymphocytes, into the developing lesion.[121,122] There is also evidence that activated endothelial cells increase their expression of scavenger receptors that bind to moLDL and drive their trafficking across the endothelium and into arterial

intima via cholesterol transcytosis within individual endothelial cells.[123,124] These pathological changes within the endothelium together result in accumulation of lipids and immune cells within the intima.

Retention of lipoproteins in the intima results in increased endothelial activation, which drives further modification of retained lipoproteins and the generation of sterile inflammation.[108,125] This state of inflammation results in the aberrant production of a number of chemokines and the recruitment of cells of the innate and adaptive immune system to the developing atheroma. These immune cells become retained within the atheroma and contribute to the generation of a highly pro-inflammatory atheroma microenvironment and a state of unresolved inflammation.[115] The development of a chronic inflammatory state within the atheroma has two major consequences: 1) sustained endothelial activation resulting in further lipoprotein retention and modification, and 2) proliferation of vascular smooth muscle cells (VSMCs) into myofibroblasts, which form a fibrous cap that overlies the plaque.[106,119] Persistent inflammation combined with growth of a necrotic core composed of foam cells and lipid-rich debris over time results in thinning of the fibrous cap and increased plaque vulnerability to rupture.[108] Rupture results from endothelial fissure or erosion, two distinct processes that result in exposure of the pro-thrombotic contents of the plaque to the circulation.[126] There, phospholipids, tissue factor and other pro-thrombotic plaque contents react with platelets and fibrin to quickly form large thrombi that can rapidly occlude entire vessels.[127]

For decades, a focus of therapeutic intervention in atherosclerosis has been LDL cholesterol reduction.[128] Lowering the level of LDL in patients with a previous coronary event using statins along with ezetimibe and/or proprotein convertase subtilisin/kexin type 9 (PCSK9) inhibitors has been shown repeatedly to confer a mortality benefit.[129] However, even with reduction of LDL to optimal levels, the rate of further cardiovascular events is not completely eliminated.[129,130] The remaining risk of a recurrent cardiovascular event, called the residual risk, has widely been believed to be attributable to the inflammatory component of atherosclerotic disease, which is not adequately addressed with LDL lowering therapy alone.[130] The first indication that inflammation had a role in atherosclerotic disease in humans came from the Justification for the Use of Statins in

Primary Prevention: An Intervention Trial Evaluation Rosuvastatin (JUPITER) trial, which demonstrated that treating patients with low-to-normal LDL levels but high C-reactive protein (CRP) levels (not causative for atherosclerosis but potentially indicative of on-going inflammatory processes) lowered their risk of a major cardiovascular event by 0.2-0.6% over one year.[131] More recently, the 2017 Canakinumab Antiinflammatory Thrombosis Outcome Study (CANTOS) trial was able to definitively show that in patients with a previous coronary event and optimally controlled LDL levels but high levels of high sensitivity CRP, treatment with canakinumab, a monoclonal antibody that inhibits IL-1β, could lower the risk of a recurrent cardiovascular event without affecting lipid levels.[132] CANTOS provides strong evidence that targeting inflammation is a viable strategy for treating atherosclerotic disease in humans.

1.2.2 Role of macrophages in atherosclerosis

Macrophages play a central role in the pathogenesis of atherosclerosis, both in efferocytic removal of apoptotic debris in early stage of disease and in retention, pathologic differentiation into lipid-laden foam cells and production of pro-inflammatory factors in late-stage disease.[116,121,133] They are arguably the central inflammatory cell of the atherosclerotic plaque, acting as the major source of a number of key pathologic pro-inflammatory cytokines including TNF-α, IL-6 and IL-1β.[134] Macrophage content has been shown to be an indicator of atherosclerotic plaque progression, and in murine plaque regression models, decrease in lesional macrophage content is observed to correlate with the degree of disease regression.[135,136] The number of circulating monocytes has also been found to be increased in mouse models of atherosclerosis, suggesting that atherosclerotic conditions have a systemic impact on hematopoiesis in addition to its local effects in the vasculature.[32,137]

It is thought that activation of the endothelium in response to accumulation and modification (particularly oxidation) of lipoproteins in the underlying intima results in the release of chemokines such as CCL2 and CCL5 that recruit circulating monocytes to the site of the lesion.[138] Importantly, blockage of either these chemokines or their cognate receptors abrogate monocyte migration into lesions and inhibit atherosclerosis progression.[111] Simultaneously, activated endothelial cells express a number of cell surface

adhesion molecules, including P- and E-selectin, which interact with their cognate receptor on the cell surface of monocytes to induce monocyte rolling.[117,139] The monocyte integrins very late antigen-4 (VLA-4) and lymphocyte function-associated antigen-1 (LFA-1) then bind to their respective ligands on activated endothelial cells, vascular cell adhesion molecule-1 (VCAM-1) and intercellular adhesion molecule-1 (ICAM-1) to mediate tethering and transmigration of the monocyte into the intima, where they proceed to differentiate into macrophages.[111,121]

Initially, these macrophages play a protective role through the efferocytic removal of apoptotic cells and debris, thereby limiting the size and expansion of the early atheroma.[140,141] However, a certain proportion of atheromas can progress to a more advanced pathologic state, characterized by a breakdown of the ability to efficiently efferocytose apoptotic cells (discussed in greater detail in **Chapter 1.3**).[142] The accumulation of cholesterol within these macrophages, through both uptake of modified lipoproteins in the intima and efferocytosis of cholesterol-laden apoptotic cells drive the formation of foam cells, described in greater detail in **Chapter 1.2.4**.[143] Within the lesional microenvironment, macrophages also experience inflammatory activation as a result of cholesterol loading and the chronic inflammatory state of the plaque microenvironment, described in detail in **Chapter 1.2.3**.[13]

Within advanced atherosclerotic plaques, macrophages contribute to the development of necrotic cores and fibrous cap thinning, two features of vulnerable plaques.[144] Macrophages contribute to fibrous cap thinning through induction of vascular smooth muscle cell (VSMC) death through induction of VSMC apoptosis through engagement of their Fas death receptors and through the production of pro-apoptotic cytokines such as TNF-α.[145] Another mechanism of macrophage-mediated thinning of the fibrous cap is through production of matrix metalloproteinases (MMPs), which degrade collagen that stabilizes the cap.[144] In particular, macrophage production of MMP-2 and MMP-9 have been shown to be involved in fibrous cap thinning in mouse models of atherosclerosis.[146] Additionally, in mice lacking MMP-13, the collagen content of fibrous caps was found to be increased.[147]

Macrophages also contribute to the generation of necrotic cores, which serve to destabilize plaques and increase the risk of rupture, through two distinct mechanisms: apoptosis of advanced lesional macrophages, and a failure of surrounding macrophages to efferocytose these apoptotic cells.[148,149] Macrophage cell death within advanced atherosclerotic lesions is the result of a combination of factors, including increased oxidative stress, activation of death receptors by ligands that exist uniquely within advanced lesions and signaling from Toll-like receptors (TLRs).[126,150] Recently, endoplasmic reticulum (ER) stress pathways, and the unfolded protein response (UPR) pathway in particular, have been recognized as important contributors to macrophage cell death in atherosclerosis.[144,151] Activation of the UPR mediator C/EBP-homologous protein (CHOP) is associated with lesion progression and with plaques with vulnerable features.[151] Deletion of CHOP in animal models of atherosclerosis has been shown to protect against lesional cell death and formation of large necrotic cores.[152]

An overview of the many roles played by macrophages in the development of atherosclerosis is provided in **Figure 1.4**.

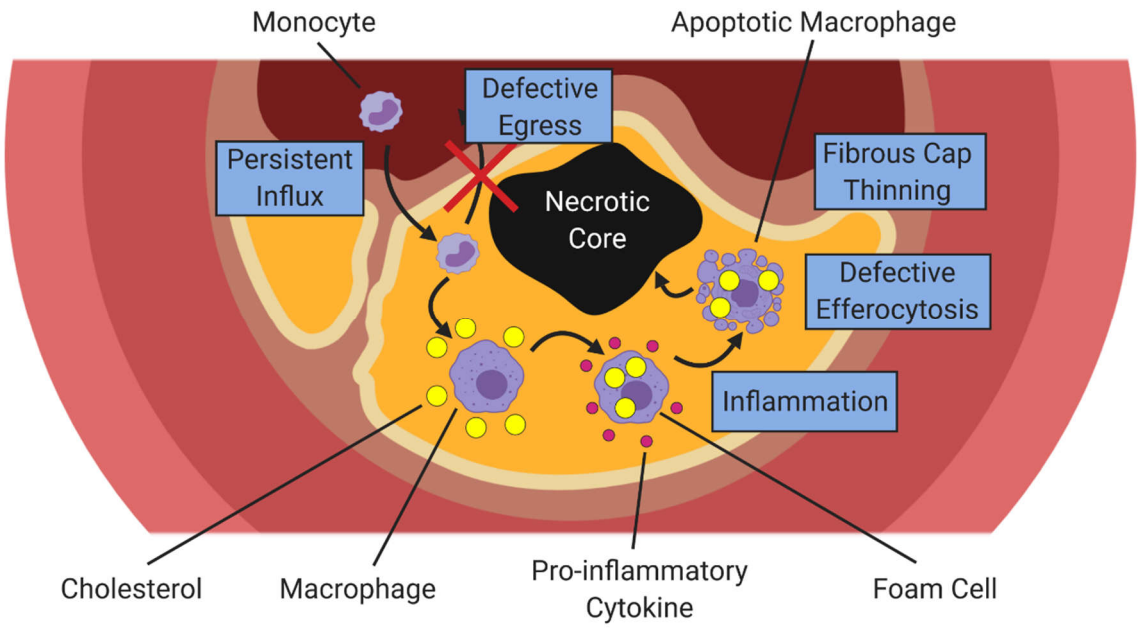

Figure 1.4 Features characteristic of pathologic monocyte/macrophage function in atherosclerosis.

Monocytes and macrophages play a central role in the pathogenesis of atherosclerosis. Activation of the endothelium overlying regions of lipoprotein accumulation results in persistent monocyte influx. Within the lesion, monocytes differentiate into macrophages, which produce pro-inflammatory cytokines and accumulate cholesterol through uptake of modified lipoproteins and efferocytosis of cholesterol-laden apoptotic cells. Excessive cholesterol accumulation results in the pathologic differentiation of macrophages into foam cells, which are retained within the plaque and fail to egress. In advanced atherosclerotic lesions, a combination of accelerated macrophage cell death and defective efferocytosis results in the formation of a large necrotic core. Generation of pro-apoptotic factors and matrix metalloproteinases by macrophages within advanced lesions also contributes to fibrous cap thinning. A combination of necrotic core formation and fibrous cap thinning increase the risk of plaque rupture and contribute to the vulnerable plaque phenotype. Figure adapted from Tabas (2009).[144]

1.2.3 Influence of the plaque microenvironment on macrophages

The presence of a chronic inflammatory state is an important factor in the pathogenesis of atherosclerosis.[115] There is ample evidence from gene expression studies of plaque-resident macrophages and in knockout mice that the presence of inflammation drives accelerated lesion progression and the absence or reduction of inflammation slows progression.[150,153] Inflammatory activation of macrophages within the plaque appears to be at least partially driven by signaling through the TLRs.[126,154] In particular, TLR4 has been shown to bind oxidized LDL (oxLDL) cooperatively with CD36 to activate NF-κB signaling and expression of pro-inflammatory cytokines.[155] Another pro-inflammatory pathway in atherosclerotic macrophages involves accumulation of free cholesterol within the macrophage cytoplasm which activates the Nod-like receptor pyrin domain containing 3 (NLRP3) inflammasome, driving the subsequent production of IL-1β and IL-18.[156] Bone marrow transplantation experiments using donor mice lacking NLRP3 results in decreased lesion size compared to transplantation with wild type bone marrow.[157] An overview of pro- and anti-inflammatory signaling with atherosclerotic macrophages is presented in **Figure 1.5**.

This aberrant activation of lesion-resident macrophages into an inflammatory phenotype has important consequences for the progression of atherosclerosis.[133] Indeed, analyses of human atherosclerotic plaques have revealed a greater proportion of pro-inflammatory macrophages compared to tissue remodeling macrophages within progressing lesions, and in particular within vulnerable plaques.[136] A number of studies have shown that experimental models of atherosclerosis regression, including delivery of an apoE-encoding adenovirus vector in *Apoe*$^{-/-}$ mice and transplantation of atheroma-laden aortic arch from *Apoe*$^{-/-}$ mice into recipient C57BL6 mice with varying levels of HDL, demonstrate that macrophage numbers and polarization state are significantly impacted.[158,159] In these models of atherosclerosis regression, investigators have consistently found lower overall macrophage numbers within the atheromas and a greater proportion of tissue remodeling macrophages.[135,158,159]

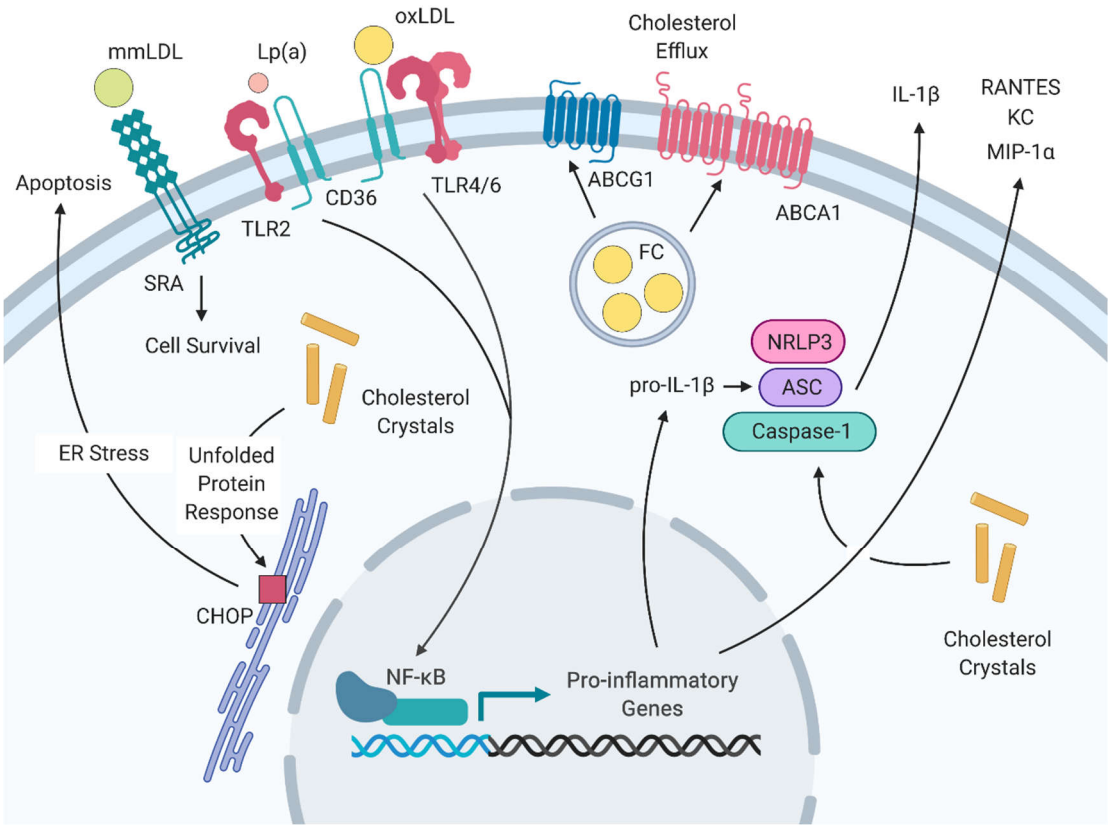

Figure 1.5 Pro-inflammatory and anti-inflammatory signaling within lesion-resident macrophages.

The atherosclerotic lesion microenvironment activates a number of pro-inflammatory signaling pathways that converge on NF-κB activation. Simultaneously, inflammatory activation is counterbalanced by anti-inflammatory signaling that upregulate pathways and receptors involved in response to cholesterol loading. Lipid ligands within the plaque, including oxLDL, minimally modified LDL (mmLDL) and lipoprotein(a) (LPa) induce signaling through TLRs and scavenger receptors to induce the generation of pro-inflammatory cytokines, including RANTES (CCL5), KC (CXCL1) and MIP-1α (CCL3). Accumulation of free cholesterol within endosomes result in endosomal damage and activation of the NLRP3 inflammasome along with generation of IL-1β. Excess cholesterol also activates the UPR pathway of the ER stress response, leading to further pro-inflammatory activation and ultimately cell apoptosis. Along with inflammatory activation, lipoprotein exposure also drives upregulation of ABCA1 and ABCG1, which mediate cholesterol efflux from the cell. Figure adapted from Moore & Tabas.[111]

Beyond the classical paradigm of the simple dichotomy between pro-inflammatory and tissue remodeling macrophage phenotypes, macrophages *in vivo* rarely fall nicely into either subset.[160] As such, a number of unique atherosclerosis-associated macrophage subsets have been identified in murine models of atherosclerosis and in patients. Kadl *et al.* identified a Mox macrophage phenotype in murine macrophages treated with oxLDL, which demonstrated a distinct gene expression pattern characterized by upregulation of redox-regulatory genes driven by the transcription factor Nrf2.[161] Boyle *et al.* identified another novel atherosclerotic macrophage subset that is associated with intra-plaque hemorrhage called hemorrhage-associated (HA)- or Mhem macrophages.[162] The presence of heme and hemoglobin at the site of hemorrhage drives expression of heme oxygenase 1 (HO-1) through activating transcription factor 1 (ATF-1).[163] These macrophages also upregulate gene targets of LXR-α/β, including ABCA1. The net result is a macrophage subset that is highly resistant to oxidative stress and cholesterol loading.[162,163]

1.2.4 Cholesterol uptake and foam cell formation

Uptake of lipoproteins by macrophages within the atheroma results in accumulation of cholesterol esters within the macrophage, which is converted into free cholesterol by lysosomal acid lipase in the lysosome.[164] Free cholesterol must be either removed from the cell through the cholesterol efflux transporters ABCA1 and ABCG1 or re-esterified and stored as cholesterol ester intracellularly as neutral lipid droplets.[100,143] Excess intracellular free cholesterol results in macrophage inflammatory activation through the induction of ER stress, TLR4 signaling and inflammasome activation.[151,157,165] Furthermore, delivery of excess cholesterol into the macrophage leads to enrichment of free cholesterol within the plasma membrane and may serve to enhance inflammatory signaling through cholesterol microdomain-mediated activation of pro-inflammatory signaling receptors.[166] Thus, cholesterol loading of macrophages can further contribute to the generation of a chronic inflammatory state within the lesion.

Accumulation of esterified cholesterol stored in both membrane-bound and free lipid droplets within the cytoplasm confers unto lesion-resident macrophages the “foamy” appearance first described by Nikolai N. Anichkov in his classic studies on cholesterol-fed rabbits in 1913.[167] There is also evidence from electron microscopy studies of macrophages

from advanced atherosclerotic lesions demonstrating the presence of minimally degraded and fully intact moLDL within foam cell.[168]

1.2.5 Generation of autoimmunity

Beyond dysfunction of the innate immune system, there is growing evidence that impaired antigen presentation and autoimmunity also play a role in atherosclerosis.[122,169] Strikingly, autoimmune disorders appear to be an independent risk factor for the development of atherosclerosis and CVD.[11,170] In patients with systemic lupus erythematous (SLE) and rheumatoid arthritis, the incidence of CVD is significantly increased compared to age- and sex-matched controls from the general population.[170] Similar patterns are observed in non-autoimmune patients, where patients who develop IgG-isotype antibodies against plaque components develop more severe disease than those who remain immunologically quiescent.[171] In animal models, these athero-reactive antibodies result in immune complex deposition within the vascular intima, further exacerbating inflammation in the atheroma, thereby hastening disease and destabilizing the plaque.[172] Importantly, presentation of atheroma-derived antigens on MHC II, by cells such as macrophages, is a pre-requisite for antibody class-switch to IgG subtypes.[173–175] This indicates that mis-presentation of atheroma antigens following ingestion of plaque components such as apoptotic foam cells has an important role in atheroma development. Indeed, T-cell-deficient nude mice fed a high-fat diet developed significantly smaller atheromas than controls.[176]

The majority of T lymphocytes present within the atheroma are TH1 $CD4^+$ cells.[122,177] These cells are likely atherogenic, as inhibition of TH1 polarization in *Apoe*$^{-/-}$ mice results decreases plaque burden. TH1 cells infiltrate the atheroma and contribute to the chronic inflammatory state of the atheroma including through IFN-γ production.[122,178] Furthermore, these T cells have a restricted repertoire and appear to respond specifically to a number of atheroma-specific antigens, including ApoB-100, native LDL and moLDL—particularly oxLDL.[175,178] In advanced atheromas, antigen presentation is primarily carried out by macrophages and conventional dendritic cells that expression CD11b and CD11c, and which are pre-disposed to TH1 priming of $CD4^+$ T cells through production of IL-12 and CCL17.[179] Presentation of self-lipid antigens by the CD1 family of MHC I-like glycoproteins is another potential source of T cell activation in

atherosclerosis.[180,181] CD1 molecules surveil the endocytic pathway and are capable of presenting both foreign- and self-lipid antigens to CD1-restricted T cells, in particular CD1d-restricted iNKT cells.[182] While the role of endogenous lipid antigens in the pathogenesis of atherosclerosis is current poorly characterized, investigators have shown that administration of α-galactosylceramide (a synthetic antigen that activates iNKT cells) resulted in a 50% increase in plaque size in *Apoe*$^{-/-}$ mice.[181]

1.2.6 Impaired inflammation resolution

Resolution of an inflammatory response is a necessary step in maintenance of homeostasis and avoiding unnecessary tissue damage.[65] However, in the setting of atherosclerosis, resolution of inflammation is impaired and instead a chronic, low-grade inflammatory state persists within the plaque microenvironment.[65,121] Mediators of inflammation resolution include anti-inflammatory cytokines, other signaling molecules and transcription factors. The most prominent anti-inflammatory cytokines in atherosclerosis are TGF-β and IL-10.[91] IL-10 signaling induces expression of the suppressor of cytokine signaling 3 (SOCS3), which antagonizes the NF-κB signaling pathway and downregulates expression of a number of pro-inflammatory cytokines.[144] IL-10 also induces expression of signal transducer and activator of transcription 3 (STAT3), a transcription factor that helps polarize macrophages into an anti-inflammatory phenotype.[9] TGF-β, in contrast, appears to primarily act on T cells in the context of atherosclerosis and induces the migration and generation of regulatory T cells.[183,184] Within the atherosclerotic plaque, macrophage production of both IL-10 and TGF-β have been shown to be reduced within advanced plaques.[185] IL-10 levels in the serum are also lower in patients with coronary artery disease.[186]

In addition to anti-inflammatory cytokines, inflammation resolution is also mediated by lipid specialized pro-resolving mediators (SPMs), including lipoxin A4, resolvin D1 and protectin D1.[115] SPMs are generated through the activity of lipoxygenase (LOX) enzymes on arachidonic acid (AA), eicosapentaenoic acid (EPA) and docosahexaenoic acid (DHA), and function through several mechanisms including the suppression of lipopolysaccharide (LPS)-mediated pro-inflammatory signaling.[187,188] Variants in LOX enzymes have been associated with CVD and patients with CVD have lower levels of circulating SPMs

compared to healthy controls.[189,190] Several experiments have shown that SPMs are produced following efferocytosis and during atherosclerotic lesion regression.[144] Direct administration of a number of SPMs in mouse models of atherosclerosis have been shown to decrease the rate of plaque progression.[191] Fredman *et al.* showed that SPMs are involved in atherosclerosis progression by demonstrating the ratio of SPMs, especially resolvin D1, and pro-inflammatory leukotriene B_4 is decreased in advanced atherosclerotic plaques and in regions of plaque vulnerability in *Ldlr*$^{-/-}$ mice.[192]

1.3 Efferocytic removal of apoptotic cells by macrophages in the atherosclerotic plaque

1.3.1 Apoptosis in the atherosclerotic plaque

Apoptosis is a key feature of progression in atherosclerosis.[148] While pre-atherosclerotic and early atherosclerotic lesions contain few if any apoptotic cells, advanced atherosclerotic plaques have been shown to be relatively abundant in uncleared apoptotic cells.[142] Several factors drive cell apoptosis within the atherosclerotic lesion, including oxidative stress, hypoxia, pro-apoptotic cytokines and the cellular response to cholesterol loading.[13,118,149,193] All cells types present within the lesion experience apoptosis, and the death of these cells have differing impacts on plaque biology. Apoptotic death of endothelial cells and VSMCs, for example, is thought to destabilize the fibrous cap through removal of cells and collagen that form the structure of the cap, resulting in increased plaque vulnerability and risk of rupture.[145]

The role of macrophage apoptosis on plaque progression appears to be more nuanced and may indeed exert opposing effects depending on the stage of plaque development (see **Figure 1.6**).[140] In the early atherosclerotic lesion, macrophage apoptosis is thought to be protective against disease progression by removing cells from the plaque and reducing the generation of inflammation.[140] Studies that transplanted the bone marrow of mice lacking the pro-apoptotic factors Bcl-2-associated X (Bax) or apoptosis signal-regulating kinase 1 (Ask-1) into *Ldlr*$^{-/-}$ mice and feeding a high fat diet for 10-12 weeks resulted in an increase in total lesion area.[194] In contrast, induction of macrophage apoptosis in later stages of

disease may be detrimental. In experiments using *Chop*$^{-/-}$ *Apoe*$^{-/-}$ mice, Thorp *et al.* showed that the rate of ER stress-induced apoptosis was decreased, and that plaque apoptosis and necrotic core formation was reduced in these mice.[152] These results suggest that macrophage apoptosis occurring later during plaque progression leads to additional necrotic cell burden, potentially due to a lack of functioning efferocytic machinery in later stages of plaque development.[152]

Figure 1.6 Macrophage apoptosis and efferocytosis in early and advanced atherosclerosis. (on opposite page)

Macrophage apoptosis and efferocytosis have different impacts on plaque biology in early versus advanced atherosclerosis. (**a**) Within early atherosclerotic lesions, induction of macrophage apoptosis has a protective role. Apoptotic macrophages are quickly cleared by neighbouring healthy macrophages, limiting the capacity of that macrophage to contribute to the generation of inflammation and inducing an anti-inflammatory phenotype in the efferocyte characterized by release of the anti-inflammatory cytokines TGF-β and IL-10. (**b**) In advanced atherosclerotic lesions, in contrast, apoptotic macrophages are not cleared by neighbouring efferocytes and instead undergo secondary necrosis. This in turn drives disease progression through contributing to the formation and growth of a necrotic core within the lesion and the release of pro-inflammatory factors into the plaque microenvironment. Figure adapted from Tabas (2009).[144]

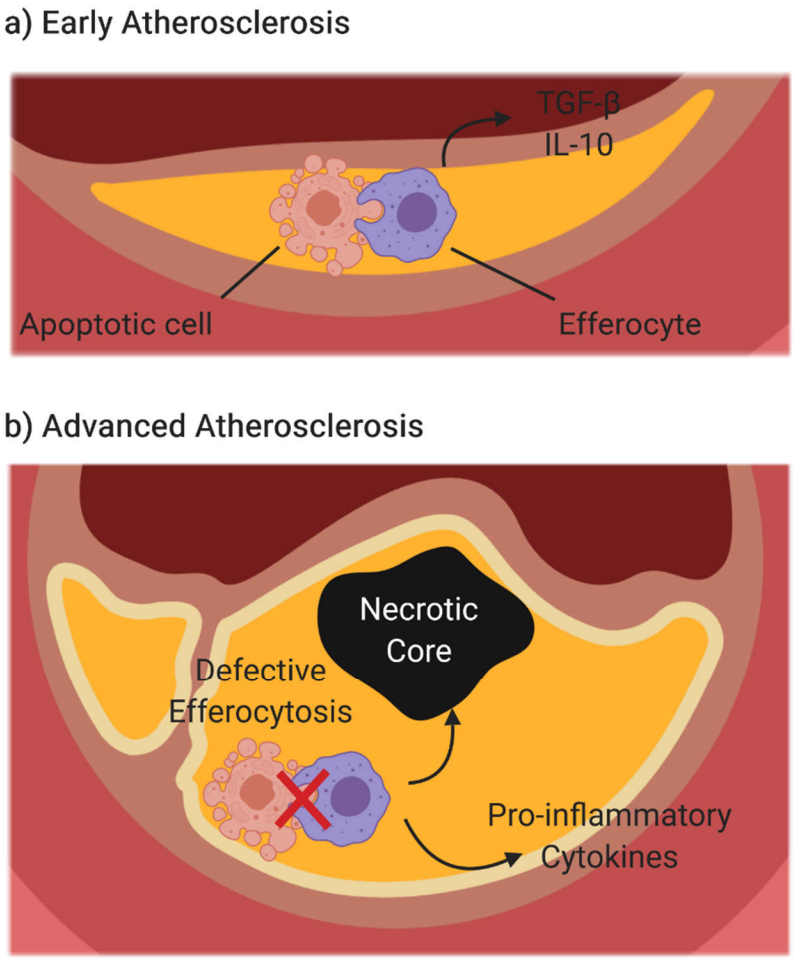

1.3.2 Evidence of defective efferocytosis in atherosclerotic disease

Defective efferocytosis is a hallmark of advanced atherosclerotic lesions and the presence of impaired efferocytosis is associated with increased plaque vulnerability.[195] The lack of efferocytic apoptotic cell clearance probably contributes more than any other single mechanism to necrotic core formation.[144] Schrijvers *et al.* demonstrated the presence of uncleared terminal deoxynucleotidyl transferase-mediated dUTP nick end-labeling $(TUNEL)^{+}$ necrotic cells within advanced atherosclerotic lesions in human carotid endarterectomy specimens while in the tonsils—a tissue with comparably high rates of apoptosis—very few uncleared apoptotic cells could be detected.[142] This finding implies that defective efferocytosis drives the accumulation of necrotic cells in atherosclerosis and that this is a *bona fide* feature of advanced atherosclerosis in humans.[142]

Complementing observations in human plaque, numerous studies in mouse models of atherosclerosis have demonstrated that deletion of macrophage efferocytic effectors increase lesion necrotic core size and total lesional area.[196,197] Boisvert *et al.* found that *Ldlr*$^{-/-}$ mice transplanted with bone marrow deficient in transglutaminase 2 (TG2), a co-receptor of integrin $\alpha_V\beta3$, had increased atherosclerotic lesion area and necrotic core size.[196] Further evidence for the importance of integrin $\alpha_V\beta3$ in efferocytosis within the atherosclerotic lesion came from studies using *Mfge8*$^{-/-}$ *Ldlr*$^{-/-}$ mice. MFG-E8 is the opsonin used by integrin $\alpha_V\beta3$ to bind PS, and *Mfge8*$^{-/-}$ *Ldlr*$^{-/-}$ mice develop lesions with larger necrotic cores and also have higher levels of circulating pro-inflammatory cytokines, in particular IFN-γ.[197] Further studies have also found that C1q, the opsonin used by LRP1 to bind calreticulin on the apoptotic cell surface, also plays a role in efferocytosis within the plaque.[56,198] Deletion of C1q in *Ldlr*$^{-/-}$ led to the development of larger and more complex lesions.[198] Finally, Thorp *et al.* demonstrated that mice expressing a tyrosine kinase defective MerTK mutant had increased numbers of free apoptotic cells and larger necrotic cores after 16 weeks of being on a high-fat diet.[199] However, deletion of another member of the TAM family of receptors, Axl, did not appear to impact efferocytosis within the atherosclerotic plaque or plaque progression.[200] A summary of these mechanisms that mediate macrophage efferocytosis within the atherosclerotic plaque is provided in **Figure 1.7**.

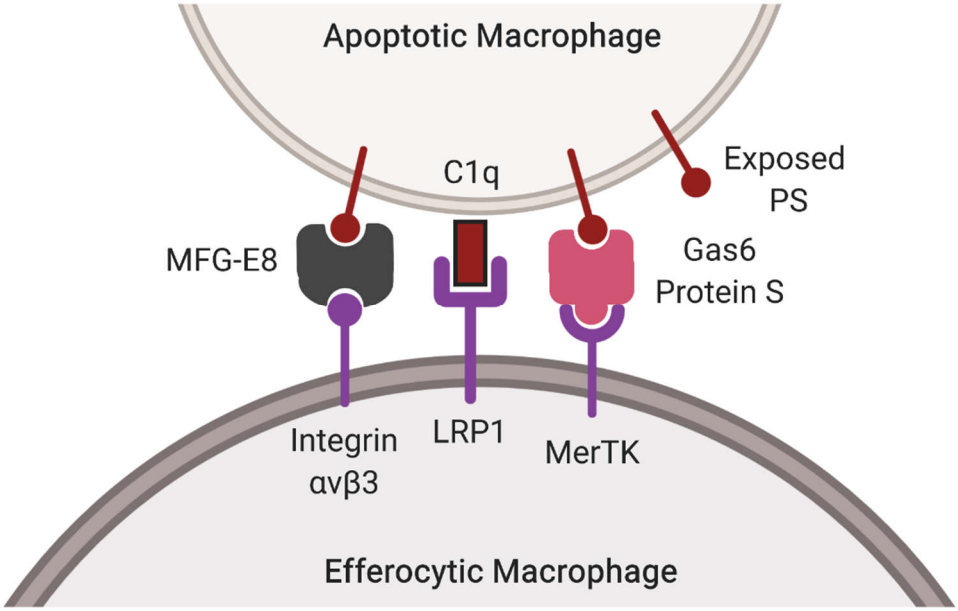

Figure 1.7 Known efferocytic receptors and pathways utilized by macrophages in atherosclerosis.

A number of efferocytic receptors and opsonins have been identified by *in vivo* studies in mouse models of atherosclerosis to be involved in macrophage efferocytosis of apoptotic cells within the atherosclerotic lesion. These include: integrin αvβ3 and its opsonin MFG-E8 and co-receptor TG2, LRP1 and its opsonin C1q, and MerTK and its opsonins Gas6 and protein S. Successful clearance of apoptotic cells induces the production of anti-inflammatory cytokines by the efferocytosing macrophage, including TGF-β and IL-10. Figure adapted from Thorp & Tabas.[201]

1.3.3 Consequences of defective efferocytosis

Beyond insufficient apoptotic cell clearance and the development of secondary necrosis leading to necrotic core formation and release of pro-inflammatory factors, defective efferocytosis also has consequences related to a lack of inflammation resolution.[65] As discussed previously in **Chapter 1.2.6**, efferocytosis induces an anti-inflammatory phenotype in macrophages that functions to partially counteract the chronic inflammatory microenvironment of the plaque.[116] Impaired efferocytosis removes macrophage-derived

anti-inflammatory cytokines from the plaque and instead promotes further inflammatory activation within the lesion.

Defective efferocytosis also leads to a reduction in the production of SPMs that normally help limit inflammation (discussed previously in **Chapter 1.2.6**) and increases the production of pro-inflammatory leukotrienes, which are synthesized from AA, the same substrate as a number of SPMs.[192] Cai *et al.* found that engagement of MerTK receptor led to translocation of 5-LOX into the nucleus, where it drives production of the SPM lipoxin A_4.[202] The authors found that impaired MerTK signaling in the context of atherosclerosis reduced the level of lipoxin A_4 production and instead increased production of the pro-inflammatory leukotriene B_4.[202]

1.3.4 Known mechanisms leading to defective efferocytosis

The molecular mechanisms that lead to defective macrophage efferocytosis in atherosclerosis remain poorly understood. One potential mechanism identified by Cai *et al.* involves cleavage of MerTK within the atherosclerotic plaque through the activity of the metalloproteinase ADAM17.[202] The authors found that in *Ldlr*$^{-/-}$ mice expressing a cleavage-resistant MerTK variant, atherosclerotic plaques possessed smaller necrotic cores and thicker fibrous caps. In human carotid atherosclerosis, cleavage of MerTK from the cell surface of macrophages and the presence of the resultant soluble form of MerTK correlated with increased plaque necrosis and ischemic symptoms in these patients.[203] Separately, the same group found that MerTK cleavage also limited SPM production by macrophages and led to higher levels of circulating pro-inflammatory cytokines in mice.[204]

Disruption of anti-phagocytic "don't eat me" signals has also been shown to have an impact on atherosclerotic disease.[10,205] Kojima *et al.* showed that blocking the anti-phagocytic molecule CD47 using antibodies in *Apoe*$^{-/-}$ mice led to restoration of efferocytosis within advanced atherosclerotic plaques and a resultant decrease in lesion necrotic core size.[205] Within the plaque, elevated levels of TNF-α appears to induce CD47 expression on VSMCs via activation of NF-κB signaling. In patient carotid endarterectomy specimens, CD47 was found to be elevated compared to non-atherosclerotic surrounding vascular tissue. This up-

regulation of CD47 could be reproduced in a mouse model of atherosclerosis through feeding of a high fat diet in *Apoe*$^{-/-}$ mice.[205]

Finally, macrophage cholesterol loading may impair efferocytosis through disruption of proper efferosome maturation.[206] Free cholesterol accumulation in macrophages leads to the induction of several adaptive processes that could alter the regulation of intracellular trafficking and efferosome maturation. Huynh *et al.* showed that inhibition of cholesterol exit from lysosomes using the small molecule inhibitor U18666A resulted in impaired phagolysosome formation.[206] The authors found that this defect was due to inactivity of Rab7 recruited to the late phagosome, leading to a failure to recruit the effector molecules RILP and ORLP1 which are required to drive migration of phagosomes towards the perinuclear region to permit efficient fusion with lysosomes.[87,206] Another example of such an adaptive process is the increased biosynthesis of phospholipids, in particular phosphatidylcholine and phospholipid species with polyunsaturated acyl chains.[207] Since the recruitment of many regulators of the maturation process depends on interactions with phospholipid species present in the efferosomal membrane, alterations to phospholipid synthesis may result in maturation defects–although this remains to be experimentally demonstrated.[207]

1.4 Current limitations in our understanding of atherosclerosis

1.4.1 Animal models of atherosclerosis and their limitations

Due to the complexity of atherosclerosis and the slow rate of disease progression in humans, a range of small and large animal models have been developed to study the biology of this disease.[208,209] Each model system carries distinct advantages and drawbacks and are typically used to study specific components of atherosclerotic disease (e.g. genetics, lipoprotein profiles, hemodynamics, etc.).[208]

The most frequently used animal models of atherosclerosis are by far the murine models of atherosclerosis.[210] Although the lipoprotein profile and lesion distribution in mice differ

from those in humans, many of the critical features of disease are preserved.[208,210] The ease of genetic manipulation in mice and the relatively fast rate at which atherosclerosis develop in atherosclerosis-prone mice make them an attractive model organism for studying the impact of specific genes and proteins on disease pathogenesis. Mice are HDL monotypic animals, meaning that HDL is the dominant lipoprotein in their circulation. This makes mice naturally resistant to atherosclerosis.[211] Mouse models of atherosclerosis therefore rely on generating a non-HDL based hypercholesterolemia. A number of murine model systems now exist for studying atherosclerosis, but the most well-known and best-studied models are the apoE-knockout and the LDLR-knockout animals.[210] Deletion of apoE or LDLR inhibit cholesterol reverse transport and the animals develop hypercholesterolemia on a high fat diet as a result.[208]

Despite the widespread use of *Ldlr*$^{-/-}$ and *Apoe*$^{-/-}$ mice in experimental investigations into the biology of atherosclerosis, there are still critical differences between human and mouse atherosclerosis that call into the question the extent to which the mouse is an accurate model of atherosclerotic disease.[212,213] First, most mouse models of atherosclerosis never develop the vulnerable, rupture-prone plaque that drives atherosclerotic CVD in humans.[210] The distribution of lesions in the vasculature also differs significantly between mouse and human.[117] Importantly, mice rarely develop significant atherosclerosis within their coronary circulation, instead preferentially developing atherosclerosis within the aortic root.[117] This stands in contrast to humans, where the aortic root and ascending aorta are usually relatively spared from severe disease.[214] Finally, mice do not possess the cholesteryl ester transfer protein (CETP), a serum transporter of cholesteryl esters and triglycerides that has been implicated in atherosclerosis in humans.[215]

The small size of the mouse imposes an additional limitation on the extent to which important disease parameters such as hemodynamics may be measured in these animals. As such, a number of large animal models of atherosclerosis have been used.[208] A full discussion of large animal models of atherosclerosis is beyond the scope of this thesis but is reviewed in detail by Getz & Reardon.[208] We will briefly summarize the most important large animal models of atherosclerosis here. Amongst these are pigs, which spontaneously develop atherosclerosis on a high fat diet.[216] A number of seminal studies on the impact of

vascular hemodynamics on atherosclerosis development and on endothelial activation in response to atherogenic stimuli have been performed in pigs.[217] Pigs also do develop complex lesions in their coronary circulation and these plaques do experience vulnerability and rupture.[218] Rabbits have also been used in the study of atherosclerosis. These animals are extraordinarily sensitive to cholesterol feeding and have been used in a number of studies on how the body's circulating lipid profile changes with a high cholesterol diet.[219] Finally, non-human primates can also be used to study atherosclerosis. Although they are expensive and difficult to maintain, non-human primates have the most similar lipoprotein profile to humans of any model organism.[220] Some of the first studies on plaque regression upon return to a low-fat diet was conducted in Rhesus monkeys.[221]

1.4.2 Challenges of studying atherosclerosis in humans

The majority of what is currently known about the biology of atherosclerosis and particularly its pathogenesis and progression is derived from studies in animal models of disease.[128] In particular, studies in mice have generated much insight into the role of macrophages and other cell types in the atherosclerotic plaque.[209] However, the degree to which these findings may be translated into the human context remains a topic of controversy.[128,222] Indeed, a number of promising therapeutic targets identified through research on mouse models of atherosclerosis have not been borne out in humans.[128] In a systematic review of disease-causing genes identified in mouse models of atherosclerosis and the association of the human orthologs of these genes with CVD, Pasterkamp *et al.* found few associations between genes found to be important in mice and human disease.[213] In contrast, von Scheidt *et al.* used the same approach but concluded that there was a significant overlap between genes found to be important for the pathogenesis of atherosclerosis in mice and genes that have been implicated in atherosclerosis and CVD in humans.[210] To illustrate the stark differences that can be present between atherosclerosis in the mouse and in humans, a recent study by Gomez *et al.* found that IL-1β had a protective effect in advanced atherosclerotic plaques in *Apoe*$^{-/-}$ mice, which stands in contrast with the results of the CANTOS trial.[223]

However, despite the sometimes questionable validity of animal models of atherosclerosis, it is technically difficult to study this disease in humans for a variety of reasons. First,

atherosclerosis develops over the course of decades in humans, making it very difficult to study disease progression.[127] Second, obtaining plaque specimens for study in humans is difficult due to the anatomical location of these plaques.[224] The most commonly used source of plaque material in human studies is plaque obtained from carotid endarterectomies.[225–227] However, it has been established there are significant differences in macrophage gene expression between plaques isolated from different anatomical sites.[228] Therefore, it is difficult to determine how representative the carotid plaque is of disease situated in other vessels. Finally, the ubiquitous nature of atherosclerosis in industrialized nations makes it difficult to identify individuals who are truly free of atherosclerosis that may be utilized as a control.[229] Due to these factors, it is likely that the field will continue to rely on mouse models of atherosclerosis as the major means of studying atherosclerosis biology.

1.5 Rationale, objective and aims

1.5.1 Rationale

Defective macrophage efferocytosis is widely acknowledged as a major driver of disease progression and plaque vulnerability in atherosclerosis. Despite this, relatively little is known about the molecular mechanisms that drive defective efferocytosis in the setting of atherosclerotic disease. The few mechanisms that have been identified to date have been described either *in vitro* or almost exclusively in mouse models of atherosclerosis. Therefore, we do not have a clear understanding of how efferocytosis becomes defective in human atherosclerotic disease.

1.5.2 Objective

The overall objective of this thesis is to explore gene expression in human atherosclerotic lesion-resident macrophages in order to identify potential genes and pathways that contribute to defective efferocytosis in human atherosclerosis.

1.5.3 Aims

Our first aim, described in **Chapter 3**, was to gain a more complete understanding of how efferosome maturation is regulated in macrophages under homeostatic conditions. We employed ectopic expression of fluorescently labelled proteins in combination with bead-based efferocytosis assays and live- and fixed-cell fluorescence microscopy to identify novel proteins that differentially regulate phagosome and efferosome maturation.

Our second aim, described in **Chapter 4**, was to study the gene expression profile of human atherosclerotic macrophages to determine globally which pathways and cellular functions were dysregulated and specifically which pathways related to efferocytosis and apoptotic cell clearance were affected. This was accomplished using a microarray to analyze gene expression in macrophages isolated from aortic punch samples compared to macrophages derived *ex vivo* from peripheral blood monocytes from healthy donors.

The final aim, described in **Chapter 5**, was to validate the role of a transcription factor identified in the previous aim as being potentially involved in driving efferocytic defects. This was done through generating stably-transduced macrophage cell lines that overexpressed or knocked down our protein of interest and using these cell lines in functional assays that test macrophage efferocytosis and efferosome maturation proceeds correctly. We also examined the upstream signaling pathways employed to drive upregulation of our protein-of-interest.

1.6 Importance

Atherosclerosis is the major pathological feature that contributes to CVD. In Canada, the impact of atherosclerotic CVD is so large that approximately 1 in 3 Canadians will be affected by atherosclerosis or one of its complications.[110] Despite the importance of atherosclerosis, there are still gaps in our understanding of the biology of atherosclerosis in humans and a lack of therapeutic agents that completely eliminate the risk of CVD. As such, identification of specific defects in the efferocytosis of apoptotic cells that forms the overarching goal of this thesis has the potential to uncover novel therapeutic targets and approaches for atherosclerosis.

1.7 References

1. Henson PM. Cell Removal : Efferocytosis. *Annu Rev Cell Dev Biol*. 2017;33:1-18.

2. Nagata S. Apoptosis and Clearance of Apoptotic Cells. *Annu Rev Immunol*. 2018;361829(1):1-18. doi:10.1146/annurev-immunol

3. Gordon S, Plüddemann A. Macrophage Clearance of Apoptotic Cells: A Critical Assessment. *Front Immunol*. 2018;9(January):127. doi:10.3389/fimmu.2018.00127

4. Grootaert MOJ, Schrijvers DM, Hermans M, Hoof VO Van, Meyer GRY De, Martinet W. Caspase-3 Deletion Promotes Necrosis in Atherosclerotic Plaques of ApoE Knockout Mice. *Oxid Med Cell Longev*. 2016. doi:10.1155/2016/3087469

5. Green DR, Oguin TH, Martinez J. The clearance of dying cells: table for two. *Cell Death Differ*. 2016;23(6):915-926. doi:10.1038/cdd.2015.172

6. Sachet M, Liang YY, Oehler R. The immune response to secondary necrotic cells. *Apoptosis*. 2017. doi:10.1007/s10495-017-1413-z

7. Stanford JC, Young C, Hicks D, et al. Efferocytosis produces a prometastatic landscape during postpartum mammary gland involution. *J Clin Invest*. 2014;124(11):4737-4752. doi:10.1172/JCI76375DS1

8. Aurora AB, Porrello ER, Tan W, et al. Macrophages are required for neonatal heart regeneration. *J Clin Invest*. 2014;124(3). doi:10.1172/JCI72181DS1

9. Michalski MN, Koh AJ, Weidner S, Roca H, McCauley LK. Modulation of Osteoblastic Cell Efferocytosis by Bone Marrow Macrophages. *J Cell Biochem*. 2016;117(12):2697-2706. doi:10.1002/jcb.25567

10. Kojima Y, Weissman IL, Leeper NJ. The Role of Efferocytosis in Atherosclerosis. *Circulation*. 2017;135(5):476-489. doi:10.1161/CIRCULATIONAHA.116.025684

11. Muñoz LE, Lauber K, Schiller M, Manfredi A a, Herrmann M. The role of

defective clearance of apoptotic cells in systemic autoimmunity. *Nat Rev Rheumatol*. 2010;6(5):280-289. doi:10.1038/nrrheum.2010.46

12. Abdolmaleki F, Farahani N, Hayat SMG, et al. The role of efferocytosis in autoimmune diseases. *Front Immunol*. 2018;9(JUL):1-13. doi:10.3389/fimmu.2018.01645

13. Gregory CD, Pound JD. Cell death in the neighbourhood: Direct microenvironmental effects of apoptosis in normal and neoplastic tissues. *J Pathol*. 2011;223(2):177-194. doi:10.1002/path.2792

14. Cummings RJ, Barbet G, Bongers G, et al. Different tissue phagocytes sample apoptotic cells to direct distinct homeostasis programs. *Nature*. 2016;539(7630):565-569. doi:10.1038/nature20138

15. Oka K, Sawamura T, Kikuta K, et al. Lectin-like oxidized low-density lipoprotein receptor 1 mediates phagocytosis of aged/apoptotic cells in endothelial cells. *Proc Natl Acad Sci*. 2002;95(16):9535-9540. doi:10.1073/pnas.95.16.9535

16. Sandahl M, Hunter DM, Strunk KE, Earp HS, Cook RS. Epithelial cell-directed efferocytosis in the post-partum mammary gland is necessary for tissue homeostasis and future lactation. *BMC Dev Biol*. 2010;10. doi:10.1186/1471-213X-10-122

17. Hermetet F, Jacquin E, Launay S, et al. Efferocytosis of apoptotic human papillomavirus-positive cervical cancer cells by human primary fibroblasts. *Biol Cell*. 2016;108(7):189-204. doi:10.1111/boc.201500090

18. Morioka S, Maueröder C, Ravichandran KS. Living on the Edge: Efferocytosis at the Interface of Homeostasis and Pathology. *Immunity*. 2019:1149-1162. doi:10.1016/j.immuni.2019.04.018

19. Shelby SJ, Feathers KL, Ganios AM, Jia L, Miller JM, Thompson D a. MERTK signaling in the retinal pigment epithelium regulates the tyrosine phosphorylation of GDP dissociation inhibitor alpha from the GDI/CHM family of RAB GTPase

effectors. *Exp Eye Res*. 2015;140:28-40. doi:10.1016/j.exer.2015.08.006

20. Elliott MR, Zheng S, Park D, et al. Unexpected requirement for ELMO1 in clearance of apoptotic germ cells in vivo. *Nature*. 2010;467(7313):333-337. doi:10.1038/nature09356

21. Finnemann SC, Bonilha VL, Marmorstein AD, Rodriguez-Boulan E. Phagocytosis of rod outer segments by retinal pigment epithelial cells requires alpha(v)beta5 integrin for binding but not for internalization. *Proc Natl Acad Sci U S A*. 1997;94(24):12932-12937.

22. Evans AL, Blackburn JWD, Taruc K, et al. Antagonistic Coevolution of MER Tyrosine Kinase Expression and Function. *Mol Biol Evol*. 2017. doi:10.1093/molbev/msx102

23. Elliott MR, Ravichandran KS. The dynamics of apoptotic cell clearance. *Dev Cell*. 2016;38(2):147-160. doi:10.1016/j.devcel.2016.06.029

24. Medina CB, Ravichandran KS. Do not let death do us part: “Find-me” signals in communication between dying cells and the phagocytes. *Cell Death Differ*. 2016;23(6):979-989. doi:10.1038/cdd.2016.13

25. Ariel A, Ravichandran KS. ‘This way please’: Apoptotic cells regulate phagocyte migration before and after engulfment. *Eur J Immunol*. 2016:1-4. doi:10.1002/eji.201646505

26. Elliott MR, Chekeni FB, Trampont PC, et al. Nucleotides released by apoptotic cells act as a find-me signal to promote phagocytic clearance. *Nature*. 2009;461(7261):282-286. doi:10.1038/nature08296

27. Chekeni FB, Elliott MR, Sandilos JK, et al. Pannexin 1 channels mediate “find-me” signal release and membrane permeability during apoptosis. *Nature*. 2010;467(7317):863-867. doi:10.1038/nature09413

28. Truman LA, Wilkinson SJ, Combadiere C, et al. CX3CL1/fractalkine is released

from apoptotic lymphocytes to stimulate macrophage chemotaxis. *Blood*. 2008;112(13):5026-5036. doi:10.1182/blood-2008-06-162404

29. Ludwig A, Hundhausen C, Lambert M, et al. Metalloproteinase Inhibitors for the Disintegrin-Like Metalloproteinases ADAM10 and ADAM17 that Differentially Block Constitutive and Phorbol Ester-Inducible Shedding of Cell Surface Molecules. *Comb Chem High Throughput Screen*. 2005;8(2):161-171. doi:10.2174/1386207053258488

30. Pulanco MC, Cosman J, Ho M, et al. Complement Protein C1q Enhances Macrophage Foam Cell Survival and Efferocytosis. *J Immunol*. 2016;198. doi:10.4049/jimmunol.1601445

31. White GE, McNeill E, Channon KM, Greaves DR. Fractalkine promotes human monocyte survival via a reduction in oxidative stress. *Arterioscler Thromb Vasc Biol*. 2014;34(12):2554-2562. doi:10.1161/ATVBAHA.114.304717

32. Landsman L, Liat BO, Zernecke A, et al. CX3CR1 is required for monocyte homeostasis and atherogenesis by promoting cell survival. *Blood*. 2009;113(4):963-972. doi:10.1182/blood-2008-07-170787

33. Hoffman RD, Kligerman M, Sundt TM, Anderson ND, Shin HS. Stereospecific chemoattraction of lymphoblastic cells by gradients of lysophosphatidylcholine. *Proc Natl Acad Sci*. 1982;79(10):3285-3289. doi:10.1073/pnas.79.10.3285

34. McKean ML, Smith JB, Silver MJ. Formation of lysophosphatidylcholine by human platelets in response to thrombin. *J Biol Chem*. 1981;256(4):1522-1524.

35. Peter C, Waibel M, Radu CG, et al. Migration to apoptotic “find-me” signals is mediated via the phagocyte receptor G2A. *J Biol Chem*. 2008;283(9):5296-5305. doi:10.1074/jbc.M706586200

36. Tran HB, Barnawi J, Ween M, et al. Cigarette smoke inhibits efferocytosis via deregulation of sphingosine kinase signaling : reversal with exogenous S1P and the S1P analogue FTY720. 2016;100(July):1-8. doi:10.1189/jlb.3A1015-471R

37. Penberthy KK, Ravichandran KS. Apoptotic cell recognition receptors and scavenger receptors. *Immunol Rev*. 2016;269:44-59.

38. Kimani SG, Geng K, Kasikara C, et al. Contribution of defective PS recognition and efferocytosis to chronic inflammation and autoimmunity. *Front Immunol*. 2014;5(NOV):1-9. doi:10.3389/fimmu.2014.00566

39. Segawa K, Kurata S, Yanagihashi Y, Brummelkamp TR, Matsuda F, Nagata S. Caspase-mediated cleavage of phospholipid flippase for apoptotic phosphatidylserine exposure. *Science (80-)*. 2014;344(6188):1164-1168.

40. Suzuki J, Imanishi E, Nagata S. Xkr8 phospholipid scrambling complex in apoptotic phosphatidylserine exposure. *Proc Natl Acad Sci*. 2016;113(34):9509-9514. doi:10.1073/pnas.1610403113

41. Borisenko GG, Matsura T, Liu SX, et al. Macrophage recognition of externalized phosphatidylserine and phagocytosis of apoptotic Jurkat cells - Existence of a threshold. *Arch Biochem Biophys*. 2003;413(1):41-52. doi:10.1016/S0003-9861(03)00083-3

42. Oldenborg PA, Harada T, Christian DA, Pantano DA, Tsai RK, Discher DE. Role of CD47 as a Marker of Self on Red Blood Cells. *Science (80-)*. 2013;288(5473):2051-2054. doi:10.1126/science.288.5473.2051

43. Barkal AA, Weiskopf K, Kao KS, et al. Engagement of MHC class i by the inhibitory receptor LILRB1 suppresses macrophages and is a target of cancer immunotherapy article. *Nat Immunol*. 2018;19(1):76-84. doi:10.1038/s41590-017-0004-z

44. Soto-Pantoja DR, Kaur S, Roberts DD. CD47 signaling pathways controlling cellular differentiation and responses to stress. *Crit Rev Biochem Mol Biol*. 2015;50(3):212-230. doi:10.3109/10409238.2015.1014024

45. Murata Y, Kotani T, Ohnishi H, Matozaki T. The CD47-SIRPα signalling system: Its physiological roles and therapeutic application. *J Biochem*. 2014;155(6):335-

344. doi:10.1093/jb/mvu017

46. Freeman SA, Grinstein S. Phagocytosis: receptors, signal integration, and the cytoskeleton. *Immunol Rev*. 2014;262(1):193-215. doi:10.1111/imr.12212

47. Miyanishi M, Tada K, Koike M, Uchiyama Y, Kitamura T, Nagata S. Identification of Tim4 as a phosphatidylserine receptor. *Nature*. 2007;450(7168):435-439. doi:10.1038/nature06307

48. Park D, Tosello-Trampont AC, Elliott MR, et al. BAI1 is an engulfment receptor for apoptotic cells upstream of the ELMO/Dock180/Rac module. *Nature*. 2007;450(7168):430-434. doi:10.1038/nature06329

49. Park SY, Jung MY, Kim HJ, et al. Rapid cell corpse clearance by stabilin-2, a membrane phosphatidylserine receptor. *Cell Death Differ*. 2008;15(1):192-201. doi:10.1038/sj.cdd.4402242

50. Nakahashi-Oda C, Tahara-Hanaoka S, Honda S ichiro, Shibuya K, Shibuya A. Identification of phosphatidylserine as a ligand for the CD300a immunoreceptor. *Biochem Biophys Res Commun*. 2012;417(1):646-650. doi:10.1016/j.bbrc.2011.12.025

51. He M, Kubo H, Morimoto K, et al. Receptor for advanced glycation end products binds to phosphatidylserine and assists in the clearance of apoptotic cells. *EMBO Rep*. 2011;12(4):358-364. doi:10.1038/embor.2011.28

52. Savill J, Dransfieldt I, Hoggt N, Haslett C. Vitronectin receptor-mediated phagocytosis of cells undergoing apoptosis. *Nature*. 1990;343(January):170-173.

53. Meer JHM Van Der, Poll T Van Der, Veer C Van. TAM receptors, Gas6, and protein S: roles in inflammation and hemostasis. *Blood*. 2014;123(16):2460-2470. doi:10.1182/blood-2013-09-528752.insights

54. Blackburn JWD, Lau DHC, Liu EY, et al. Soluble CD93 is an apoptotic cell opsonin recognized by $\alpha_x \beta_2$. *Eur J Immunol*. 2019:1-23.

doi:10.1002/eji.201847801

55. Gregory CD, Devitt A, Moffatt O. Roles of ICAM-3 and CD 14 in the recognition and phagocytosis of apoptotic cells by macrophages. *Biochem Soc Trans*. 2015;26(4):644-649. doi:10.1042/bst0260644

56. Ogden CA, deCathelineau A, Hoffmann PR, et al. C1q and mannose binding lectin engagement of cell surface calreticulin and CD91 initiates macropinocytosis and uptake of apoptotic cells. *J Exp Med*. 2001;194(6):781-795.

57. Greenberg ME, Sun M, Zhang R, Febbraio M, Silverstein R, Hazen SL. Oxidized phosphatidylserine–CD36 interactions play an essential role in macrophage-dependent phagocytosis of apoptotic cells. *J Exp Med*. 2006;203(12):2613-2625. doi:10.1084/jem.20060370

58. Elliott MR, Koster KM, Murphy PS. Efferocytosis Signaling in the Regulation of Macrophage Inflammatory Responses. *J Immunol*. 2017;198(4):1387-1394. doi:10.4049/jimmunol.1601520

59. Hanayama R, Tanaka M, Miwa K, Shinohara A, Iwamatsu A, Nagata S. Identification of a factor that links apoptotic cells to phagocytes. *Nature*. 2002;417(6885):182-187. doi:10.1038/417182a

60. Project S, Cal- GDV, Marshall WA, et al. Autoimmune Disease and Impaired Uptake of Apoptotic Cells in MFG-E8 – Deficient Mice. *Science (80-)*. 2004;304(May):1147-1151. doi:10.1126/science.1094359

61. Caberoy NB, Zhou Y, Li W. Tubby and tubby-like protein 1 are new MerTK ligands for phagocytosis. *EMBO J*. 2010;29(23):3898-3910. doi:10.1038/emboj.2010.265

62. Heckenlively JR, Chang B, Erway LC, et al. Mouse model for Usher syndrome: linkage mapping suggests homology to Usher type I reported at human chromosome 11p15. *Proc Natl Acad Sci*. 1995;92(24):11100-11104. doi:10.1073/pnas.92.24.11100

63. Ikeda S, Shiva N, Ikeda A, et al. Retinal degeneration but not obesity is observed in null mutants of the tubby-like protein 1 gene. *Hum Mol Genet*. 2000;9(2):155-163. doi:10.1093/hmg/9.2.155

64. Kinchen JM, Ravichandran KS. Phagosome maturation: going through the acid test. *Nat Rev Mol Cell Biol*. 2008;9(10):781-795. doi:10.1038/nrm2515

65. Yurdagul A, Doran AC, Cai B, Fredman G, Tabas IA. Mechanisms and Consequences of Defective Efferocytosis in Atherosclerosis. 2017;4(January):1-10. doi:10.3389/fcvm.2017.00086

66. Freeman SA, Grinstein S. Phagocytosis: Receptors, signal integration, and the cytoskeleton. *Immunol Rev*. 2014;262(1):193-215. doi:10.1111/imr.12212

67. Heit B, Kim H, Cosío G, et al. Multimolecular signaling complexes enable syk-mediated signaling of CD36 internalization. *Dev Cell*. 2013;24(4):372-383. doi:10.1016/j.devcel.2013.01.007

68. Wu Y, Singh S, Georgescu M-M, Birge RB. A role for Mer tyrosine kinase in αvβ5 integrin-mediated phagocytosis of apoptotic cells. *J Cell Sci*. 2005;118(3):539-553. doi:10.1242/jcs.01632

69. Flannagan RS, Canton J, Furuya W, Glogauer M, Grinstein S. The phosphatidylserine receptor TIM4 utilizes integrins as coreceptors to effect phagocytosis. *Mol Biol Cell*. 2014;25(9):1511-1522. doi:10.1091/mbc.e13-04-0212

70. Flannagan RS, Jaumouillé V, Grinstein S. The Cell Biology of Phagocytosis. *Annu Rev Pathol Mech Dis*. 2011;7(1):61-98. doi:10.1146/annurev-pathol-011811-132445

71. Reddien PW, Horvitz HR. CED-2/CrkII and CED-10/Rac control phagocytosis and cell migration in Caenorhabditis elegans. *Nat Cell Biol*. 2000;2(March):131-136.

72. Hedgecock EM, Sulston JE, Thomson JN. Mutations Affecting Programmed Cell Deaths in the Nematode Caenorhabditis elegans. *Science (80-)*. 1983;220(4603):1277-1279.

73. Van Buul JD, Geerts D, Huveneers S. Rho GAPs and GEFs: Controling switches in endothelial cell adhesion. *Cell Adhes Migr*. 2014;8(2):108-124. doi:10.4161/cam.27599

74. Nakaya M, Tanaka M, Okabe Y, Hanayama R, Nagata S. Opposite effects of Rho family GTPases on engulfment of apoptotic cells by macrophages. *J Biol Chem*. 2006;281(13):8836-8842. doi:10.1074/jbc.M510972200

75. Tosello-Trampont AC, Nakada-Tsukui K, Ravichandran KS. Engulfment of Apoptotic Cells Is Negatively Regulated by Rho-mediated Signaling. *J Biol Chem*. 2003;278(50):49911-49919. doi:10.1074/jbc.M306079200

76. Olazabal IM, Caron E, May RC, Schilling K, Knecht DA, Machesky LM. Rho-kinase and myosin-II control phagocytic cup formation during CR, but not FcγR, phagocytosis. *Curr Biol*. 2002;12(16):1413-1418. doi:10.1016/S0960-9822(02)01069-2

77. Kim SY, Kim S, Bae DJ, et al. Coordinated balance of Rac1 and RhoA plays key roles in determining phagocytic appetite. *PLoS One*. 2017;12(4):1-19. doi:10.1371/journal.pone.0174603

78. Kitano M, Nakaya M, Nakamura T, Nagata S, Matsuda M. Imaging of Rab5 activity identifies essential regulators for phagosome maturation. *Nature*. 2008;453(7192):241-245. doi:10.1038/nature06857

79. Levin R, Grinstein S, Canton J. The life cycle of phagosomes: formation, maturation, and resolution. *Immunol Rev*. 2016;273(1):156-179. doi:10.1111/imr.12439

80. Mills IG, Jones AT, Clague MJ. Involvement of the endosomal autoantigen EEA1 in homotypic fusion of early endosomes. *Curr Biol*. 1998;8(15):881-884.

doi:10.1016/S0960-9822(07)00351-X

81. Kinchen JM, Doukoumetzidis K, Almendinger J, et al. A pathway for phagosome maturation during engulfment of apoptotic cells. *Nat Cell Biol*. 2008;10(5):556-566. doi:10.1038/ncb1718

82. Kinchen JM, Ravichandran KS. Identification of two evolutionarily conserved genes regulating processing of engulfed apoptotic cells. *Nature*. 2010;464(7289):778-782. doi:10.1038/nature08853

83. Poteryaev D, Datta S, Ackema K, Zerial M, Spang A. Identification of the switch in early-to-late endosome transition. *Cell*. 2010;141(3):497-508. doi:10.1016/j.cell.2010.03.011

84. Dhar K, Moulton AM, Rome E, et al. Targeted myocardial gene expression in failing hearts by RNA sequencing. *J Transl Med*. 2016;14(1):327. doi:10.1186/s12967-016-1083-6

85. Harrison RE, Bucci C, Vieira O V, Schroer TA, Grinstein S. Phagosomes fuse with late endosomes and/or lysosomes by extension of membrane protrusions along microtubules: role of Rab7 and RILP. *Mol Cell Biol*. 2003;23(18):6494-6506. doi:10.1128/MCB.23.18.6494

86. Johansson M, Rocha N, Zwart W, et al. Activation of endosomal dynein motors by stepwise assembly of Rab7-RILP-p150Glued, ORP1L, and the receptor ??III spectrin. *J Cell Biol*. 2007;176(4):459-471. doi:10.1083/jcb.200606077

87. Cantalupo G, Alifano P, Roberti V, Bruni CB, Bucci C. Rab-interacting lysosomal protein (RILP): The Rab7 effector required for transport to lysosomes. *EMBO J*. 2001;20(4):683-693. doi:10.1093/emboj/20.4.683

88. Johnson DE, Ostrowski P, Jaumouillé V, Grinstein S. The position of lysosomes within the cell determines their luminal pH. *J Cell Biol*. 2016;212(6):677-692. doi:10.1083/jcb.201507112

89. De Luca M, Cogli L, Progida C, et al. RILP regulates vacuolar ATPase through interaction with the V1G1 subunit. *J Cell Sci*. 2015;128(14):2565-2565. doi:10.1242/jcs.175323

90. Han CZ, Ravichandran KS. Metabolic connections during apoptotic cell engulfment. *Cell*. 2011;147(7):1442-1445. doi:10.1016/j.cell.2011.12.006

91. Korns D, Frasch SC, Fernandez-Boyanapalli R, Henson PM, Bratton DL. Modulation of macrophage efferocytosis in inflammation. *Front Immunol*. 2011;2(NOV):1-10. doi:10.3389/fimmu.2011.00057

92. Trahtemberg U, Mevorach D. Apoptotic Cells Induced Signaling for Immune Homeostasis in Macrophages and Dendritic Cells. *Front Immunol*. 2017;8(October). doi:10.3389/fimmu.2017.01356

93. Allavena P, Guglielmetti S, Marelli G, et al. Heme-oxygenase-1 Production by Intestinal CX3CR1 + Macrophages Helps to Resolve Inflammation and Prevents Carcinogenesis . *Cancer Res*. 2017;77(16):4472-4485. doi:10.1158/0008-5472.can-16-2501

94. Tomkowicz B, Walsh E, Cotty A, et al. TIM-3 suppresses anti-CD3/CD28-induced TCR activation and IL-2 expression through the NFAT signaling pathway. *PLoS One*. 2015;10(10):1-21. doi:10.1371/journal.pone.0140694

95. Sen P, Wallet MA, Yi Z, et al. Apoptotic cells induce Mer tyrosine kinase − dependent blockade of NF- κ B activation in dendritic cells Apoptotic cells induce Mer tyrosine kinase – dependent blockade of NF- □ B activation in dendritic cells. 2014;109(2):653-660. doi:10.1182/blood-2006-04-017368

96. A-Gonzalez N, Bensinger SJ, Hong C, et al. Apoptotic cells promote their own clearance and immune tolerance through activation of the nuclear receptor LXR. *Immunity*. 2009;31(2):245-258. doi:10.1016/j.immuni.2009.06.018

97. Röszer T. Transcriptional control of apoptotic cell clearance by macrophage nuclear receptors. *Apoptosis*. 2016;0(0):0. doi:10.1007/s10495-016-1310-x

98. Mukundan L, Odegaard JI, Morel CR, et al. PPAR- δ senses and orchestrates clearance of apoptotic cells to promote tolerance. *Nat Med*. 2009;15(11):1266-1273. doi:10.1038/nm.2048

99. Costet P, Lalanne F, Gerbod-Giannone MC, et al. Retinoic Acid Receptor-Mediated Induction of ABCA1 in Macrophages. *Mol Cell Biol*. 2003;23(21):7756-7766. doi:10.1128/mcb.23.21.7756-7766.2003

100. Yvan-Charvet L, Pagler T a., Seimon T a., et al. ABCA1 and ABCG1 protect against oxidative stress-induced macrophage apoptosis during efferocytosis. *Circ Res*. 2010;106(12):1861-1869. doi:10.1161/CIRCRESAHA.110.217281

101. Cui D, Thorp E, Li Y, et al. Pivotal advance: macrophages become resistant to cholesterol-induced death after phagocytosis of apoptotic cells. *J Leukoc Biol*. 2007;82(5):1040-1050. doi:10.1189/jlb.0307192

102. Park D, Han CZ, Elliott MR, et al. Continued clearance of apoptotic cells critically depends on the phagocyte Ucp2 protein. *Nature*. 2011;477(7363):220-224. doi:10.1038/nature10340

103. Wang Y, Subramanian M, Yurdagul A, et al. Mitochondrial Fission Promotes the Continued Clearance of Apoptotic Cells by Macrophages. *Cell*. 2017;171(2):331-345.e22. doi:10.1016/j.cell.2017.08.041

104. Morioka S, Perry JSA, Raymond MH, et al. Efferocytosis induces a novel SLC program to promote glucose uptake and lactate release. *Nature*. 2018. doi:10.1038/s41586-018-0735-5

105. Falk E. Pathogenesis of Atherosclerosis. *J Am Coll Cardiol*. 2006;47(8):0-5. doi:10.1016/j.jacc.2005.09.068

106. Westover E. Cholesterol in Health and Disease. *J Clin Invest*. 2002;110(5):583-590. doi:10.1172/JCI200216381.Imagine

107. Thorp E, Subramanian M, Tabas I. The role of macrophages and dendritic cells in

the clearance of apoptotic cells in advanced atherosclerosis. *Eur J Immunol*. 2011;41(9):2515-2518. doi:10.1002/eji.201141719

108. Hansson GK, Libby P, Tabas I. Inflammation and plaque vulnerability. *J Intern Med*. 2015;278:483-493. doi:10.1111/joim.12406

109. Herrington W, Lacey B, Sherliker P, Armitage J, Lewington S. Epidemiology of Atherosclerosis and the Potential to Reduce the Global Burden of Atherothrombotic Disease. *Circ Res*. 2016;118(4):535-546. doi:10.1161/CIRCRESAHA.115.307611

110. Canada S. Table 13-10-0801-01 Leading causes of death, total population (age standardization using 2011 population). 2017. doi:https://doi.org/10.25318/1310080101-eng

111. Moore KJ, Tabas I. Macrophages in the pathogenesis of atherosclerosis. *Cell*. 2011;145(3):341-355. doi:10.1016/j.cell.2011.04.005

112. Strong JP, Malcom GT, Mcmahan CA, et al. Prevalence and Extent of Atherosclerosis in Adolescents and Young Adults. *Jama*. 1999;281(8):727-735. doi:10.1001/jama.281.8.727

113. Wissler RW, Strong JP. Risk Factors and Progression of Atherosclerosis in Youth. *Am J Pathol*. 1998;153(4):1023-1033. doi:10.1016/S0002-9440(10)65647-7

114. Dron JS, Hegele RA. Genetics of Lipid and Lipoprotein Disorders and Traits. *Curr Genet Med Rep*. 2017;5(2):115-115. doi:10.1007/s40142-017-0117-6

115. Viola J, Soehnlein O. Atherosclerosis – A matter of unresolved inflammation. *Semin Immunol*. 2015;27(3):184-193. doi:10.1016/j.smim.2015.03.013

116. Tabas I. 2016 Russell Ross Memorial Lecture in Vascular Biology. *Arterioscler Thromb Vasc Biol*. 2016:ATVBAHA.116.308036. doi:10.1161/ATVBAHA.116.308036

117. VanderLaan P a., Reardon C a., Getz GS. Site Specificity of Atherosclerosis: Site-Selective Responses to Atherosclerotic Modulators. *Arterioscler Thromb Vasc Biol*. 2004;24(1):12-22. doi:10.1161/01.ATV.0000105054.43931.f0

118. Messner B, Bernhard D. Smoking and cardiovascular disease: Mechanisms of endothelial dysfunction and early atherogenesis. *Arterioscler Thromb Vasc Biol*. 2014;34(3):509-515. doi:10.1161/ATVBAHA.113.300156

119. Aronson D, Rayfield EJ. How hyperglycemia promotes atherosclerosis: molecular mechanisms. *Cardiovasc Diabetol*. 2002;1(1):1. doi:10.1186/1475-2840-1-1

120. Schürmann C, Rezende F, Kruse C, et al. The NADPH oxidase Nox4 has anti-atherosclerotic functions. *Eur Heart J*. 2015;36(48):3447-3456. doi:10.1093/eurheartj/ehv460

121. Moore KJ, Sheedy FJ, Fisher E a. Macrophages in atherosclerosis: a dynamic balance. *Nat Rev Immunol*. 2013;13(10):709-721. doi:10.1038/nri3520

122. Tse K, Tse H, Sidney J, Sette A, Ley K. T cells in atherosclerosis. *Int Immunol*. 2013;25(11):615-622. doi:10.1093/intimm/dxt043

123. Armstrong SM, Sugiyama MG, Fung KYY, et al. A novel assay uncovers an unexpected role for SR-BI in LDL transcytosis. *Cardiovasc Res*. 2015;108(2):268-277. doi:10.1093/cvr/cvv218

124. Moore KJ, Freeman MW. Scavenger Receptors in Atherosclerosis: Beyond Lipid Uptake. *Arterioscler Thromb Vasc Biol*. 2006. doi:10.1161/01.ATV.0000229218.97976.43

125. Moore KJ, Freeman MW. Scavenger receptors in atherosclerosis: beyond lipid uptake. *Arterioscler Thromb Vasc Biol*. 2006;26(8):1702-1711. doi:10.1161/01.ATV.0000229218.97976.43

126. Roshan M, Tambo A, Pace N. The role of TLR2, TLR4, and TLR9 in the pathogenesis of atherosclerosis. *Int J Inflam*. 2016:1-11.

doi:10.1056/NEJM197608192950805

127. Yahagi K, Kolodgie FD, Otsuka F, et al. Pathophysiology of native coronary, vein graft, and in-stent atherosclerosis. *Nat Rev Cardiol*. 2015;advance on. doi:10.1038/nrcardio.2015.164

128. Libby P, Ridker PM, Hansson GK. Progress and challenges in translating the biology of atherosclerosis. *Nature*. 2011;473(7347):317-325. doi:10.1038/nature10146

129. Vincent J. Lipid Lowering Therapy for Atherosclerotic Cardiovascular Disease: It Is Not So Simple. *Clin Pharmacol Ther*. 2018;104(2):220-224. doi:10.1002/cpt.1138

130. Ridker PM. Residual inflammatory risk: addressing the obverse side of the atherosclerosis prevention coin. *Eur Heart J*. 2016;37(22):1720-1722. doi:10.1093/eurheartj/ehw024

131. Ridker PM, Danielson E, Fonseca F, et al. Rosuvastatin to Prevent Vascular Events in Men and Women with Elevated C-Reactive Protein. *N Engl J Med*. 2008;359(21):2195-2207. doi:10.1056/NEJMoa1109071

132. Ridker PM, Dellborg M, Kastelein JJP, et al. Antiinflammatory Therapy with Canakinumab for Atherosclerotic Disease. *N Engl J Med*. 2017;377(12):1119-1131. doi:10.1056/nejmoa1707914

133. Mills CD, Lenz LL, Ley K. Macrophages at the fork in the road to health or disease. *Front Immunol*. 2015;6(February):1-6. doi:10.3389/fimmu.2015.00059

134. Tabas I, Bornfeldt KE. Macrophage Phenotype and Function in Different Stages of Atherosclerosis. *Circ Res*. 2016;118(4):653-667. doi:10.1161/CIRCRESAHA.115.306256

135. Arsenault BJ, Kritikou EA, Tardif JC. Regression of atherosclerosis. *Curr Cardiol Rep*. 2012;14(4):443-449. doi:10.1007/s11886-012-0285-7

136. de Gaetano M, Crean D, Barry M, Belton O. M1- and M2-Type Macrophage Responses Are Predictive of Adverse Outcomes in Human Atherosclerosis. *Front Immunol*. 2016;7(July). doi:10.3389/fimmu.2016.00275

137. Rahman K, Vengrenyuk Y, Ramsey SA, et al. Inflammatory Ly6Chimonocytes and their conversion to M2 macrophages drive atherosclerosis regression. *J Clin Invest*. 2017;127(8):2904-2915. doi:10.1172/JCI75005

138. McNeill E, Iqbal AJ, Jones D, et al. Tracking Monocyte Recruitment and Macrophage Accumulation in Atherosclerotic Plaque Progression Using a Novel hCD68GFP/ApoE $^{-/-}$ Reporter Mouse. *Arterioscler Thromb Vasc Biol*. 2016:ATVBAHA.116.308367. doi:10.1161/ATVBAHA.116.308367

139. Bunting M, Harris ES, McIntyre TM, Prescott SM, Zimmerman GA. Leukocyte adhesion deficiency syndromes: adhesion and tethering defects involving β 2 integrins and selectin ligands. *Curr Opin Hematol*. 2002;9(1).

140. Gautier EL, Huby T, Witztum JL, et al. Macrophage apoptosis exerts divergent effects on atherogenesis as a function of lesion stage. *Circulation*. 2009;119(13):1795-1804. doi:10.1161/CIRCULATIONAHA.108.806158

141. Linton MF, Babaev VR, Huang J, Linton EF, Tao H, Yancey PG. Macrophage Apoptosis and Efferocytosis in the Pathogenesis of Atherosclerosis. *Circ J*. 2016. doi:10.1253/circj.CJ-16-0924

142. Schrijvers DM, De Meyer GRY, Kockx MM, Herman AG, Martinet W. Phagocytosis of apoptotic cells by macrophages is impaired in atherosclerosis. *Arterioscler Thromb Vasc Biol*. 2005;25(6):1256-1261. doi:10.1161/01.ATV.0000166517.18801.a7

143. Chistiakov DA, Melnichenko AA, Myasoedova VA, Grechko A V., Orekhov AN. Mechanisms of foam cell formation in atherosclerosis. *J Mol Med*. 2017;95(11):1153-1165. doi:10.1007/s00109-017-1575-8

144. Tabas I. Macrophage death and defective inflammation resolution in

atherosclerosis. *Nat Rev Immunol*. 2009;10(1):36-46. doi:10.1038/nri2675

145. Clarke M, Bennett M. The emerging role of vascular smooth muscle cell apoptosis in atherosclerosis and plaque stability. *Am J Nephrol*. 2007;26(6):531-535. doi:10.1159/000097815

146. Dick W, Zhu C, Björkegren J, Skogsberg J, Eriksson P. MMP-2 and MMP-9 are prominent matrix metalloproteinases during atherosclerosis development in the Ldlr -/- Apob 100/100 mouse. *Int J Mol Med*. 2011;28(2):247-253. doi:10.3892/ijmm.2011.693

147. Quillard T, Tesmenitsky Y, Croce K, et al. Selective inhibition of matrix metalloproteinase-13 increases collagen content of established mouse atherosclerosis. *Arterioscler Thromb Vasc Biol*. 2011;31(11):2464-2472. doi:10.1161/ATVBAHA.111.231563

148. Tabas I. Apoptosis and plaque destabilization in atherosclerosis: the role of macrophage apoptosis induced by cholesterol. *Cell Death Differ*. 2004;11 Suppl 1:S12-S16. doi:10.1038/sj.cdd.4401444

149. Gonzalez L, Trigatti BL. Macrophage apoptosis and necrotic core development in atherosclerosis: A rapidly advancing field with clinical relevance to imaging and therapy. *Can J Cardiol*. 2016;33(3):303-312. doi:10.1016/j.cjca.2016.12.010

150. Puig O, Yuan J, Stepaniants S, et al. A gene expression signature that classifies human atherosclerotic plaque by relative inflammation status. *Circ Cardiovasc Genet*. 2011;4(6):595-604. doi:10.1161/CIRCGENETICS.111.960773

151. Li Y, Schwabe RF, DeVries-Seimon T, et al. Free cholesterol-loaded macrophages are an abundant source of tumor necrosis factor-α and interleukin-6: Model of NF-κB- and map kinase-dependent inflammation in advanced atherosclerosis. *J Biol Chem*. 2005;280(23):21763-21772. doi:10.1074/jbc.M501759200

152. Thorp E, Li G, Seimon TA, Kuriakose G, Ron D, Tabas I. Reduced Apoptosis and Plaque Necrosis in Advanced Atherosclerotic Lesions of Apoe-/- and Ldlr-/- Mice

Lacking CHOP. *Cell Metab*. 2009;9(5):474-481. doi:10.1016/j.cmet.2009.03.003

153. Angsana J, Chen J, Liu L, Haller CA, Chaikof EL. Efferocytosis as a regulator of macrophage chemokine receptor expression and polarization. *Eur J Immunol*. 2016;46(7):1592-1599. doi:10.1002/eji.201546262

154. Zhu X, Owen JS, Wilson MD, et al. Macrophage ABCA1 reduces MyD88-dependent Toll-like receptor trafficking to lipid rafts by reduction of lipid raft cholesterol. *J Lipid Res*. 2010;51(11):3196-3206. doi:10.1194/jlr.M006486

155. Chávez-Sánchez L, Garza-Reyes MG, Espinosa-Luna JE, Chávez-Rueda K, Legorreta-Haquet MV, Blanco-Favela F. The role of TLR2, TLR4 and CD36 in macrophage activation and foam cell formation in response to oxLDL in humans. *Hum Immunol*. 2014;75(4):322-329. doi:10.1016/j.humimm.2014.01.012

156. Sheedy FJ, Grebe A, Rayner KJ, et al. CD36 coordinates NLRP3 inflammasome activation by facilitating intracellular nucleation of soluble ligands into particulate ligands in sterile inflammation. *Nat Immunol*. 2013;14(8):812-820. doi:10.1038/ni.2639

157. Duewell P, Kono H, Rayner KJ, et al. NLRP3 inflammasomes are required for atherogenesis and activated by cholesterol crystals. *Nature*. 2010;464(7293):1357-1361. doi:10.1038/nature08938

158. Desurmont C, Caillaud JM, Emmanuel F, et al. Complete atherosclerosis regression after human ApoE gene transfer in ApoE-deficient/nude mice. *Arterioscler Thromb Vasc Biol*. 2000;20(2):435-442. doi:10.1161/01.ATV.20.2.435

159. Feig JE, Rong JX, Shamir R, et al. HDL promotes rapid atherosclerosis regression in mice and alters inflammatory properties of plaque monocyte-derived cells. *Proc Natl Acad Sci*. 2011;108(17):7166-7171. doi:10.1073/pnas.1016086108

160. Rojas J, Salazar J, Martínez MS, et al. Macrophage Heterogeneity and Plasticity: Impact of Macrophage Biomarkers on Atherosclerosis. *Scientifica (Cairo)*.

2015;2015:1-17. doi:10.1155/2015/851252

161. Kadl A, Meher AK, Sharma PR, et al. Identification of a novel macrophage phenotype that develops in response to atherogenic phospholipids via Nrf2. *Circ Res*. 2010;107(6):737-746. doi:10.1161/CIRCRESAHA.109.215715

162. Boyle JJ, Harrington H a, Piper E, et al. Coronary intraplaque hemorrhage evokes a novel atheroprotective macrophage phenotype. *Am J Pathol*. 2009;174(3):1097-1108. doi:10.2353/ajpath.2009.080431

163. Boyle JJ, Johns M, Kampfer T, et al. Activating transcription factor 1 directs Mhem atheroprotective macrophages through coordinated iron handling and foam cell protection. *Circ Res*. 2012;110(1):20-33. doi:10.1161/CIRCRESAHA.111.247577

164. Chistiakov DA, Bobryshev Y V., Orekhov AN. Macrophage-mediated cholesterol handling in atherosclerosis. *J Cell Mol Med*. 2015;XX(X):n/a-n/a. doi:10.1111/jcmm.12689

165. Yang K, Wang X, Liu Z, et al. Oxidized Low-Density Lipoprotein Promotes Macrophage Lipid Accumulation via the Toll-Like Receptor 4-Src Pathway. *Circ J*. 2015. doi:10.1253/circj.CJ-15-0345

166. Maxfield FR, Tabas I. Role of cholesterol and lipid organization in disease. *Nature*. 2005;438(7068):612-621. doi:10.1038/nature04399

167. Konstantinov IE, Mejevoi N, Anichkov NM. Nikolai N. Anichkov and his theory of atherosclerosis. *Texas Hear Inst J*. 2006;33(4):417-423.

168. Elsegood CL, Mamo JCL. An investigation by electron microscopy of chylomicron remnant uptake by human monocyte-derived macrophages. *Atherosclerosis*. 2006;188(2):251-259. doi:10.1016/j.atherosclerosis.2005.10.043

169. Wolf D, Zirlik A, Ley K. Beyond vascular inflammation—recent advances in understanding atherosclerosis. *Cell Mol Life Sci*. 2015. doi:10.1007/s00018-015-

1971-6

170. Wade NS, Major AS. The problem of accelerated atherosclerosis in systemic lupus erythematosus: insights into a complex co-morbidity. *Thromb Haemost*. 2011;106(5):849-857. doi:10.1016/j.biotechadv.2011.08.021.Secreted

171. Montecucco F, Vuilleumier N, Pagano S, et al. Anti-Apolipoprotein A-1 auto-antibodies are active mediators of atherosclerotic plaque vulnerability. *Eur Heart J*. 2011;32(4):412-421. doi:10.1093/eurheartj/ehq521

172. Sobenin IA, Salonen JT, Zhelankin A V, et al. Low Density Lipoprotein-Containing Circulating Immune Complexes: Role in Atherosclerosis and Diagnostic Value. *Biomed Res Int*. 2014;2014:1-7.

173. Rocha N, Neefjes J. MHC class II molecules on the move for successful antigen presentation. *EMBO J*. 2008;27(1):1-5. doi:10.1038/sj.emboj.7601945

174. Hansson GK, Jonasson L, Holm J, Claesson-Welsh L. Class II MHC antigen expression in the atherosclerotic plaque: smooth muscle cells express HLA-DR, HLA-DQ and the invariant gamma chain. *Clin Exp Immunol*. 1986;64(2):261-268.

175. Hermansson A, Ketelhuth DFJ, Strodthoff D, et al. Inhibition of T cell response to native low-density lipoprotein reduces atherosclerosis. *J Exp Med*. 2010;207(5):1081-1093. doi:10.1084/jem.20092243

176. Emeson EE, Shen ML, Bell CG, Qureshi A. Inhibition of atherosclerosis in CD4 T-cell-ablated and nude (nu/nu) C57BL/6 hyperlipidemic mice. *Am J Pathol*. 1996;149(2):675-685.

177. Laurat E, Poirier B, Tupin E, et al. In Vivo Downregulation of T Helper Cell 1 Immune Responses Reduces Atherogenesis in Apolipoprotein E-Knockout Mice. *Circulation*. 2001;104(2):197-202. doi:10.1161/01.CIR.104.2.197

178. Stemme S, Faber B, Holmt J, et al. T lymphocytes from human atherosclerotic plaques recognize oxidized low density lipoprotein. *Med Sci*. 1995;92(April):3893-

3897. doi:10.1073/pnas.92.9.3893

179. Koltsova EK, Ley K. How dendritic cells shape atherosclerosis. *Trends Immunol*. 2011;32(11):540-547. doi:10.1016/j.it.2011.07.001

180. Elzen P van den, Garg S, León L, et al. Apolipoprotein-mediated pathways of lipid antigen presentation. *Nature*. 2005;437(7060):906-910. doi:10.1038/nature04001

181. Tupin E, Nicoletti A, Elhage R, et al. CD1d-dependent Activation of NKT Cells Aggravates Atherosclerosis. *J Exp Med*. 2004;199(3):417-422. doi:10.1084/jem.20030997

182. Barral DC, Brenner MB. CD1 antigen presentation: how it works. *Nat Rev Immunol*. 2007;7(12):929-941. doi:10.1038/nri2191

183. Gojova A, Esposito B, Gourdy P, Ardouin P, Tedgui A, Mallat Z. Specific abrogation of transforming growth factor-β signaling in T cells alters atherosclerotic lesion size and composition in mice. *Blood*. 2003;102(12):4052-4059. doi:10.1182/blood-2003-05-1729.Z.M.

184. Konkel JE, Zhang D, Zanvit P, et al. Transforming Growth Factor-β Signaling in Regulatory T Cells Controls T Helper-17 Cells and Tissue-Specific Immune Responses. *Immunity*. 2017;46(4):660-674. doi:10.1016/j.immuni.2017.03.015

185. Frostegård J, Zhang Y, Sun J, Yan K, Liu A. Oxidized Low-Density Lipoprotein (OxLDL)-Treated Dendritic Cells Promote Activation of T Cells in Human Atherosclerotic Plaque and Blood, Which Is Repressed by Statins: MicroRNA let-7c Is Integral to the Effect. *J Am Heart Assoc*. 2016;5(9):1-15. doi:10.1161/JAHA.116.003976

186. George J, Schwartzenberg S, Medvedovsky D, et al. Regulatory T cells and IL-10 levels are reduced in patients with vulnerable coronary plaques. *Atherosclerosis*. 2012;222(2):519-523. doi:10.1016/j.atherosclerosis.2012.03.016

187. Lehmann C, Homann J, Ball AK, et al. Lipoxin and resolvin biosynthesis is

dependent on 5-lipoxygenase activating protein. *FASEB J*. 2015;29(12):5029-5043. doi:10.1096/fj.15-275487

188. Baker LA, Martin NRW, Kimber MC, Pritchard GJ, Lindley MR, Lewis MP. Resolvin E1 (R v E 1) attenuates LPS induced inflammation and subsequent atrophy in C2C12 myotubes. *J Cell Biochem*. 2018;119(7):6094-6103. doi:10.1002/jcb.26807

189. Gammelmark A, Nielsen MS, Lundbye-Christensen S, Tjønneland A, Schmidt EB, Overvad K. Common polymorphisms in the 5-Lipoxygenase pathway and risk of incident myocardial infarction: A danish case-cohort study. *PLoS One*. 2016;11(11):1-19. doi:10.1371/journal.pone.0167217

190. Elajami TK, Colas RA, Dalli J, Chiang N, Serhan CN, Welty FK. Specialized proresolving lipid mediators in patients with coronary artery disease and their potential for clot remodeling. *FASEB J*. 2016;30(8):2792-2801. doi:10.1096/fj.201500155R

191. Fredman G, Tabas I. Boosting Inflammation Resolution in Atherosclerosis: The Next Frontier for Therapy. *Am J Pathol*. 2017;187(6):1211-1221. doi:10.1016/j.ajpath.2017.01.018

192. Fredman G, Hellmann J, Proto JD, et al. An imbalance between specialized pro-resolving lipid mediators and pro-inflammatory leukotrienes promotes instability of atherosclerotic plaques. *Nat Commun*. 2016;7:1-11. doi:10.1038/ncomms12859

193. Li Y, Gerbod-Giannone MC, Seitz H, et al. Cholesterol-induced apoptotic macrophages elicit an inflammatory response in phagocytes, which is partially attenuated by the Mer receptor. *J Biol Chem*. 2006;281(10):6707-6717. doi:10.1074/jbc.M510579200

194. Liu J, Thewke DP, Su YR, Linton MF, Fazio S, Sinensky MS. Reduced macrophage apoptosis is associated with accelerated atherosclerosis in low-density lipoprotein receptor-null mice. *Arterioscler Thromb Vasc Biol*. 2005;25(1):174-

179. doi:10.1161/01.ATV.0000148548.47755.22

195. Kojima Y, Weissman IL, Leeper NJ. The Role of Efferocytosis in Atherosclerosis. *Circulation*. 2017;135(5):476-489. doi:10.1161/CIRCULATIONAHA.116.025684

196. Boisvert W a., Rose DM, Boullier a., et al. Leukocyte transglutaminase 2 expression limits atherosclerotic lesion size. *Arterioscler Thromb Vasc Biol*. 2006;26(3):563-569. doi:10.1161/01.ATV.0000203503.82693.c1

197. Ait-oufella H, Kinugawa K, Zoll J, et al. Lactadherin Deficiency Leads to Apoptotic Cell Accumulation and Accelerated Atherosclerosis in Mice. *Circulation*. 2007;115(16):2168-2177. doi:10.1161/CIRCULATIONAHA.106.662080

198. Bhatia VK, Yun S, Leung V, et al. Complement C1q reduces early atherosclerosis in low-density lipoprotein receptor-deficient mice. *Am J Pathol*. 2007;170(1):416-426. doi:10.2353/ajpath.2007.060406

199. Thorp E, Cui D, Schrijvers DM, Kuriakose G, Tabas I. Mertk Receptor Mutation Reduces Efferocytosis Efficiency and Promotes Apoptotic Cell Accumulation and Plaque Necrosis in Atherosclerotic Lesions of Apoe ⁻/⁻ Mice. *Arterioscler Thromb Vasc Biol*. 2015;28(8):1421-1428. doi:10.1161/ATVBAHA.108.167197

200. Subramanian M, Proto JD, Matsushima GK, Tabas I. Deficiency of AXL in Bone Marrow-Derived Cells Does Not Affect Advanced Atherosclerotic Lesion Progression. *Sci Rep*. 2016;6(November):39111. doi:10.1038/srep39111

201. Thorp E, Tabas I. Mechanisms and consequences of efferocytosis in advanced atherosclerosis. *J Leukoc Biol*. 2009;86(5):1089-1095. doi:10.1189/jlb.0209115

202. Cai B, Thorp EB, Doran AC, et al. MerTK receptor cleavage promotes plaque necrosis and defective resolution in atherosclerosis. *J Clin Invest*. 2017:1-5. doi:10.1172/JCI90520

203. Cai B, Thorp EB, Doran AC, et al. MerTK receptor cleavage promotes plaque

necrosis and defective resolution in atherosclerosis. *J Clini*. 2017;127(2):564-568. doi:10.1172/JCI90520.We

204. Cai B, Thorp EB, Doran AC, et al. MerTK cleavage limits proresolving mediator biosynthesis and exacerbates tissue inflammation. *Proc Natl Acad Sci*. 2016;113(23):6526-6531. doi:10.1073/pnas.1524292113

205. Kojima Y, Volkmer J-P, McKenna K, et al. CD47-blocking antibodies restore phagocytosis and prevent atherosclerosis. *Nature*. 2016;536(7614):86-90. doi:10.1038/nature18935

206. Huynh KK, Gershenzon E, Grinstein S. Cholesterol accumulation by macrophages impairs phagosome maturation. *J Biol Chem*. 2008;283(51):35745-35755. doi:10.1074/jbc.M806232200

207. Tabas I. Consequences of cellular cholesterol accumulation : Basic concepts and physiological implications. *J Clin Invest*. 2002;110(7):905-911. doi:10.1172/JCI200216452.The

208. Getz GS, Reardon C a. Animal models of Atherosclerosis. *Arterioscler Thromb Vasc Biol*. 2012;32(5):1104-1115. doi:10.1161/ATVBAHA.111.237693

209. Getz GS, Reardon C a. ApoE knockout and knockin mice: The history of their contribution to the understanding of atherogenesis. *CEUR Workshop Proc*. 2015;1542(773):33-36. doi:10.1017/CBO9781107415324.004

210. von Scheidt M, Zhao Y, Kurt Z, et al. Applications and Limitations of Mouse Models for Understanding Human Atherosclerosis. *Cell Metab*. 2017;25(2):248-261. doi:10.1016/j.cmet.2016.11.001

211. Gordon SM, Li H, Zhu X, Shah AS, Lu LJ, Davidson WS. A comparison of the mouse and human lipoproteome: Suitability of the mouse model for studies of human lipoproteins. *J Proteome Res*. 2015;14(6):2686-2695. doi:10.1021/acs.jproteome.5b00213

212. Seok J, Warren HS, Cuenca AG, et al. Genomic responses in mouse models poorly mimic human inflammatory diseases. *Proc Natl Acad Sci U S A*. 2013;110(9):3507-3512. doi:10.1073/pnas.1222878110

213. Pasterkamp G, Van Der Laan SW, Haitjema S, et al. Human validation of genes associated with a murine atherosclerotic phenotype. *Arterioscler Thromb Vasc Biol*. 2016;36(6):1240-1246. doi:10.1161/ATVBAHA.115.306958

214. Nakashima Y, Chen YX, Kinukawa N, Sueishi K. Distributions of diffuse intimal thickening in human arteries: Preferential expression in atherosclerosis-prone arteries from an early age. *Virchows Arch*. 2002;441(3):279-288. doi:10.1007/s00428-002-0605-1

215. Hogarth CA, Roy A, Ebert DL. Genomic evidence for the absence of a functional cholesteryl ester transfer protein gene in mice and rats. *Comp Biochem Physiol - B Biochem Mol Biol*. 2003;135(2):219-229. doi:10.1016/S1096-4959(03)00046-0

216. Hamamdzic D, Wilensky RL. Porcine Models of Accelerated Coronary Atherosclerosis: Role of Diabetes Mellitus and Hypercholesterolemia. *J Diabetes Res*. 2013;2013:1-7. doi:10.1155/2013/761415

217. Wentzel JJ, Chatzizisis YS, Gijsen FJH, Giannoglou GD, Feldman CL, Stone PH. Endothelial shear stress in the evolution of coronary atherosclerotic plaque and vascular remodelling: Current understanding and remaining questions. *Cardiovasc Res*. 2012;96(2):234-243. doi:10.1093/cvr/cvs217

218. van Ditzhuijzen NS, van den Heuvel M, Sorop O, et al. Serial Coronary Imaging of Early Atherosclerosis Development in Fast-Food-Fed Diabetic and Nondiabetic Swine. *JACC Basic to Transl Sci*. 2016;1(6):449-460. doi:10.1016/j.jacbts.2016.08.006

219. Fan J, Kitajima S, Watanabe T, et al. Rabbit models for the study of human atherosclerosis: From pathophysiological mechanisms to translational medicine. *Pharmacol Ther*. 2015;146:104-119. doi:10.1016/j.pharmthera.2014.09.009

220. Cox LA, Olivier M, Spradling-Reeves K, Karere GM, Comuzzie AG, VandeBerg JL. Nonhuman primates and translational research-Cardiovascular disease. *ILAR J*. 2017;58(2):235-250. doi:10.1093/ilar/ilx025

221. Armstrong ML, Warner ED, Connor WE. Regression of coronary atheromatosis in rhesus monkeys. *Circ Res*. 1970;27(1):59-67. doi:10.1161/01.RES.27.1.59

222. Aluganti Narasimhulu C, Fernandez-Ruiz I, Selvarajan K, et al. Atherosclerosis — do we know enough already to prevent it? *Curr Opin Pharmacol*. 2016;27(Ldl):92-102. doi:10.1016/j.coph.2016.02.006

223. Gomez D, Baylis RA, Durgin BG, et al. Interleukin-1β has atheroprotective effects in advanced atherosclerotic lesions of mice. *Nat Med*. 2018. doi:10.1038/s41591-018-0124-5

224. Fernández-Friera L, Peñalvo JL, Fernández-Ortiz A, et al. Prevalence, vascular distribution, and multiterritorial extent of subclinical atherosclerosis in a middle-aged cohort the PESA (Progression of Early Subclinical Atherosclerosis) study. *Circulation*. 2015;131(24):2104-2113. doi:10.1161/CIRCULATIONAHA.114.014310

225. Frostegård J, Ulfgren A, Nyberg P, et al. Cytokine expression in advanced human atherosclerotic plaques : dominance of pro-inflammatory (Th1) and macrophage-stimulating cytokines. *Atherosclerosis*. 1999;9150(99):7-8.

226. Papaspyridonos M, Smith A, Burnand KG, et al. Novel candidate genes in unstable areas of human atherosclerotic plaques. *Arterioscler Thromb Vasc Biol*. 2006;26(8):1837-1844. doi:10.1161/01.ATV.0000229695.68416.76

227. Chai JT, Ruparelia N, Goel A, et al. Differential Gene Expression in Macrophages From Human Atherosclerotic Plaques Shows Convergence on Pathways Implicated by Genome-Wide Association Study Risk Variants. *Arterioscler Thromb Vasc Biol*. 2018;38(11):2718-2730. doi:10.1161/ATVBAHA.118.311209

228. Sulkava M, Raitoharju E, Levula M, et al. Differentially expressed genes and

canonical pathway expression in human atherosclerotic plaques-Tampere Vascular Study. *Sci Rep*. 2017;7(December 2016):1-10. doi:10.1038/srep41483

229. Kuller L, Borhani N, Furberg C, et al. Prevalence of subclinical atherosclerosis and cardiovascular disease and association with risk factors in the Cardiovascular Health Study. *Am J Epidemiol*. 1994;139(12):1164-1179.

Chapter 2

2 Materials and Methods

2.1 Reagents, cell lines, plasmids/oligos, and antibodies

2.1.1 Reagents

RPMI, DMEM, Trypsin-EDTA and fetal bovine serum (FBS) were purchased from Wisent. Recombinant human M-CSF, GM-CSF, IFNγ and IL-4 were purchased from Peprotech. No. 1.5 thickness 8-mm round coverslips and 16% paraformaldehyde (PFA) were purchased from Electron Microscopy Supplies. Colloidal Coomassie Blue, PUREZOL RNA isolation reagent and iScript Select cDNA Synthesis Kit were purchased from Bio-Rad. Lympholyte-poly was purchased from Cedarlane Laboratories. Cell Proliferation Dyes eFluor 450 and eFluor 670 were purchased from eBioscience. Phosphatidylserine (PS), phosphatidylcholine (PC), biotin-phosphatidylethanolamine (biotin-PE), rhodamine-phosphatidylethanolamine (rhodamine-PE), cholesterol and BODIPY-cholesterol were purchased from Avanti Polar Lipids. Salmonella lipopolysaccharide (LPS), rAPID alkaline phosphatase, Polybrene Infection Reagent, mammalian protease inhibitor cocktail, Oil Red O, Nile Red, phorbol 12-myristate-13-acetate (PMA), methyl-β-cyclodextran, TRITC-dextran, human IgG and the Anti-Citrulline (Modified) Detection Kit were purchased from Sigma-Aldrich. Phusion DNA polymerase, FugeneHD, dithiobis[succinimidyl propionate], dithio-bismaleimidoethane, Permafluor mounting reagent, Fast SYBR Green master mix, EZ-link NHS-LC-biotin, CellTrace dyes and nitro blue tetrazolium chloride were purchased from Thermo Fisher. Restriction enzymes and T4 DNA ligase were purchased from New England Biolabs. Polystyrene beads, silica beads and silica-functionalized magnetic beads were purchased from Bangs Laboratories. Tissue-Tek OCT compound was purchased from VWR. Lipofectamine 3000 transfection reagent was purchased from Life Technologies. Polyjet In Vitro DNA transfection reagent was purchased from SignaGen Laboratories. Human plasma oxidized low density lipoprotein (oxLDL) was purchased from Alfa Aesar. Trypsin Enzymatic Antigen Retrieval Kit was purchased from Abcam. Vector DAB HRP substrate was purchased from Vector Laboratories. Cytoseal 60 was purchased from Thomas

Scientific. pHrodo Red Microscale Labeling Kit was purchased from Invitrogen. Normal rabbit and donkey sera were purchased from Jackson Immunoresearch. All other chemicals were purchased from Canada BioShop.

2.1.2 Mice, cell lines and bacteria

LDL receptor-deficient C57BL/6J mice were generously provided by Dr. Lillian Barra (Western University). THP-1 monocytes (ATCC TIB-202) were a gift from Dr. Joe Mymryk (Western University). Jurkat T cells (ATCC TIB-152) were a gift from Dr. Jimmy Dikeakos (Western University). J774.2 murine macrophage cells (ATCC TIB-67) were a gift from Dr. Sergio Grinstein (Hospital for Sick Children). HEK 293 cells (ATCC CRL-1573) were a gift from Dr. David Litchfield (Western University). *Escherichia coli* DH5α and ML35 strains were gifts from Drs. John McCormick and Susan Koval, respectively (Western University).

2.1.3 Plasmids and oligos

PM-RFP, Rab5-GFP, Rab7-mCherry, TfR-GFP, TfR-mCherry and LAMP1-mCherry expression constructs were gifts from Dr. Sergio Grinstein (Hospital for Sick Children). pBabePuro-GATA2 (Addgene Plasmid #1285) was purchased from Addgene. pLVX-IRES-ZsGreen1, pGFP-C-shLenti, pMD2.G and pDR8.2 were gifts from Dr. Jimmy Dikeakos (Western University). Human Rab17 cDNA was purchased from the Harvard PlasmID Repository. Primers and shRNA oligos were purchased from IDT. ON-TARGETplus siRNA was purchased from Thermo Fisher.

2.1.4 Antibodies

Mouse anti-human LAMP-1 monoclonal IgG1 antibody (H4A3) and mouse anti-human GAPDH monoclonal IgG1 antibody (2G7) were purchased from Developmental Studies Hybridoma Databank. Rat anti-mouse MHC class II monoclonal IgG2b antibody (M5/114.15.2; eBioscience 14-5321-82) was purchased from eBioscience. Rabbit anti-human Rab17 polyclonal IgG antibody (Proteintech 28274-1-AP) was purchased from Proteintech. Rabbit anti-human CD163 polyclonal IgG antibody (Abcam ab87099), mouse anti-human CD68 monoclonal IgG1 antibody (KP1; Abcam ab955) and rabbit anti-human

GATA2 polyclonal IgG antibody (Abcam ab153820) were purchased from Abcam. Rabbit anti-citrulline polyclonal IgG antibody (Sigma 07-377) was purchased as part of the Anti-Citrulline (Modified) Detection Kit from Sigma-Aldrich. All fluorescent secondary antibodies were purchased as IgG F(ab')$_2$ fragments from Jackson ImmunoResearch.

2.2 Cell culture

2.2.1 Cell lines

HEK 293 cells were maintained at 37 °C and 5% CO_2 in DMEM media supplemented with 10% FBS, L-glutamine and sodium bicarbonate, and buffered with 25 mM HEPES to a pH = 7.2. Cells were sub-cultured 1:5 by scraping once cells reached 80-90% confluency or approximately once every 3 to 4 days.

J774.2 murine macrophage cells were maintained at 37 °C and 5% CO_2 in RPMI media supplemented with 10% FBS, L-glutamine and sodium bicarbonate, and buffered with 25 mM HEPES to a pH = 7.2. Cells were sub-cultured 1:5 by enzymatic digestion with 0.05% trypsin supplemented with 0.53 mM EDTA once cells reached 80-90% confluency or approximately once every 3 to 4 days.

THP-1 human monocyte-like cells were maintained at 37 °C and 5% CO_2 in RPMI media supplemented with 10% FBS, L-glutamine and sodium bicarbonate, and buffered with 25 mM HEPES to a pH = 7.2. Cells were sub-cultured 1:5 or 1:10 through addition of fresh media once cells reached a concentration of 1×10^6 cells/mL. For differentiation into macrophages, cells are incubated with 100 nM PMA for 48-72 hrs. Differentiated THP-1 cells are washed at least 1× with PBS to remove excess PMA prior to use in downstream assays.

Jurkat human T lymphocyte-like cells were maintained at 37 °C and 5% CO_2 in RPMI media supplemented with 10% FBS, L-glutamine and sodium bicarbonate, and buffered with 25 mM HEPES to a pH = 7.2. Cells were sub-cultured 1:5 or 1:10 through addition of fresh media once cells reached a concentration of 1×10^6 cells/mL.

2.2.2 Primary cells

Primary human macrophages and dendritic cells were prepared from monocytes isolated from whole blood isolated from healthy adult donors with ethics approval from the Office of Human Research Ethics at Western University Health Sciences Research Ethics Board (HSREB Reference Number: 104010). Blood was collected through venipuncture into vacuum tubes coated with heparin and monocytes were isolated using Lympholyte-poly cell separation media (Cedarlane) according to the manufacturer's instructions. Briefly, approximately 4 mL of blood was layered over an equal volume of Lympholyte-poly and centrifuged for 25 min at 500 ×g at 50% acceleration and zero deceleration. The monocyte layer was carefully removed using a transfer pipette to a clean 50 mL tube and resuspended in approximately 50 mL of PBS and subsequently centrifuged for 6 min at 300 ×g at full acceleration and deceleration. Monocytes were re-suspended in 200 µL of warm RPMI per well to fill of a 12-well plate. Sterile, acid-washed glass coverslips were placed into 12-well plates and the monocyte suspension was pipetted onto coverslips. Cells were incubated for 1 hr at 37 °C and 5% CO_2 to allow monocytes to adhere to glass and coverslips were washed 3× with PBS to remove any non-adherent cells. Cells were maintained in culture with RPMI supplemented with 10% FBS, L-glutamine and sodium bicarbonate, 10,000 U/mL penicillin, 10 mg/mL streptomycin and 25 µg/mL amphotericin B and buffered with 25 mM HEPES to a pH = 7.2.

To generate dendritic cells, adherent monocytes were additionally supplemented with 1000U/mL rhGM-CSF and 500U/mL rhIL-4 for 48 hrs. To generate macrophages, adherent monocytes were additionally supplemented with various cytokines and allowed to incubate for five days to induce cell differentiation and polarization. For M0 or M2 macrophages, adherent monocytes were supplemented with 10 ng/mL rhM-CSF. For M1 macrophages, adherent monocytes were supplemented with 20 ng/mL rhGM-CSF. Following the five-day incubation, culture media was replaced with fresh complete RPMI free of antibiotics and supplemented with the following combination of cytokines to induce specific macrophage polarization: M0 macrophages – 10 ng/mL rhM-CSF; M1 macrophages – 20 ng/mL rhGM-CSF, 250 ng/mL LPS and 10 ng/mL IFNγ; M2 macrophages – 10 ng/mL rhM-CSF and 10 ng/mL rhIL-4.

2.3 Molecular cloning

2.3.1 Recombinant DNA preparation

Recombinant expression vectors were prepared through restriction enzyme digestion and subsequent ligation of appropriate insert sequences and vector backbones (see **Appendix A** for a complete list of constructs used in this thesis). Briefly, a DNA insert consisting of the consensus coding sequence (CDS) of the gene of interest or simply the sequence of interest (in the case of shRNA inserts) were amplified using standard PCR with primers designed to add flanking restriction enzyme sites compatible with the multiple cloning site of the vector backbone. A list of all PCR primers used for cloning can be found in **Appendix A**. PCR reaction was run for 30 cycles with Phusion DNA polymerase (New England Biolabs) according to the manufacturer's instructions.

Subsequently, the insert and backbone were digested with appropriate restriction enzymes for 1 hr at 37 °C and gel purified using a 1% agarose gel and the Monarch Nucleic Acid Preparation Kit (New England Biolabs) according to the manufacturer's instructions. Optionally, prior to gel purification, backbone DNA sequences can be dephosphorylated with rAPID alkaline phosphatase (Sigma-Aldrich) according to the manufacturer's instructions. Purified cut insert and backbone were ligated at a ratio of 10:1 insert to backbone overnight at 16 °C with 20,000 U/mL T4 ligase. Ligated vectors were transformed into chemically-competent *Escherichia coli* DH5α cells by heat shock for 1 min at 42 °C.

Transformed *E. coli* were plated on LB agar supplemented with the appropriate selective antibiotic(s) and incubated overnight at 37 °C. Colonies appearing following incubation were screened by colony PCR where feasible and propagated in liquid LB media overnight at 37 °C and shaking at 200 RPM. Following overnight incubation, plasmids were harvested from cultures using the High-Speed Plasmid Mini Kit (Geneaid) according to the manufacturer's instructions. Correct insertion of insert into backbone was confirmed by Sanger sequencing at the London Regional Genomics Centre.

2.3.2 Transfection of cell lines

HEK 293 cells were transfected using Lipofectamine 3000 (Life Technologies) according to the manufacturer's instructions. Briefly, cells were seeded at 30-40% confluency the day prior to transfection. Vector DNA and Lipofectamine 3000 reagent were prepared in separate tubes in serum-free RPMI media. Equal volumes of DNA and Lipofectamine reagent were combined and the mixture allowed to incubate for 5 min at room temperature. The entirety of the mixture was then added dropwise to the desired well of J774.2 cells to be transfected. The transfection mix was incubated with cells for 5-16 hrs at 37 °C and 5% CO_2, after which it was replaced by fresh complete RPMI media and allowed to incubate for at least 12 hrs at 37 °C and 5% CO_2 prior to use in downstream applications.

J774.2 cells were transfected using FuGENE HD transfection reagent (Promega) according to the manufacturer's instructions. Briefly, the DNA to be transfected was diluted in serum-free media and FuGENE reagent was added to 3:1 transfection reagent to DNA ratio. The mixture was vortexed briefly and allowed to incubate for 10-15 min at room temperature. Following incubation, the transfection mixture was added to the well to be transfected and allowed to incubate for at least 16 hrs at 37 °C and 5% CO_2 prior to use in downstream applications.

2.3.3 Viral transduction of cell lines

THP-1 macrophages were transduced using lentiviral vectors to establish cell lines stably expressing the gene or sequence of interest. Insert sequences cloned into an appropriate lentiviral transfer plasmid backbone were packaged into lentiviral vectors in HEK 293 cells using Polyjet In Vitro DNA Transfection Reagent (SignaGen Laboratories) according to the manufacturer's instructions. Briefly, HEK 293 cells were seeded at 10-20% confluency on 10-cm dishes and allowed to proliferate to 50-60% confluency over approximately two days. A DNA mixture containing 5 µg of the lentiviral vector, 2 µg of the pMD2.G envelope plasmid and 5 µg of the pDR8.2 packaging plasmid in serum-free DMEM media. This mixture was combined with an equal volume of Polyjet reagent diluted in serum-free DMEM and allowed to incubate for 12 min at room temperature. Following incubation, the transfection mixture was added dropwise to HEK 293 cells. Cells were incubated for

three days at 37 °C and 5% CO_2, with the media being changed with fresh complete DMEM 24 hrs post-transfection. At the end of the three-day period, cell supernatants were collected and FBS was added to a final concentration of 20%. Supernatants were centrifuged for 5 min at 1,500 ×g and then filtered using a 2-µm filter. Filtered supernatant containing lentivirus was aliquoted and stored at -80 °C until needed.

THP-1 monocytes were transduced using prepared lentivirus using a Spinfection protocol. Approximately 1 × 10^6 cells were re-suspended in 500 µL of lentivirus-containing supernatant prepared previously. Polybrene Infection Reagent (Sigma-Aldrich) was added to a final concentration of 8 µg/mL and the mix was centrifuged for 45 min at 800 ×g. Cell pellet was washed 1× with PBS to remove excess virus and Polybrene reagent and transferred into complete RPMI media. Transduced cells were incubate for a minimum of 48 hrs at 37 °C and 5% CO_2 prior to use in downstream applications.

2.4 RNA preparation and RT-qPCR

2.4.1 RNA preparation

Total RNA was isolated from cells or patient tissues through acid guanidinium thiocyanate-phenol-chloroform extraction uysing PureZOL RNA isolation reagent (Bio-Rad). Cells or tissues were suspended in an appropriate volume of PureZOL reagent (1 mL of reagent per 50-100 mg of tissue or 10^7 cells), vortexed briefly and allowed to incubate for 5 min at room temperature. Chloroform was added 1:5 v/v and the mix was allowed to incubate for another 5 min at room temperature with intermittent agitation. Samples were centrifuged for 15 min at 12,000 ×g and 4 °C, and subsequently the upper aqueous layer containing RNA was transferred to a fresh tube. An equal volume of isopropanol and 0.5 µL of 20 mg/mL glycogen were added to the RNA and the mixture was incubated at -80 °C for at least 30 min. Samples were again centrifuged for 15min at 12,000 ×g and 4 °C to pellet precipitated RNA. The RNA pellet was washed 2× with 75% ethanol, air dried for approximately 5 min at room temperature and reconstituted in a minimal amount of RNase-free ddH_2O. RNA concentration and quality were measured using a NanoDrop 1000 Spectrophotometer (Thermo Fisher) prior to use in downstream applications.

2.4.2 RT-qPCR

cDNA was generated from total RNA using the iScript Select cDNA Synthesis Kit (Bio-Rad) according to the manufacturer's instructions, with an equal amount of starting RNA an equal mix of the random and oligo$(dT)_{20}$ primer mixes. cDNA concentration and quality were checked using a NanoDrop 1000 Spectrophotometer prior to use in qPCR reactions. qPCR was performed using the Fast SYBR Green Master Mix (Thermo Fisher) an equal amount of starting cDNA. All qPCR primers used in this thesis can be found in **Appendix A**. PCR reactions were run on a QuantStudio 5 Real-Time PCR System (Thermo Fisher) for 40 cycles. Relative expression of genes of interest was calculated using the ΔΔCt method with either GAPDH or 18S serving as the reference gene.

2.5 Western blotting

Western blotting was employed to detect proteins of interest in cultured cells. A sufficient number of cells (at least 5×10^5) was cultured and was 1× with PBS immediately prior to lysis. Lysis was performed using either Triton X-100 (for cytoplasmic or membrane proteins; 150 mM NaCl, 1% Triton X-100, 50 mM pH 8.0 Tris-HCl) or RIPA (for nuclear proteins; 150 mM NaCl, 1% Triton X-100, 0.5% sodium deoxycholate, 0.1% SDS and 50 mM pH 8.0 Tris-HCl). Appropriate lysis buffer containing 1:100 v/v mammalian protease inhibitor was added to the cells and cells were scraped into suspension. The lysate was transferred to a clean tube and incubated for 40 min at 4 °C on a rotator. The lysate was subsequently centrifuged for 15 min at 12,000 ×g and 4 °C. Following centrifugation, supernatants were transferred to a clean tube and 1:4 v/v 4× Laemmli's buffer (1:5 v/v 1M pH 6.8 Tris-HCl, 0.08 g/mL SDS, 2:5 v/v glycerol and 0.02% bromophenol blue in ddH_2O) and 1:10 v/v β-mercaptoethanol were added. Supernatants were subsequently incubated for 5 min at 95 °C to fully denature proteins.

Denatured cell lysates were run on a 10% SDS-PAGE gel for 60 min at 120 V or until the leading edge of the lysates have nearly reached the bottom of the gel. Proteins were transferred to a nitrocellulose membrane for 1 hr at 100 V or overnight at 40 V on ice or at 4 °C. Following transfer, membranes were washed 1× with TBST prior to processing.

Membranes were blocked with 5% BSA in TBST for a minimum of 1 hr at room temperature with gentle agitation. The primary antibody was added to blocking buffer at an appropriate concentration and allowed to incubate for at least 1 hr at room temperature. Membranes were washed 3× with TBST and incubated in blocking buffer with an appropriate concentration of infrared dye-conjugated secondary antibody added. Membranes were allowed to incubate for at least 30 min at room temperature with gentle agitation. Subsequently, membranes were again washed 3× with TBST and imaged on an Odysey CLx Imaging System (LI-COR). If necessary, band densitometry was carried out using the Analyze Gels tools on ImageJ.[1]

2.6 Phagocytosis and efferocytosis assays

2.6.1 Preparation of synthetic phagocytic and efferocytic targets

IgG-coated beads were used as synthetic phagocytic targets. An equal mixture of 10 µL of 10% 5-µm polystyrene beads (vortexed and washed 1× with PBS prior to use) and 10 µL of 10 µg/mL human IgG were combined in PBS. Mixture was incubated for 90 min at room temperature or overnight at 4 °C rotating. Following incubation, beads were washed 3× with PBS (3,000 ×g, 1 min per wash) and re-suspended in 100 µL of PBS and stored for up to two weeks at 4 °C prior to use. If desired, beads may be labelled with 1 µg/mL of a fluorescently-conjugated secondary anti-human IgG antibody prior to use.

PS-coated beads were used as synthetic efferocytic targets. A lipid mixture consisting of 80% PC and 20% PS was prepared in a glass vial. If desired, a portion of the PS can be replaced with 0.1% rhodamine-conjugated PE and/or 0.1% biotin-conjugated PE to allow for fluorescent labelling of the beads. A 10 µL volume of 10% 3-µm silica beads was washed 1× with PBS (3,000 ×g, 1 min per wash) and then 1× with methanol. Beads were dried completely by incubating them for 5 min at 60 °C. Dried beads were re-suspended in 100 µL of chloroform and added to the lipid mixture. The lipid/bead mixture was vortexed well and dried under a stream of nitrogen gas for approximately 10 min or until the chloroform had completely evaporated. Beads were subsequently washed 3× with PBS

(3,000 ×g, 20 sec per wash) to completely remove any liposomes. Beads were then re-suspended in 100 µL of PBS and stored for up to two weeks at 4 °C prior to use.

2.6.2 Preparation of physiologic phagocytic and efferocytic targets

2.6.2.1 Heat killed bacteria

An overnight culture of *E. coli* ML35 prepared to provide a sufficient number of bacteria for the phagocytosis assay. Typically, a ratio between 10:1 to 100:1 bacteria-to-phagocyte was used. The desired number of bacteria was pelleted for 1 min at 6,000 ×g. Pellet was re-suspended in 500 µL of PBS. At this stage, if necessary, bacteria were heat-killed by incubating for 10 min at 70 °C. Bacteria were washed 2× with PBS.

When required, bacteria were surface biotinylated and/or labelled with a covalent fluorescent dye for downstream applications. Surface biotinylation was performed using NHS-LC-biotin. Bacteria were re-suspended in 500 µL of pH 8.0 PBS, to which 0.2 mg of NHS-LC-biotin re-suspended in 10 µL of DMSO was added. The mixture was incubated for 30 min at room temperature with gentle agitation. Excess NHS-biotin was quenched using an equal volume of PBS containing 100 mM glycine for 10 min at room temperature with gentle agitation. Biotinylated bacteria were washed 2× with PBS and re-suspended in PBS at the desired concentration. Fluorescent labelling was performed using either a CellTrace dye or an eFluor cell proliferation dye. Bacteria were re-suspended in 500 µL of PBS and 0.5 µL of the dye was added to the suspension. The mixture was incubated for 20 min at room temperature with gentle agitation away from light. Excess dye was quenched with an equal volume of PBS containing 100 mM glycine for 10 min at room temperature with gentle agitation away from light. Labelled bacteria were washed 2× with PBS and re-suspended in PBS at the desired concentration. Heat-killed bacteria were stored 4 °C up to five days whereas live bacteria were used immediately following preparation.

In some experiments, bacteria were opsonized with human serum prior to use. A solution of 20% human serum was prepared in serum-free DMEM or RPMI media. Equal volumes of bacteria and opsonin solution were mixed and incubated for 20 min at room temperature or overnight at 4 °C rotating. Opsonized bacteria were washed 1× with serum-free DMEM or RPMI prior to use.

2.6.2.2 Apoptotic cells

Apoptotic Jurkat cells were used as physiologic efferocytotic targets. Jurkat cells were grown in culture to provide a sufficient number of apoptotic cells. Typically a ratio of 10:1 apoptotic cells-to-phagocytes was used. 1×10^6 Jurkat cells were re-suspended in 1 mL of serum-free RPMI media, to which staurosporine was added to a final concentration of 1 µM. Cells were incubated for 3-16 hrs (ideally closer to 16 hrs) at 37 °C and 5% CO_2. Apoptotic cells were washed 3× with PBS to remove excess staurosporine and re-suspended in complete RPMI media prior to use.

When required, apoptotic cells were surface biotinylated and/or labelled with a covalent fluorescent dye for downstream applications. Apoptotic cells were re-suspended in 500 µL of PBS. For surface biotinylation, 0.2 mg of NHS-LC-biotin was re-suspended in 10 µL of DMSO and added to the apoptotic cells. For direct fluorescent labelling, a CellTracker dye was added to a final concentration of 2 µg/mL to apoptotic cells. The mixture was incubated for 20 min at room temperature with gentle agitation away from light. Excess biotin and/or dye was quenched with RPMI media containing 10% FBS for 5 min at room temperature with gentle agitation away from light. Labelled apoptotic cells were centrifuged for 5 min at 500 ×g and cells were re-suspended in an appropriate volume of complete RPMI or PBS.

In some experiments, apoptotic cells were opsonized with human serum prior to use. A solution of 20% human serum was prepared in serum-free DMEM or RPMI media. Equal volumes of bacteria and opsonin solution were mixed and incubated for 20 min at room temperature or overnight at 4 °C rotating. Opsonized apoptotic cells were washed 1× with serum-free RPMI prior to use.

2.6.3 Phagocytosis/efferocytosis assay

Phagocytosis and efferocytosis assays were carried out according to our labs previously published methods (Evans *et al.* and Taruc *et al.*).[2,3] A desired number of phagocytes/efferocytes along with the appropriate phagocytic/efferocytic targets were prepared as specified above. Phagocytes/efferocytes were allowed to equilibrate to room temperature in order to prevent premature target uptake. The desired number of phagocytic

and/or efferocytic targets were added and the mixture was centrifuged for 1 min at 500 ×g to force contact between phagocytes/efferocytes and targets. Assays were incubated for 30 min (IgG-coated beads), 60 min (PS-coated beads or bacteria) or 90 min (apoptotic cells). Following incubation, assays were allowed to equilibrate to room temperature to prevent any further target internalization and washed at least 2× with PBS to remove any unbound targets.

2.7 Immunofluorescence staining

2.7.1 Staining of tissue sections

Immunofluorescence staining was performed on 10-µm thick tissue sections adhered to glass slides. Sections were immersed in cold 4% PFA for 15 min at -20 °C. Sections were subsequently washed 3× 5 min with PBS and excess liquid was carefully removed from slide surface. Tissue sections were demarcated with a PAP pen to facilitate further staining. Sections were blocked using 200 µL blocking buffer (10% serum from species used for generation of secondary antibody, 0.3 M glycine, 0.1% Tween-20 and 1% BSA in PBS) for at least 1 hr at room temperature. For intracellular staining, cells were permeabilized by supplementing blocking buffer with 0.1% Triton X-100. Following blocking, the blocking buffer was removed and 200 µL of primary antibody at an appropriate concentration in blocking buffer was added to the sections. Sections were incubated with primary antibody for at least 1 hr at room temperature or overnight at 4 °C and subsequently washed 3× 15 min using 0.1% BSA and 0.1% Tween-20 in PBS. Sections were then incubated with 200 µL of 1 µg/mL secondary antibody for at least 30 min at room temperature and subsequently washed 3× 15 min using 0.1% BSA and 0.1% Tween-20 in PBS. Coverslips were glued to sections using Permafluor mounting reagent and stained sections were kept at 4 °C until imaging.

2.7.2 Staining of cells

Cells to be stained were grown on 18 mm, #1.5 thickness round coverslips placed into the wells of a 12-well tissue culture plate. Prior to staining, cells were equilibrated to room

temperature to prevent membrane turnover and washed 1× with PBS. Cells were fixed with 4% PFA for 20 min at room temperature and subsequently washed 3× 5 min with PBS to remove excess PFA. Fixed cells were blocked with 5% PBS (supplemented with 10% serum if the cells to be stained were FcγR-expressing phagocytes) for at least 20 min at room temperature. For intracellular staining, cells were permeabilized by supplementing the blocking buffer with 0.1% Triton X-100, and the length of the blocking period increased to at least 1 hr. Blocking buffer was removed and primary antibody in blocking buffer was added to the cells and allowed to incubate for 30 min (without permeabilization) or 60 min (with permeabilization) at room temperature. Cells were washed 3× 5 min (without permeabilization) or 3× 15 min (with permeabilization). Secondary antibodies in blocking buffer was added and allowed to incubate for 30 min at room temperature. Cells were again washed 3× 5 min (without permeabilization) or 3× 15 min (with permeabilization). Coverslips were mounted onto glass slides using Permafluor mounting reagent and stored at 4 °C until imaging.

2.8 Patient tissue samples

2.8.1 Human research ethics

Patient tissues used in this study were obtained under a discarded tissue protocol from patients undergoing elective coronary artery bypass graft (CABG) surgery at London Health Sciences Centre. This study was reviewed and approved by the Office of Human Research Ethics at Western University Health Sciences Research Ethics Board (HSREB Reference Number: 107566). Since this is a discarded tissue study, we did not collect any personal health information, personal identifying information or clinical data nor were we required to obtain informed consent from patients' whose tissues were used in this study.

2.8.2 Surgical specimen preparation

Aortic punch tissue specimens were obtained intra-operatively by a cardiac surgeon using a 4.0-mm diameter CleanCut RCL Aortic Punch (QUEST Medical) and placed into cold

saline. Specimens were then bisected evenly using clean surgical scissors, with one half of the tissue used to prepare frozen sections and the other for preparing paraffin sections.

2.8.3 Tissue sectioning

2.8.3.1 Frozen sections

For laser capture microdissection, tissue specimens used for frozen sections were immediately embedded in OCT freezing compound and frozen on dry ice over a period of 5-10 min and placed into -80 °C for storage. No more than 30 min was allowed to elapse between the time at which aortic punch tissue specimens were excised and placement of the frozen, OCT-embedded tissue into -80 °C for storage. Frozen sections were subsequently obtained from OCT-embedded tissue on a cryostat at a 10-µm thickness onto clean, RNase-free glass microscope slides.

For immunofluorescence, Oil Red O staining and all other downstream applications, tissue specimens were fixed in fresh (< 1 week old) 4% paraformaldehyde for 24 hr at 4 °C. Fixed specimens were placed into PBS with 15% sucrose for approximately 4 hr (or until the tissue sinks) and then into PBS with 30% sucrose overnight at 4 °C. Fixed, cryopreserved tissue specimens were then embedded in OCT freezing compound and frozen on dry ice over a period of 5-10 min and placed into -80 °C for storage. Frozen sections were subsequently obtained from OCT-embedded tissue on a Leica CM1900 Cryostat at a 10-µm thickness onto clean Superfrost Plus microscope slides (Fisherbrand).

2.8.3.2 Formalin sections

Tissue specimens used for formalin-fixed, paraffin-embedded (FFPE) sections were fixed in fresh (< 1 week old) 4% paraformaldehyde for 24 hr at 4 °C. Fixed specimens were stored in 70% ethanol until ready for further processing. For paraffin infiltration, specimens were dehydrated through immersion in changes of ethanol of increasing concentration (70% ethanol for 1 hr, 95% ethanol for 1 hr, and four changes of 100% ethanol for 1/1.5/1.5/2 hr), cleared with two changes of xylene for 1 hr each and immersed in two changes of paraffin wax at 58 °C for 1 hr. Processed tissues were embedded into paraffin

blocks. FFPE tissues were subsequently sectioned on a microtome at a 5-µm thickness onto clean glass microscope slides.

2.9 Mouse work

Use of animals for this study was obtained from the Western University Animal Care Committee under Animal Use Protocol (AUP) 2018-131:1. LDL receptor-deficient (*Ldlr*$^{-/-}$) C57BL/6J mice were put on either a high-fat, high-cholesterol (15% fat, 1% cholesterol) diet or a chow control for a period of 12 weeks. Animals were subsequently sacrificed, with thoracic aortas being subsequently surgically isolated for further processing.

2.10 Microscopy

Microscopy was used to visualize tissue histology and perform quantification of fluorescence intensity. In all cases, at least three biological replicates were analyzed. For measurement of fluorescence within individual cells, a minimum of 30 cells were quantified. To minimize observer bias, random fields of view were captured whenever possible.

2.10.1 White light

Tissue section immunohistochemistry, TUNEL assay and Oil Red O-stained cells were imaged using an inverted-stage white light microscope equipped with a digital camera running Northern Eclipse image analysis software (EMPIX Imaging) using a 5× or 10× objective lens.

2.10.2 Epifluorescence

Imaging of immunofluorescently-stained frozen sections and immunofluorescently-stained cells was performed using a Leica DMI6000B epifluorescence microscope equipped with a Sedat Quad filter set (Chroma) and operated by Leica LAX software.

For imaging of Rab protein recruitment to phagosomes and efferosomes or for co-localization experiments, samples were imaged using a 100×/1.40NA objective lens and an Evolve-512 delta EM-CCD camera (Teledyne Photometrics).

For imaging of phagocytosis and efferocytosis assays, peptide citrullination assays, dextran fusion assays, nitro blue tetrazolium assays or for confirming the expression of a fluorescently-tagged protein, samples were imaged using a 63×/1.40 NA objective lens and the Evolve EM-CCD camera. If needed, z-sections were captured for apoptotic cell efferocytosis assays across the entire depth of the efferocyte separated by 0.5 µm between stacks.

For imaging of whole immunofluorescently-stained tissue sections, samples were imaged using a 40×/1.00NA objective lens and the ORCA-Flash4.0 V3 Digital CMOS camera (Hamamatsu Photonics) with the Leica LAX Tile Scan Merge function to capture the entirety of the aortic wall intima.

2.10.3 Live cell

Cells to be imaged were grown on No. 1.5 thickness 8-mm round glass coverslips and transferred to a Leiden chamber and placed into a heated and CO_2-perfused chamber attached to the piezoelectric stage of a Leica DMI6000B epifluorescence microscope. Between 5-10 cells of interest were marked using the Mark and Find feature of the Leica LAX software and live cell acquisitions of each cell were obtained at 0.5-1 frames/min over a period of 1-8 hrs.

2.11 Image analysis

All image analysis was performed using the FIJI distribution of ImageJ unless otherwise stated.[1,4] Specific methods are described in detail in individual methods sections for each following chapter.

In general, measurement of fluorescence intensity was performed by forming a selection around the region of interest (ROI) and using the Measure feature to obtain the area and

integrated density of the ROI. Background fluorescence was measured by drawing a ROI around a region free of any cells or other features and measuring the mean. Background subtraction was performed on fluorescence intensity measurements by subtracting from integrated density the product of background mean and the measurement ROI area.

Unless otherwise specified, co-localization analysis was performed using the JACoP plugin on ImageJ to determine Pearson's coefficient.[5]

2.12 Statistical analysis

All statistical analysis was performed on GraphPad Prism 6 software. Comparison between two means made use of an unpaired, two-tailed Student's t test or Mann-Whitney U test when the sample distribution was noted to be non-normal. For comparison of multiple means, we employed 1-way or 2-way ANOVA as appropriate with the Holm-Sidak multiple comparisons test when comparing multiple means with a single mean or the Tukey's range test when comparison multiple means with every single other mean.

2.13 References

1. Schneider CA, Rasband WS, Eliceiri KW. NIH Image to ImageJ: 25 years of image analysis. *Nat Methods*. 2012;9(7):671-675. doi:10.1038/nmeth.2089

2. Evans AL, Blackburn JWD, Yin C, Heit B. Quantitative efferocytosis assays. *Methods Mol Biol*. 2017;1519:25-41. doi:10.1007/978-1-4939-6581-6

3. Taruc K, Yin C, Wootton DG, Heit B. Quantification of Efferocytosis by Single-cell Fluorescence Microscopy. *J Vis Exp*. 2018;(138):1-12. doi:10.3791/58149

4. Schindelin J, Arganda-Carreras I, Frise E, et al. Fiji: an open-source platform for biological-image analysis. *Nat Methods*. 2012;9(7):676-682. doi:10.1038/nmeth.2019

5. Bolte S, Cordelieres FP. A guided tour into subcellular colocalisation analysis in light microscopy. *J Microsc*. 2006;224(3):13-232.

Chapter 3

3 The Small GTPase Rab17 is a Key Regulator of Efferosome Maturation Under Homeostatic Conditions

3.1 Introduction

3.1.1 Regulation of efferosome maturation under homeostatic conditions

Appropriate regulation of efferocytic clearance of apoptotic cells and subsequent maturation of the resultant efferosome are crucial for the proper maintenance of tissue homeostasis.[1–3] Much of what is currently known about the regulation of efferosome maturation is derived from studies in a *Caenorhabditis elegans* model, where the early stages of efferosome maturation appears to proceed similarly to canonical phagosome maturation.[4] Efferosome and phagosome maturation is described in detail in **Chapter 1.1.5**, but briefly, the small GTPase Rab5 is recruited to the surface of the nascent efferosome, followed by a rapid exchange of Rab5 for Rab7 mediated by the Mon1-Ccz1 complex.[5,6] Rab7 subsequently mediates the recruitment of effector molecules such as RILP and ORPL1, which are required for efferosomal-lysosomal fusion, and VTPases that drive efferosomal acidification.[7–10] The result of this process is the formation of an efferolysosome where, akin to a phagolysosome, the apoptotic cell cargo is degraded.[11]

3.1.2 Differential regulation of phagosome and efferosome maturation

Although the mechanisms that govern phagosome and efferosome maturation are similar, there are drastic differences in the immunological outcomes of phagocytosis versus efferocytosis.[11,12] Whereas phagocytosis is a pro-inflammatory process that results in inflammation and antigen presentation, efferocytosis is immunologically silent and instead drives resolution of inflammation.[12] The ultimate fate of efferocytic and phagocytic cargoes must therefore also differ.[13,14] Phagocytic cargoes are degraded and subsequently loaded onto MHC class II molecules for antigen presentation, whereas efferocytosis does not result in antigen presentation.[13]

3.1.3 The Rab family of GTPases

The Rab ("Ras-related in brain") family is a part of the Ras superfamily of small GTPases and function as master regulators of intracellular vesicular trafficking.[15] Rab GTPases are found ubiquitously across all eukaryotes studied to date, with more than 60 family members identified in the human genome alone.[16,17] Members of the Rab family all possess a distinctive set of five α helices surrounding a six-stranded β sheet. This structure is common to all members of the Ras superfamily and contain structures responsible for guanine nucleotide binding activity.[18] Additionally, Rab GTPases contain two regions termed switch I and switch II, which contain distinctive RabF regions that can be used to identify Rab GTPases and undergo conformational changes depending on whether the Rab is in an active GTP-bound or an inactive GDP-bound state. Finally, individual Rab family members contain RabSF regions, which are thought to be responsible for binding with specific effector molecules.[15,16] An illustration of the common structural features of the Rab GTPases is provided in **Figure 3.1**.

Figure 3.1 Common structural features of the Rab family of small GTPases. (on opposite page)

Ribbon diagram of the crystal structure of Rab3A complexed with the GTP analog GppNHp. Purple – bound nucleotide; orange sphere – Mg^{2+} ion; blue – switch I and II regions; green – α helices and β sheets; yellow – loops. (**a**) A consensus amino acid sequence of the Rab GTPase family. Red – Rab-specific residues (RabF1-5); dark blue – subfamily-specific motifs (RabSF1-4); cyan – highly conserved nucleotide-binding motifs; G – guanine base-binding motif; PM – phosphate/magnesium-binding motif. (**b**) The secondary structure units (α helices, β strands, and loops, λ) are indicated above the sequence. Figure modified from Stenmark and Olkkonen.[15]

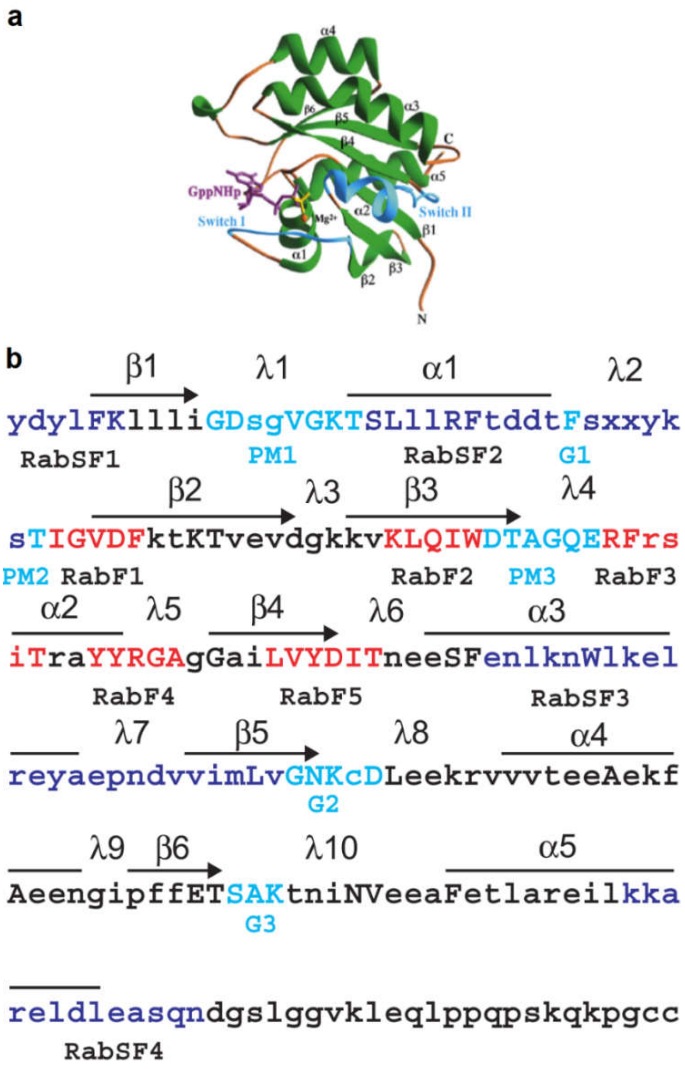

Newly-synthesized Rab GTPases are bound by a Rab escort protein (REP), which first recruits a geranylgeranyl transferase enzyme that mediates transfer of a hydrophobic geranylgeranyl group to the carboxyl terminus of the protein.[19,20] This post-translational modification allows the Rab to anchor itself to cellular membranes.[20] Specific targeting of Rab GTPases to the appropriate membrane surface is thought to result from an interaction between the Rab-REP complex and receptors on the target membrane.[21] At this stage, the Rab is in an inactive, GDP-bound conformation. Inactive Rab's can become activated via GTP-GDP exchange mediated by a GEF. The activate Rab is then able to recruit specific downstream effector molecules. Active Rab's can be inactivated by a GAP, which cleaves the bound GTP to GDP.[22,23]

Table 3.1 Rab-family GTPases implicated in phagosome maturation. Modified from Kinchen and Ravichandran.[11]

Protein	Function
Rab1	ER-to-Golgi transport
Rab2	ER-to-Golgi transport
Rab3	Exocytosis
Rab4	Membrane and receptor recycling
Rab5	Marker of the early endosome
Rab6	Retrograde transport, Golgi-to-ER transport
Rab7	Trafficking from early to late endosome or lysosome
Rab8	Trafficking between Golgi, endosomes and plasma membrane
Rab9	Lysosomal enzyme trafficking, late endosome-to-Golgi transport
Rab10	Transport from Golgi to polarized membranes (basolateral face)
Rab11	Marker of the recycling endosome, trafficking of between the recycling endosome and cell surface
Rab14	Phagosome and early endosome fusion, trafficking between early endosomes and Golgi
Rab20	Localized to apical membranes and Golgi complexes, potentially involved in vacuolar-ATPase trafficking
Rab22	*Trans*-Golgi-to-endosome transport
Rab23	Localized to endosomes and plasma membrane
Rab32	Localized to the mitochondrion
Rab33	Retrograde transport from Golgi to ER
Rab35	Cytokinesis

Rab GTPases play many key functions in the regulation of almost every component of intracellular vesicular trafficking.[11,22,24] Rab5 and Rab7 are key markers of the early and late phagosome/efferosome respectively and play crucial functions in the regulation of proper phagosome and efferosome maturation.[6,25] Rab4 and Rab11 are members of this family that have been implicated in membrane and receptor recycling. Rab4 is required for the recycling of receptors from the early endosome to the cell membrane while Rab11 is a marker of the recycling endosome and required for trafficking of receptors from the RE to the cell surface.[26–28] A final example is Rab27, which plays an important role in regulated secretion across multiple cell types and appears to play a key role in mediating granule release from secretory cells such as melanocytes, neurons and neutrophils.[29–31]

Unsurprisingly, there are a multitude of Rab GTPases involved in the regulation of phagosome/efferosome maturation (**Table 3.1**). These include the classical Rab5 and Rab7 but also a number of Rab family members involved in transport between the endoplasmic reticulum and Golgi and the Golgi and other vesicles.

3.1.3.1 Rab17

One member of the Rab GTPase family of particular interest to us is Rab17 as it appears as a protein that is uniquely recruited to the efferosomal surface in the mass spectrometry experiments described below. Rab17 was initially identified in the 1990's in epithelial cells and enterocytes as a key regulator of transcytosis and membrane recycling in polarized cells.[32–34]

Since then, the presence and function of Rab17 has been described in a number of polarized and secretory cells, including hepatocytes[35,36], neurons[37] and melanocytes[38]. In the liver, Rab17 appears to play a key role in regulating the basolateral-to-apical transcytosis in hepatocytes and that sumoylation was required in addition to GTP-binding for Rab17 activity.[35,36] In the brain, Rab17 is expressed in neurons of the hippocampus and regulates formation and post-synaptic growth of dendrites.[37] It is also found in brain epithelial cells, where it again appears to regulate the formation of "sorting tubules" that mediate the transcytosis of cargoes across the blood-brain barrier.[39] In melanocytes, Rab17 is found to be associated with the RE and Rab17 knockdown resulted in impaired filopodia formation and melanosome release.[38] A detailed mechanistic study of Rab17 involvement in transcytosis by Striz *et al.*[36] revealed that it is able to associate with transcytotic vesicle-specific VAMP's and interact with syntaxin 2 at the apical membrane to initiate vesicle fusion.

Importantly, a dominant-negative (DN) mutant of Rab17 has been previously described and characterized.[32] This mutant contains a single asparagine to isoleucine mutation in the NKXD motif, which is highly conserved within GTPase proteins and is required for binding to GTP and conversion to the protein's active form.[40,41] DN-Rab17 does not appear to interact with syntaxin 2 and cells expressing DN-Rab17 displayed impair trafficking of

apical proteins via transcytosis, suggesting that expression of DN-Rab17 impairs proper cargo trafficking.[35]

3.1.4 Rationale and importance

Despite being a crucial mechanism for the maintenance of tissue homeostasis, efferocytosis and the mechanisms that regulate efferosome maturation remain poorly understood. Much of what is known about efferosome maturation is derived from either knowledge of phagosome maturation or from studies in model organisms such as *C. elegans*.[6] As phagocytosis and efferocytosis have radically different immunological outcomes, it is reasonable to expect that phagosomes and efferosomes undergo different maturation programs.[12] To date, we still lack a clear understanding of how phagosome and efferosome maturation are differentially regulated.

In the present chapter, we use a mass spectrometric approach towards identifying proteins that are uniquely recruited to phagosomes vs. efferosomes as potential regulators of differential maturation. We then utilize fluorescence microscopy to track differential recruitment of regulators to the phagosome and efferosome surfaces and examine the effects of the knockdown of regulators on phagosomal and efferosomal cargo fate.

Efferocytosis plays an important role in limiting inflammation and promoting resolution.[3,42] Failure of efferocytosis has been implicated in the pathophysiology of a number of inflammatory and autoimmune diseases, including atherosclerosis,[43–45] systemic lupus erythematosus[46,47] and multiple sclerosis.[48] Despite this, factors that regulate efferosome maturation under homeostatic conditions remain poorly understood. A clearer picture of how efferosome maturation is regulated will allow us to gain a better understanding of how efferosomal cargo is degraded without antigen presentation and will form the basis of investigating how this process begins to break down in autoimmune disease.

3.2 Methods

3.2.1 Rab17 cloning

Human Rab17 was cloned into pEGFP-C1 and pmCherry-C1 backbones using the method described in **Chapter 2.3.1**. A dominant-negative (N132I) Rab17 construct[35] was prepared by amplifying the above construct with DN Rab17-specific 5′ phosphorylated primers using the standard PCR cycle with a 7 min elongation time. Parental plasmid was removed by the addition of 1:50 (vol/vol) DpnI to the reaction and incubating for 1 h at 37 °C. The resulting PCR product was then gel purified, re-circularized by incubating overnight at 16 °C with T4 ligase and subsequently transformed into *E. coli* as described in **Chapter 2.5.1**. See **Appendix A** for primer sequences.

3.2.2 Phagocytosis/efferocytosis assays

Synthetic IgG- and PS-coated beads were prepared using the methods described in **Chapter 2.6.1** while heat-killed *E. coli* and apoptotic Jurkat cells were prepared as described in **Chapter 2.6.2**. Phagocytosis and efferocytosis assays were performed following the methods described in **Chapter 2.6.3** with proteins of interest labelled following blocking/permeabilization by addition of primary antibodies (1:1000 anti-MHC class II, 1:500 anti-LAMP1, 1:200 anti-Rab17) followed by fluorescently tagged Fab's (1:1000 to 1:2500).

3.2.3 Quantification of Rab17 recruitment to phagosomes/efferosomes

Quantification of Rab17 recruitment was performed in MATLAB using modified forms of previously published vesicle-tracking and intensity quantification algorithms.[49–51] Briefly, 90-120 min time-lapse videos were captured of macrophages ectopically expressing the plasmalamellar marker PM-RFP, GFP-tagged Rab17 and far-red-labeled phagocytic/efferocytic targets. TIFF stacks of individual cells were then exported, and a local threshold applied to the target channel using a local neighborhood 2× the size of the targets. Targets were then identified using the 'bwlabel' command in MATLAB and the targets tracked using a robust tracking algorithm.[50,52] Image channels corresponding to PM-RFP and Rab17 were subjected to a global background subtraction, with no other

processing applied, to maintain linearity of intensity data. Internalized targets were defined as targets that colocalized with a distinct PM-RFP structure that was no more than 1.4× (beads) or 2× (*E. coli* or apoptotic cells) the diameter of the phagocytic/efferocytic target, and the first frame in which the target colocalized with a distinct PM-RFP structure was set as the 0 min timepoint of phagocytosis/efferocytosis. All tracks were manually curated to ensure accuracy, with any tracks lasting less than 15 min rejected from subsequent analyses. Recruitment of Rab17 to the PM-RFP/target structure was then measured at all subsequent timepoints and normalized to the maximum intensity Rab17 structure in the cell.

3.2.4 Colocalization analysis

Colocalization of signaling molecules with phagosomes and efferosomes in fixed cells was also quantified using MATLAB. Z-stack images of cells were captured and deconvolved using an iterative deconvolution approach. A ROI was manually drawn around each cell and the mean ± SEM of the fluorescence intensity of each channel within the ROI determined. Phagocytic/efferocytic targets were then identified using the local background subtraction and thresholding approach described in the previous subsection but using the 'bwlabeln' MATLAB command to identify targets in the 3D images. Each target was converted into a 3D ROI by identifying the bounding pixels of each target using the 'convhull' command. These ROIs were then expanded by a factor of 1.4× to ensure that the bounding PM-RFP and any recruited signaling molecules would be captured without significant inclusion of cytosolic staining. Targets were scored as associated with a molecule of interest if the mean intensity of the molecule of interest in each ROI was two SD higher than the mean intensity of the molecule throughout the entire cell. As with the Rab17 recruitment analysis described above, no intensity adjustments other than a global background subtraction were applied to the images of the signaling molecules to preserve linearity of the image intensity data.

3.2.5 Efferosome mimics quantification

Quantification of mimic-containing efferosomes was performed to measure the formation of efferosome-derived vesicles (EDVs). Time-to-fragmentation was measured from the

timepoint of complete efferosome closure to timepoint when fission of the first Rab17^{+} EDV was observed. The number of EDVs formed from each efferosome was recorded and the diameter of each EDV was quantified using the line measurement tool.

3.2.6 Efferosome fission, fusion and movement

Efferosomes were tracked in fluorescent images. At the timepoint of complete efferosome closure an ROI was drawn around the cell using the freehand selection tool, and the x/y coordinates of the cell barycentre determined with the measure tool. The MTrack2 plugin was used to track the efferosome, EDVs, and any EDV-interacting Rab17^{+} vesicles. Track positions were imported into MATLAB, the timing and location of all fission and fusion events annotated, and the track divided into pre- vs. post-initial fission segments. Pre-fission tracks were translated such that all measurements were made relative to a vector linking efferosome closure site to the cell barycentre, and post-fission tracks translated such that all measurements were made relative to a vector linking the fission site to the cell barycentre. The directionality of movement of each track was then quantified as the ratio between the Euclidian distance covered by the vesicle from its start- to end-point vs. the total distance traveled.[53,54]

3.2.7 Efferosome positioning

Efferosome positioning was quantified using the method of Johnson *et al.*[55] Images were imported into FIJI[56,57] and the cell boundary, as defined by the Rab17 staining, traced using the freehand tool. This ROI was then degraded inwards in 1 mm increments to create 3 shells of 1 mm thickness. The number of EDVs in each shell, EDV diameter (sub-resolution EDVs were recorded as 0.2 mm in diameter), and colocalization with LAMP or TfR was quantified in each image using the methods described above.

3.3 Results

3.3.1 Efferosomes and phagosomes share a common early maturation pathway

Phagocytic cargos are degraded by a well-characterized maturation pathway in which the sequential acquisition of Rab5 and Rab7 mediates the sequential fusion of early endosomes, late endosomes and lysosomes with the phagosome.[8] Evidence from *C. elegans* and mammalian cell lines indicate that this same maturation pathway degrades efferocytosed apoptotic cells.[4] However, these studies did not use professional antigen presenting cells (pAPCs), which may use an alternative pathway to avoid antigen presentation following uptake of apoptotic cells.

To test whether apoptotic cells were trafficked through a novel maturation pathway in pAPCs, we tracked the recruitment of ectopically expressed Rab5-GFP and Rab7-RFP in J774.2 macrophages engaged in phagocytosis (**Figures 3.2a** and **3.2c**) or efferocytosis (**Figures 3.2b** and **3.2d**) of 5 μm diameter synthetic phagocytic or efferocytic targets. Both efferosomes and phagosomes sequentially recruited Rab5 and Rab7, with efferosomes transitioning from a Rab5-positive to Rab7-positive compartment with slightly slower temporal dynamics than phagosomes (**Figures 3.2c** and **3.2d**). To confirm that both phagosomes and efferosomes were completing maturation, we immunostained human PBMC-derived M0 macrophages for the lysosomal marker LAMP1 40 min after engulfment of synthetic phagocytic or efferocytic targets (**Figure 3.2e**). Significant LAMP1 accumulation was observed on phagosomes and efferosomes, confirming that vacuoles containing both types of cargo fuse with lysosomes. Finally, we assessed the possibility that macrophage polarization may result in the selective uptake of phagocytic versus efferocytic targets (**Figure 3.2f**).

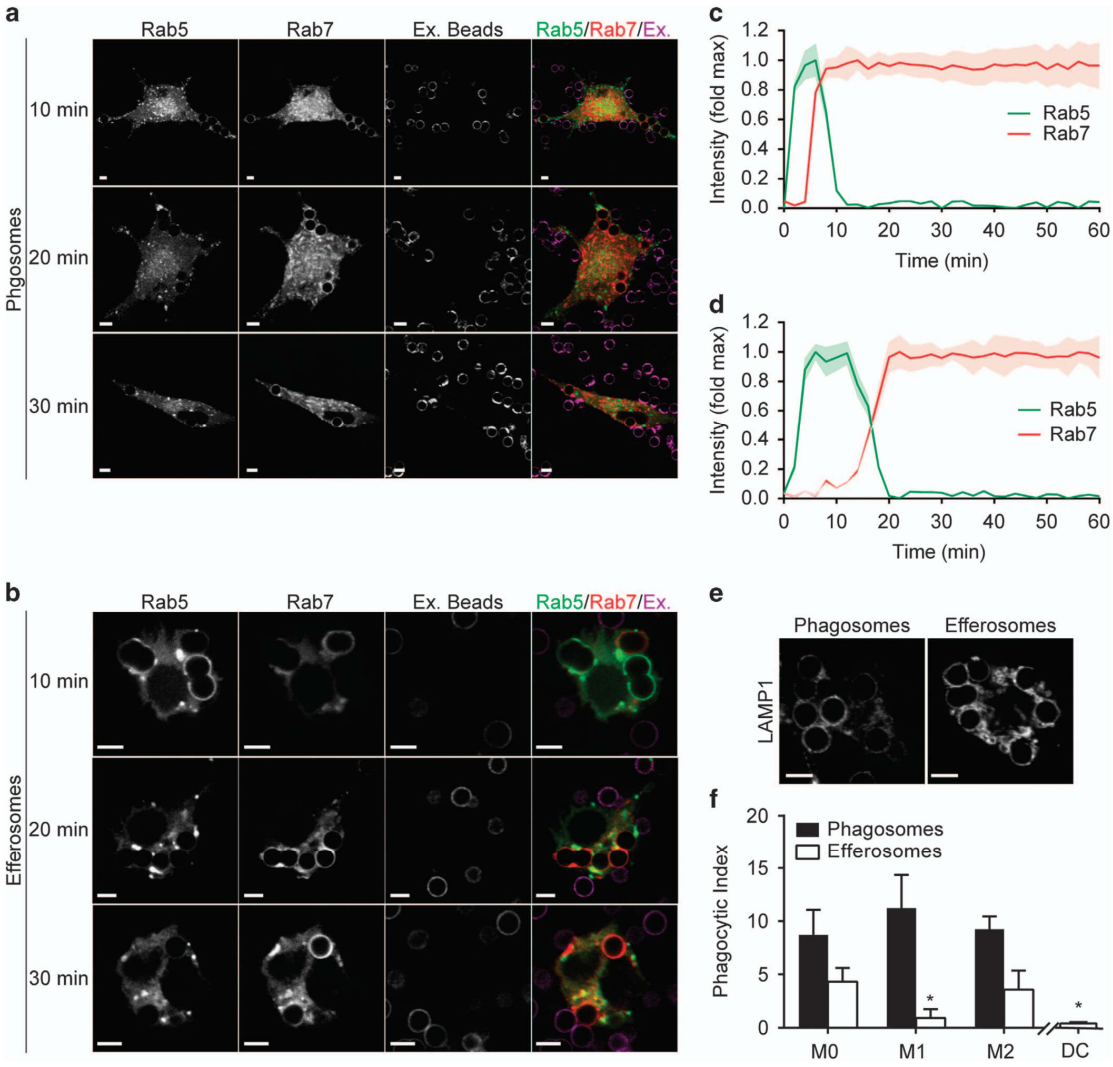

Figure 3.2 Efferosomes and phagosomes share a common early maturation pathway. (on opposite page)

Fixed and live cell microscopy was used to assess the localization of Rab5, Rab7 and the lysosomal marker LAMP1 to efferosomes and phagosomes containing 5 μm diameter bead-based mimics of apoptotic cells and bead-based mimics of pathogens. (**a** and **b**) Recruitment of Rab5 and Rab7 to phagosomes (**a**) and efferosomes (**b**) 10, 20 and 30 min following engulfment by J774.2 macrophages. Ex. Beads indicates noninternalized (i.e. extracellular) beads. (**c** and **d**) Dynamics of Rab5 and Rab7 recruitment to phagosomes (**c**) and efferosomes (**d**). T = 0 is set as the video frame when complete sealing of the

phagosome/efferosome was observed; data are normalized to maximum Rab5 or Rab7 intensity on each individual phagosome. (**e**) Immunostaining of LAMP1 accumulation in phagosomes or efferosomes in human PBMC-derived M0 macrophages. (**f**) Uptake of apoptotic cell mimics (Efferosomes) and IgG-opsonized pathogen mimics (Phagosomes) by human PBMC-derived M0-, M1- and M2-polarized macrophages and DCs, expressed as the number of beads engulfed per cell. Data are representative of (**a**, **b** and **e**) or quantifies (**c**, **d** and **f**) at least 30 cells imaged across five independent experiments. Data are presented as mean or mean ± S.E.M. *$p < 0.05$ compared with uptake of the same type of target by M0 macrophages. Scale bars are 5 μm.

M0 and M2 macrophages were highly efferocytic, while M1 macrophages and primary human dendritic cells were poorly efferocytic. Furthermore, no selectivity was observed for phagocytic targets, indicating that any capacity to differentially present efferosomal versus phagosomal antigens must occur following both target engulfment and the canonical Rab5/Rab7-mediated maturation pathway.

3.3.2 Mass spectrometric identification of late regulators of efferosome and phagosome maturation

Given that efferosomes and phagosomes shared the same early maturation pathway, any selective processing of these targets likely occurs at a later timepoint. As such, we recovered efferosomes and phagosomes using 3 μm diameter magnetic bead mimics of efferocytic and phagocytic targets from M0-polarized human macrophages, 40 min after initiation of efferocytosis or phagocytosis. Proteins from the recovered efferosomes and phagosomes were resolved using SDS-PAGE, revealing several proteins selectively recruited to efferosomes versus phagosomes (**Figure 3.3**).

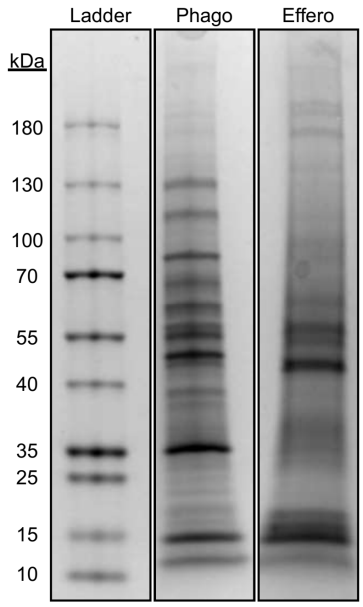

Figure 3.3 Efferosomes and phagosomes interact with unique subsets of proteins.

Coomassie staining of SDS-PAGE gels of proteins recovered from phagosomes (phago) and efferosomes (effero) 40 min following phagocytosis or efferocytosis of 3 μm IgG- or PS-coated magnetic beads. Phagosomes and efferosomes were recovered by magnet from human PBMC-derived M0-polarized macrophages following cell lysis.

These unique proteins were subsequently excised and identified by liquid-chromatography/mass spectrometry. Phagosomes (**Table 3.2**) contained many of the proteins expected of a vesicle maturing into an MHC class II loading compartment, notably MHC class II and indicators of Golgi-to-lysosome trafficking (Rab6b, PIK4). In addition, phagosomes were enriched in several proteins involved in GTPase and kinase signaling. In marked contrast, efferosomes (**Table 3.3**) lacked MHC class II and the markers of Golgi-to-lysosome trafficking observed on phagosomes. Efferosomes instead recruited proteins that mediate vesicular trafficking, cytoskeletal organization and ubiquitination/ ISG15ylation. Of particular interest to us were the Rab family GTPases Rab17 and RASEF (Rab45), both of which have been implicated in trafficking to recycling endosomes and exocytosis.[34,38,58,59] Combined, these results suggest that efferocytic cargos are intercepted before formation of the MHC class II loading compartment and are redirected to a recycling or exocytic cellular compartment.

Table 3.2 Unique proteins recruited to phagosomes 40 min post-phagocytosis.

Protein name	Symbol	Peptides[a]	% Coverage[b]
Vesicular trafficking and antigen presentation			
MHC class I	MR1	62	34.3
MHC class II	HLADQB1	58	22.2
Annexin A2	ANXA2	57	19.9
Phosphatidylinositol-4-kinase	PIK4	56	20.1
Rab6B	Rab6b	83	39.9
CTTNBP2NL	CTTNBP2NL	204	31
GTPase and kinase signaling			
Insulin-like growth factor binding protein 2	IGFBP2	126	38.8
Misshapen-like kinase 1	MINK1	91	7.01
Cyclin-Y-like protein 2	CCNYL2	58	33.3
Lymphoid enhancer-binding factor 1	LEF1	89	29.4
RalA-binding protein 1	RALBP1	82	17.7
Serine/threonine-protein kinase 4	STK4	29	10.6
NOD3	NLRC3	111	15.5
5′-AMP-activated protein kinase β1	PRKAB1	15	6.05
GIMD1	GIMD1	24	11.1
Cyclin-dependent kinase 4	CDK4	20	18.0
DOCK10	DOCK10	58	10.7
Other			
Acylphosphatase-1	ACYP1	37	43.5
Cytotoxic T-lymphocyte protein 4	CTLA4	46	26.4
Type I inositol(1,4,5)trisphosphate 5 phosphatase	INPP5A	30	96.8
Abhydrolase domain containing 1	ABHD1	63	33.9
Lactate dehydrogenase c	LDHC	41	42.7
Striatin, calmodulin-binding protein 3	STRN3	48	10.8
CKLF-like MARVEL transmembrane domain-containing protein 1	CMTM1	14	11.5
Interferon-stimulated 20 kDa exonuclease-like 2	ISG20L2	12	8.70

[a]Peptides = total number of peptides from each protein identified across three independent experiments.
[b]% Coverage = portion of protein sequence covered by the identified peptides

Table 3.3 Unique proteins recruited to efferosomes 40 min post-efferocytosis.

Protein name	Symbol	Peptides[a]	% Coverage[b]
Vesicular trafficking and cytoskeleton			
Rab17	Rab17	69	36.3
RASEF (Rab45)	RASEF	32	72.7
Vacuolar protein sorting-associated protein 33B	VPS33B	95	16.6
Talin 1	TLN1	198	7.79
Rac2	RAC2	19	12.8
MAP4	MAP4	119	13.9
Liprin β1	PPFIBP1	86	31.6
Prostaglandin F2 receptor-negative regulator	PTGFRN	89	11.3
WAS/WASL-interacting protein family member 3	WIPF3	48	14.7
Ubiquitination/ISG15ylation			
E3 ubiquitin/ISG15 ligase TRIM25	TRIM25	85	20.1
Ubiquitin carboxyl-terminal hydrolase 15	USP15	115	12.1
F-box-only protein 6	FBXO6	74	21.9
Kinase and calcium signaling			
Serine/threonine-protein phosphatase 2A regulatory subunit B	PPP2RC3	46	10.2
MAP kinase-interacting serine/threonine-protein kinase 1	MKNK1	12	5.29
Calsyntenin 2	CLSTN2	49	8.06
Glycogen synthase kinase-3β	GSK3B	18	100
Receptors and opsonins			
Galectin-3	LGALS3	69	47.3
Mannan-binding lectin serine protease 1	MASP1	13	15.5
CD36	SCARB1	18	58.1
Other			
Leucine-rich repeat neuronal protein 1	LRRN1	48	57.1
Inositol monophosphatase 2	IMPA2	72	27.6
Alkaline phosphatase, tissue-nonspecific isozyme	ALPL	10	66.7

[a]Peptides = total number of peptides from each protein identified across 3 independent experiments.
[b]% Coverage = portion of protein sequence covered by the identified peptides

3.3.3 Rab17 is persistently recruited to efferosomes but not phagosomes

To assess the role of Rab17 in phagocytosis and efferocytosis, we performed live cell microscopy of J774.2 macrophages ectopically expressing the plasma membrane marker PM-RFP and Rab17-GFP as they engulfed beads mimicking efferocytic or phagocytic targets. As expected, both phagocytic and efferocytic targets were internalized into plasma membrane-derived vacuoles demarcated by PM-RFP (**Figures 3.4a** and **3.4b**). Rab17 transiently localized to phagosomes, with dynamics similar to that of Rab5 (**Figures 3.4a** and **3.4c**). In marked contrast, Rab17 was persistently recruited to efferosomes, displaying only a modest decrease in recruitment over the hour following engulfment of the efferocytic target (**Figures 3.4b** and **3.4c**). Close inspection of individual efferosomes revealed that this recruitment was not constant, and rather that Rab17 is repeatedly recruited in a series of waves, suggestive of repeat sampling of efferosomes by Rab17 (**Figure 3.4d**).

Figure 3.4 Rab17 is selectively retained on efferosomes. (on opposite page)

Live cell microscopy was performed on J774.2 macrophages expressing PM-RFP and Rab17-GFP engulfing apoptotic cell (Efferosomes) or IgG-opsonized pathogen (Phagosomes) mimics. (**a** and **b**) Representative images of Rab17-GFP recruitment to phagosomes (**a**) or efferosomes (**b**). Star/arrowhead tracks the same phagosome/efferosome through successive time points. (**c**) Dynamics of Rab17 recruitment to phagosomes and efferosomes. (**d**) Recruitment dynamics of Rab17-GFP to three representative efferosomes. (**c** and **d**) T = 0 is set as the video frame when complete sealing of the phagosome/efferosome was observed and data are normalized to maximum Rab17 intensity on each individual phagosome. Data are presented as mean ± SEM (**c**) or mean (**d**). Data are representative of (**a**, **b** and **d**) or quantifies (**c**) a minimum of 22 cells imaged over four independent experiments. Scale bars are 5 μm.

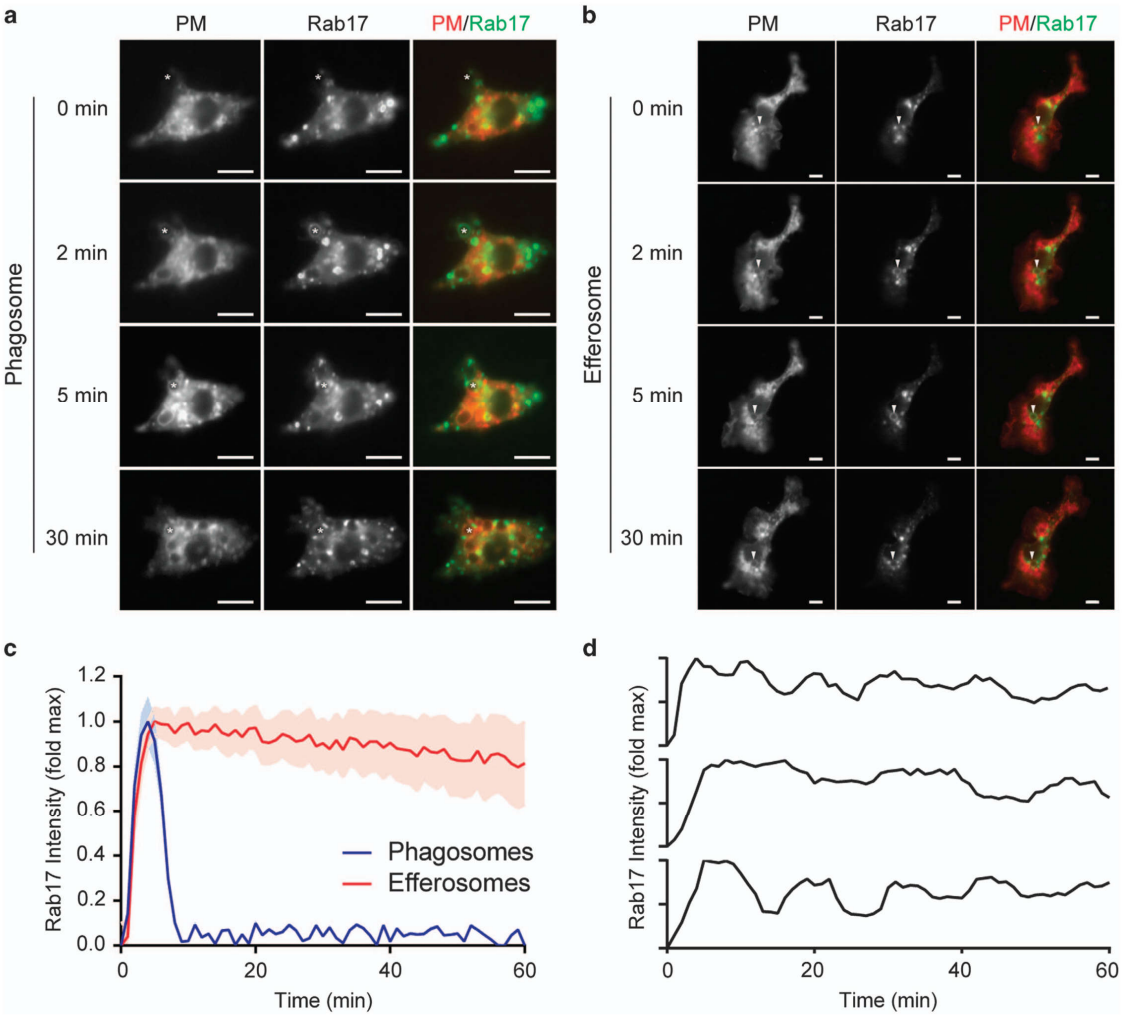

Rab17 expression was observed in primary human PBMC-derived M0-, M1- and M2-polarized macrophages as well as primary human PBMC-derived DCs, with late recruitment of Rab17 observed to efferosomes in M0- and M2-polarized macrophages and DCs (**Figure 3.5**). RASEF and Rab6b, the other Rab-family GTPases identified in our mass spectrometry screen, did not significantly associate with either phagosomes or efferosomes (**Figures 3.6a** and **3.6b**).

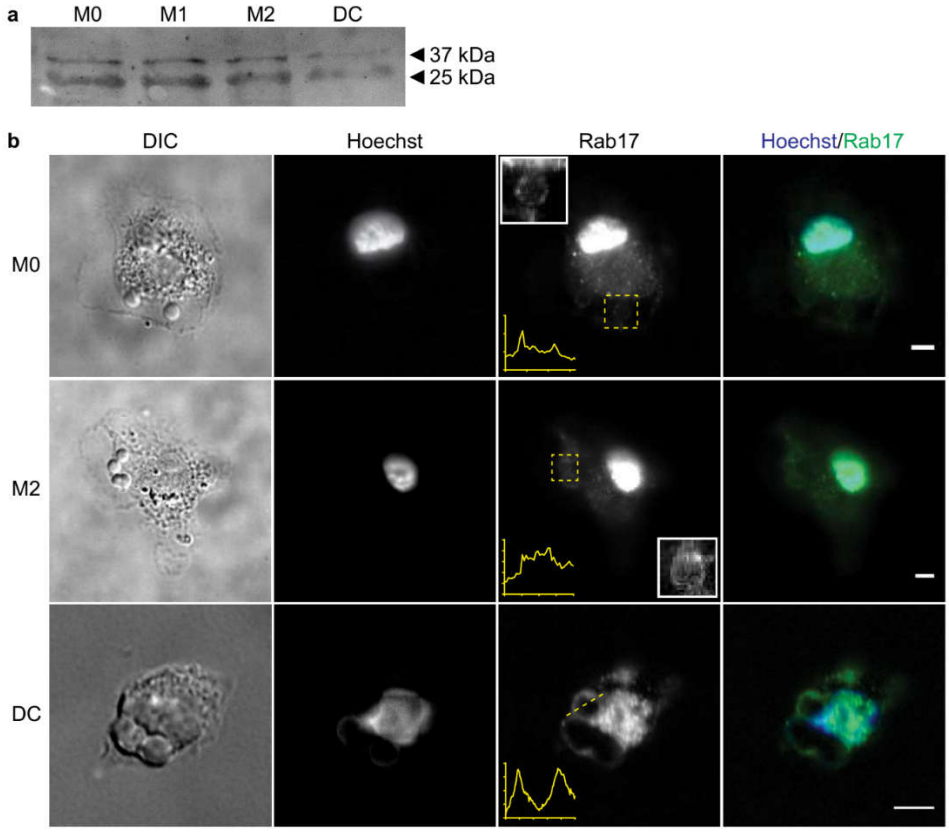

Figure 3.5 Rab17 is expressed in human phagocytes and is recruited to efferosomes late in maturation.

Macrophages and dendritic cells were derived by ex vivo differentiation of human PBMC's into the respective cell types. Rab17 immunoblot of M0-, M1- and M2-polarized macrophages and dendritic cells (DCs). (**a**) Immunostaining of Rab17 30 min following efferosome closure. (**b**) Plots indicate the intensity of Rab17 staining along the dashed yellow line (DC) or horizontally across the center of the insert (M0/M2). Data from M1-polarized macrophages are not presented as no efferosomes were observed in these cells. Images are representative of 3 independent experiments. Scale bars are 5 µm.

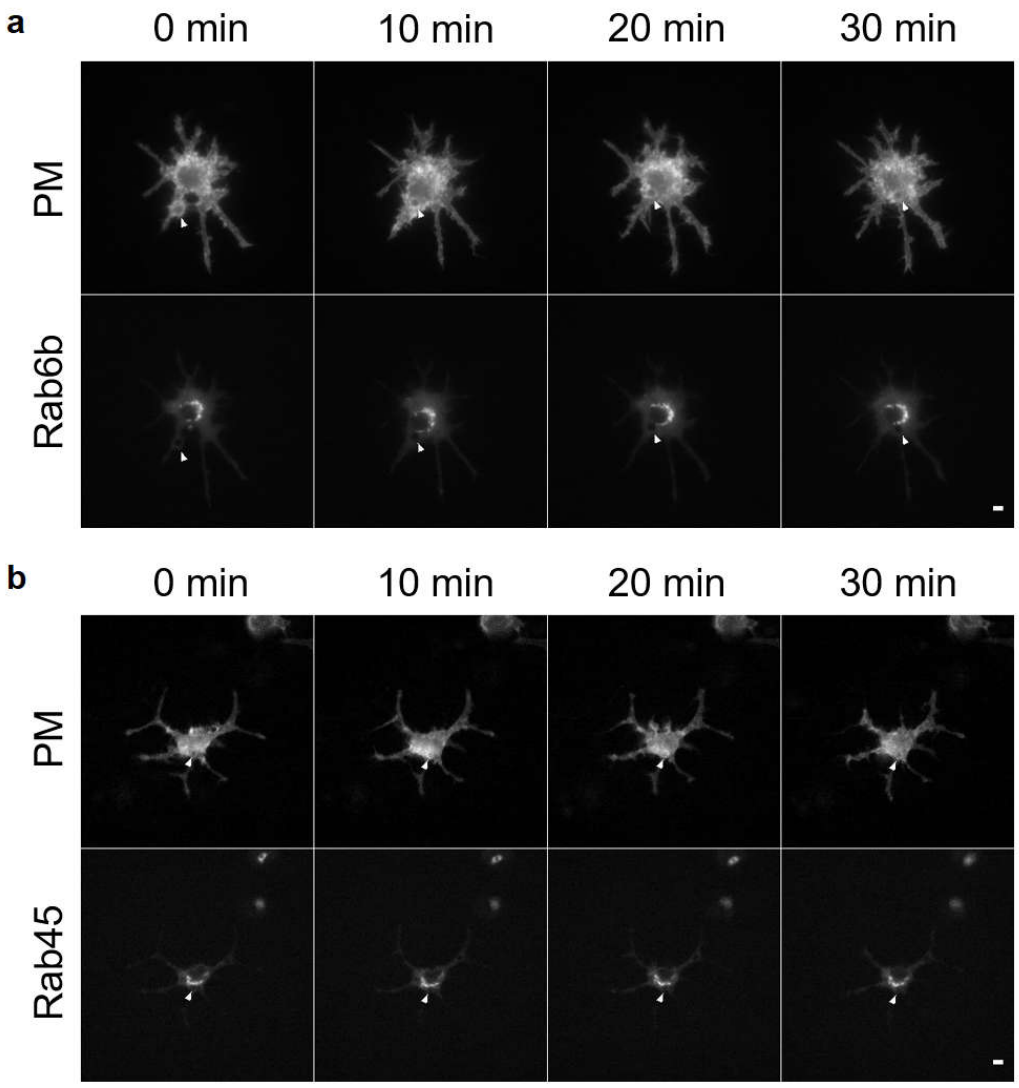

Figure 3.6 Rab6b and Rab45 are not recruited to the maturing phagosome and efferosome.

Live cell microscopy was performed on J774.2 macrophages expressing PM-RFP and either Rab6b-GFP engulfing IgG-opsonized pathogen mimics (**a**) or Rab45-GFP engulfing apoptotic cell mimics (**b**) Representative images demonstrating lack of Rab6b and Rab45 recruitment are shown. The arrowhead tracks the same phagosome/efferosome through successive time points. T = 0 is set as the video frame when complete sealing of the phagosome/efferosome was observed. Data are representative of a minimum of 10 cells imaged over three independent experiments. Scale bars are 5 μm.

Since our model system used non-digestible mimics of bacterial and apoptotic cells, we could not assess whether Rab17 altered the trafficking of degraded materials derived from efferosomes or phagosomes. As such, we performed live cell imaging of Rab17-GFP- and PM-RFP-expressing macrophages as they engulfed *E. coli* or apoptotic cells covalently labeled with a degradation-resistant, pH-stable, far-red fluorophore. Bacterial phagocytosis did not differ from the mimics, with *E. coli* internalized into a compartment that transiently colocalized with Rab17 and retained PM-RFP for at least 90 min (**Figures 3.7a**, **3.7c** and **3.7d**). In marked contrast, macrophages efferocytosed small fragments (apoptotic bodies) from apoptotic cells into PM-RFP-demarcated efferosomes, on which Rab17 was retained for prolonged periods of time (**Figures 3.7b**, **3.7c** and **3.7e**). Interestingly, at later time points, degraded apoptotic cell materials were observed to move into a compartment negative for PM-RFP (**Figure 3.7d**), a phenomenon not observed with non-degradable targets (**Figure 3.4b**), suggesting that degraded efferocytosed materials were being directed out of the canonical maturation pathway—a process not observed with *E. coli* (**Figure 3.7e**), indicating that the degraded apoptotic cells and *E. coli* had been trafficked into different cellular compartments.

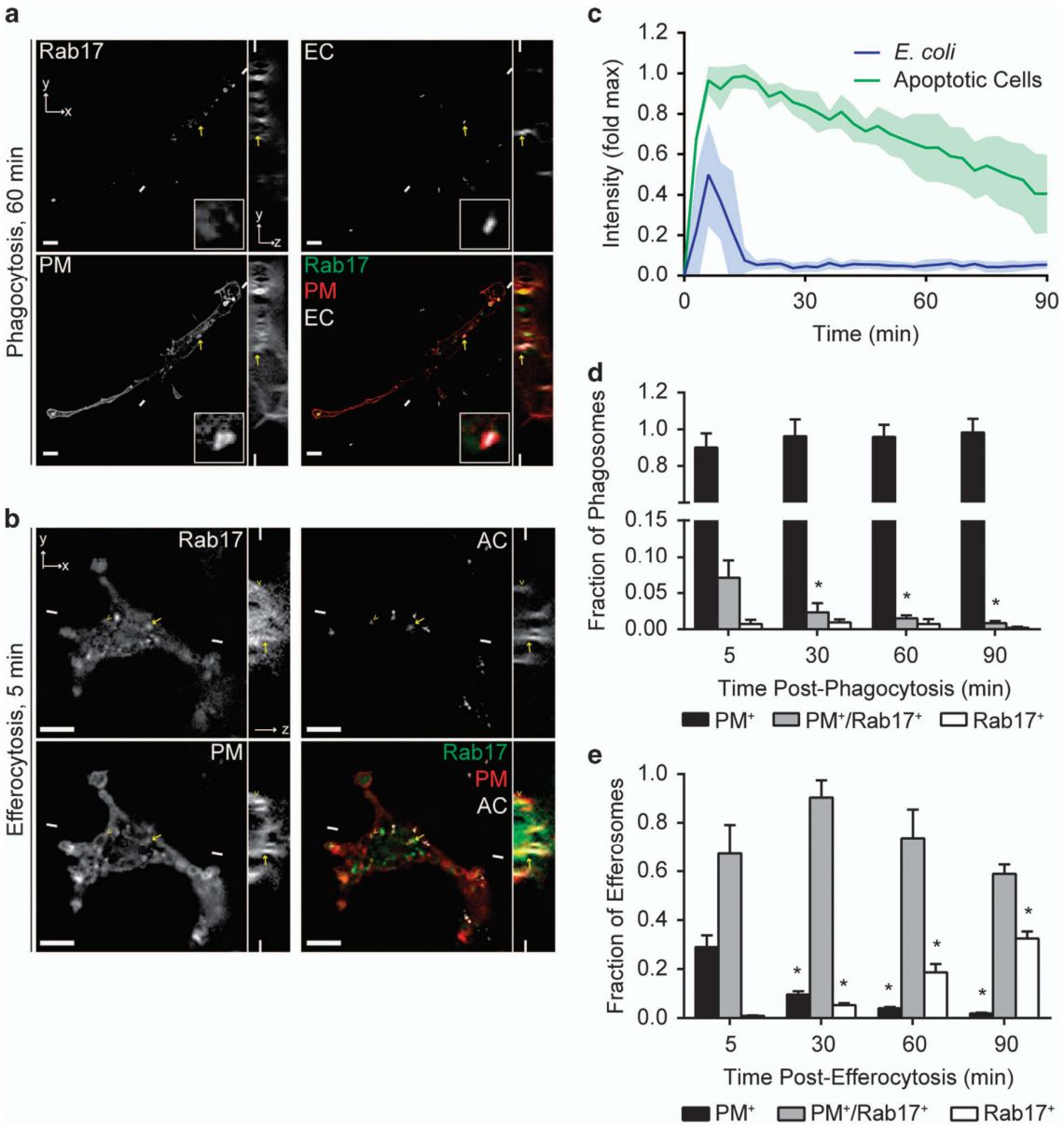

Figure 3.7 Rab17 is selectively retained on apoptotic cell containing efferosomes.

Live cell microscopy was performed on J774.2 macrophages expressing PM-RFP and Rab17-GFP engulfing fluorescently tagged apoptotic cells (AC) or *E. coli* (*E. coli* or EC). (**a**) Representative slice from a z-stack of Rab17-GFP and PM-RFP recruitment to *E. coli* containing phagosomes 60 min following phagocytosis. Arrow indicates the phagosome magnified in the insert. (**b**) Representative slice of a z-stack of Rab17-GFP and PM-RFP recruitment to an apoptotic cell containing efferosome 5 min following efferocytosis. Arrow indicates the same Rab17^{+}/PM-RFP^{+} efferosome, and arrowhead indicates the same

Rab17$^-$/PM-RFP$^+$ efferosome, in all panels. (**c**) Recruitment dynamics of Rab17-GFP to phagosomes and efferosomes, normalized to the brightest Rab17$^+$ cell structure. (**d** and **e**) Portion of *E. coli* containing phagosomes (**d**) or apoptotic cell containing efferosomes (**e**), which are positive for PM-RFP only (PM$^+$), positive for PM-RFP and Rab17 (PM$^+$/Rab17$^+$) or positive for Rab17 alone (Rab17$^+$). Scale bars are 5 μm. Small lines indicate the position of the cross-section shown in the corresponding xy and z images. (**c**–**e**) T = 0 is set as the video frame when complete sealing of the phagosome/efferosome was observed, and data are normalized to maximum Rab17 intensity observed in each cell and is presented as mean ± SEM. Data are representative of (**a** and **b**) or quantifies (**c**–**e**) a minimum of 52 cells imaged over four independent experiments. *$p < 0.05$ compared with the 5 min timepoint for the same group.

3.3.4 Rab17 mediates the trafficking of degraded apoptotic cell materials to the recycling endosome

The previous data are consistent with a model in which phagocytosed materials traffic through the canonical maturation pathway, whereas efferocytosed materials are redirected into another cellular compartment by Rab17. Given that Rab17 has previously been found to regulate recycling and exocytosis, it was likely that efferocytosed materials were being trafficked from the efferosome to the recycling endosome.[38,58] We therefore assessed the recruitment of Rab17, a recycling endosome marker (transferrin receptor, TfR) and MHC class II to phagosomes and efferosomes. Consistent with the canonical maturation process, 90 min following engulfment most phagosomes had recruited MHC class II but not Rab17 or TfR (**Figures 3.8a** and **3.8b**). In contrast, efferocytosed materials did not colocalize with MHC class II, which remained diffusively distributed throughout the cell (**Figure 3.8c**). Instead, efferosomes strongly colocalized with TfR, with a portion colocalizing with both Rab17 and TfR (**Figure 3.8d**). We next attempted to knockdown Rab17, but transfection with siRNA concentrations that reliably knocked down Rab17 expression also inhibited phagocytosis and efferocytosis (**Figure 3.8e**). Instead, we transfected J774.2 cells with a mCherry-tagged dominant negative (DN)-Rab17 at a dose that inhibited ~ 50% of efferocytosis and phagocytosis (0.5 μg per well; **Figure 3.8e**). DN-Rab17 was not recruited to phagosomes and was recruited to a significantly lower fraction of efferosomes compared

with wild-type Rab17 (**Figure 3.8f**). Importantly, expression of DN-Rab17 significantly increased the association of MHC class II, and decreased the association of TfR, with efferosomes (**Figure 3.8f**). Combined, these results indicate that Rab17 is selectively recruited to efferosomes, where it mediates the transfer of degraded apoptotic cell material into the recycling endosome and away from the MHC class II loading compartment.

Figure 3.8 Rab17 mediates trafficking of degraded apoptotic cell materials. (on opposite page)

Z-stacks were captured of fixed J774.2 macrophages expressing Rab17-mCherry and either co-expressing TfR-GFP (TfR) or immunostained for MHC class II (MHCII) 90 min following engulfment of *E. coli* (EC) or apoptotic cells (AC). (**a**-**d**) Localization of Rab17 and MHC class II (**a** and **c**) or TfR (**b** and **d**), relative to phagocytosed *E. coli* (**c** and **d**) or efferocytosed apoptotic cells (**a** and **b**). Uptake of E. coli and apoptotic cells by J774.2 macrophages that were untreated/non-transfected (UT), treated with scrambled (Scm) or Rab17 siRNA (Rab17), or transfected with 0.1–1.0 μg per well of a construct expressing DN-Rab17, expressed as the number of *E. coli* or apoptotic cells engulfed per cell. (e) Quantification of the fraction of phagocytosed *E. coli* or efferocytosed apoptotic cells that recruited Rab17, MHC class II and TfR in cells expressing mCherry-tagged wild-type or dominant-negative (DN) Rab17. (f) Images are representative of (**a**-**d**), and graphs quantify (**e** and **f**), a minimum of 15 images captured in three independent experiments. Scale bars are 5 μm. Small lines indicate the position of the cross-section shown in the corresponding xy and z images. *$p < 0.05$ compared with the same group in untreated cells (**e**) or cells expressing wild-type Rab17 (**f**).

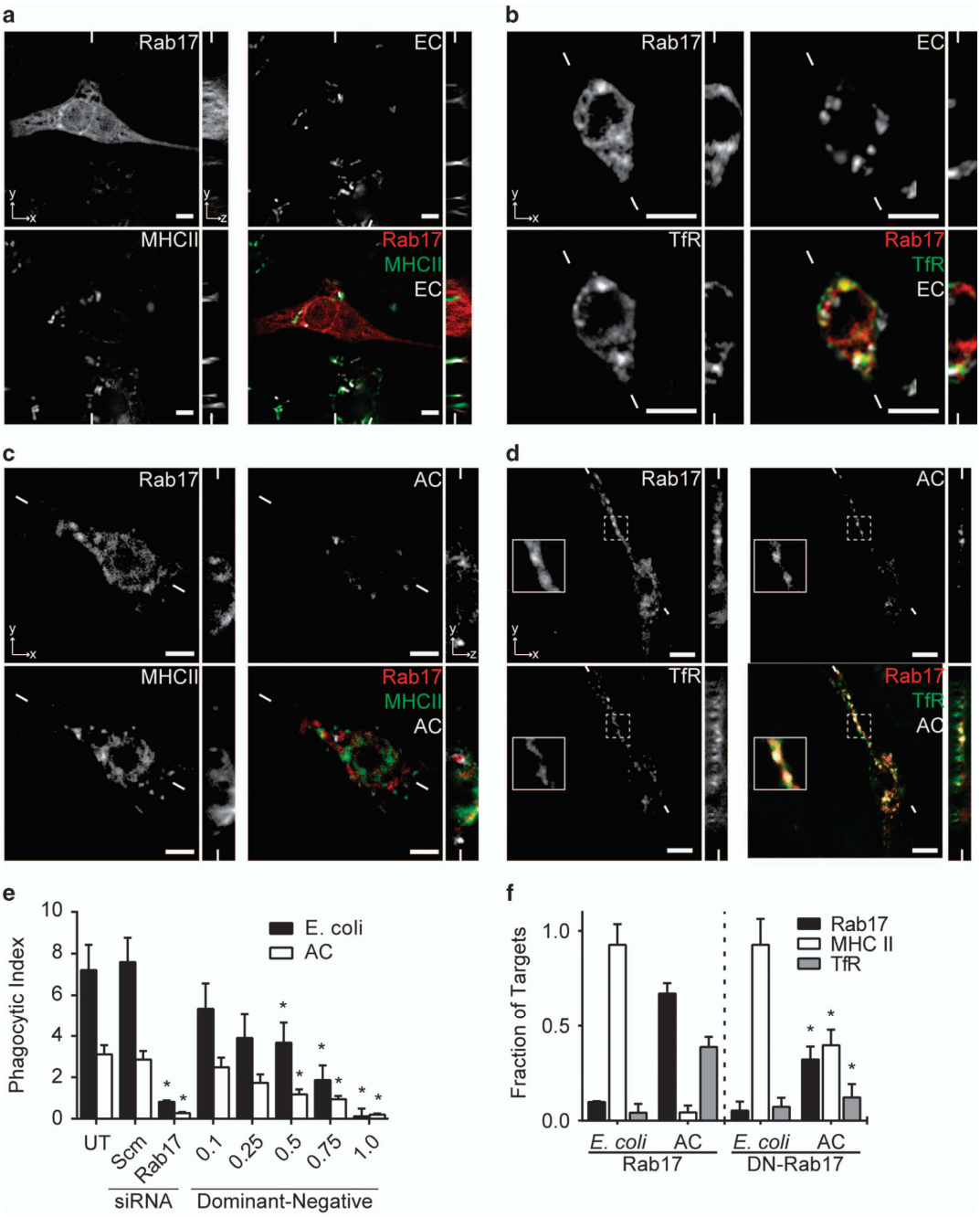

3.3.5 Rab17 sorts materials on maturing efferosomes

Having demonstrated that Rab17 mediates the transfer of degraded apoptotic cell materials from the efferosome to recycling endosomes, we next sought to elucidate the mechanism by which Rab17 mediates the transfer of materials from efferosomes to recycling endosomes. Firstly, the distribution of Rab17 relative to recycling endosomes (demarcated by transferrin receptor, TfR) and plasma-membrane derived vesicles (demarcated by PM-

RFP) was assessed in resting macrophages. PM-RFP was found to be largely excluded from Rab17$^+$ vesicles (**Figure 3.9a** and **3.9c**). More interestingly, while all but a minute portion of Rab17$^+$ vesicles were positive for TfR, there was a significant portion of TfR$^+$ vesicles which lacked Rab17 (**Figures 3.9b** and **3.9c**). Therefore, in resting macrophages, Rab17 demarcates a subset of the recycling endosome system and is not significantly recruited to plasma membraned-derived vesicles such as endosomes.

Figure 3.9 Rab17 dynamics on efferosome mimics. (on opposite page)

Colocalization of Rab17-GFP and Rab17-mCherry with PM-RFP-derived vesicles or with TfR-GFP-positive vesicles in resting J774.2 cells. (**a** and **b**) Percent of Rab17$^+$ vesicles co-staining with TfR (Rab17:TfR), TfR$^+$ vesicles co-staining with Rab17 (TfR:Rab17) and PM-derived vesicles co-staining with Rab17 (PM:Rab17). (**c**) Dynamics of Rab17-GFP and PM-RFP on efferosomes containing non-digestible apoptotic cell mimics. (**d**) Arrows indicate Rab17$^+$ vesicles fissioning from the efferosome. Images are representative of (**a** and **b**) or quantifies (**c**) 47 images captured over 4 independent experiments or is representative of 12 time-lapse videos captured over 5 independent experiments (**d**). Data are presented as mean ± SEM. Scale bars are 5 μm (**a** and **b**) or 10 μm (**d**).

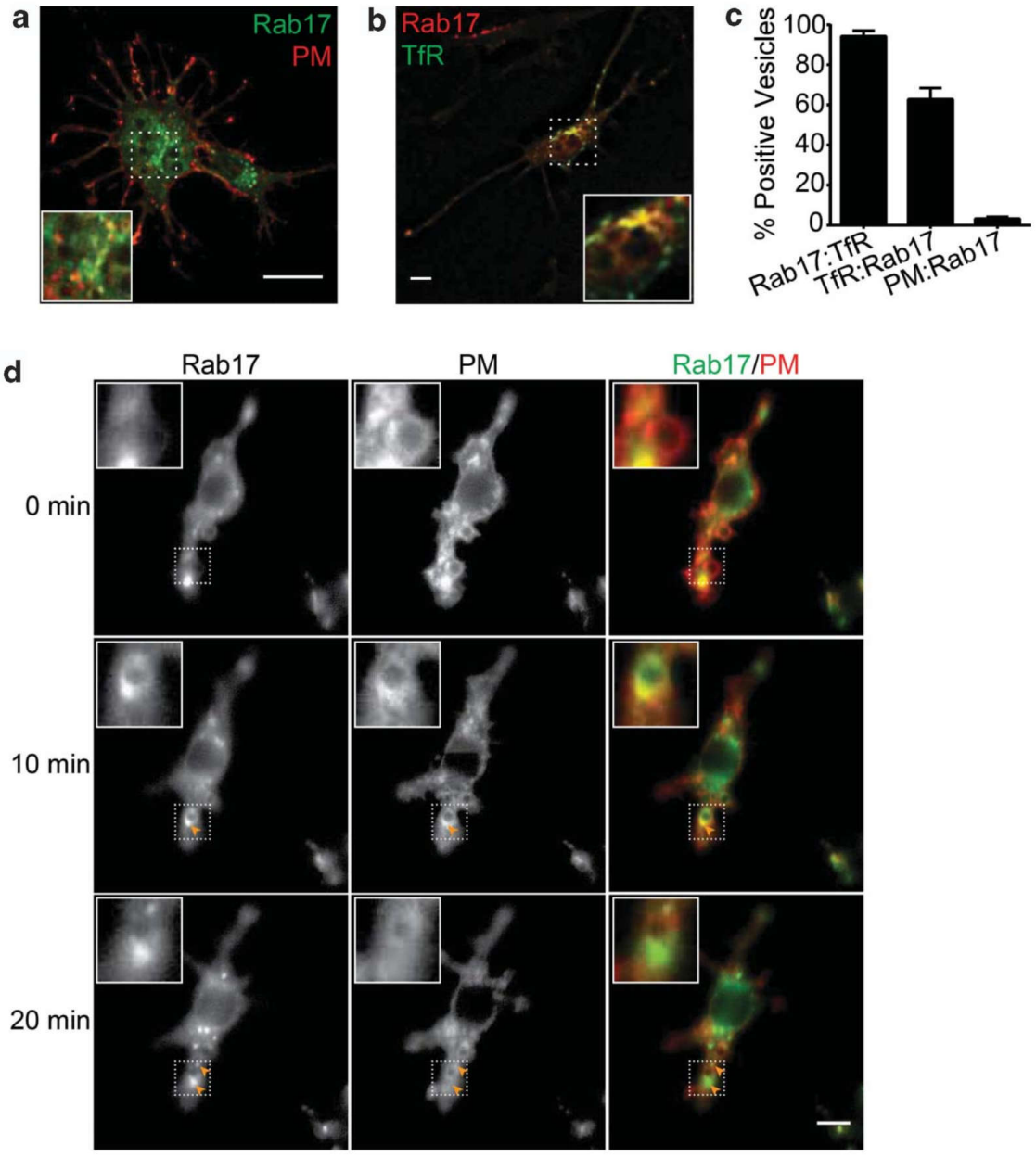
a
Rab17
PM
b
Rab17
TfR
c
% Positive Vesicles
100
80
60
40
20
0
Rab17:TfR
TfR:Rab17
PM:Rab17
d
Rab17
PM
Rab17/PM
0 min
10 min
20 min

Next, live cell microscopy was used to quantify Rab17 dynamics during efferocytosis, using large (5 µm) apoptotic cell mimics to provide higher spatial resolution (**Figure 3.9d**). These mimics were internalized into a PM-RFP-demarcated compartment which was positive for Rab17-GFP. A few minutes following closure, the efferosome vesiculated through the fission of $Rab17^+$ vesicles, depleting approximately 60% of the Rab17 initially recruited to the efferosome (**Figure 3.9d**, **Table 3.4**). Interestingly, the fissioning vesicles were devoid of PM-RFP, suggesting that materials were being selectively sorted by vesiculation of the efferosome. The efferosome remained weakly positive for Rab17 following vesiculation, with the occasional $Rab17^+$ vesicle interacting with the efferosome during this stage.

Table 3.4 Efferosome fission and fusion characteristics.

Efferosome Characteristics	Mimics	Apoptotic Cells
Diameter at Closure	5.20 ± 1.4 μm	2.87 ± 0.13 μm
Diameter at Vesiculation	4.97 ± 2.6 μm	2.74 ± 0.11 μm
Time to Vesiculation	7.25 ± 3.72 min	22.40 ± 3.78 min
Number of EDVs/Efferosome	1.25 ± 0.45	4.05 ± 0.58
Vesiculation Time	3.25 ± 1.29 s	*
Size of EDVs	1.08 ± 0.29 μm	**
Time from Vesiculation to First Fusion	n.o.	10.77 ± 2.23 min
DN-Rab17 Efferosome Characteristics		
Time to Vesiculation	—	64.1 ± 10.3 min
Number of EDVs/Efferosomes	—	0.79 ± 0.51
Size of EDVs	—	2.28 ± 0.46 μm

*Vesiculation time was shorter than the time between video frames (120 s)
**Many vesicles were sub-resolution in size and could not be measured
n.o. Not Observed

3.3.6 Fission and fusion of efferosome-derived vesicles

Our results from the previous section used indigestible apoptotic cell mimics, thus preventing us from relating Rab17 dynamics to the processing of the efferosomal cargo. To address this limitation, Rab17 dynamics were quantified on efferosomes containing labeled apoptotic Jurkat cells in macrophages expressing Rab17-mCherry and PM-GFP. Macrophages engulfed apoptotic bodies, not intact cells (**Table 3.4**, **Figure 3.10a**), with the level of Rab17 retained on efferosomes and the size of the efferosomes remaining

constant during the early stages of maturation (**Table 3.4**, **Figure 3.10b**). Despite some photobleaching, it was apparent that newly formed efferosomes migrated toward the cell center where they then vesiculated into multiple EDV's (**Figures 3.10b** and **3.10c**). Interestingly, the intensity of PM-GFP staining on EDV's was variable, consistent with the sorting observed during the vesiculation of non-digestible efferosome mimics (**Figure 3.10b**).

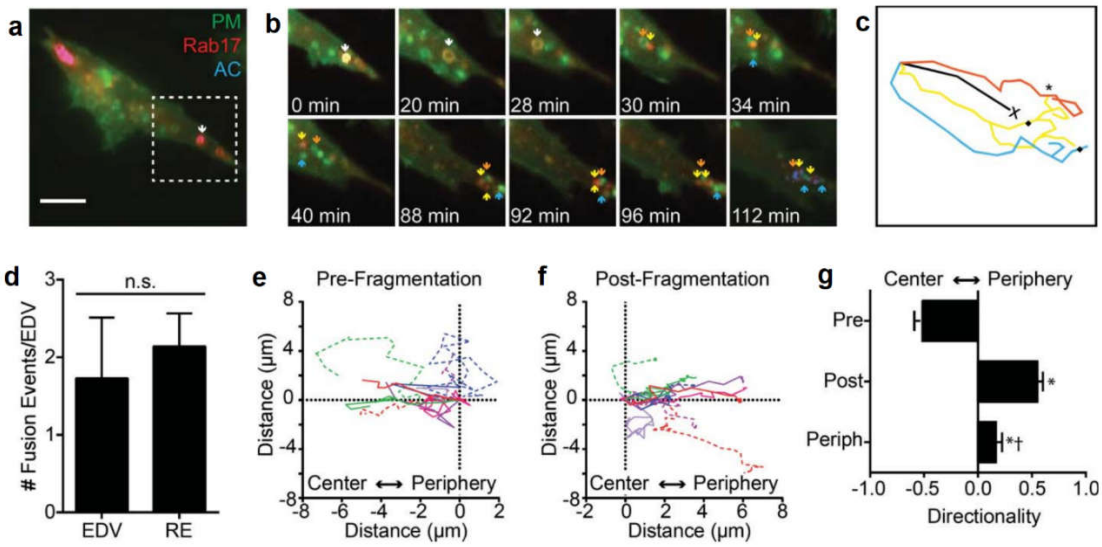

Figure 3.10 Fission, fusion and movement of Rab17-positive efferosomes.

Efferosome and Rab17 dynamics were quantified using live cell microscopy of efferocytosed fluorescently-labeled apoptotic bodies by macrophages expressing Rab17-mCherry and PM-GFP. (**a**) Fluorescent image of a macrophage immediately following engulfment of an apoptotic body (arrow/AC). Scale bar is 5 μm. Time-lapse micrograph of the insert from panel a. (**b**) The intact efferosome is tracked by the white arrow, colored arrows track individual EDVs. The staining of the apoptotic body is shown only for the first and final frames, to emphasize the differential sorting of Rab17 and PM-GFP into EDV's. Track of efferosome and EDV's from panel b. 'X' indicates the efferosome starting position, asterisk indicates fusion between two EDV's, and diamonds indicate sites of fusion with $Rab17^{+}$ recycling endosomes. (**c**) Number of fusion events between EDV's, and between EDV and recycling endosomes (RE). (**d**) Representative motion tracks of 10 pre-fission efferosomes, measured relative to a vector between the cell

barycentre and the site of efferosome formation. (**e**) Representative motion tracks of a single post-fission vesicle derived from each efferosome in panel e, measured relative to a vector between the cell barycentre and the efferosome fission point. (**f**) Directionality of efferosome movement pre-fission (Pre), Post-fission (Post), and once the EDV's reach the periphery (Periph). (**g**) Data are representative of (**a-c**, **e** and **f**), or quantifies (**d** and **g**) 124 efferosomes imaged over 3 independent experiments. *$p < 0.05$ comparted to Pre, $^{\dagger}p < 0.05$ compared with Post, n.s. $p > 0.05$ by Students t-test (**d**) or one-way ANOVA with Tukey post-hoc (**g**).

By tracking the fluorescent signal of the apoptotic bodies, we were able to track EDV's for prolonged periods of time, revealing that newly vesiculated EDV's migrated toward the cell periphery, and once at the cell periphery, ceased moving (**Figures 3.10b** and **3.10c**). During this migration most EDV's underwent further vesiculation, as well as fusion with other EDV's and with $Rab17^{+}$ recycling endosomes that were otherwise devoid of apoptotic bodies (**Figures 3.10c-d**, **Table 3.4**), consistent with our previous findings demonstrating cargo transfer from efferosomes to TfR^{+} recycling endosomes. Both the inward movement of the nascent efferosome, and the subsequent outward movement of the EDV's were highly linear but became non-directional once EDV's reached the cell periphery (**Figures 3.10e-g**).

3.3.7 Rab17 is required for efferosome-derived vesicle migration

The inward migration of the newly formed efferosome is required for efficient fusion with lysosomes and cargo degradation,[10,60] and indeed, we have demonstrated here that efferosome-lysosome fusion is concordant with Rab17 recruitment to the efferosome. In contrast, the subsequent peripheral migration of phagocytosed cargo is, to our knowledge, previously unreported. To determine if Rab17 was required for peripheral efferosome migration, we expressed DN- or WT-Rab17-GFP in macrophages and quantified the intracellular localization of efferosomes, using DN-Rab17 at a modest expression level to prevent the inhibition of efferocytosis observed when Rab17 siRNA is used (**Figure 3.8e**). As expected, a significant fraction of efferosomes were located in the periphery of cells expressing WT-Rab17, whereas efferosomes remained in the perinuclear region of cells expressing DN-Rab17 (**Figures 3.11a** and **3.11b**). Efferosomes in DN-Rab17 expressing

cells underwent limited fission (**Figures 3.11c** and **3.11d**, **Table 3.4**), but fused normally with LAMP1-demarkated lysosomes (**Figures 3.11e** and **3.11g**). Consistent with our findings above, expression of DN-Rab17 significantly impaired the transfer of efferosome cargos from EDV's to TfR^+ recycling endosomes (**Figures 3.11f** and **3.11g**)

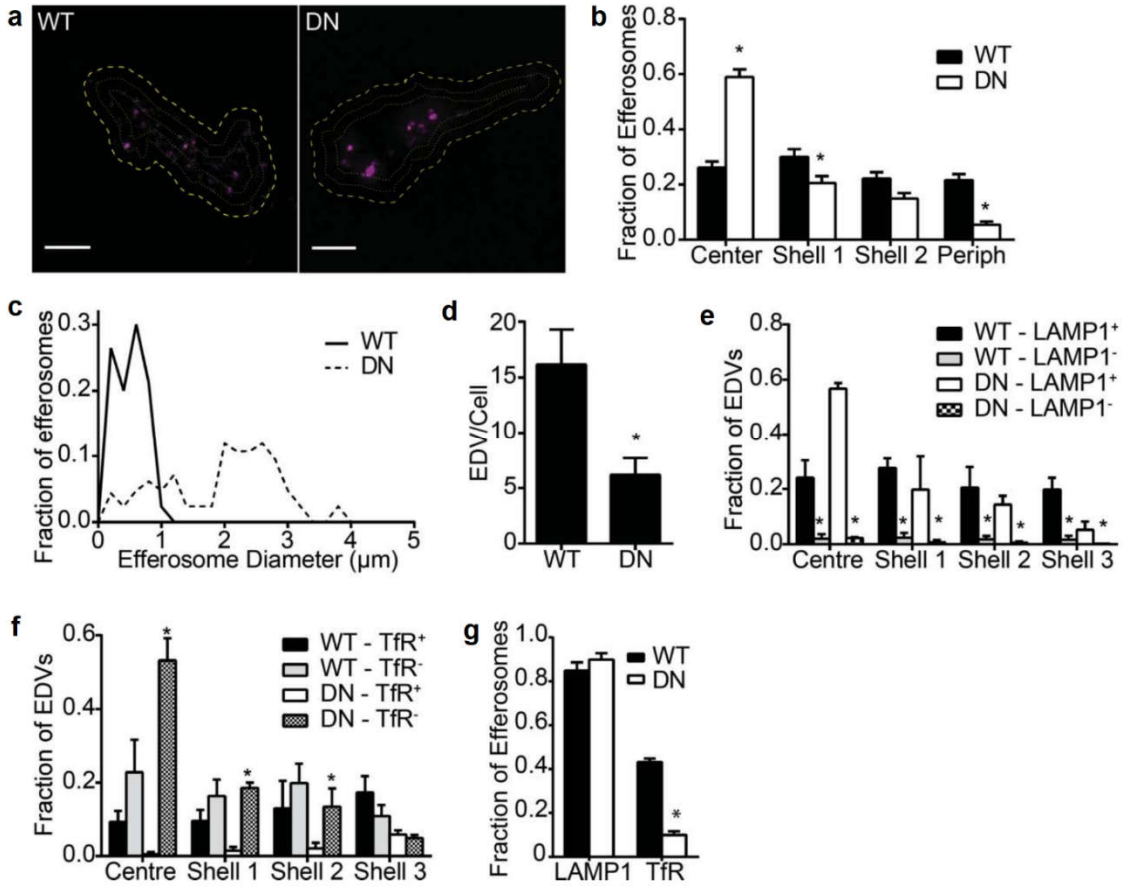

Figure 3.11 Peripheral migration of EDV's and cargo transfer to recycling endosomes requires Rab17.

Localization of fluorescently-labeled, apoptotic Jurkat cell-derived EDV's in macrophages expressing WT- or DN-Rab17-GFP, and either the lysosomal marker LAMP1-mCherry or the recycling endosome marker TfR-mCherry, was quantified 90 min post-efferocytosis. Representative images of EDV location in cells expressing WT- or DN-Rab17. (**a**) Large dashed line indicates the cell periphery; fine dotted lines indicate "shells" positioned at 1 μm increments inwards from the cell periphery. Quantification of the fraction of EDV's observed in each "shell" of cells expressing WT- or DN-Rab17. (**b**) Quantification of

diameter (**c**) and number (**d**) of EDV's in macrophages expressing WT- and DN-Rab17. Effect of WT- vs. DN-Rab17 on the distribution of EDV's colocalizing with ($LAMP1^+$) or lacking ($LAMP1^-$) the lysosomal marker LAMP1. (**e**) Effect of WT- vs. DN-Rab17 on the distribution of EDV's colocalizing with (TfR^+) or lacking (TfR^-) the recycling endosome marker TfR. (**f**) Comparison of the colocalization of efferosomes with LAMP1 and TfR in cells expressing WT- or DN-Rab17. Data are representative of (**a**) or quantifies (**b**-**g**) at least 28 cells over 3 independent experiments. *$p < 0.05$ compared with WT (**b**, **g**), $LAMP^+$ in the same group (**e**) or TfR^+ in the same group (**f**), 2-way ANOVA with Tukey post-hoc (**b**, **e** and **f**), or Students t-test (**d** and **g**). Scale bars are 5 μm.

3.4 Discussion

Proper efferosome maturation is essential for avoidance of self-antigen presentation and the induction of inflammation and autoimmunity.[3] To date, our understanding of the mechanisms that regulate efferosome maturation has been limited and it has been thought that efferosome maturation proceeds similarly to phagosome maturation.[11] However, it is apparent that efferosome and phagosome maturation must be differentially regulated processes since the immunological outcomes of these two processes are diametrically opposed, with phagocytosis resulting in the initiation of an inflammatory response and efferocytosis resulting instead in resolution of inflammation.[1,3] The ultimate fate of phagocytic cargo is to be trafficked to the MHC class II loading compartment, where antigenic peptides from pathogens are loaded onto cognate MHC class II molecules and trafficked to the cell surface for antigen presentation.[61]

Some investigators have suggested that the differences observed with efferocytosis in contrast to phagocytosis is driven by differences in the kinetics of efferosome vs. phagosome maturation.[11,62] Efferosome maturation in macrophages appears to be delayed in comparison with phagosomes.[13,62] It has been suggested that TLR signaling within phagosomes drive accelerated maturation and subsequent loading of antigenic peptides derived from phagosomal cargo onto MHC class II molecules.[13,62] Indeed, murine macrophages deficient in either TLR2, TLR4 or MyD88 exhibited a decreased capacity to

phagocytose either *E. coli* or *Salmonella typhimurium*, and phagosome maturation in these macrophages was significantly delayed.[62] However, other studies that have examined the rate of phagosome maturation in the presence and absence of TLR ligands showed no difference in the rate of acquisition of late phagosomal and lysosomal markers.[63] We therefore set out to determine whether, in professional phagocytes such as macrophages, there is an intrinsic mechanism that differentially regulates efferosome maturation and allows efferocytic cargo to bypass the MHC class II loading compartment.

Our data agree with existing literature that suggest efferosome and phagosome maturation share a common regulatory pathway.[4,6,11] Indeed, we recapitulate the key finding that the small GTPases Rab5 and Rab7 are recruited sequentially to the maturing efferosome and phagosome.[6] We further demonstrate that the kinetics of Rab5 and Rab7 recruit does not differ between efferocytosis and phagocytosis. This is perhaps unsurprising as it is well established that Rab7 is responsible for the recruitment of key downstream effector molecules that: 1) guide the assembly of a dynein-dynactin complex that drives migration of the efferosome/phagosome along microtubules towards the cell centre,[10,64] and 2) mediates the fusion of lysosomes to the maturing phagosome, which delivers the vATPses that mediate efferosome/phagosome acidification.[9,65]

However, through our mass spectrometry analysis, we identified Rab GTPases that were differentially recruited to efferosomes vs. phagosomes. Of these, we were particularly interested in the recruitment of Rab17 to efferosomes, given its established role in the literature as a key regulator of receptor and cargo recycling[34,58]. This led to the hypothesis that Rab17 may mediate trafficking through the recycling endosome as a mechanism by which efferocytic cargo can bypass the MHC class II loading compartment.[34,36] Indeed, we observe that while Rab17 is transiently recruited to the surface of phagosome, it is persistently recruited to efferosomes. Consistent with others who have shown that Rab17 regulates trafficking through the recycling endosome,[58] we demonstrate here that $Rab17^{+}$ vesicles containing efferocytic cargo colocalize with TfR, which is a marker of the recycling endosome system.[66] Importantly, we also demonstrate that $Rab17^{+}$ vesicles containing apoptotic cell-derived materials do not colocalize with MHC II, suggesting that Rab17 mediates re-direction of this cargo away from the MHC class II loading

compartment and to the recycling endosome. Strikingly, when we interfere with Rab17 activity through ectopic expression of a DN-Rab17, efferocytic cargo is then observed to colocalize with MHC class II. Taken together, these data suggest that Rab17 is an essential regulator of efferosome maturation and allows antigens derived from efferocytic cargo to avoid being presented on MHC class II.

Furthermore, we go on to show that the dynamics of efferosome trafficking in macrophages following internalization of efferocytic cargo differs significantly from that of a phagosome. Phagosomes undergo migration towards the cell center during their maturation process in a dynamin-dependent process.[7] This brings phagosomes into close proximity to lysosomes, which are localized around the nucleus of the cell, and facilitate phagolysosomal fusion and degradation of phagocytic cargo.[55,60] Following phagolysosome formation, these bodies remain localized perinuclearly to facilitate MHC class II loading compartment formation.[67] While the role of phagosomelysosome position within the cell is not entirely clear, studies have shown that lysosomes closer to the perinuclear area have lower pH and greater degradative capabilities.[55] We find that in efferosome maturation, while the efferosome initially migrates towards the cell centre and undergoes fusion with lysosomes, the efferosome undergoes fission events and generates multiple EDVs, which then migrate back towards the cell periphery. This is presumably to facilitate trafficking of degraded efferocytic cargo to the recycling endosomes, which are located peripherally within the cell.[68] Moreover, as the Golgi is a perinuclear organelle, this may act to decrease the efficiency of Golgi-to-efferosome trafficking, thus limiting the delivery of newly synthesized MHC II to the efferosome. Remarkably, Rab17 again appears to be required to facilitate EDV formation and the migration of EDVs back towards the cell periphery. In macrophages expressing DN-Rab17, initial migration of the efferosome towards the cell centre and subsequent lysosomal fusion remain unaffected. However, EDV formation and migration of EDVs towards the cell periphery are abrogated in DN-Rab17-expressing macrophages, and trafficking of cargo to the recycling endosome does not occur. Therefore, Rab17 appears to be required for driving efferosomal fission and subsequent migration of EDVs towards the cell periphery.

Peripheral migration of EDVs is likely a kinesin-driven process[69] and it is tempting to imagine that Rab17 either directly recruits kinesin or recruits an effector that then recruits kinesin to mediate peripheral migration of EDVs along the microtubule system. Although this remains to be demonstrated experimentally, the role of Rab proteins in regulation of vesicular traffic through recruitment of kinesin has been well documented. Several Rab proteins, including Rab3, Rab6, Rab9, Rab11 and Rab27, have been shown to be capable of recruiting kinesin, either director or through adaptor proteins.[70] The fate of efferocytic cargo following trafficking to the recycling endosome also remains unclear. Degraded efferocytic cargo may be expelled from the phagocyte through exocytosis or it may be recycled by the cell through nutrient recovery.[49,71] Rab17 has been associated with both transcytosis and exocytosis of melanosomes, which are lysosome-derived organelles, while the recycling endosome is well established as a nutrient absorption site.[38,68] The ultimate fate of efferocytosed materials remains an open question at this point. Despite these remaining questions, we propose a model of efferosome maturation whereby Rab17 is selectively recruited to the efferosome and mediates efferosome fission and trafficking towards the cell periphery to facilitate escape from the MHC class II loading compartment and instead mediate trafficking of cargo to the recycling endosome (**Figure 3.12**).

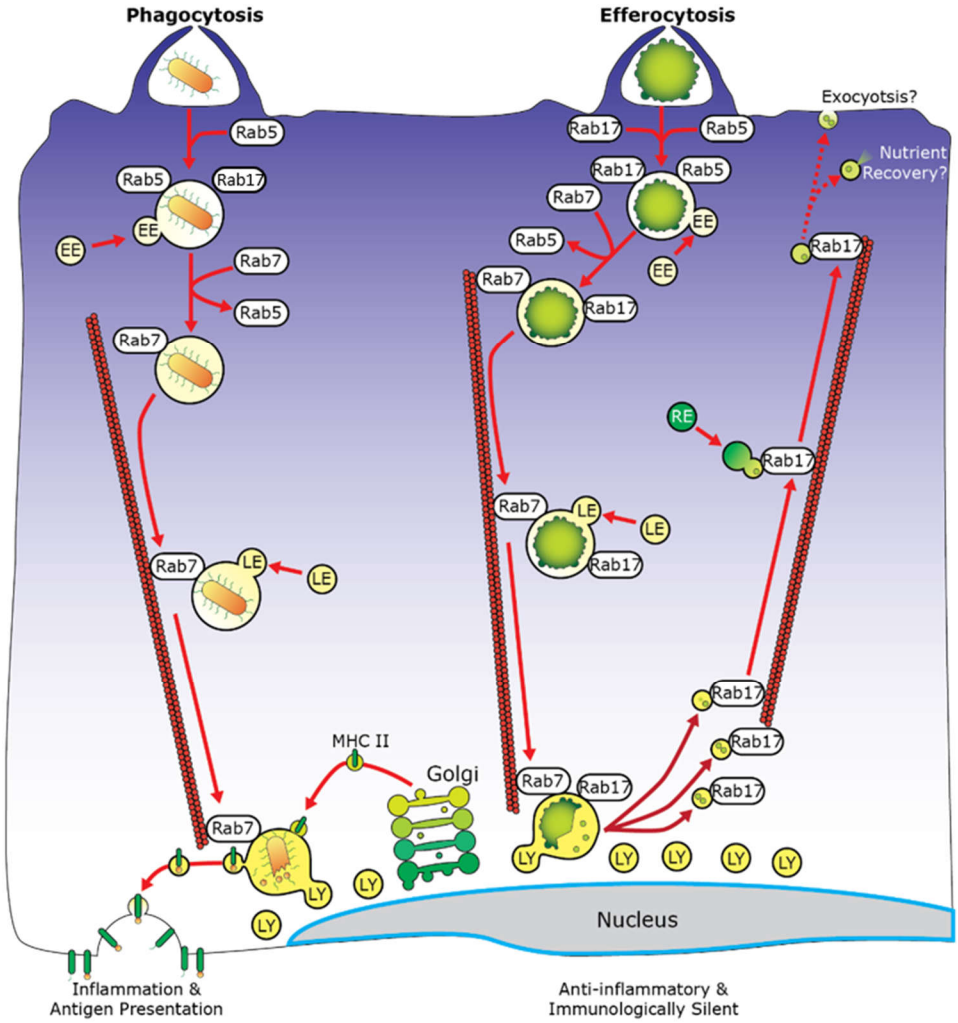

Figure 3.12 A model of differential regulation of phagosome and efferosome maturation.

Phagocytic uptake of pathogen results in the formation of a phagosome that subsequently undergoes multiple fusions with early endosomes. Rab17 is transiently recruited to the early phagosome but rapidly lost. Rab5 is a key marker of the early phagosome and is swapped for Rab7 as part of the process of transition from early to late phagosomes. Rab7 drives migration of the late phagosome towards the cell centre along microtubules, fusion of the phagosome with late endosomes and phagosomal acidification. At the cell centre, the late phagosome undergoes fusion with lysosomes to form the phagolysosome where the phagocytic cargo is degraded by lysosome proteases. MHC class II molecules are recruited to the phagolysosome from the Golgi and drives formation of the MHC class II

loading compartment. Antigenic peptides derived from degraded phagocytic cargo are loaded onto cognate MHC class II molecules and trafficked to the cell surface for antigen presentation. Efferosome maturation follows a similar pathway, with the additional recruitment of Rab17 to the efferosome surface. The efferosome undergoes lysosomal fusion but Rab17 then drives efferosomal fission and trafficking of efferosome-derived vesicles along microtubules towards the cell periphery where efferocytic cargo is trafficked to the recycling endosome and subsequently undergoes exocytosis and/or nutrient recovery. EE = early endosome, LE = late endosome, LY = lysosome.

Our findings in this chapter represent a concrete advancement in our understanding of the regulation of efferosome maturation under homeostatic conditions. Our data suggest that in professional phagocytes such as macrophages, there is an intrinsic Rab17-mediated pathway that acts to prevent improper antigen presentation following efferocytosis. This supports the idea that the differential regulation of efferosome vs. phagosome maturation is at least partially independent of Toll-like receptor signaling. These findings may also have important implications in future studies that examine defects in efferocytosis in the context of inflammatory and autoimmune diseases. Dysregulation of Rab GTPase function has previously been implicated in several pathologies. For example, Rab7 function is impaired in the presence of hypercholesterolemia and results in defects in phagosome maturation.[72] Further studies that examine the role of Rab17 in inflammatory and autoimmune diseases where efferocytosis has been implicated in disease pathogenesis are warranted and may indeed demonstrate that Rab17 is a viable therapeutic target in the treatment of these diseases.

3.5 References

1. Henson PM. Cell Removal : Efferocytosis. *Annu Rev Cell Dev Biol*. 2017;33:1-18.

2. Sachet M, Liang YY, Oehler R. The immune response to secondary necrotic cells. *Apoptosis*. 2017. doi:10.1007/s10495-017-1413-z

3. Nagata S. Apoptosis and Clearance of Apoptotic Cells. *Annu Rev Immunol*.

2018;361829(1):1-18. doi:10.1146/annurev-immunol

4. Kinchen JM, Doukoumetzidis K, Almendinger J, et al. A pathway for phagosome maturation during engulfment of apoptotic cells. *Nat Cell Biol*. 2008;10(5):556-566. doi:10.1038/ncb1718

5. Cui Y, Zhao Q, Gao C, et al. Activation of the Rab7 GTPase by the MON1-CCZ1 complex is essential for PVC-to-vacuole trafficking and plant growth in Arabidopsis. *Plant Cell*. 2014;26(5):2080-2097. doi:10.1105/tpc.114.123141

6. Kinchen JM, Ravichandran KS. Identification of two evolutionarily conserved genes regulating processing of engulfed apoptotic cells. *Nature*. 2010;464(7289):778-782. doi:10.1038/nature08853

7. Johansson M, Rocha N, Zwart W, et al. Activation of endosomal dynein motors by stepwise assembly of Rab7-RILP-p150Glued, ORP1L, and the receptor ??III spectrin. *J Cell Biol*. 2007;176(4):459-471. doi:10.1083/jcb.200606077

8. Flannagan RS, Jaumouillé V, Grinstein S. The Cell Biology of Phagocytosis. *Annu Rev Pathol Mech Dis*. 2011;7(1):61-98. doi:10.1146/annurev-pathol-011811-132445

9. Canton J, Khezri R, Glogauer M, Grinstein S. Contrasting phagosome pH regulation and maturation in human M1 and M2 macrophages. *Mol Biol Cell*. 2014;25(21):3330-3341. doi:10.1091/mbc.E14-05-0967

10. Cantalupo G, Alifano P, Roberti V, Bruni CB, Bucci C. Rab-interacting lysosomal protein (RILP): The Rab7 effector required for transport to lysosomes. *EMBO J*. 2001;20(4):683-693. doi:10.1093/emboj/20.4.683

11. Kinchen JM, Ravichandran KS. Phagosome maturation: going through the acid test. *Nat Rev Mol Cell Biol*. 2008;9(10):781-795. doi:10.1038/nrm2515

12. Gordon S, Plüddemann A. Macrophage Clearance of Apoptotic Cells: A Critical Assessment. *Front Immunol*. 2018;9(January):127.

doi:10.3389/fimmu.2018.00127

13. Blander JM, Medzhitov R. On regulation of phagosome maturation and antigen presentation. *Nat Immunol*. 2006;7(10):1029-1035. doi:10.1038/ni1006-1029

14. Levin R, Grinstein S, Canton J. The life cycle of phagosomes: formation, maturation, and resolution. *Immunol Rev*. 2016;273(1):156-179. doi:10.1111/imr.12439

15. Stenmark H, Olkkonen VM. The Rab GTPase family. *Genome Biol*. 2001;2(5):REVIEWS3007. doi:10.1186/gb-2001-2-5-reviews3007

16. Pfeffer SR. Structural clues to rab GTPase functional diversity. *J Biol Chem*. 2005;280(16):15485-15488. doi:10.1074/jbc.R500003200

17. Bock JB, Matern HT, Peden AA, Scheller RH. A genomic perspective on membrane compartment organization. *Nature*. 2001;409(6822):839-841. doi:10.1038/35057024

18. Shima F, Ijiri Y, Muraoka S, et al. Structural basis for conformational dynamics of GTP-bound ras protein. *J Biol Chem*. 2010;285(29):22696-22705. doi:10.1074/jbc.M110.125161

19. Seabra MC. Nucleotide Dependence of Rab Geranylgeranylation. *J Biol Chem*. 2017;271(24):14398-14404. doi:10.1074/jbc.271.24.14398

20. Alexandrov K, Horiuchi H, Steele-Mortimer O, Seabra MC, Zerial M. Rab escort protein-1 is a multifunctional protein that accompanies newly prenylated rab proteins to their target membranes. *EMBO J*. 1994;13(22):5262-5273. doi:10.1002/j.1460-2075.1994.tb06860.x

21. Grosshans BL, Ortiz D, Novick P. Rabs and their effectors: Achieving specificity in membrane traffic. *Proc Natl Acad Sci*. 2006;103(32):11821-11827. doi:10.1073/pnas.0601617103

22. Seabra MC, Wasmeier C. Controlling the location and activation of Rab GTPases. *Curr Opin Cell Biol*. 2004;16(4):451-457. doi:10.1016/j.ceb.2004.06.014

23. Müller MP, Goody RS. Molecular control of Rab activity by GEFs, GAPs and GDI. *Small GTPases*. 2018;9(1-2):5-21. doi:10.1080/21541248.2016.1276999

24. Novick P, Zerialt M. The diversity of Rab proteins in vesicle transport GDI GDP-dissociation inhibitor GEF guanine nucleotide exchange factor NSF N-ethylmaleimide-sensitive factor REP Rab escort protein SNAP soluble NSF-attachment protein SNARE SNAP receptor TGN frans-Golgi n. *Curr Opin Cell Biol*. 1997;9:496-504.

25. Rink J, Ghigo E, Kalaidzidis Y, Zerial M. Rab conversion as a mechanism of progression from early to late endosomes. *Cell*. 2005;122(5):735-749. doi:10.1016/j.cell.2005.06.043

26. Strick DJ, Elferink LA. Rab15 effector protein: a novel protein for receptor recycling from the endocytic recycling compartment. *Mol Biol Cell*. 2005;16(12):5699-5709. doi:10.1091/mbc.E05-03-0204

27. Jiang C, Liu Z, Hu R, et al. Inactivation of Rab11a GTPase in Macrophages Facilitates Phagocytosis of Apoptotic Neutrophils. *J Immunol*. 2017:1601495. doi:10.4049/jimmunol.1601495

28. Khvotchev M V, Ren M, Takamori S, Jahn R, Südhof TC. Divergent functions of neuronal Rab11b in Ca2+-regulated versus constitutive exocytosis. *J Neurosci*. 2003;23(33):10531-10539.

29. Monfregola J, Johnson JL, Meijler MM, Napolitano G, Catz SD. MUNC13-4 protein regulates the oxidative response and is essential for phagosomal maturation and bacterial killing in neutrophils. *J Biol Chem*. 2012;287(53):44603-44618. doi:10.1074/jbc.M112.414029

30. Brzezinska AA, Johnson JL, Munafo DB, et al. The Rab27a effectors JFC1/Slp1 and Munc13-4 regulate exocytosis of neutrophil granules. *Traffic*.

2008;9(12):2151-2164. doi:10.1111/j.1600-0854.2008.00838.x

31. Munafó DB, Johnson JL, Ellis BA, Rutschmann S, Beutler B, Catz SD. Rab27a is a key component of the secretory machinery of azurophilic granules in granulocytes. *Biochem J*. 2007;402(2):229-239. doi:10.1042/BJ20060950

32. Lütcke A, Jansson S, Parton RG, et al. Rab17, a novel small GTPase, is specific for epithelial cells and is induced during cell polarization. *J Cell Biol*. 1993;121(3):553-564.

33. Hansen GH, Niels-Christiansen LL, Immerdal L, Hunziker W, Kenny AJ, Danielsen EM. Transcytosis of immunoglobulin A in the mouse enterocyte occurs through glycolipid raft- and Rab17-containing compartments. *Gastroenterology*. 1999;116(3):610-622. doi:10.1016/S0016-5085(99)70183-6

34. Hunziker W, Peters PJ. Rab17 localizes to recycling endosomes and regulates receptor-mediated transcytosis in epithelial cells. *J Biol Chem*. 1998;273(25):15734-15741. doi:10.1074/jbc.273.25.15734

35. Striz AC, Tuma PL. The GTP-bound and sumoylated form of the Rab17 small molecular weight GTPase selectively binds syntaxin 2 in polarized hepatic WIF-B cells. *J Biol Chem*. 2016;291(18):9721-9732. doi:10.1074/jbc.M116.723353

36. Striz AC, Stephan AP, López-coral A, Tuma PL. *Rab17 Regulates Apical Delivery of Hepatic Transcytotic Vesicles*.

37. Mori Y, Matsui T, Furutani Y, Yoshihara Y, Fukuda M. Small GTPase Rab17 regulates dendritic morphogenesis and postsynaptic development of hippocampal neurons. *J Biol Chem*. 2012;287(12):8963-8973. doi:10.1074/jbc.M111.314385

38. Beaumont KA, Hamilton NA, Moores MT, et al. The recycling endosome protein Rab17 regulates melanocytic filopodia formation and melanosome trafficking. *Traffic*. 2011;12(5):627-643. doi:10.1111/j.1600-0854.2011.01172.x

39. Villaseñor R, Schilling M, Sundaresan J, Lutz Y, Collin L. Sorting Tubules

Regulate Blood-Brain Barrier Transcytosis. *Cell Rep*. 2017;21(11):3256-3270. doi:10.1016/j.celrep.2017.11.055

40. Pai EF, Kabsch W, Krengel U, Holmes KC, John J, Wittinghofer A. Structure of the guanine-nucleotide-binding domain of the Ha-ras oncogene product p21 in the triphosphate conformation. *Nature*. 1989;341(6239):209-214. doi:10.1038/341209a0

41. Gorvel JP, Chavrier P, Zerial M, Gruenberg J. Rab5 Controls Early Endosome Fusion in Vitro. *Cell*. 1991;64(5):915-925. doi:10.1016/0092-8674(91)90316-Q

42. Tabas I. Macrophage death and defective inflammation resolution in atherosclerosis. *Nat Rev Immunol*. 2009;10(1):36-46. doi:10.1038/nri2675

43. Thorp E, Cui D, Schrijvers DM, Kuriakose G, Tabas I. Mertk receptor mutation reduces efferocytosis efficiency and promotes apoptotic cell accumulation and plaque necrosis in atherosclerotic lesions of ApoE-/- mice. *Arterioscler Thromb Vasc Biol*. 2015;28(8):1421-1428. doi:10.1161/ATVBAHA.108.167197

44. Thorp E, Cui D, Schrijvers DM, Kuriakose G, Tabas I. Mertk receptor mutation reduces efferocytosis efficiency and promotes apoptotic cell accumulation and plaque necrosis in atherosclerotic lesions of apoe-/- mice. *Arterioscler Thromb Vasc Biol*. 2008;28(8):1421-1428. doi:10.1161/ATVBAHA.108.167197

45. Schrijvers DM, De Meyer GRY, Kockx MM, Herman AG, Martinet W. Phagocytosis of apoptotic cells by macrophages is impaired in atherosclerosis. *Arterioscler Thromb Vasc Biol*. 2005;25(6):1256-1261. doi:10.1161/01.ATV.0000166517.18801.a7

46. Muñoz LE, Lauber K, Schiller M, Manfredi A a, Herrmann M. The role of defective clearance of apoptotic cells in systemic autoimmunity. *Nat Rev Rheumatol*. 2010;6(5):280-289. doi:10.1038/nrrheum.2010.46

47. Wade NS, Major AS. The problem of accelerated atherosclerosis in systemic lupus erythematosus: insights into a complex co-morbidity. *Thromb Haemost*.

2011;106(5):849-857. doi:10.1016/j.biotechadv.2011.08.021.Secreted

48. Zipp F. Apoptosis in multiple sclerosis. *Cell Tissue Res*. 2000;301(1):163-171. doi:10.1007/s004410000179

49. Azizi PM, Zyla RE, Guan S, et al. Clathrin-dependent entry and vesicle-mediated exocytosis define insulin transcytosis across microvascular endothelial cells. *Mol Biol Cell*. 2014;26(4):740-750. doi:10.1091/mbc.e14-08-1307

50. Armstrong SM, Sugiyama MG, Fung KYY, et al. A novel assay uncovers an unexpected role for SR-BI in LDL transcytosis. *Cardiovasc Res*. 2015;108(2):268-277. doi:10.1093/cvr/cvv218

51. Pillon NJ, Azizi PM, Li YE, et al. Palmitate-induced inflammatory pathways in human adipose microvascular endothelial cells promote monocyte adhesion and impair insulin transcytosis. *Am J Physiol Metab*. 2015;309(1):E35-E44. doi:10.1152/ajpendo.00611.2014

52. Crocker JC, Grier DG. Methods of Digital Video Microscopy for Colloidal Studies. *J Colloid Interface Sci*. 1996;179:298-310.

53. Heit B, Tavener S, Raharjo E, Kubes P. An intracellular signaling hierarchy determines direction of migration in opposing chemotactic gradients. *J Cell Biol*. 2002;159(1):91-102. doi:10.1083/jcb.200202114

54. Heit B, Kubes P. Measuring Chemotaxis and Chemokinesis: The Under-Agarose Cell Migration Assay. *Sci Signal*. 2003;2003(170):pl5-pl5. doi:10.1126/stke.2003.170.pl5

55. Johnson DE, Ostrowski P, Jaumouillé V, Grinstein S. The position of lysosomes within the cell determines their luminal pH. *J Cell Biol*. 2016;212(6):677-692. doi:10.1083/jcb.201507112

56. Schneider CA, Rasband WS, Eliceiri KW. NIH Image to ImageJ: 25 years of image analysis. *Nat Methods*. 2012;9(7):671-675. doi:10.1038/nmeth.2089

57. Schindelin J, Arganda-Carreras I, Frise E, et al. Fiji: an open-source platform for biological-image analysis. *Nat Methods*. 2012;9(7):676-682. doi:10.1038/nmeth.2019

58. Zacchi P, Stenmark H, Parton RG, et al. Rab17 regulates membrane trafficking through apical recycling endosomes in polarized epithelial cells. *J Cell Biol*. 1998;140(5):1039-1053. doi:10.1083/jcb.140.5.1039

59. Shintani M, Tada M, Kobayashi T, Kajiho H, Kontani K, Katada T. Characterization of Rab45/RASEF containing EF-hand domain and a coiled-coil motif as a self-associating GTPase. *Biochem Biophys Res Commun*. 2007;357(3):661-667. doi:10.1016/j.bbrc.2007.03.206

60. Harrison RE, Bucci C, Vieira O V, Schroer T a, Grinstein S. Phagosomes fuse with late endosomes and/or lysosomes by extension of membrane protrusions along microtubules: role of Rab7 and RILP. *Mol Cell Biol*. 2003;23(18):6494-6506. doi:10.1128/MCB.23.18.6494

61. Rocha N, Neefjes J. MHC class II molecules on the move for successful antigen presentation. *EMBO J*. 2008;27(1):1-5. doi:10.1038/sj.emboj.7601945

62. Blander JM. Regulation of Phagosome Maturation by Signals from Toll-Like Receptors. *Science*. 2011;1014(2004):1014-1018. doi:10.1126/science.1096158

63. Yates RM, Russell DG. Phagosome maturation proceeds independently of stimulation of toll-like receptors 2 and 4. *Immunity*. 2005;23(4):409-417. doi:10.1016/j.immuni.2005.09.007

64. Harrison RE, Bucci C, Vieira O V, Schroer TA, Grinstein S. Phagosomes fuse with late endosomes and/or lysosomes by extension of membrane protrusions along microtubules: role of Rab7 and RILP. *Mol Cell Biol*. 2003;23(18):6494-6506. doi:10.1128/MCB.23.18.6494

65. Becken U, Jeschke A, Veltman K, Haas A. Cell-free fusion of bacteria-containing phagosomes with endocytic compartments. *Proc Natl Acad Sci U S A*.

2010;107(48):20726-20731. doi:10.1073/pnas.1007295107

66. Fan G-H, Lapierre LA, Goldenring JR, Richmond A. Differential regulation of CXCR2 trafficking by Rab GTPases. *Blood*. 2003;101(6):2115-2124. doi:10.1182/blood-2002-07-1965

67. Fairn GD, Grinstein S. How nascent phagosomes mature to become phagolysosomes. *Trends Immunol*. 2012;33(8):397-405. doi:10.1016/j.it.2012.03.003

68. Goldenring JR. Recycling endosomes. *Curr Opin Cell Biol*. 2015;35:117-122. doi:10.1016/j.ceb.2015.04.018

69. Saric A, Hipolito VEB, Kay JG, Canton J, Antonescu CN, Botelho RJ. mTOR controls lysosome tubulation and antigen presentation in macrophages and dendritic cells. *Mol Biol Cell*. 2016;27(2):321-333. doi:10.1091/mbc.E15-05-0272

70. Horgan CP, McCaffrey MW. Rab GTPases and microtubule motors. *Biochem Soc Trans*. 2012;39(5):1202-1206. doi:10.1042/bst0391202

71. Eskelinen EL. Roles of LAMP-1 and LAMP-2 in lysosome biogenesis and autophagy. *Mol Aspects Med*. 2006;27(5-6):495-502. doi:10.1016/j.mam.2006.08.005

72. Huynh KK, Gershenzon E, Grinstein S. Cholesterol accumulation by macrophages impairs phagosome maturation. *J Biol Chem*. 2008;283(51):35745-35755. doi:10.1074/jbc.M806232200

Chapter 4

4 Macrophages in Early Human Atherosclerosis Exhibit Dysregulated Expression of Genes Involved in Cholesterol Metabolism and Efferocytosis

4.1 Introduction

4.1.1 Challenge of studying human atherosclerotic macrophages

The role of macrophages in atherosclerotic disease has been studied intensively for many years, yet our understanding of macrophage phenotype and function in human atherosclerosis remains limited.[1] This lack of progress can be at least partially attributed to the inherent challenges of studying atherosclerosis in humans, and the limitations in available animal models of atherosclerosis (discussed in further detail in **Chapters 1.4.1** and **1.4.2**).[2,3]

Much of our understanding of the mechanisms driving macrophage dysfunction in atherosclerosis has come from animal studies in *Apoe*$^{-/-}$ or *Ldlr*$^{-/-}$ knockout mice.[3,4] These mouse models, while widely utilized, have some significant drawbacks and features that diverge from human disease. Mice are naturally HDL-predominant and are thus resistant to atherosclerosis.[3] Indeed, mice do not naturally develop atherosclerosis when fed a high fat diet and mouse models of atherosclerosis rely on genetically perturbing LDL homeostasis to generate disease.[4] The anatomical distribution of atherosclerotic lesions is also dramatically different in mouse models when compared to human disease.[5,6] Mice rarely develop atherosclerotic plaques within the coronary arteries, and differences in mouse hemodynamics means that they have greatest atherosclerotic burden in the aortic root and ascending aorta.[5]

On the other hand, studying atherosclerosis in humans is challenging for several reasons. First, atherosclerosis in humans takes decades to develop into clinically significant disease,[7] making it challenging to study the underlying disease pathogenesis.[2] Atherosclerosis is also ubiquitous amongst people living in developed, post-industrial nations.[8,9] The PDAY study, which examined the burden of atherosclerotic disease from

young people who died between the ages of 15 and 34 at 15 centres in the United States, found that atherosclerotic lesions at the early stages of disease were present starting in the 15-20 age group, and that lesions that occupied > 5% of intimal surface area were present in the aorta at rates in excess of 95% across all subjects.[9,10] This makes it difficult to identify subjects who can be considered "disease-free" when studying atherosclerosis in humans.

Finally, the site of disease—the atherosclerotic plaque—is difficult to access. The most common source of atherosclerotic plaque used to study macrophage phenotype and gene expression has been carotid plaque.[11,12] While carotid plaque can be obtained following carotid endarterectomy procedures and carotid plaque is involved in ischemic stroke, findings from carotid plaque may not be entirely translatable to coronary and aortic plaques. Transcriptomics studies that have examined plaque-resident macrophage gene expression in lesions from different anatomical sites have shown site-specific changes in gene expression patterns.[13] It is difficult to access coronary and aortic plaque material outside of autopsy studies, and as a result atherosclerosis in these vessels remain poorly studied. More creative approaches to studying atherosclerosis at these anatomical sites are needed. A recent study by Sulkava *et al.* was able to make use of left internal thoracic arteries obtained in the course of CABG surgery,[13] highlighting the need to leverage collaboration with surgical colleagues to advance our understanding of human atherosclerotic disease.

4.1.2 Cholesterol metabolism in macrophages

Macrophage cholesterol metabolism is well established as being dysregulated in atherosclerosis.[14,15] Formation of cholesterol-laden macrophages, known as foam cells, is perhaps the most well-established feature of atherosclerosis—having first been described by the Russian pathologist Nikolai Anitchkov in 1914.[16]

A summary of cholesterol metabolism in macrophages is provided in **Figure 4.1**. Macrophages recognize and take up modified lipoproteins through the scavenger receptors SR-A, CD36 and the lectin-like low-density lipoprotein receptor 1 (LOX-1).[17] Following uptake, these modified lipoproteins are trafficked into the lysosome, where lysosomal acid lipase (LAL) releases free cholesterol from the lipoprotein.[18] Free cholesterol within the

lysosome is transported out of the lysosome and into the ER through the concerted activity of the membrane-bound cholesterol transport proteins Niemann-Pick disease, type C1 (NPC1) and Niemann-Pick disease, type C2 (NPC2).[19] In the ER, acyl coenzyme A:cholesterol acyltransferase 1 (ACAT1) catalyzes the conversion of free cholesterol into cholesterol esters, which are stored as lipid droplets within the ER and cytoplasm of the macrophage.[18,20] Neutral cholesterol ester hydrolase (NCEH) catalyzes the hydrolysis of these cholesterol esters back into free cholesterol.[19] This free cholesterol can subsequently be removed from the cell through the efflux activity of the transporters ABCA1 and ABCG1, upon which they are shuttled onto the cholesterol acceptors HDL and ApoA1 for transport to the liver for further processing and removal.[20]

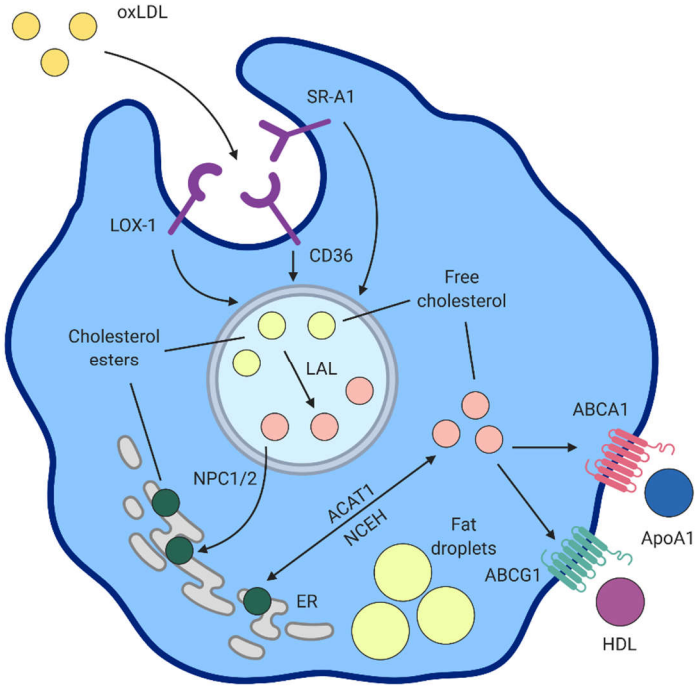

Figure 4.1 Cholesterol uptake, metabolism and efflux by macrophages.

Overview of cholesterol metabolism in macrophages. SR-A1 = scavenger receptor-A1, LOX-1 = lectin-like low-density lipropotein receptor-1, LAL = lysosomal acid lipase, NPC1/2 = Niemann-Pick disease, type C1/2, ACAT1 = acyl coenzyme A: cholesterol acyltransferase-1, NCEH = neural cholesterol ester hydrolase, ER = endoplasmic reticulum, HDL = high-density lipoprotein. Figure modified from Chistiakov *et al.*[20]

In atherosclerosis, pro-inflammatory stimuli and hypercholesterolemic stress induce increased expression of scavenger receptors and ACAT1, along with downregulation of cholesterol transporters required for cholesterol efflux.[21] This results in accumulation of lipid droplets and intracellular free cholesterol, giving the macrophage it's characteristic "foamy" appearance.[1,21] Additionally, accumulation of free cholesterol within the cytoplasm of these macrophages induces a pro-inflammatory response that results in production of TNF-α, IL-1β and IL-6, thus contributing to the maintenance of the inflammatory plaque microenvironment.[22,23]

4.1.3 Efferocytosis and efferosome maturation

Efferocytic removal of apoptotic cells (primarily apoptotic macrophages) within the atherosclerotic plaque is a crucial mechanism for limiting plaque progression and vulnerability.[24,25] In early atherosclerotic disease, it is thought that macrophage efferocytosis of apoptotic cells contributes to the generation of anti-inflammatory cytokines such as TGF-β and IL-10, which function to induce generation of a protective fibrotic cap and restraint of inflammation within the plaque microenvironment.[24] In the late stages of atherosclerosis, macrophage efferocytosis becomes defective, contributing secondary necrosis of uncleared apoptotic cells that contributes to generation of large necrotic cores that increase the likelihood of plaque rupture and thrombosis.[24]

Mechanisms leading to defective efferocytosis remain poorly defined, especially in human disease. Macrophages recognize apoptotic cells through efferocytic receptors that recognize specific signals on the cell surface of apoptotic cells (such as phosphatidylserine), usually through an intermediary opsonin.[25,26] These efferocytic receptors are thought to then function in cooperation with cell surface integrins (including the integrin α_x and β_2)[27] to mediate internalization of the apoptotic cell.[26] Activation of integrins results in the induction of several cell signaling pathways, including signaling through the Src family kinases and integrin-linked kinases to drive actin remodeling, efferocytic cup formation and efficient efferocytosis.[26,28] Following internalization, the nascent efferosome undergoes a series of maturation steps that result in efficient degradation of apoptotic cell contents without generation of inflammation or antigen presentation (discussed in detail in **Chapter 3**).

Available evidence supports the notion that both efferocytic uptake and efferosome maturation may be dysregulated in the setting of atherosclerosis. Cardiac and vascular macrophages utilize the TAM family of receptors in binding to apoptotic cells through their opsonin Gas6. Linkage studies in humans have demonstrated that SNPs in MERTK and TYRO3, but not AXL or GAS6, are associated with carotid atherosclerosis.[29,30] In particular MerTK appears to play a critical role in mediating efferocytic clearance of apoptotic cells within the atherosclerotic plaque.[31] Mutations in MerTK reduce efferocytic efficiency and increases necrotic core size in mouse models of atherosclerosis,[32] and ADAM17-mediated cleavage of MerTK also reduced atherosclerotic burden in *Ldlr*$^{-/-}$ mice.[33] Dysregulation in efferosome maturation in atherosclerosis has been studied to a far lesser extent. However, there is some evidence that Rab GTPase activity and antigen presentation are altered in atherosclerotic macrophages.[34,35]

4.1.4 Rationale and importance

Several decades of intensive study into the mechanisms of atherogenesis have yielded a wealth of knowledge on potential mechanisms that drive atherosclerosis initiation, progression and reversal. However, translation of these findings into clinical interventions that better diagnose, monitor and treat atherosclerotic disease has remained limited.[2] One reason for this lack of clinical translation is that the vast majority of these mechanistic studies have been done either *in vitro* or in animal models of atherosclerosis. These model systems, while extremely useful, fail to capture the whole complexity of human disease and, as a result, mechanisms that drive human atherosclerotic disease remain poorly understood.[2,3] Evidence from both animal and human studies implicate macrophages as key players in the pathogenesis of atherosclerosis.[24] However, macrophage dysfunction in atherosclerosis is challenging to study due to the inaccessibility of human plaque tissue and the inherent challenges of separating out a pure macrophage cell population from the plaque for analysis.

In this chapter, we describe a novel approach towards studying macrophage dysfunction in the setting of human aortic atherosclerosis. In collaboration with cardiac surgeons, we were able to collect small punch biopsies of the wall of the ascending aorta that are routinely obtained by the surgeon during CAGB operations. We proceed to obtain macrophages from

the atherosclerotic lesions present on these aortic punch samples by laser capture microdissection (LCM) and use these macrophages in a gene expression study to examine dysfunction in macrophage cholesterol metabolism and efferocytosis in the setting of human atherosclerotic disease.

A clearer picture of macrophage dysfunction in human atherosclerosis will provide us with a better understanding of which pathological mechanisms established from *in vitro* and animal work may be of importance in human atherosclerotic disease. Furthermore, uncovering changes in gene expression patterns in pathways related to efferocytosis and efferosome maturation will provide new insight into how critical function of macrophage efferocytosis becomes defective in the setting in atherosclerotic disease.

4.2 Methods

4.2.1 Histology

All histology was performed by Caroline O'Neil at the Robarts Research Institute Molecular Pathology Core Facility. Prior to staining, all frozen sections were fixed in 10% buffered formalin for 20 min and washed in ddH_2O. FFPE sections were deparaffinized by immersion in two changes of xylene for 10 min each and subsequently rehydrated by immersion in three changes of 100% ethanol, two changes of 95% ethanol and one change of 70% ethanol. Slides were then immersed in ddH_2O for 5 min.

4.2.1.1 Hematoxylin and eosin

Hematoxylin and eosin (H&E) staining was performed on both frozen and FFPE sections. Slides were first immersed in Mayer's hematoxylin solution for 3 min, followed by a brief wash in ddH_2O. Slides were the immersed in 0.2% ammonia water solution for 30 sec to allow for bluing and washed in ddH_2O. Slides were dipped briefly into 95% ethanol and stained in eosin Y solution for 3 min, followed by a brief wash in ddH_2O. Slides were then dehydrated by immersing in 95% ethanol for 1 min, and then in three changes of 100% ethanol for 10 dips each. Slides were mounted onto glass coverslips.

4.2.2 Oil Red O

Oil Red O staining was performed only on frozen sections. Slides were allowed to air dry at room temperature for 30 min prior to fixing in 10% buffered formalin. Slides were air dried again for 30 min at room temperature and washed in three changes of ddH_2O. Slides were transferred into 100% isopropanol for 5 min and then stained in per-warmed Oil Red O solution (3 parts 1:200 w/v Oil Red O powder 100% isopropanol to 2 parts ddH_2O) for 10 min at 60 °C. Following Oil Red O staining, slides were immersed in 85% isopropanol for 5 min and then washed in two changes of ddH_2O. Slides were then immersed in Mayer's hematoxylin solution for 30 sec and washed with ddH_2O for 5 min. Slides were mounted onto glass coverslips.

4.2.3 Movat's stain

Modified Russell-Movat pentachrome staining was performed on both frozen and FFPE sections. Slides were immersed in Verhoeff's elastic stain (2:1:1 5% hematoxylin in 100% ethanol, 10% ferric chloride, Verhoeff's iodine solution – 2% w/v iodine and 4% w/v potassium iodide in ddH_2O) for 30 min and subsequently washed with ddH_2O for 5 min. Slides were immersed in three changes of 2% ferric chloride solution for 10 sec each, immersed in 5% sodium thiosulfate solution for 1 min and washed with ddH_2O for 5 min. Slides were then immersed in 3% glacial acetic acid for 3 min, then 1% Alcian blue solution for 15 min, and finally washed with running ddH_2O for 10 min. Slides were then immersed in Crocein scarlet-acid fuchsin solution (0.08% w/v Crocein scarlett, 0.02% w/v acid fuchsin and 0.5% v/v acetic acid in ddH_2O) for 2 min, washed in two changes of ddH_2O for five dips each and then in one change of 1% acetic acid for five dips. Next, slides are immersed in 5% phosphotungstic acid for 1 min, and washed in one change of 1% acetic acid, one change of ddH_2O and one change of 100% ethanol for five dips each. Slides are dehydrated in two changes of 100% ethanol for 3 min each and then immersed in alcoholic saffron solution (6% w/v Saffron du Gatinais in ethanol) for 15 min. Finally, slides are dried in two changes of xylene for 3 min each and mounted onto glass coverslips.

4.2.3.1 TUNEL stain

TUNEL staining was performed on FFPE sections only to assess the number of uncleared apoptotic cells present.[36,37] Following deparaffinization, sections were digested with 20 µg/mL proteinase K for 15 min at room temperature to permeabilize tissue. Slides were rinsed with two changes of PBST for 2 min each. Slides were then immersed in 3% H_2O_2 in PBS for 10 min and washed again with two changes of PBST for 2 min each. Slides were then immersed in TdT reaction mixture (1:9 terminal transferase enzyme, biotin-16-UTP prepared according to the manufacturer's instructions) for 2 hr at 37 °C in a humidity chamber. The labelling reaction was stopped by incubation in a buffer containing 300 mM NaCl and 30 mM sodium citrate for 10 min. Following washing with PBST, slides were immersed in streptavidin-HRP for 20 min at room temperature and then DAB chromogen with a PBST wash in between. Slides were rinsed in running tap water for 30 sec and counterstained with Mayer's hematoxylin solution for 30 sec. Slides were washed in running ddH_2O for 5 min and then dehydrated through subsequent immerse in one change of 95% ethanol and two changes of 100% ethanol for 3 min each. Sections were cleared by immerse in two changes of xylene for 5 min each and mounted onto a glass coverslip.

4.2.4 Laser capture microdissection

Patient aortic punch frozen sections as described in **Chapter 2.2** on Superfrost Plus Microscope Slides (Fisher Scientific) and stored at -80 °C prior to use. Immediately prior to beginning tissue staining and dehydration, slides were removed from -80 °C storage and allowed to thaw briefly (~ 30 sec) at room temperature to completely remove condensation. Slides were fixed in ice-cold acetone for 2 mins, followed by air drying for 30 sec to remove excess acetone. A PAP pen was used to circumscribe each tissue section adhering to the slide. In a humidity chamber, sections were washed with 200 µL of PBS and 100 µL of 30-60 µg/mL anti-CD163 antibody (Abcam, polyclonal Ab ab87099) was applied for 3 min at room temperature. Sections were washed 2× with PBS and 100 µL of 1:100 diluted secondary antibody was applied for 3 min at room temperature. Sections were again washed 2× with PBS and then sequentially dehydrated with application of 200 µL of 75%, 95% and 100% ethanol for durations of 30 sec each. Slides were dried by immersion in

xylene for 5 min and excess xylene was allowed to evaporate under a fume hood. Processed slides were used immediately for LCM.

LCM was performed on an ArcturusXT Laser Capture Microdissection System (Applied Biosystems) running ArcturusXT Operating Software (Applied Biosystems). Due to the small size of the sections in question, CapSure HS LCM Caps (Applied Biosystems) were used to capture dissected samples. Samples were captured using IR capture laser of 15 µm diameter at 70 mW, 1,500 µsec and 1 hit per capture. A minimum of 200 captures per section across four consecutive sections was performed to obtain sufficient cell numbers for downstream analysis. Following laser capture microdissection, dissected samples were immediately processed in TRIzol reagent to stabilize RNA. Total RNA was extracted from dissected samples using the protocol described in **Chapter 2.6.1**.

4.2.5 Microarray

RNA quality checks, cDNA preparation, array hybridization and microarray data analysis (in part) were all performed by David Carter and Jen Biltcliffe at the London Regional Genomics Centre.

Total RNA for microarray was prepared from patient aortic punch macrophages prepared according to **Chapter 4.2.4** and control peripheral blood monocyte-derived macrophages prepared according to **Chapter 2.4.2**. Prior to the microarray, RNA quality was checked using a 2100 Bioanalyzer Instrument (Agilent) and a minimum A260/280 of 1.5 and minimum RIN of 7 was required before the RNA could be used in the microarray. A minimum of 2.0 µg of total RNA was from each sample was used in the microarray.

RNA samples were prepared for array hybridization using the GeneChip WT Pico Reagent Kit (Applied Biosystems) according to the manufacturer's instructions with 12 cycles of pre-*in vitro* transcription amplification. Poly-A RNA standards provided by the manufacturer were used as exogenous positive controls. Samples were analyzed on the GeneChip Human Gene 2.0 ST Array chip (Applied Biosystems) hybridized on the GeneChip Scanner 3000 7G System (Applied Biosystems) according to the manufacturer's recommended instructions.

4.2.6 Identification of differentially expressed genes

Raw microarray data were analyzed using the Partek Genomics Suite platform (Partek). Reads were normalized using the Robust Multi-array Average (RMA) procedure with quantile normalization. Subsequently, a mixed-model ANOVA was used to identify differentially expressed genes with a foldchange cutoff of 2.0 and p-value cutoff of $p<0.05$. Unsupervised hierarchical clustering of all differentially expressed genes was performed to generate a heat map of differential gene expression.

Results were verified using open-access tools in R Statistical Software (R Project for Statistical Computing) available through the Bioconductor project.[38] The oligo package was used to read in raw microarray data files and perform RMA normalization.[39] The limma package was used to identify differentially expressed genes using a linear models approach along with an empirical Bayes method to better estimate errors in log-fold change.[40,41]

4.2.7 GO term enrichment analysis

Gene ontology (GO) term enrichment analysis was performed on the Partek Genomics Suite (Partek) using the GO ANOVA feature, with analysis restricted to functional groups with more than two and fewer than 150 genes. The top 100 GO biological function terms were used for GO term visualization using the REVIGO online software platform (Rudjer Boskovic Institute), where terms were visualized by both uniqueness and connectivity.[42]

4.2.8 Gene set enrichment analysis

Gene set enrichment analysis (GSEA) was performed using the Gene Set Enrichment Analysis software platform (Broad Institute) with publicly-available annotated gene sets (cholesterol_homeostasis, antigen_processing_presentation, fcr_mediated_phagocytosis, phagosome_maturation) obtained from the Molecular Signatures Database (MSigDB).[43,44] Analysis run at 10,000 permutations using default settings with FDR < 0.25.

4.2.9 KEGG pathway analysis

Pathway enrichment analysis was performed using the Partek Pathway software platform (Partek) using public-available Kyoto Encyclopedia of Genes and Genomes (KEGG) pathways (Phagosome, Oxidative Phosphorylation, Antigen Processing and Presentation).

4.3 Results

4.3.1 Quantification of mean wall and intimal thickness in patient aortic punch samples

In order to study human aortic atherosclerosis, we utilized aortic punch tissue that is routinely obtained and discarded by cardiac surgeons during procedures that involve cannulation of the ascending aorta. The surgeon creates a full-thickness, circular punch through the aortic wall. The resulting tissue sample contains all the features of a typical artery, including the tunica intima, tunica media and tunica adventitia. An example of a patient aortic punch cross-section is shown in **Figure 4.2**.

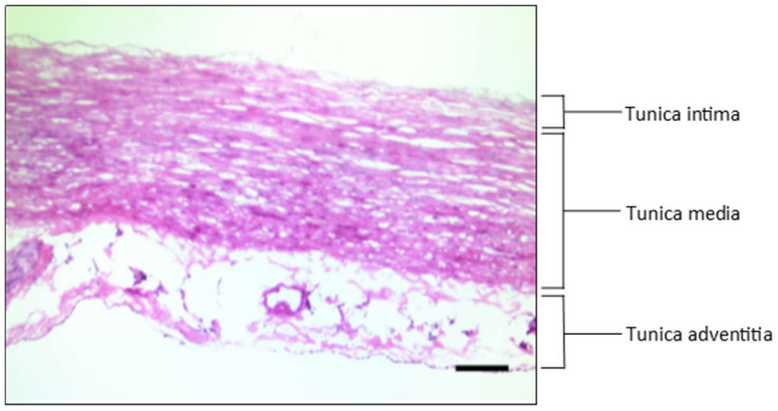

Figure 4.2 Cross-section of a typical patient aortic punch sample.

H&E staining of a sectioned patient aortic punch tissue sample demonstrating the intact layers of the aortic wall. Following excision during surgery, aortic punch tissue was embedded and frozen in OCT. 10 µm-thick frozen sections were obtained and stained using hematoxylin and eosin and imaged under white light. The section shown is representative of the appearance of a typical patient aortic punch sample. Scale bar is 500 µm.

As there are relatively few studies that have examined atherosclerotic plaques in the human aorta, we sought to assess the average wall and tunica intima thicknesses of our patient aortic punch samples. To differentiate between intima and media on histology, we utilized the Movat pentachrome stain, which allows visualization of the elastin layer that separates the intimal and medial layers as a thin black line immediately below the intimal layer (example shown in **Figure 4.3a**). Average wall thickness of our patient aortic punch samples was approximately 3.7 mm (**Figure 4.3b**) while average intimal thickness was approximately 0.2 mm (**Figure 4.3c**).

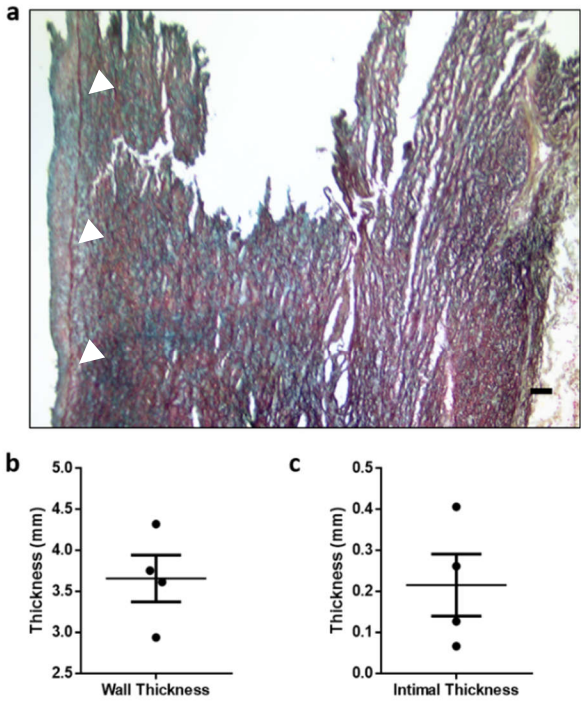

Figure 4.3 Quantification of wall and intimal thickness in patient aortic punch samples.

Following excision during surgery, patient aortic punch tissue samples were formalin-fixed and embedded in paraffin. (**a**) 10 µm-thick sections were obtained, stained using a modified Russell-Movat pentachrome stain and imaged under white light. From images, (**b**) wall thickness and (**c**) intimal thickness were directly measured. Image is representative (**a**), and graphs quantify (**b**,**c**) four punches from four separate patients. Data are shown are mean ± SEM. White arrows indicate the elastin layer. Scale bars are 100 µm.

The literature reports varying mean ascending aortic wall thickness in healthy individuals. Biancari *et al.* report that an ascending aorta wall thickness of greater than 1.8 mm increases the risk of post-operative mortality following CABG,[45] while Erbel and Eggebrecht state that a wall thickness of less than 4 mm should be considered to be normal in healthy adults.[46] Our finding of 3.7 mm in older individuals with significant atherosclerotic burden therefore lies between these two reported values. Discrepancies in reported measurements may be a result of the methodology used to assess wall thickness, with both ultrasound and direct measurement on histology being utilized.[47,48] In general, aortic wall thickness varies according to anatomical location, with the ascending aorta having the greatest thickness.[48] The size of the aorta also increases with age, with the diameter increasing by 1-2 mm/year on average.[46]

4.3.2 Patient aortic punch samples exhibit early stage atherosclerotic disease

Upon examination of H&E staining of patient aortic punch tissue sections, we observed minimal evidence of advanced atherosclerotic disease (e.g. significant accumulation of lipids, large necrotic cores, etc.). As a result, we sought to better characterize the degree of atherosclerotic disease present in our aortic punch samples by examining: 1) sub-intimal lipid accumulation, 2) intimal thickening and fibrosis, and 3) sub-intimal macrophage accumulation. Serial frozen sections of aortic punch tissue were stained with H&E to assess tissue morphology, Oil Red O to assess lipid accumulation, Movat's stain to assess intimal thickening and fibrosis, and αCD163 antibody to assess macrophage accumulation.

CD163 was used as a marker of macrophages within the atherosclerotic plaque because the most commonly used human macrophage marker, CD68, is problematic in atherosclerosis because smooth muscle cells exposed to the atheroma microenvironment can also express this marker.[48–50] Indeed, Allahverdian *et al.* demonstrated that up to 40% of $CD68^+$ cells in advanced coronary atheromas are of smooth muscle cell origin.[50] The hemoglobin-haptoglobin scavenger receptor CD163 is uniquely expressed in cells of the monocyte/ macrophage lineage and was therefore selected as a highly specific marker of macrophages within the human atherosclerotic plaque.[51] It is well-established that CD163 is highly expressed in macrophages that have been exposed to intraplaque hemorrhage, which adopt

an unique phenotype termed MHem (or HA-mac) that is characterized by ATF-1-driven up-regulation of CD163 and the HO-1 enzyme.[52,53] Originally believed to be atheroprotective, a recently seminal study from Guo *et al.* has demonstrated that MHem macrophages actually increase inflammation in human atherosclerotic plaques via induction of intraplaque angiogenesis, vascular permeability and inflammatory cell recruitment.[54] In our hands, CD163 expression can be reliably detected on human M0-, M1- and M2-polarized macrophages differentiated *in vitro* from peripheral blood monocytes (**Figure 4.4a**). We were able to further demonstrate that in our patient aortic punch tissue sections, CD163 and CD68 expression are highly correlated (**Figure 4.4b** and **4.4c**).

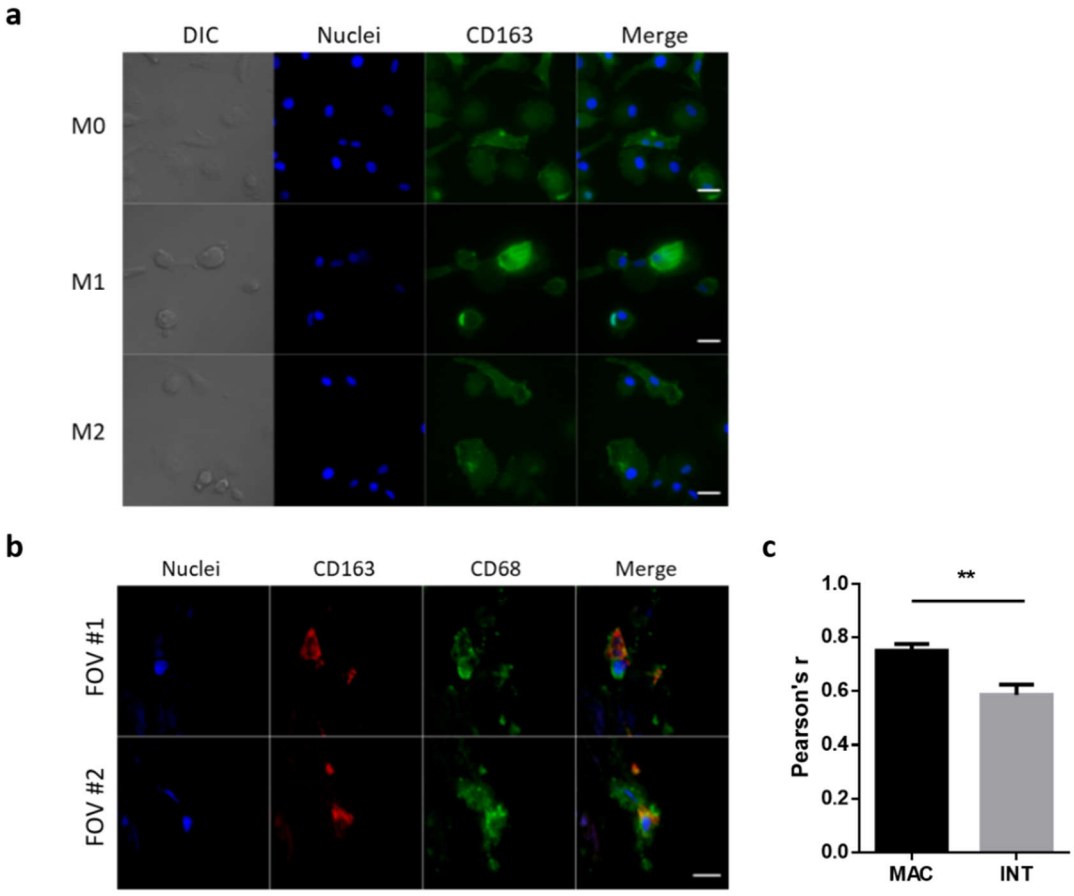

A representative example of serial sections of patient aortic punch tissue stained using the strategy described previously is provided in **Figure 4.5a**. We observed while there was a lack of extracellular lipid pools or necrotic core formation, our patient aortic punch tissues were characterized by lipid droplet accumulation beneath the intima, along with some intimal thickening and fibrosis. Furthermore, we could detect the presence of discrete macrophage populations within the intimal layer. Upon quantification of the degree of lipid accumulation, intimal thickening and macrophage accumulation, we could demonstrate that there was a significant positive correlation between the degree of lipid accumulation and number of macrophage cells (**Figure 4.5b**). Positive correlations were also observed between intimal thickness and number of macrophage cells (**Figure 4.5c**) and between intimal thickness and lipid accumulation (**Figure 4.5d**). Referencing the classic classification system for atherosclerotic plaque progression developed by Stary and colleagues in 1994, these features are characteristic of Types I-III lesions .[55]

Figure 4.4 CD163 is a reliable marker of macrophage cells. (on opposite page)

Immunofluorescence staining of cultured macrophages and aortic punch sections was used to determine whether CD163 expression can be reliably detected on macrophage cells. (**a**) Macrophages differentiated *in vitro* from peripheral blood monocytes from healthy human donors and polarized to M0, M1 and M2 phenotypes were immunostained for CD163. Images are representative of three independent replicates. Scale bars are 20 μm. (**b**) Aortic punch sections were co-immunostained for CD163 and CD68 and (**c**) Pearson's correlation coefficient between CD163 and CD68 was calculated for both clearly identifiable macrophage cells (MAC) and random regions of the intima (INT). Images show two representative fields of view (FOV#1 and FOV#2) (**b**) or quantifies five fields of view as mean ± SEM (**c**). **$p < 0.01$ by unpaired two-tailed Student's t test. Scale bar is 10 μm.

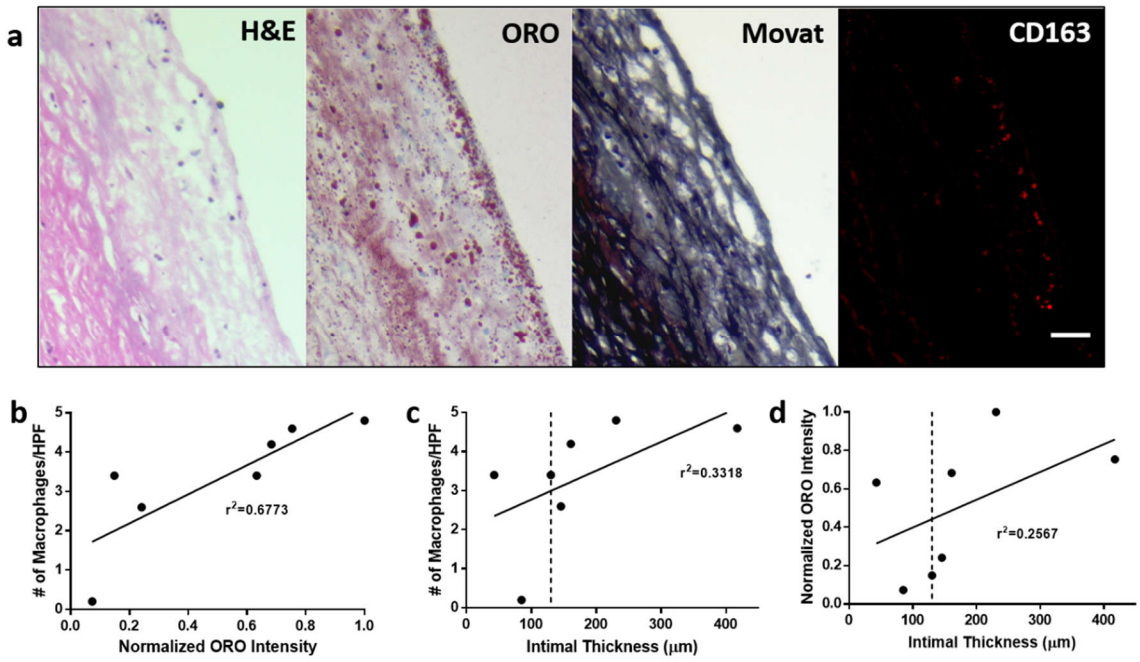

Figure 4.5 Patient aortic punch tissue samples exhibit features of early atherosclerotic disease.

Serial sections of patient aortic punch tissues were obtained and treated with a number of histological stains to characterize the degree of atherosclerotic disease present in the samples. (**a**) 10 μm-thick frozen sections were stained with hematoxylin and eosin (H&E), Oil Red O (ORO), modified Russell-Movat's pentachrome stain (Movat) and immunostained for CD163 (CD163). (**b-d**) The degree correlation was assessed between lipid accumulation and number of macrophages per high-power field (**b**), intimal thickness and number of macrophages per high-power field (**c**) or intimal thickness and lipid accumulation (**d**). Linear regression was calculated, with line of best fit and r^2 values being provided in each graph. Pearson's correlation coefficient was also calculated ($p < 0.01$ for **b**, n.s. for **c** and **d**). Images are representative of (**a**) and graphs quantify (**b-d**) seven separate aortic punch samples. Dotted line indicates the normal intimal thickness in healthy adults. Scale bar is 50 μm.

Finally, we aimed to assess the extent of necrotic cell accumulation within the intima in our aortic punch tissues. Uncleared apoptotic cells that have undergone secondary necrosis is a hallmark feature of advanced atherosclerotic disease. In accordance with our previous results, we found only a few necrotic cells could be observed (**Figure 4.6a** and **4.6b**), again indicating an earlier stage of disease progression.

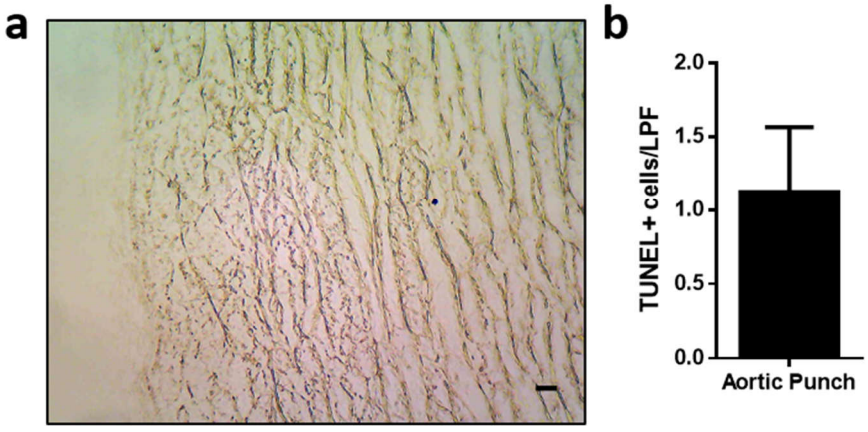

Figure 4.6 Minimal necrotic cell accumulation in patient aortic punch tissue.

TUNEL staining was used to measure the degree of necrotic cell accumulation within patient aortic punch tissues. (**a**) TUNEL staining of a 10 μm-thick frozen section of aortic punch tissue, and (**b**) quantification of the number of TUNEL stain-positive necrotic cells per low power field. Image is representative of (**a**) and graph quantifies (**b**) eight random fields of view from three separate aortic punch samples. Data are shown are mean ± SEM.

4.3.3 Isolation of a pure macrophage cell population from patient tissue

After establishing that CD163 immunostaining as a reliable means of identifying macrophage cell populations in the intima of our patient aortic punch samples (example shown in **Figure 4.7a**), we proceeded to isolate a pure macrophage cell population using LCM. Aortic punch frozen sections were rapidly immunostained for CD163 and used immediately for LCM, with CD163 staining guiding the capture of at least 800 cells per sample from four successive serial sections.

RNA was immediately isolated from captured macrophage cells and expression of the monocyte/macrophage-specific marker CD14 and the smooth muscle cell-specific ACTA2 in captured cells compared to whole sections to assess the purity of captured cell populations. Captured cell samples were significantly enriched in CD14 expression (**Figure 4.7b**) whereas they expressed ACTA2 at significantly lower levels than whole section controls (**Figure 4.7c**), suggesting that a relatively pure macrophage cell population was successfully isolated by LCM.

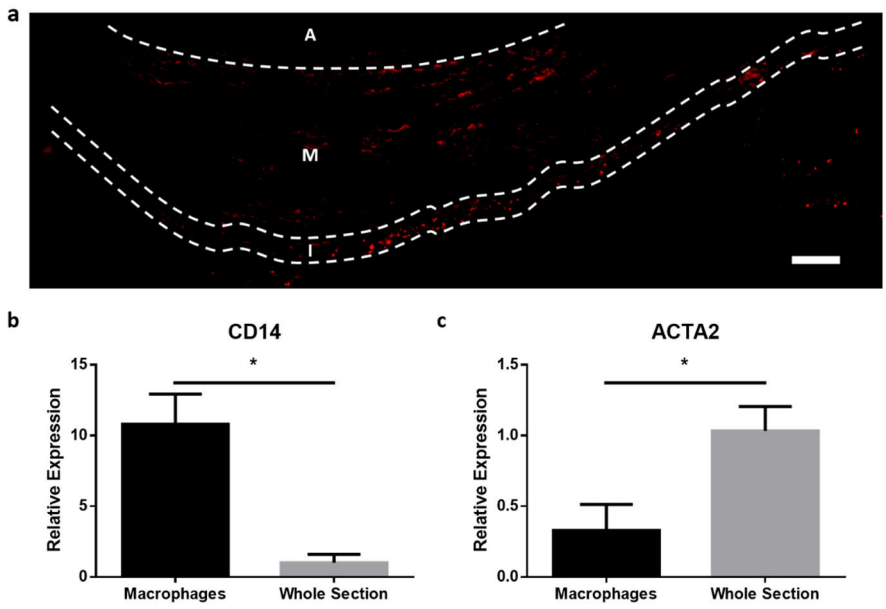

Figure 4.7 Isolation of a pure macrophage cell population from aortic punch tissue by LCM.

LCM was used to selectively isolate macrophage cell populations and the purity of LCM dissected macrophages was confirmed by RT-qPCR. (**a**) Patient aortic punch tissue sections were immunostained for CD163 and imaged using the fluorescence microscopy system built into the LCM System. Borders between the intima (I), media (M) and adventitia (A) are denoted by dashed lines. (**b**, **c**) RT-qPCR analysis of the expression of CD14 (**b**) and ACTA2 (**c**) in LCM-captured macrophages and whole section controls. The image is representative of (**a**) and graphs quantify (**b**, **c**) three independent sets of captured macrophages and whole section controls. Data are presented as mean ± SEM. *$p < 0.05$ by unpaired two-tailed Student's t test. Scale bar is 200 μm.

4.3.4 Gene expression profiling of macrophages isolated from patient aortic punch tissue

To better understand the properties of macrophages within the early pre-atherosclerotic lesions identified in our patient aortic punch tissue, gene expression profiling by microarray was performed on LCM-captured patient macrophages. As a control we utilized peripheral blood monocytes isolated from healthy age- and sex-matched donors were differentiated *in vitro* to M0-polarized macrophages. In total, three patient macrophage samples and three controls were analyzed by microarray. Concentration and integrity for each sample are reported in **Table 4.1**.

Table 4.1 Concentration and RNA integrity of samples used for microarray.

Type	ID	Concentration (ng/µL)	A260/280	A260/230	RIN
Patient Macrophages	AP-1	9.1	1.72	0.84	7.0
	AP-2	9.8	1.46	0.83	7.4
	AP-3	9.6	1.86	0.81	7.0
Control Macrophages	CT-1	39.1	1.71	1.40	7.5
	CT-2	47.7	1.78	1.46	8.6
	CT-3	112.9	1.84	1.43	7.6

Microarray analysis was performed using the GeneChip Human Gene 2.0 ST Array at London Regional Genomics Centre (London, Ontario). This chip provides comprehensive coverage of protein-coding and long intergenic non-coding RNA (lncRNA), although for the purposes of this study, lncRNA was not included in subsequent analyses because they remain poorly annotated. Gene expression profiling demonstrated significant differences in gene expression between patient and control macrophages. Principal component analysis (PCA) showed clear segregation and separation of patient and control macrophages, with the first two principal components accounting for 65.9% of variability between the two groups (**Figure 4.8a**). Following RMA normalization (**Figure 4.8b**) and differentially expressed gene identification using a mixed-model ANOVA, 3,374 protein-coding genes met the pre-specified cutoff criteria of log-foldchange > 2.0 and adjusted p value < 0.05

(**Figure 4.8c**). Compared to control macrophages, the majority of genes in patient macrophages were down-regulated (**Figures 4.8c** and **4.8d**).

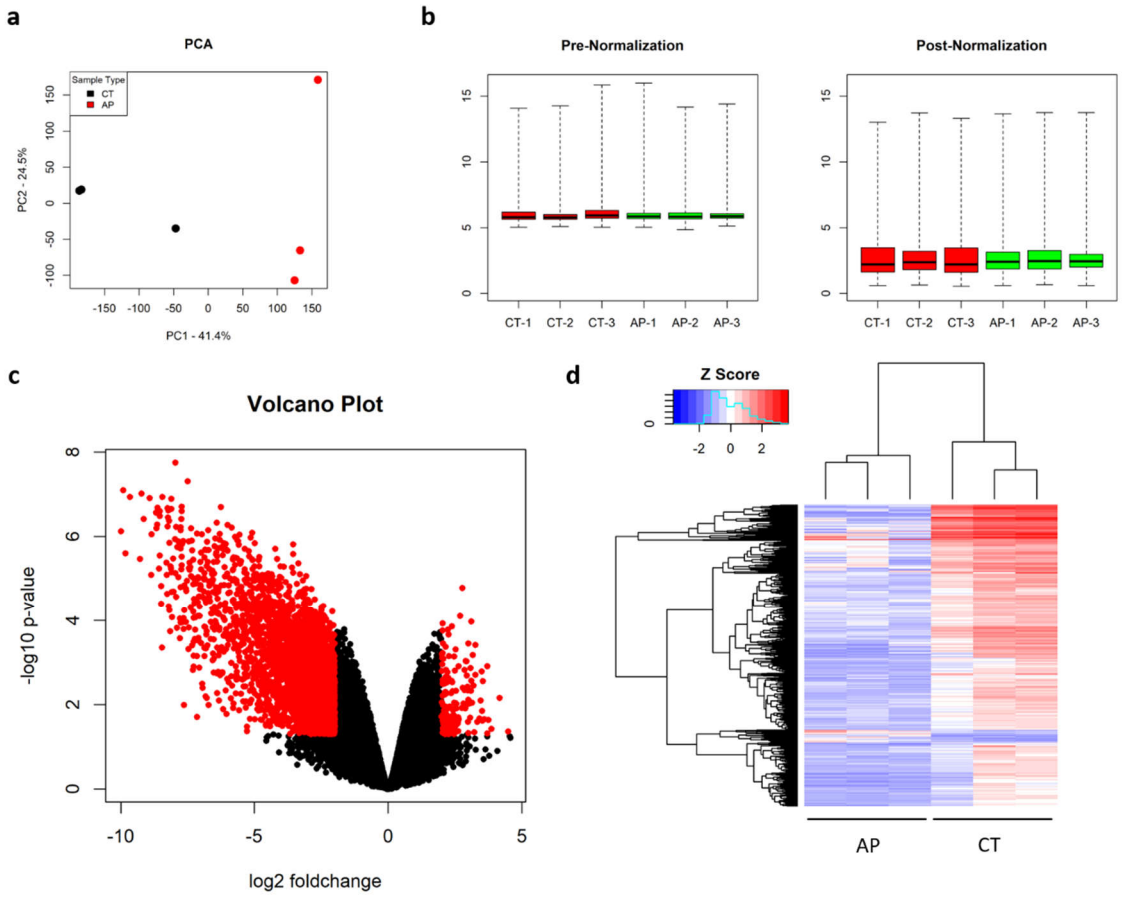

Figure 4.8 Microarray analysis of pre-atherosclerotic macrophages demonstrates profound differences in gene expression.

Microarray analysis was performed on LCM-captured patient macrophages with *ex vivo* monocyte-derived macrophages from healthy donors as controls. Three patient samples and three controls were used for microarray. (**a**) PCA of gene expression profiles from patient and control macrophages. (**b**) Average read intensities of patient and control macrophage samples pre- and post-RMA normalization. (**c**) Volcano plot demonstrating overall changes in gene expression in patient macrophages compared to controls. Each individual dot represents one gene, with red dots representing differentially expressed genes that met the pre-specified cut-offs of log-foldchange > 2.0 and adjusted p value <

0.05. In total, 3,374 protein-coding genes met cut-offs. (**d**) Heatmap generated through unsupervised hierarchical clustering of all differentially expressed genes in patient macrophages compared to controls, with colour scheme reflecting gene expression z-score. AP – patient aortic punch macrophages, CT – healthy donor control macrophages.

From the complete list of differentially expressed protein-coding genes, we manually curated a list of genes of interest on the basis of either known association with atherosclerosis or involvement in pathways of interest. These pathways of interest included: 1) phagocytosis and efferocytosis, 2) cholesterol metabolism, 3) antigen presentation, 4) peptide citrullination, and 5) regulation of gene expression. Using this method, we identified 10 differentially upregulated genes of interest and 10 differentially downregulated gene of interest (**Table 4.2**). A list of the top 100 upregulated and downregulated genes can be found in **Appendix B**.

Table 4.2 Differentially expressed genes with potential relevance to dysregulated macrophage function in atherosclerosis

GENE SYMBOL	GENE NAME	FOLD CHANGE
CLEC18A	C-type lectin domain family 18 member A	3.84465
RAB44	RAB44, member RAS oncogene family	2.63632
FOXF2	forkhead box F2	2.53369
LGALS14	lectin, galactoside-binding, soluble, 14	2.46699
YAP1	Yes-associated protein 1	2.45382
GATA2	GATA binding protein 2	2.42342
E4F1	E4F transcription factor 1	2.32076
RARG	retinoic acid receptor, gamma	2.30969
PADI3	peptidyl arginine deiminase	2.30731
IL34	interleukin 34	2.06427
HLA-DRA	major histocompatibility complex, class II, DR alpha	-249.226
RAB7A	RAB7A, member RAS oncogene family	-181.069
NPC2	Niemann-Pick disease, type C2	-103.934
CD44	CD44 molecule (Indian blood group)	-55.613
AHR	aryl hydrocarbon receptor	-52.8631
ITGAX	integrin, alpha X	-51.7944
CD47	CD47 molecule	-21.8968
NPC1	Niemann-Pick disease, type C1	-12.2608
ABCA1	ATP binding cassette subfamily A member 1	-3.95497
ILK	integrin-linked kinase	-3.20291

The set of genes that were differentially upregulated in patient macrophages in comparison to controls was limited. However, this set of genes did significantly include a number of transcription factors (FOXF2, YAP1, GATA2, E4F1 and RARG). This was of interest to us because these transcription factors may drive part or all of the differences in gene expression observed in our patient macrophages. Of these five transcription factors, GATA2, E4F1 and RARG have previously been implicated in atherosclerosis. Briefly, SNP's in GATA2 have been found to be associated with CAD in genome-wide association and linkage studies.[56,57] E4F1 is an estrogen-responsive gene that is up-regulated in the aortas of postmenopausal women with atherosclerotic disease.[58] Finally, activation of RARG *in vitro* has been shown to induce up-regulation of ABCA1, which encodes a protein that plays a key role in transport of cholesterol out of the cell.[59] Interestingly, another gene that is upregulated in patient macrophages is PADI3, which encodes the type III peptidyl arginine deiminase – an enzyme that is responsible for peptide citrullination and plays a role in the pathogenesis of rheumatoid arthritis.[60] Peptide citrullination has been reported to occur in atherosclerosis and is thought to be involved in the acceleration of atherosclerotic disease development in patients with rheumatoid arthritis.[61]

4.3.5 Confirmation of changes in gene expression by RT-qPCR

Since microarray data is inherently noisy, we next sought to confirm that the changes in gene expression identified in the microarray analysis could be reproduced by RT-qPCR. Furthermore, to control for the possibility of bias from using a limited number of patients and controls, we assessed gene expression in five independent patient and control macrophage samples. Genes assessed included those involved in regulation of gene expression: GATA2, E4F1, RARG (**Figure 4.9a**); those involved in cholesterol metabolism: ABCA1, NPC1, NPC2 (**Figure 4.9b**); and those involved in phagocytosis/ efferocytosis (**Figure 4.9c**).

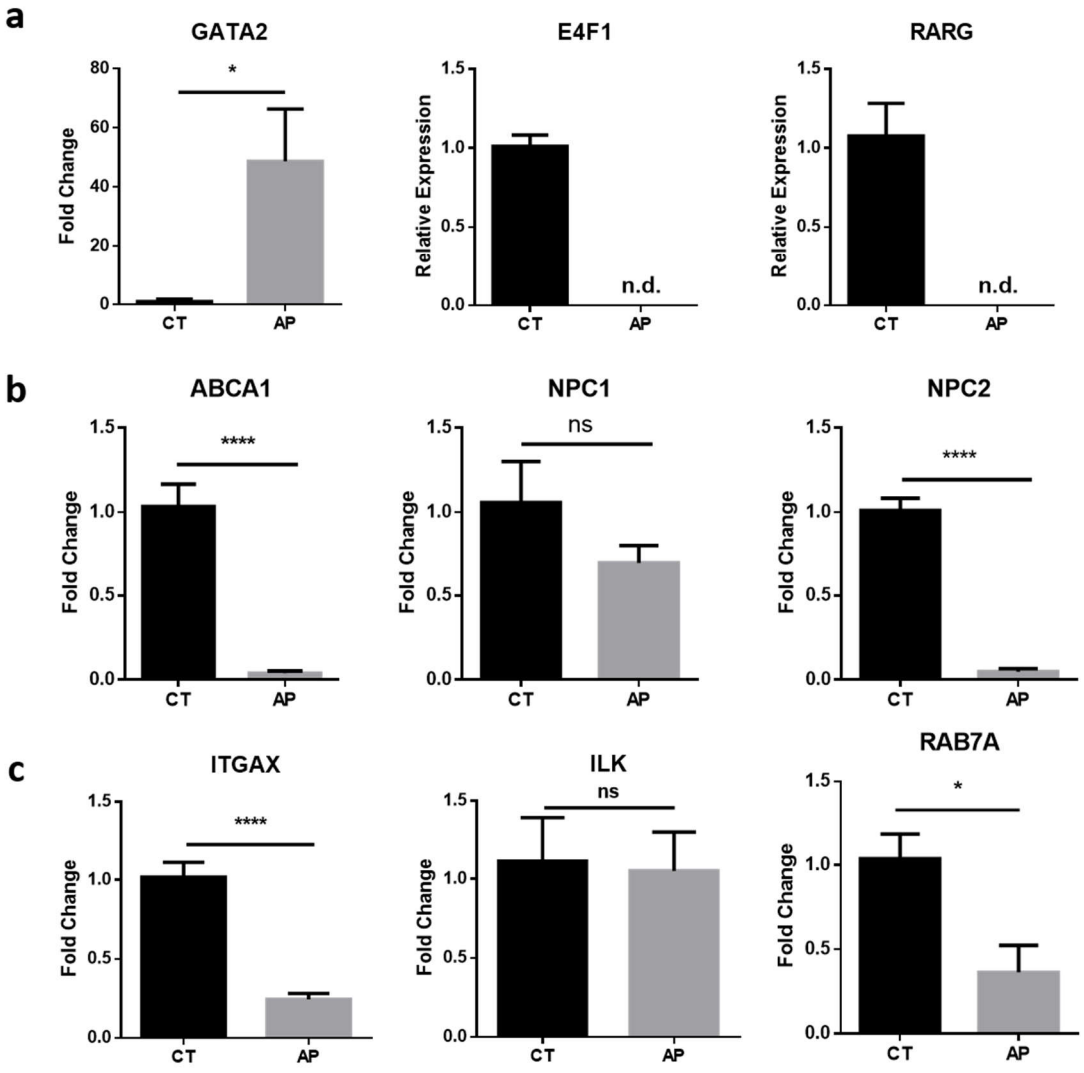

Figure 4.9 RT-qPCR validation of key microarray results. (on opposite page)

RT-qPCR analysis was performed on independent patient macrophage and control macrophage samples to validate microarray results. Genes assessed included those involved in regulation of gene expression (**a**), cholesterol metabolism (**b**) and phagocytosis/ efferocytosis (**c**). Graphs quantify five independent patient and control macrophage samples that had not been used in the microarray. CT – control macrophages from healthy donors, AP –macrophages from patient aortic punch tissue. Data are presented mean ± SEM. *$p < 0.05$, **$p < 0.01$, ****$p < 0.001$ by Mann Whitney U test. ns = not significant, n.d. = not detected.

As expected, we observed upregulation of GATA2 and downregulation of ABCA1, NPC2, ITGAX and RAB7A in the patient macrophages in comparison to the controls. There was no difference in the expression of ILK between patients and controls, which may be due to inter-individual differences between the subjects used in the microarray study versus for RT-qPCR or random variability in the original microarray data. Unexpected, neither E4F1 nor RARG was detectable in our RT-qPCR assay. Conversely, we found that GATA2 was upregulated in excess of 50-fold in patient macrophages.

4.3.6 Functional analysis of gene expression data reveals potential defects in cholesterol metabolism and in phagocytosis/ efferocytosis

To translate differences in gene expression profile determined by microarray to altered patient macrophage function within the pre-atherosclerotic environment, we took functional and pathway-based approaches to assigning biological significance to differences in gene expression. We first examined GO classifications that were significantly enriched in our gene expression dataset. Using the 100 most significantly over-represented biological processes in our dataset, we generated plots of GO terms on the basis of uniqueness (**Figure 4.10a**) and connectivity (**Figure 4.10b**).

Figure 4.10 Highly over-represented GO terms from microarray data. (on opposite page)

The 100 most highly significant biological processes GO terms from the microarray dataset were visualized on the basis of uniqueness (**a**) or connectivity (**b**) using the REVIGO online GO term analysis platform. Plots assign *x* and *y* coordinates to terms by semantic similarity such that GO terms representing processes similar in function are grouped closer together (**a**) or by connectivity between terms such that similar GO terms are connected pairwise, with the line width indicating the degree of similarity (**b**). Colours represent p values and the size of each circle represents the number of differentially expressed genes from the microarray dataset that are categorized as part of that particular GO term (**a**, **b**).

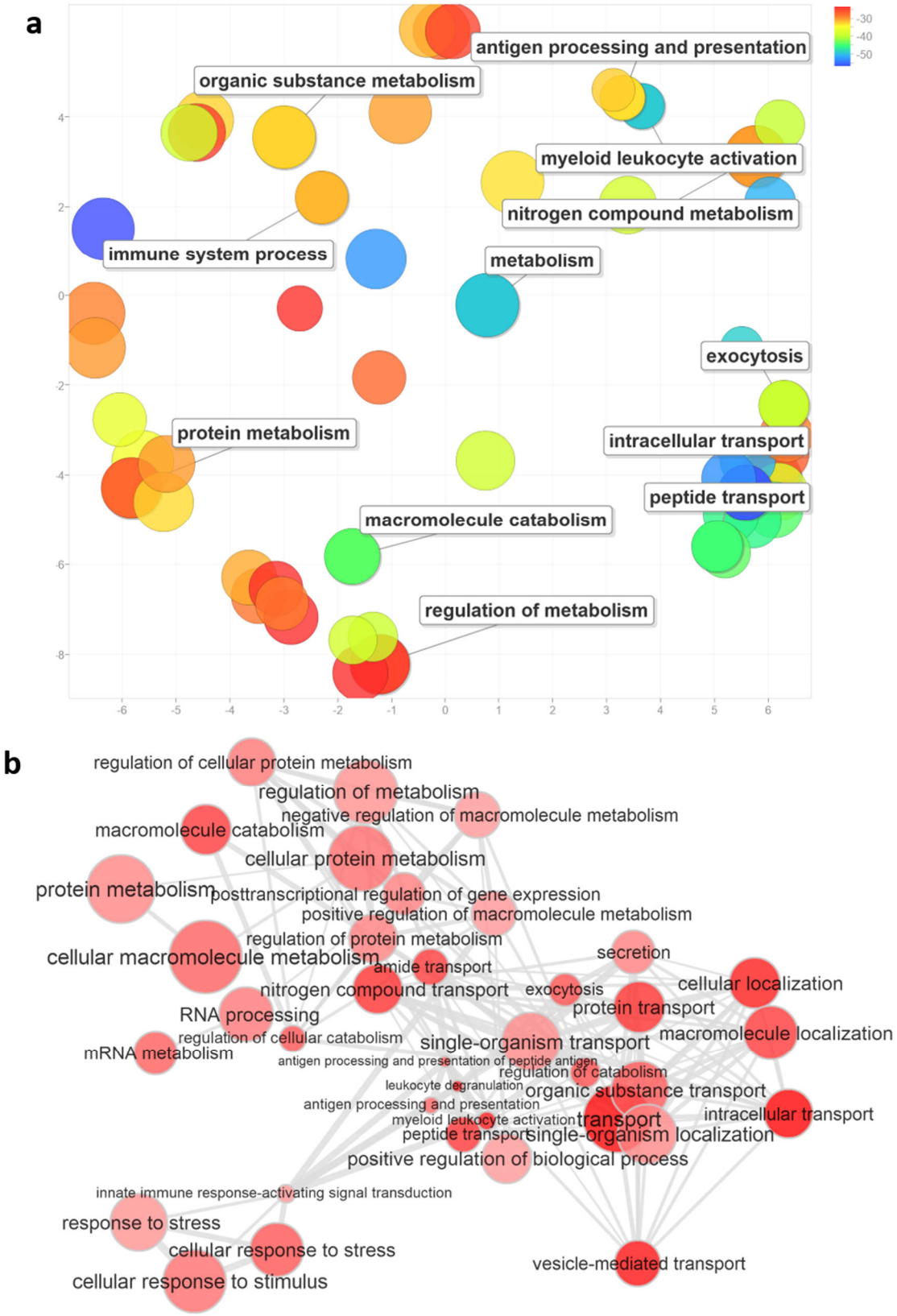
a
antigen processing and presentation
organic substance metabolism
myeloid leukocyte activation
nitrogen compound metabolism
immune system process
metabolism
exocytosis
protein metabolism
intracellular transport
peptide transport
macromolecule catabolism
regulation of metabolism
-30
-40
-50
b
regulation of cellular protein metabolism
regulation of metabolism
negative regulation of macromolecule metabolism
macromolecule catabolism
cellular protein metabolism
protein metabolism
posttranscriptional regulation of gene expression
positive regulation of macromolecule metabolism
regulation of protein metabolism
cellular macromolecule metabolism
amide transport
secretion
nitrogen compound transport
exocytosis
cellular localization
protein transport
RNA processing
regulation of cellular catabolism
single-organism transport
macromolecule localization
mRNA metabolism
antigen processing and presentation of peptide antigen
regulation of catabolism
leukocyte degranulation
organic substance transport
antigen processing and presentation
myeloid leukocyte activation
transport
intracellular transport
peptide transport
single-organism localization
positive regulation of biological process
innate immune response-activating signal transduction
response to stress
cellular response to stress
cellular response to stimulus
vesicle-mediated transport

From this basic analysis of GO term enrichment data, a number of key biological processes that involve differentially expressed genes can be identified. These processes include: cellular metabolism, intracellular transport, antigen presentation and cellular stress response. We proceeded to validate these observations through gene set enrichment analysis looking at over-representation of differentially expressed genes in the following processes with defined gene sets: cholesterol homeostasis (**Figure 4.11a**), Fcγ-mediated phagocytosis (**Figure 4.11b**), phagosome maturation (**Figure 4.11c**), and antigen processing and presentation (**Figure 4.11d**). Indeed, we found that all four gene sets were significantly enriched in our microarray results (false discovery rate [FDR]-adjusted p-value = 0.083664).

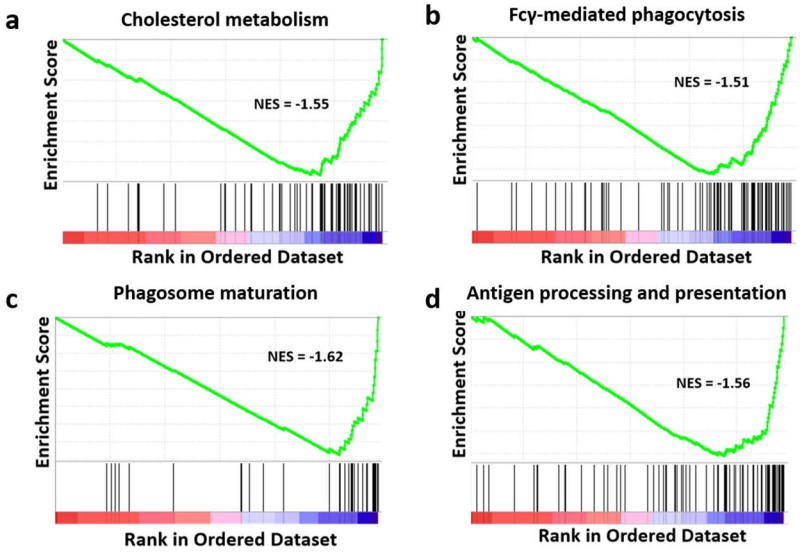

Figure 4.11 Gene set enrichment analysis of differentially expression genes in patient macrophages.

GSEA was performed to analyze genes sets enriched in patient macrophages compared to controls. Enrichment plots were generated for all gene sets tested. All four gene sets tested were found to be significantly enriched using a FDR-adjusted p-value cutoff of 0.25. (**a**) Cholesterol metabolism (adjusted p-value = 0.083664), (**b**) Fcγ-mediated phagocytosis (adjusted p-value = 0.083664), (**c**) Phagosome maturation (adjusted p-value = 0.083664) and (**d**) Antigen processing and presentation (adjusted p-value = 0.083664). NES = normalized enrichment score.

Finally, we mapped differentially expressed genes onto several key pathways of interest in order to visualize the potential impact of altered gene expression in patient macrophages on the function of biological pathways. Specifically, we examined pathways related to phagocytosis and phagosome maturation (**Figure 4.12a**) and antigen processing and presentation (**Figure 4.12b**). Both phagocytosis and antigen processing were pathways that were previously implicated by the results of our GO term enrichment and gene set enrichment analyses. As expected, we found that key components of both of these pathways were significantly downregulated in the gene expression profile of patient macrophages. Looking at phagosome maturation, several key components of this process appear to be impaired, including Rab7, the vacuolar ATPase, and several components of the NADPH oxidase complex. As for antigen processing and presentation, components of this pathway appear to be almost universally affected, with expression of the key regulators calreticulin and γ-interferon-inducible lysosomal thiol reductase (GILT) being significantly downregulated (**Figure 4.12a** and **4.12b**).

Figure 4.12 Visualization of differentially expressed genes on KEGG pathways. (on opposite page)

Differentially expressed genes obtained from microarray results were mapped onto KEGG pathways using the Partek Pathway software platform. Pathway data for phagocytosis (**a**) and antigen presentation (**b**) were obtained from the Kyoto Encyclopedia of Genes and Genomes. Red indicates downregulation of gene expression in the microarray dataset, with darker shades indicating greater magnitudes of downregulation.

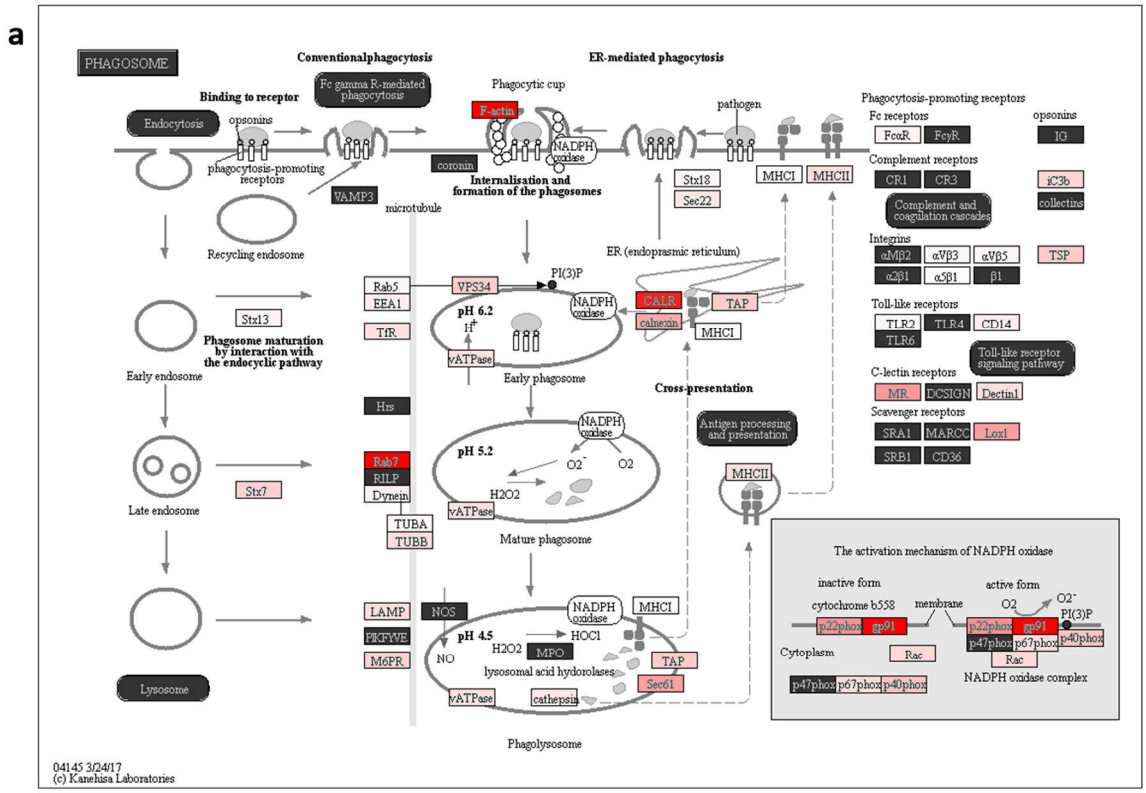
a
PHAGOSOME
Conventionalphagocytosis
ER-mediated phagocytosis
Binding to receptor
Fc gamma R-mediated phagocytosis
Phagocytic cup
F-actin
pathogen
Endocytosis
opsonins
phagocytosis-promoting receptors
VAMP3
coronin
NADPH oxidase
Internalisation and formation of the phagosomes
Stx18
Sec22
MHCI
MHCII
microtubule
Recycling endosome
ER (endoprasmic reticulum)
Rab5
EEA1
VPS34
PI(3)P
pH 6.2
H+
vATPase
CALR
calnexin
TAP
TfR
Stx13
Phagosome maturation by interaction with the endocyclic pathway
Early endosome
Early phagosome
Cross-presentation
Antigen processing and presentation
Hrs
Rab7
RILP
Dynein
pH 5.2
O2-
O2
H2O2
Stx7
Late endosome
TUBA
TUBB
Mature phagosome
LAMP
NOS
PIKFWE
M6PR
pH 4.5
HOCl
MPO
NO
lysosomal acid hydorolases
Sec61
cathepsin
Lysosome
Phagolysosome
Phagocytosis-promoting receptors
Fc receptors
FcαR
FcγR
opsonins
IG
Complement receptors
CR1
CR3
iC3b
collectins
Complement and coagulation cascades
Integrins
αMβ2
αVβ3
αVβ5
α2β1
α5β1
β1
TSP
Toll-like receptors
TLR2
TLR4
CD14
TLR6
Toll-like receptor signaling pathway
C-lectin receptors
MR
DCSIGN
Dectin1
Scavenger receptors
SRA1
MARCO
Lox1
SRB1
CD36
The activation mechanism of NADPH oxidase
inactive form
active form
cytochrome b558
membrane
O2
O2-
PI(3)P
p22phox
gp91
p47phox
p67phox
p40phox
Rac
Cytoplasm
NADPH oxidase complex
04145 3/24/17
(c) Kanehisa Laboratories
b
ANTIGEN PROCESSING AND PRESENTATION
MHC I pathway
IFNγ
TNFα
PA28
Immuno-proteasome
Cytosolic antigens
Proteasome
HSP70
HSP90
TAP1/2
Endoplasmic reticulum
BiP
CANX
MHCI
BRp57
CALR
β2M
TAPBP
MHCI
β2m
CD8
TCR
CD8 T cell
T cell receptor signaling pathway
Killing of target cells
KIR
NK cell
Natural killer cell mediated cytotoxicity
Regulation of NK cell activity
MHC II pathway
Endocytosed antigens
GILT
AEP
CTSB
Endosome
MIIC / CIIV
Ii
MHCII
AEP
SLIP
CTSB/L/S
CLIP
HLA-DM
CD4
TCR
CD4T cell
T cell receptor signaling pathway
Cytokine production, activation of other immune cells
Nucleus
CIITA
RFX
CREB
NFY
?
DNA
04612 5/20/10
(c) Kanehisa Laboratories

4.4 Discussion

Macrophages play a complex and multifaceted role in the development and progression of atherosclerosis.[62,63] Studying gene expression in human atherosclerotic plaque-resident macrophages poses challenges in both accessing the relevant tissues in patients and in isolating the macrophage cell population from the rest of the plaque. To date, there have been a limited number of studies that have examined gene expression in human atherosclerotic plaques.[11,13,64–70] The majority of these studies have focused carotid plaques, which can be obtained following carotid endarterectomy.[11,65,68,70] Significantly fewer studies have examined coronary arteries[64,67,69] and only a select number of these have actually taken the additional step of separating the macrophages from the rest of the plaque tissue prior to analysis.[65,66]

To the best of my knowledge, the current study is the first to examine gene expression profiles in isolated macrophages from atherosclerotic plaques located in the human aorta. Histopathological examination of the aortic punch tissue samples demonstrated that the aortic wall is characterized by early pre-atherosclerotic lesions that fall under type III lesions or earlier in the classic Stary classification scheme of atherosclerotic plaque progression.[55,71] At this stage of plaque development, there is moderate intimal thickening and fibrosis, along with accumulation of small populations of macrophages and limited amounts of intracellular and extracellular lipid deposits, which aligns well with our observations.[55] This was not completely surprisingly to us because atherosclerotic burden in humans is predominantly focused in the coronary and carotid vessels, along with the abdominal aorta and common iliac arteries.[6,72] The ascending aorta, where our punch samples originated, in comparison is relatively spared of severe atherosclerotic disease.[3,5] While the lack of advanced plaques precluded us from studying macrophage gene expression in late atherosclerotic disease, when efferocytosis is already impaired, it offered us the opportunity to instead focus on early stages of atherosclerotic plaque development and characterize macrophage phenotype in early pre-atherosclerotic disease. This represents another novel aspect of our approach, since the existing literature has focused almost exclusively on late-stage, established disease that is present in the majority of clinical specimens recovered. At these later stages of disease development, the mechanisms

that drive the development of efferocytic defect may be masked by changes induced by the complex interactions between macrophages and the late plaque microenvironment, including prior plaque rupture and thrombosis and intra-plaque hemorrhages – both of which have been previously shown to induce distinct macrophage phenotypes.[11,52,73]

The isolation of a pure macrophage cell population from the pre-atherosclerotic lesion presents another challenge. While some previous gene expression studies have utilized whole plaques, a number of cell types besides macrophages exist within the plaque. This includes large populations of smooth muscle cells, fibroblasts and endothelial cells that comprise the plaque,[7,63] as well as smaller numbers of infiltrating immune cell populations including $CD4^+$ and $CD8^+$ lymphocytes, NKT cells and dendritic cells.[74–76] It is therefore difficult to attribute any observed changes in gene expression to macrophages alone when whole plaques are used in gene expression profiling studies. However, isolation of macrophages from plaques is not a trivial task. The traditional approach of enzymatic digestion followed by magnetic- or FACS-based cell separation presents a challenge when the goal is to analyze gene expression because the conditions under which macrophages cells are subjected to during these procedures (e.g. enzymatic digestion, separation from the atheroma microenvironment) may contribute to significant changes in their gene expression profiles due to the incredible plasticity of these cells and their ability to rapidly adapt to new external environments.[77] Indeed, recently single-cell RNA sequencing studies have demonstrated that murine microglia cells removed from the brain and placed into culture *ex vivo* exhibited dramatic changes in gene expression within six hours.[78] Therefore, we opted to immediately freeze our tissue samples and isolate macrophages by LCM. While freezing subjects RNA to some level of degradation, it carries the important advantage of preserving the integrity of overall gene expression profile.[79] Several previous studies have used LCM to isolate macrophages from within atherosclerotic plaques. Following labelling of macrophages by CD163, we were able to selectively isolate macrophage cells from pre-atherosclerotic lesions and isolate enough RNA of sufficient quality to perform both microarray and RT-qPCR analysis.

We examined gene expression changes in patient macrophages by microarray using M0-polarized macrophages differentiated *in vitro* from peripheral blood monocytes as a

control. The lack of a more comparable source of control macrophages is a significant drawback of this approach, yet a suitable source of control cells is difficult to identify. In the healthy artery, there is not a substantial population of sub-intimal macrophages that could act as a control. Several groups have identified a population of "arterial macrophages" that are associated with arteries throughout the body, these are primarily located within the adventitia or in close association with the smooth muscle rather than the intima.[80,81] Ensan *et al.* found that in C57BL/6J mice, only 2% of all arterial macrophages could be found in the intima.[81] Further, studies have demonstrated that these macrophages are entirely tissue resident cells with an embryonic origin.[81] In contrast, atherosclerotic plaque-resident macrophages are thought to be mostly derived from circulating monocytes, although they do exhibit limited self-proliferative potential.[63,82] Some studies that have examined apoptotic cell clearance in human atherosclerotic plaque have used the tonsils as a control tissue with a highly active efferocytic activity.[36] However, it is questionable in our particular situation whether tonsillar macrophages would serve as a superior control to monocyte-derived macrophages. Nevertheless, since our control macrophages are derived from a different source than patient pre-atherosclerotic macrophages, that should be taken into account when interpreting the results of our gene expression profiling study.

From the results of our microarray study, it is apparent that even in the early stages of atherosclerotic plaque development, lesion-resident macrophages have a very different gene expression profile. We observed that over 3,000 protein-coding genes are differentially expressed in patient macrophages in comparison to controls. Undoubtedly, some of this difference we observe can be attributed to the comparison between lesion-resident macrophages and monocyte-derived macrophage controls. However, many of the features that we identify as unique in the pre-atherosclerotic lesion-resident macrophage population are not obviously connected to inherent differences between macrophages isolated from a tissue and macrophages cultured *in vitro*. These features include marked downregulation of genes involved in cholesterol homeostasis, phagocytosis and phagosome maturation and antigen processing and presentation but not inflammatory activation. Rather, we contend that these features define a novel macrophage phenotype associated with early, pre-atherosclerotic lesions (**Figure 4.13**). Within the early atherosclerotic lesion, the dominant microenvironmental factor that drives macrophage

dysfunction is probably an excess of lipids and modified lipoproteins rather than the chronic inflammation that characterizes advanced plaques. Hypercholesterolemia has been previously described by Huynh *et al.* to impair phagosome maturation by interfering with the activity of Rab7,[34] which, as described in the previous chapter, is a key regulator of proper phagosome and efferosome maturation. Rab7 regulates phagosome acidification and phagolysosomal formation and its downregulation in pre-atherosclerotic lesion-resident macrophages suggests that phagosome and efferosome maturation may be impaired in these cells.

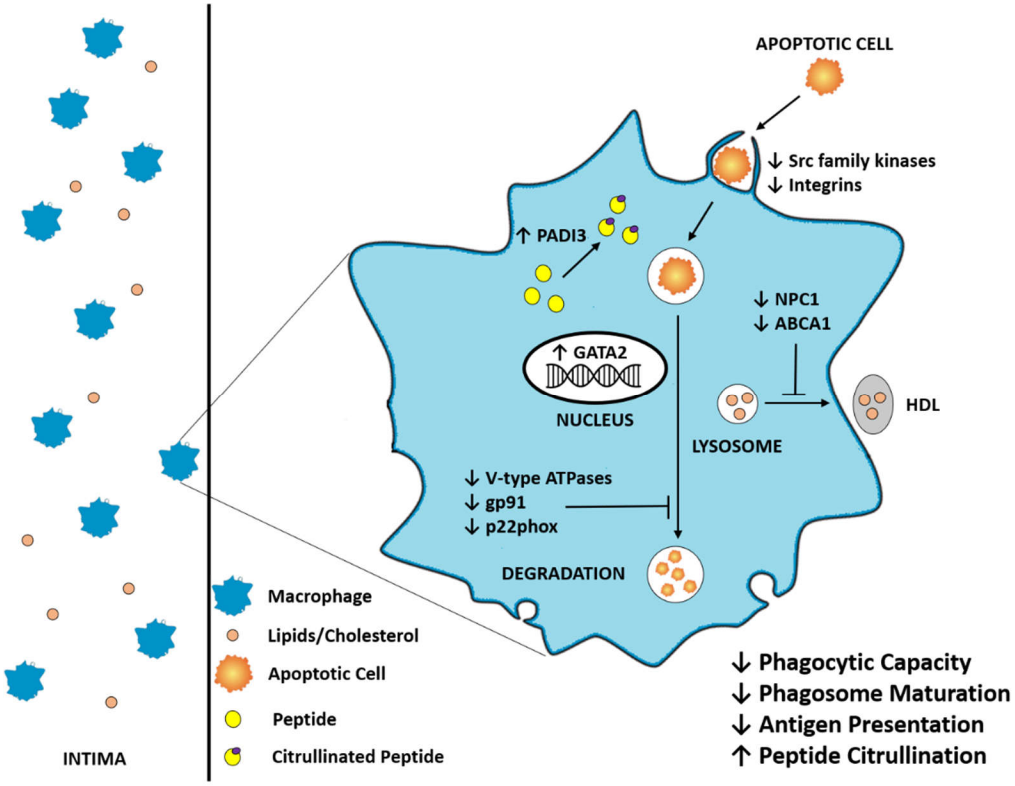

Figure 4.13 Novel macrophage phenotype associated with early, pre-atherosclerotic lesions.

We defined a novel macrophage phenotype associated with early, pre-atherosclerotic lesions located in the human ascending aorta. Upon histological examination, the vessel intima is observed to possess diffuse thickening in combination with accumulation of lipids and small, discrete macrophage cell populations. These intima-infiltrating macrophages are characterized by dysregulated gene expression in pathways related to cellular cholesterol

handling, intracellular vesicular trafficking and phagocytosis/efferocytosis. Specifically, we observed downregulation in the expression of the cholesterol efflux genes NPC1 and ABCA1, downregulation of genes encoding components of the vATPase, NADPH oxidase (gp91, p22phox), and downregulation of Src kinases and integrins involved in pathogen and apoptotic cell internalization. We observed upregulation of several transcription factors, notably the hematopoietic transcription factor GATA2 and upregulation of the PADI3 enzyme.

The phenotype we have described herein appears to be distinct from any other previously established macrophage phenotypes. Defining a consistent phenotype for atherosclerotic macrophages has been difficult and the precise phenotype varies on the basis of whether investigators studied human or animal plaques, the location of the plaque and the stage of plaque development. In general, it is thought that atherosclerotic macrophages in later stages of disease are predominantly M1-like and proinflammatory in nature.[83] Indeed, immunohistochemistry studies of advanced atherosclerotic plaques show an increase in the proportion of pro-inflammatory macrophages and an association between these macrophages and sites of plaque instability.[84] Additionally, in animal models of atherosclerosis regression, decrease plaque size is associated with an increase in the number of M2-like macrophages.[85,86] In advanced atherosclerosis, macrophages are shaped by the inflammatory microenvironment of the plaque to adopt a pro-inflammatory phenotype and contribute to inflammation, cytokine production and plaque instability.[24,87] The M1-M2 paradigm however fails to capture the full complexity of macrophage behaviours within the atherosclerotic plaque. Non-classical macrophage phenotypes have also been described in the setting of atherosclerosis.[88] For example, Boyle *et al.* describe a heme-induced macrophage polarization stated (Mhem) that is associated with intraplaque hemorrhage.[53] These macrophages upregulate ATF-1 and heme oxygenase-1 and are able to efficient clear excess hemoglobin.[53] Kadl *et al.* describe another unique macrophage characterized by upregulation of Nrf2 in response to oxidized phospholipids, which express high levels of redox-regulating genes such as Srxn1 and Txnrd1 to control the oxidative stress induced by oxidized phospholipids.[89] In contrast, our pre-atherosclerotic macrophages do not appear to overexpress markers of the macrophage M1-polarization, nor is there a particularly strong effect in genes involved in iron metabolism or redox

regulation. In contrast, we observe a non-inflammatory phenotype in our pre-atherosclerotic macrophages along with features suggestive of ER stress and regulation of proteasome activity.

Macrophage efferocytosis undoubtedly plays a critical role in the pathogenesis of atherosclerotic disease. Work to date has indicated that defective efferocytosis is a feature of advanced, late-stage atherosclerotic disease. While the mechanisms that drive defective efferocytosis remain poorly defined, there is some evidence to suggest that the inflammatory microenvironment of the atheroma drives matrix metalloproteinase-mediated cleavage of efferocytic receptors, thereby impairing efferocytic uptake of apoptotic cells. Our findings here challenge these paradigms in two key ways: first, we find that defects in phagocytosis and efferocytosis are present (at least at the level of gene expression) very early on in atherosclerotic disease; second, we find that in addition to impairments in phagocytic and efferocytic uptake, phagosome/efferosome maturation may also be implicated in impaired macrophage efferocytosis. Critically, these findings are based on analysis of isolated macrophage cell populations from human disease and are therefore potentially more indicative of clinically-relevant macrophage dysfunction in atherosclerosis than what has been previously identified in animal models of disease or studies that have examined whole plaques.

4.5 References

1. Aluganti Narasimhulu C, Fernandez-Ruiz I, Selvarajan K, et al. Atherosclerosis — do we know enough already to prevent it? *Curr Opin Pharmacol*. 2016;27(Ldl):92-102. doi:10.1016/j.coph.2016.02.006

2. Libby P, Ridker PM, Hansson GK. Progress and challenges in translating the biology of atherosclerosis. *Nature*. 2011;473(7347):317-325. doi:10.1038/nature10146

3. Getz GS, Reardon C a. Animal models of Atherosclerosis. *Arterioscler Thromb Vasc Biol*. 2012;32(5):1104-1115. doi:10.1161/ATVBAHA.111.237693

4. Getz GS, Reardon C a. ApoE knockout and knockin mice: The history of their contribution to the understanding of atherogenesis. *CEUR Workshop Proc*. 2015;1542(773):33-36. doi:10.1017/CBO9781107415324.004

5. VanderLaan P a., Reardon C a., Getz GS. Site Specificity of Atherosclerosis: Site-Selective Responses to Atherosclerotic Modulators. *Arterioscler Thromb Vasc Biol*. 2004;24(1):12-22. doi:10.1161/01.ATV.0000105054.43931.f0

6. Fernández-Friera L, Peñalvo JL, Fernández-Ortiz A, et al. Prevalence, vascular distribution, and multiterritorial extent of subclinical atherosclerosis in a middle-aged cohort the PESA (Progression of Early Subclinical Atherosclerosis) study. *Circulation*. 2015;131(24):2104-2113. doi:10.1161/CIRCULATIONAHA.114.014310

7. Falk E. Pathogenesis of Atherosclerosis. *J Am Coll Cardiol*. 2006;47(8):0-5. doi:10.1016/j.jacc.2005.09.068

8. Kuller L, Borhani N, Furberg C, et al. Prevalence of subclinical atherosclerosis and cardiovascular disease and association with risk factors in the Cardiovascular Health Study. *Am J Epidemiol*. 1994;139(12):1164-1179.

9. Strong JP, Malcom GT, Mcmahan CA, et al. Prevalence and Extent of Atherosclerosis in Adolescents and Young Adults. *Jama*. 1999;281(8):727-735. doi:10.1001/jama.281.8.727

10. Wissler RW, Strong JP. Risk Factors and Progression of Atherosclerosis in Youth. *Am J Pathol*. 1998;153(4):1023-1033. doi:10.1016/S0002-9440(10)65647-7

11. Papaspyridonos M, Smith A, Burnand KG, et al. Novel candidate genes in unstable areas of human atherosclerotic plaques. *Arterioscler Thromb Vasc Biol*. 2006;26(8):1837-1844. doi:10.1161/01.ATV.0000229695.68416.76

12. Frostegård J, Ulfgren A, Nyberg P, et al. Cytokine expression in advanced human atherosclerotic plaques : dominance of pro-inflammatory (Th1) and macrophage-stimulating cytokines. *Atherosclerosis*. 1999;9150(99):7-8.

13. Sulkava M, Raitoharju E, Levula M, et al. Differentially expressed genes and canonical pathway expression in human atherosclerotic plaques-Tampere Vascular Study. *Sci Rep*. 2017;7(December 2016):1-10. doi:10.1038/srep41483

14. Cruz MT, Sviridov D, Woollard K, Vieira O V, Gibson MS, Domingues N. Lipid and Non-lipid Factors Affecting Macrophage Dysfunction and Inflammation in Atherosclerosis. *Front Physiol*. 2018;1(June):654. doi:10.3389/fphys.2018.00654

15. Westover E. Cholesterol in Health and Disease. *J Clin Invest*. 2002;110(5):583-590. doi:10.1172/JCI200216381.Imagine

16. Konstantinov IE, Mejevoi N, Anichkov NM. Nikolai N. Anichkov and his theory of atherosclerosis. *Texas Hear Inst J*. 2006;33(4):417-423.

17. Moore KJ, Freeman MW. Scavenger receptors in atherosclerosis: beyond lipid uptake. *Arterioscler Thromb Vasc Biol*. 2006;26(8):1702-1711. doi:10.1161/01.ATV.0000229218.97976.43

18. Jerome WG. Advanced atherosclerotic foam cell formation has features of an acquired lysosomal storage disorder. *Rejuvenation Res*. 2006;9(2):245-255. doi:10.1089/rej.2006.9.245

19. Tabas I. Consequences of cellular cholesterol accumulation : Basic concepts and physiological implications. *J Clin Invest*. 2002;110(7):905-911. doi:10.1172/JCI200216452.The

20. Chistiakov DA, Bobryshev Y V., Orekhov AN. Macrophage-mediated cholesterol handling in atherosclerosis. *J Cell Mol Med*. 2015;XX(X):n/a-n/a. doi:10.1111/jcmm.12689

21. Chistiakov DA, Melnichenko AA, Myasoedova VA, Grechko A V., Orekhov AN. Mechanisms of foam cell formation in atherosclerosis. *J Mol Med*. 2017;95(11):1153-1165. doi:10.1007/s00109-017-1575-8

22. Li Y, Gerbod-Giannone MC, Seitz H, et al. Cholesterol-induced apoptotic

macrophages elicit an inflammatory response in phagocytes, which is partially attenuated by the Mer receptor. *J Biol Chem*. 2006;281(10):6707-6717. doi:10.1074/jbc.M510579200

23. Li Y, Schwabe RF, DeVries-Seimon T, et al. Free cholesterol-loaded macrophages are an abundant source of tumor necrosis factor-α and interleukin-6: Model of NF-κB- and map kinase-dependent inflammation in advanced atherosclerosis. *J Biol Chem*. 2005;280(23):21763-21772. doi:10.1074/jbc.M501759200

24. Tabas I. Macrophage death and defective inflammation resolution in atherosclerosis. *Nat Rev Immunol*. 2009;10(1):36-46. doi:10.1038/nri2675

25. Kojima Y, Weissman IL, Leeper NJ. The Role of Efferocytosis in Atherosclerosis. *Circulation*. 2017;135(5):476-489. doi:10.1161/CIRCULATIONAHA.116.025684

26. Linton MF, Babaev VR, Huang J, Linton EF, Tao H, Yancey PG. Macrophage Apoptosis and Efferocytosis in the Pathogenesis of Atherosclerosis. *Circ J*. 2016. doi:10.1253/circj.CJ-16-0924

27. Blackburn JWD, Lau DHC, Liu EY, et al. Soluble CD93 is an apoptotic cell opsonin recognized by $\alpha_x \beta_2$. *Eur J Immunol*. 2019:1-23. doi:10.1002/eji.201847801

28. Widmaier M, Rognoni E, Radovanac K, Azimifar SB, Fassler R. Integrin-linked kinase at a glance. *J Cell Sci*. 2012;125(8):1839-1843. doi:10.1242/jcs.093864

29. Hurtado B, Abasolo N, Muñoz X, et al. Association study between polymorphims in GAS6-TAM genes and carotid atherosclerosis. *Thromb Haemost*. 2010;104(3):592-598. doi:10.1160/TH09-11-0787

30. DeBerge M, Yeap XY, Dehn S, et al. MerTK cleavage on resident cardiac macrophages compromises repair after myocardial ischemia reperfusion injury. *Circ Res*. 2017;121(8):930-940. doi:10.1161/CIRCRESAHA.117.311327

31. Evans AL, Blackburn JWD, Taruc K, et al. Antagonistic Coevolution of MER

Tyrosine Kinase Expression and Function. *Mol Biol Evol*. 2017. doi:10.1093/molbev/msx102

32. Thorp E, Cui D, Schrijvers DM, Kuriakose G, Tabas I. Mertk Receptor Mutation Reduces Efferocytosis Efficiency and Promotes Apoptotic Cell Accumulation and Plaque Necrosis in Atherosclerotic Lesions of Apoe ⁻/⁻ Mice. *Arterioscler Thromb Vasc Biol*. 2015;28(8):1421-1428. doi:10.1161/ATVBAHA.108.167197

33. Cai B, Thorp EB, Doran AC, et al. MerTK receptor cleavage promotes plaque necrosis and defective resolution in atherosclerosis. *J Clini*. 2017;127(2):564-568. doi:10.1172/JCI90520.We

34. Huynh KK, Gershenzon E, Grinstein S. Cholesterol accumulation by macrophages impairs phagosome maturation. *J Biol Chem*. 2008;283(51):35745-35755. doi:10.1074/jbc.M806232200

35. Elzen P van den, Garg S, León L, et al. Apolipoprotein-mediated pathways of lipid antigen presentation. *Nature*. 2005;437(7060):906-910. doi:10.1038/nature04001

36. Schrijvers DM, De Meyer GRY, Kockx MM, Herman AG, Martinet W. Phagocytosis of apoptotic cells by macrophages is impaired in atherosclerosis. *Arterioscler Thromb Vasc Biol*. 2005;25(6):1256-1261. doi:10.1161/01.ATV.0000166517.18801.a7

37. Thorp E, Cui D, Schrijvers DM, Kuriakose G, Tabas I. Mertk receptor mutation reduces efferocytosis efficiency and promotes apoptotic cell accumulation and plaque necrosis in atherosclerotic lesions of ApoE-/- mice. *Arterioscler Thromb Vasc Biol*. 2015;28(8):1421-1428. doi:10.1161/ATVBAHA.108.167197

38. Gentleman RC, Carey VJ, Bates DM, et al. Bioconductor: open software development for computational biology and bioinformatics. *Genome Biol*. 2004;5(10):R80. doi:10.1186/gb-2004-5-10-r80

39. Carvalho BS, Irizarry RA. A framework for oligonucleotide microarray preprocessing. *Bioinformatics*. 2010;26(19):2363-2367.

doi:10.1093/bioinformatics/btq431

40. Ritchie ME, Phipson B, Wu D, et al. limma powers differential expression analyses for RNA-sequencing and microarray studies. *Nucleic Acids Res*. 2015;43(7):e47. doi:10.1093/nar/gkv007

41. Phipson B, Lee S, Majewski IJ, Alexander WS, Smyth GK. Robust hyperparameter estimation protects against hypervariable genes and improves power to detect differential expression. *Ann Appl Stat*. 2016;10(2):946-963. doi:10.1214/16-AOAS920

42. Supek F, Bošnjak M, Škunca N, Šmuc T. Revigo summarizes and visualizes long lists of gene ontology terms. *PLoS One*. 2011;6(7). doi:10.1371/journal.pone.0021800

43. Daly MJ, Patterson N, Mesirov JP, Golub TR, Tamayo P, Spiegelman B. PGC-1α-responsive genes involved in oxidative phosphorylation are coordinately downregulated in human diabetes. *Nat Genet*. 2003;34(3):267-273.

44. Subramanian A, Subramanian A, Tamayo P, et al. Gene set enrichment analysis: a knowledge-based approach for interpreting genome-wide expression profiles. *Proc Natl Acad Sci U S A*. 2005;102(43):15545-15550. doi:10.1073/pnas.0506580102

45. Biancari F, Lahtinen J, Heikkinen J. Impact of ascending aortic wall thickness and atherosclerosis on the intermediate survival after coronary artery bypass surgery. *Eur J Cardio-thoracic Surg*. 2012;41(5):94-99. doi:10.1093/ejcts/ezs087

46. Erbel R, Eggebrecht H. Aortic dimensions and the risk of dissection. *Heart*. 2006;92(1):137-142. doi:10.1136/hrt.2004.055111

47. van den Hengel K. Abdominal aortic wall thickness and compliance. 2008.

48. Nakagawa K, Nakashima Y. Pathologic intimal thickening in human atherosclerosis is formed by extracellular accumulation of plasma-derived lipids and dispersion of intimal smooth muscle cells. *Atherosclerosis*. 2018:1-8.

doi:10.1016/j.atherosclerosis.2018.03.039

49. Shankman LS, Gomez D, Cherepanova OA, et al. KLF4-dependent phenotypic modulation of smooth muscle cells has a key role in atherosclerotic plaque pathogenesis. *Nat Med*. 2015;21(6):628-637. doi:10.1038/nm.3866

50. Allahverdian S, Chehroudi AC, McManus BM, Abraham T, Francis GA. Contribution of intimal smooth muscle cells to cholesterol accumulation and macrophage-like cells in human atherosclerosis. *Circulation*. 2014;129(15):1551-1559. doi:10.1161/CIRCULATIONAHA.113.005015

51. Nguyen TT, Schwartz EJ, West RB, Warnke RA, Arber DA, Natkunam Y. Expression of CD163 (hemoglobin scavenger receptor) in normal tissues, lymphomas, carcinomas, and sarcomas is largely restricted to the monocyte/macrophage lineage. *Am J Surg Pathol*. 2005;29(5):617-624. doi:10.1097/01.pas.0000157940.80538.ec

52. Boyle JJ, Harrington H a, Piper E, et al. Coronary intraplaque hemorrhage evokes a novel atheroprotective macrophage phenotype. *Am J Pathol*. 2009;174(3):1097-1108. doi:10.2353/ajpath.2009.080431

53. Boyle JJ, Johns M, Kampfer T, et al. Activating transcription factor 1 directs Mhem atheroprotective macrophages through coordinated iron handling and foam cell protection. *Circ Res*. 2012;110(1):20-33. doi:10.1161/CIRCRESAHA.111.247577

54. Guo L, Akahori H, Harari E, et al. CD163+ macrophages promote angiogenesis and vascular permeability accompanied by inflammation in atherosclerosis. *J Clin Invest*. 2018;128(3):1-19. doi:10.1172/JCI93025

55. Stary HC, Chandler AB, Glagov S, et al. A Definition of Initial , Fatty Streak , and Intermediate Lesions of Atherosclerosis. *Circulation*. 1994;89(5):2462-2479.

56. Muiya NP, Wakil S, Al-Najai M, et al. A study of the role of GATA2 gene polymorphism in coronary artery disease risk traits. *Gene*. 2014;544(2):152-158.

doi:10.1016/j.gene.2014.04.064

57. Connelly JJ, Wang T, Cox JE, et al. GATA2 is associated with familial early-onset coronary artery disease. *PLoS Genet*. 2006;2(8):1265-1273. doi:10.1371/journal.pgen.0020139

58. Nakamura Y, Igarashi K, Suzuki T, et al. E4F1, a novel estrogen-responsive gene in possible atheroprotection, revealed by microarray analysis. *Am J Pathol*. 2004;165(6):2019-2031. doi:10.1016/S0002-9440(10)63253-1

59. Costet P, Lalanne F, Gerbod-Giannone MC, et al. Retinoic Acid Receptor-Mediated Induction of ABCA1 in Macrophages. *Mol Cell Biol*. 2003;23(21):7756-7766. doi:10.1128/mcb.23.21.7756-7766.2003

60. Olivares-Martínez E, Hernández-Ramírez DF, Núñez-Álvarez CA, Cabral AR, Llorente L. The amount of citrullinated proteins in synovial tissue is related to serum anti-cyclic citrullinated peptide (anti-CCP) antibody levels. *Clin Rheumatol*. 2016;35(1):55-61. doi:10.1007/s10067-015-3047-2

61. Sokolove J, Sharpe O, Brennan M, et al. Citrullination within the atherosclerotic plaque: A potential target for the anti-citrullinated protein antibody response in rheumatoid arthritis. *Arthritis Rheum*. 2013;65(7):1719-1724. doi:10.1002/art.37961

62. Tabas I. 2016 Russell Ross Memorial Lecture in Vascular Biology. *Arterioscler Thromb Vasc Biol*. 2016:ATVBAHA.116.308036. doi:10.1161/ATVBAHA.116.308036

63. Wolf D, Zirlik A, Ley K. Beyond vascular inflammation—recent advances in understanding atherosclerosis. *Cell Mol Life Sci*. 2015. doi:10.1007/s00018-015-1971-6

64. Dahl TB, Yndestad A, Skjelland M, et al. Increased expression of visfatin in macrophages of human unstable carotid and coronary atherosclerosis: Possible role in inflammation and plaque destabilization. *Circulation*. 2007;115(8):972-980.

doi:10.1161/CIRCULATIONAHA.106.665893

65. Chai JT, Ruparelia N, Goel A, et al. Differential Gene Expression in Macrophages From Human Atherosclerotic Plaques Shows Convergence on Pathways Implicated by Genome-Wide Association Study Risk Variants. *Arterioscler Thromb Vasc Biol*. 2018;38(11):2718-2730. doi:10.1161/ATVBAHA.118.311209

66. Puig O, Yuan J, Stepaniants S, et al. A gene expression signature that classifies human atherosclerotic plaque by relative inflammation status. *Circ Cardiovasc Genet*. 2011;4(6):595-604. doi:10.1161/CIRCGENETICS.111.960773

67. Raitoharju E, Lyytikäinen L-P, Levula M, et al. miR-21, miR-210, miR-34a, and miR-146a/b are up-regulated in human atherosclerotic plaques in the Tampere Vascular Study. *Atherosclerosis*. 2011;219(1):211-217. doi:10.1016/j.atherosclerosis.2011.07.020

68. Saksi J, Ijäs P, Nuotio K, et al. Gene expression differences between stroke-associated and asymptomatic carotid plaques. *J Mol Med*. 2011;89(10):1015-1026. doi:10.1007/s00109-011-0773-z

69. Wang Z, Guo D, Yang B, et al. Integrated analysis of microarray data of atherosclerotic plaques: Modulation of the ubiquitin-proteasome system. *PLoS One*. 2014;9(10). doi:10.1371/journal.pone.0110288

70. Perisic L, Hedin E, Razuvaev A, et al. Profiling of atherosclerotic lesions by gene and tissue microarrays reveals pcsk6 as a novel protease in unstable carotid atherosclerosis. *Arterioscler Thromb Vasc Biol*. 2013;33(10):2432-2443. doi:10.1161/ATVBAHA.113.301743

71. Stary HC, Bleakley CA, Dinsmore RE, et al. A Definition of Advanced Types of Atherosclerotic Lesions and a Histological Classification of Atherosclerosis. *Circulation*. 1995;92(5):1355-1374. doi:10.1161/01.CIR.92.5.1355

72. Nakashima Y, Chen YX, Kinukawa N, Sueishi K. Distributions of diffuse intimal thickening in human arteries: Preferential expression in atherosclerosis-prone

arteries from an early age. *Virchows Arch*. 2002;441(3):279-288. doi:10.1007/s00428-002-0605-1

73. Kolodgie FD, Virmani R, Burke a P, et al. Pathologic assessment of the vulnerable human coronary plaque. *Heart*. 2004;90(12):1385-1391. doi:10.1136/hrt.2004.041798

74. Tse K, Tse H, Sidney J, Sette A, Ley K. T cells in atherosclerosis. *Int Immunol*. 2013;25(11):615-622. doi:10.1093/intimm/dxt043

75. Tupin E, Nicoletti A, Elhage R, et al. CD1d-dependent Activation of NKT Cells Aggravates Atherosclerosis. *J Exp Med*. 2004;199(3):417-422. doi:10.1084/jem.20030997

76. Koltsova EK, Ley K. How dendritic cells shape atherosclerosis. *Trends Immunol*. 2011;32(11):540-547. doi:10.1016/j.it.2011.07.001

77. Adam M, Potter AS, Potter SS. Psychrophilic proteases dramatically reduce single-cell RNA-seq artifacts: a molecular atlas of kidney development. *Development*. 2017;144(19):3625-3632. doi:10.1242/dev.151142

78. Gosselin D, Skola D, Coufal NG, et al. An environment-dependent transcriptional network specifies human microglia identity. *Science (80-)*. 2017;356(6344):1248-1259. doi:10.1126/science.aal3222

79. Medeiros F, Rigl CT, Anderson GG, Becker SH, Halling KC. Tissue handling for genome-wide expression analysis: A review of the issues, evidence, and opportunities. *Arch Pathol Lab Med*. 2007;131(12):1805-1816.

80. Lim HY, Lim SY, Tan CK, et al. Hyaluronan Receptor LYVE-1-Expressing Macrophages Maintain Arterial Tone through Hyaluronan-Mediated Regulation of Smooth Muscle Cell Collagen. *Immunity*. 2018;49(2):326-341.e7. doi:10.1016/j.immuni.2018.06.008

81. Ensan S, Li A, Besla R, et al. Self-renewing resident arterial macrophages arise

from embryonic CX3CR1+ precursors and circulating monocytes immediately after birth. *Nat Immunol*. 2015;17(2):159-168. doi:10.1038/ni.3343

82. Moore KJ, Sheedy FJ, Fisher E a. Macrophages in atherosclerosis: a dynamic balance. *Nat Rev Immunol*. 2013;13(10):709-721. doi:10.1038/nri3520

83. Viola J, Soehnlein O. Atherosclerosis – A matter of unresolved inflammation. *Semin Immunol*. 2015;27(3):184-193. doi:10.1016/j.smim.2015.03.013

84. de Gaetano M, Crean D, Barry M, Belton O. M1- and M2-Type Macrophage Responses Are Predictive of Adverse Outcomes in Human Atherosclerosis. *Front Immunol*. 2016;7(July). doi:10.3389/fimmu.2016.00275

85. Chistiakov DA, Myasoedova VA, Revin V V., Orekhov AN, Bobryshev Y V. The phenomenon of atherosclerosis reversal and regression: Lessons from animal models. *Exp Mol Pathol*. 2017;102(1):138-145. doi:10.1016/j.yexmp.2017.01.013

86. Rahman K, Vengrenyuk Y, Ramsey SA, et al. Inflammatory Ly6Chimonocytes and their conversion to M2 macrophages drive atherosclerosis regression. *J Clin Invest*. 2017;127(8):2904-2915. doi:10.1172/JCI75005

87. Hansson GK, Libby P, Tabas I. Inflammation and plaque vulnerability. *J Intern Med*. 2015;278:483-493. doi:10.1111/joim.12406

88. Rojas J, Salazar J, Martínez MS, et al. Macrophage Heterogeneity and Plasticity: Impact of Macrophage Biomarkers on Atherosclerosis. *Scientifica (Cairo)*. 2015;2015:1-17. doi:10.1155/2015/851252

89. Kadl A, Meher AK, Sharma PR, et al. Identification of a novel macrophage phenotype that develops in response to atherogenic phospholipids via Nrf2. *Circ Res*. 2010;107(6):737-746. doi:10.1161/CIRCRESAHA.109.215715

Chapter 5

5 The Hematopoietic Transcription Factor GATA2 is a Master Regulator of Defective Macrophage Efferocytosis in Atherosclerosis

5.1 Introduction

5.1.1 In vitro models of atherosclerotic macrophages

Studying atherosclerotic macrophages *in vitro* is a challenging task because the complexity of the atherosclerotic plaque microenvironment is difficult to re-capitulate in culture.[1] We know that at a minimum, atherosclerosis involves cross talk between three cell types: macrophages, endothelial cells and VSMCs.[2,3] Indeed, a number of investigators have attempted to create models of atherosclerosis through co-culture of some combination endothelial cells, VSMCs and monocytes in the presence of various components of the extracellular matrix (ECM).[4–6] These models can successfully re-capitulate certain aspects of atherogenesis, including SMC proliferation and migration of monocytes into the sub-endothelial cell space and their subsequent differentiation into macrophages.[4] However, due to the presence of multiple cell types, extra care is required in order to study macrophage cell biology in isolation using these approaches and it is difficult to discern how individual pro-atherogenic stimuli (such as the presence of modified lipoproteins) act directly on macrophage cells.

Another approach that has been commonly employed is the isolation and *ex vivo* culture of macrophages from patients, or more commonly, mice with atherosclerosis.[1] One strategy is to isolate macrophages from the peritoneum of atherosclerotic mice and subsequently activate and study them *in vitro*.[1] This has been key in studying the effects of various pro-atherogenic agents, cytokines and drugs on macrophages conditioned to the hypercholesterolemic environment of the atherosclerotic animal.[1,7,8] For example, Yu *et al.* used this approach to establish that treatment with rosuvastatin in *Apoe*$^{-/-}$ mice had the direct effect of inhibiting macrophage apoptosis,[7] while Kanters *et al.* found that atherosclerotic macrophages isolated from *Ldlr*$^{-/-}$ mice lacking a component of the NFκB signaling complex exhibited decreased IL-10 production following stimulation with LPS.[8]

However, while this approach is powerful and re-capitulates the systemic effects of atherosclerosis on macrophage function, it become less feasible in humans given the lack of a source that can provide large numbers of viable macrophages. Furthermore, unlike with mice or immortalized cell lines, it is very difficult to perform genetic manipulations on human macrophages cultured *ex vivo*, limiting our ability to study the effects of perturbing the expression of specific genes on macrophage phenotype.[9]

Perhaps the simplest *in vitro* model of atherosclerotic macrophages is to treat cultured macrophage with oxLDL,[10] a similar modified lipoprotein,[11] or LDL in the presence of an ACAT inhibitor.[12] The literature disagrees somewhat with the precise concentration of oxLDL to use and the duration of treatment, with studies using a range of concentrations between 25-100 μg/mL and a duration between 1-3 days.[13,14] While a very simple model, oxLDL exposure is able to re-capitulate some of the earliest pathologic features exhibited by macrophages within atherosclerotic lesions. Uptake of oxLDL has a number of consequences for macrophage. Cholesterol recovered from the lipoprotein particle accumulates within the macrophage, as both neutral cholesterol esters sequestered within lipid droplets and as free cholesterol that accumulates within the cytoplasm and lipid plasma membrane of the cell.[11] Cholesterol ester buildup as lipid droplets creates the classic "foamy" appearance of macrophage-derived foam cells.[15] Free cholesterol within the cytoplasm aggregate as cholesterol crystal, which can induce a number of biological responses within the macrophage, including UPR and activation of the UPR effector protein CHOP, which can induce apoptosis.[16,17] Cholesterol crystals also contribute to activation of the NRLP3 inflammasome and generation of IL-1β, which plays a key role in driving inflammatory responses within the atherosclerotic plaque.[18] Furthermore, oxLDL can activate endosomal Toll-like, which in addition to generating a pro-inflammatory response, also inhibits the macrophage's capacity to engage in efficient efferocytosis.[19]

5.1.2 GATA family of transcription factors

The GATA family of transcription factors is comprised of six members that have master regulatory roles during development, specifically in progenitor differentiation and renewal, and in cell lineage specification.[20,21] GATA transcription factors are highly-conserved and are evolutionarily ancient proteins, being found among animals, plants and fungi.[20] They

are characterized by the presence of two highly-conserved zinc finger domains that recognize the consensus sequence (A/T)GATA(A/G).[22] In vertebrates, there are six members of the GATA transcription factor family (GATA1-6; see **Figure 5.1**).[20] Classically, these six paralogs have been divided into two subfamilies on the basis of function. GATA1/2/3 were thought to be primarily involved in development of the hematopoietic system while GATA4/5/6 were thought to be involved in cardiac development.[21] However, more recent evidence suggests that various members of the GATA family play important roles in the development of many other tissues, including the kidneys (GATA2/3), breast (GATA3) and testes (GATA1) among others.[20] The role of GATA transcription factor during development has been discussed in detail in two recent reviews from Lentjes *et al.* and Tremblay *et al*.[20,21]

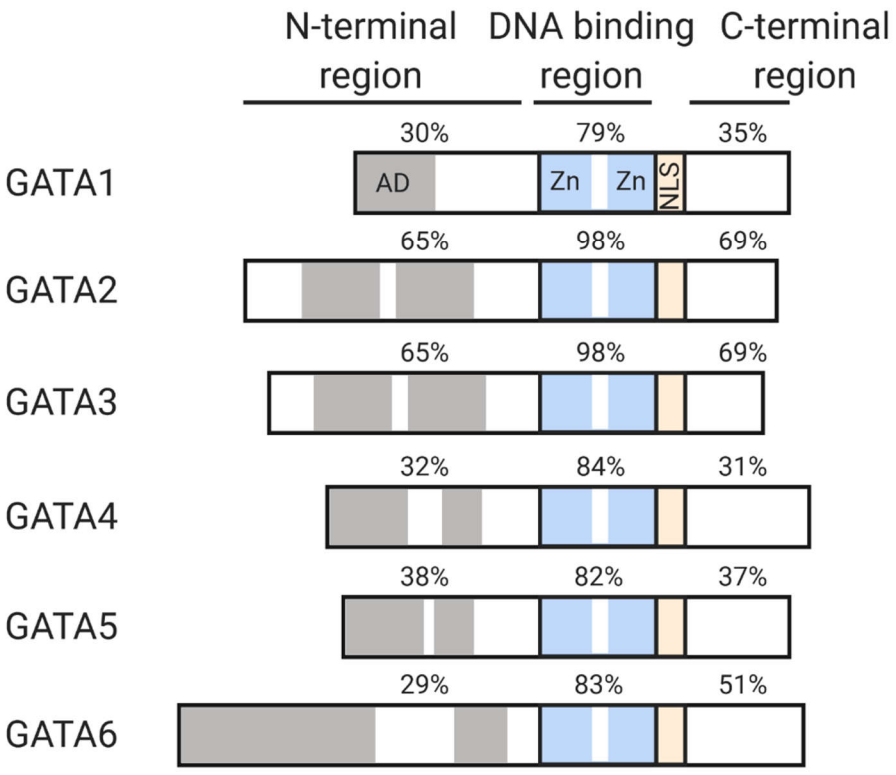

GATA family members are transcription factors with pleiotropic effects, capable of cooperative binding with a wide range of other transcription factors.[20,23] In fact, multiple members of the GATA family have demonstrated ability to act as pioneer transcription factors, binding to heterochromatic DNA sequences and promote chromatin opening to allow for other transcription factors to bind.[20] For example, GATA2 is able to regulate androgen receptor binding by recognizing and opening sections of chromatin containing androgen receptor-target genes. GATA family members typically bind cooperatively with other, tissue-specific transcription factors to regulate gene expression.[23] They are capable of regulating the activity of other transcription factors through a variety of molecular mechanisms (see **Figure 5.2**).[20] In particular, during lineage specification, pairs of GATA transcription factors tend to negatively regulate each other, where the exchange of one GATA family member for another drives cell fate commitment in a process called a "GATA switch".[20]

Figure 5.1 The GATA family of transcription factors. (on opposite page)

The six members of the GATA family of transcription factors found in vertebrates (GATA1-6). Members of the GATA family exhibit a high degree of sequence conservation within the DNA binding domain, which is comprised of two zinc finger domains that allow binding to the (A/T)GATA(A/G) consensus DNA binding sequence. Sequence conservation in the N-terminal and C-terminal regions is markedly lower. The percentage similarity of the protein sequence is calculated using the Matrix Global Alignment Tool (MatGAT).[24] AD = activation domains, Zn = zinc finger, NLS = nuclear localization signal. Figure is modified from Tremblay *et al*.[20]

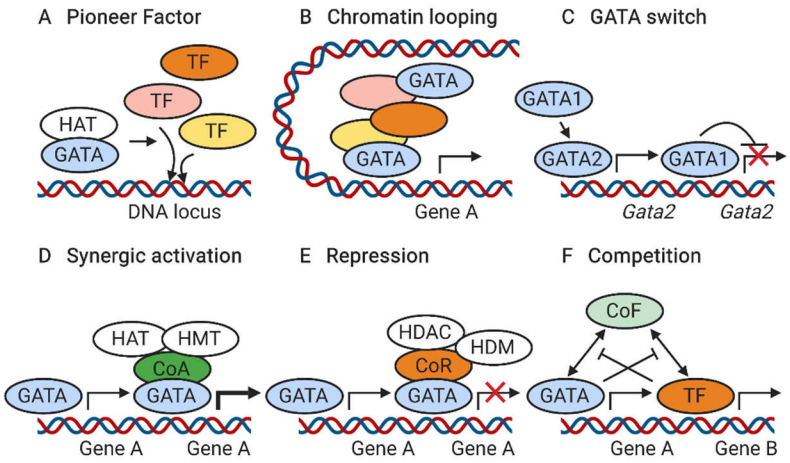

Figure 5.2 GATA transcription factor mechanisms of action.

Molecular mechanisms of action employed by members of the GATA family of transcription factors to regulate gene expression. (**A**) GATA transcription factors can act as pioneer factors and open up chromatin to allow for binding of other transcription factors. (**B**) They are able to loop chromatin to bring distant enhancer regions in closer proximity with the genes they regulate. (**C**) The replacement of one GATA factor for another is termed a "GATA switch" and has been implicated in regulating cell lineage specification. GATA transcription factors are also able to recruit mediators that affect epigenetic modification, either activating (**D**) or repressing (**E**) chromatin opening. (**F**) Finally, GATA transcription factors directly enhance or repress binding of other transcription factors. Figure is modified from Tremblay *et al*.[20]

GATA transcription factors regulate both primitive and definitive hematopoiesis. During definitive hematopoiesis, GATA factors are required for both progenitor renewal and cell lineage specification.[23] Hematopoietic stem cells require continued GATA2 expression to maintain their capacity for self-renewal.[23] Disturbing GATA2 expression, either through over-expression or knockdown, perturbs the ability of these stem cells to engage in self-renewal.[23,25] GATA factors are also markers of specific lineages of hematopoietic cells. GATA1 is expressed in erythrocytes and megakaryocytes, GATA2 is a marker of monocytic and dendritic cells, while GATA3 is only expressed in cells of the lymphoid lineage.[20]

5.1.2.1 GATA2

Of the GATA family of transcription factors, GATA2 is of particular interest to us. GATA2 was one of three non-cell cycle transcription factors found to be upregulated in patient atherosclerotic macrophages from our gene expression profiling study (see **Chapter 4**). Available evidence in the literature suggests that GATA2 could be involved in the pathogenesis of atherosclerosis in humans. Mature monocytes and macrophages do not normally express GATA2. A previous genome-wide association study (GWAS) and a linkage study have found a positive association between mutations in GATA2 and early-onset familial CAD and several risk factors associated with CAD, including obesity, low HDL and hypercholesterolemia.[26,27] Furthermore, a study that examined miRNA-regulation of gene expression in CAD patients found that GATA2 was involved in a miR-92a regulatory pathway associated with CAD.[28] GATA2 appears to regulate expression of the long non-coding RNA CDKN2B-AS, which in turns regulates miR-92a levels.[28] miR-92a has previously been identified as driving the production of inflammatory cytokines in endothelial cells under pro-atherogenic conditions.[29]

GATA2 has also been implicated in several regulatory pathways associated with inflammation. In a cohort of cardiac transplant patients receiving re-transplantation as a result of graft rejection, SENP1-mediated deSUMOylation of GATA2 in the coronary arteries was associated with graft atherosclerosis and inflammation.[30] SENP1-mediated deSUMOylation increased GATA2 stability and ability to bind DNA, thereby increasing its activity.[30] There is also evidence that GATA2 expression is regulated by inflammatory PAMP's, including LPS. Yang *et al.* show that LPS induces myeloid-derived suppressor cell formation in mice in a GATA2-dependent fashion,[31] while Wu *et al.* demonstrate that, at least *in vitro*, LPS stimulates GATA2 migration into the nucleus and activations transcription of IL-1β.[32]

Along with GATA1, GATA2 is absolutely required for both primitive and definitive hematopoiesis. GATA1/2 knockout mice die during E10-11 due to severe hematopoietic defects. GATA2 is required for proper development of the lymphatic system. In mice, complete GATA2 knockout is embryonically lethal due to lymphatic collapse, whereas partial knockouts result in lymphatic system mis-patterning.[33] In patients with loss-of-

function GATA2 mutations, lymphatic valves do not properly develop and these patients exhibit lymphedema as a result.[34] Mutations in GATA2 are also associated with diseases of the hematopoietic system, including both chronic and acute myeloid leukemia, Emberger syndrome, and MonoMAC (monocytopenia and mycobacterial infection) syndrome (also referred to as Immunodeficiency 21).[34–36] These syndromes are characterized by profound deficiencies of dendritic cells, monocytes, B cells and natural killer cells, resulting in severe immunodeficiency and increased susceptibility to infection by human papillomaviruses and nontuberculous mycobacteria.[37] Simultaneously, patients with GATA2 mutations are at increased risk of AML, pulmonary alveolar proteinosis and lymphedema. The mutations within GATA2 that give rise to these clinical manifestations are heterogeneous but can be roughly divided into three groups: missense mutations, frameshift mutations and in-frame deletions of the C-terminal zinc finger, mutations and large deletions resulting in a null allele, and mutations within the regulatory region of the GATA2 gene.[37]

GATA2 mutations have been identified in patients with chronic myeloid leukemia (CML) that have experienced progression into the blast crisis phase of disease.[20,25] In many of these patients, a distinctive L359V mutation results in increased DNA binding and coactivator recruitment, as well as repression of the transcription factor PU.1 through aberrant binding and sequestration of this protein.[25] PU.1 is a major regulator of myeloid cell proliferation and GATA2-mediated repression of PU.1 function *in vitro* appears to be sufficient to induce maturation arrest of myeloid precursor cells at the myeloblast and monoblast stages.[38] Disruption of GATA2 expression and function can also lead to AML.[20,35] In this case, both GATA2 overexpression and knockdown/loss-of-function can lead to leukemogenesis.[20] In particular, high levels of GATA2 expression correlate with poorer outcomes in pediatric AML and activation of GATA2 through a Ras-MAPK-GATA2 axis is sufficient to induce CXCL2-dependent AML proliferation.[39,40]

5.1.3 Processes involved in efferosome maturation

Efferocytosis is a complex process of removing apoptotic cells in order to prevent secondary necrosis and maintain tissue homeostasis.[41,42] We discuss efferocytosis and its regulation in detail in **Chapter 1.1** and **Chapter 3**. Broadly speaking, efferocytosis can be

divided into three distinct stages: recognition of the apoptotic cell, apoptotic cell binding and uptake, and processing and degradation of the internalized apoptotic cell.[42] In the context of atherosclerosis, a great deal of effort has gone into understanding the first two stages of efferocytosis but the final stage of efferocytosis—proper degradation and processing of internalized apoptotic cargo through regulated efferosome maturation—remains poorly understood.[43,44] Although the regulation and end result of efferocytosis is distinct, efferosome maturation utilizes the same fundamental processes to degrade apoptotic cells as phagosomes utilize to degrade pathogens. These processes include: superoxide generation within the efferosome, efferosome acidification, and fusion between efferosomes and lysosomes.[45]

The generation of superoxides within the phagosome is an efficient mechanism of pathogen killing.[46,47] In macrophages, phagosomal superoxides are generated by the phagocyte NADPH-oxidase (NOX) complex. NOX is capable of generating superoxide anions within the phagosome, which in turn can form hydrogen peroxide, a potent antimicrobial agents.[46] This mechanism is so efficient that human macrophages polarized *in vitro* to the pro-inflammatory M1 phenotype actually favour superoxide formation and hydrogen peroxide formation at the expense of consuming protons within the phagosome and delaying phagosome acidification.[48] The NOX complex is composed of two transmembrane proteins: gp91^{phox}, p22^{phox}; three cytosolic regulators: p40^{phox}, p47^{phox} and p67^{phox}; and a Rho GTPase (either Rac1 or Rac2).[46,49] The gp91phox and p22phox subunits together assemble into an inactive flavocytochrome on the membrane of nascent phagosomes. The regulatory subunits exist in the cytoplasm as a complex, which translocates to the phagosome membrane upon stimulation and, together with Rac1 or Rac2, activates the flavocytochrome complex. The activated flavocytochrome is able to reduce oxygen molecules to generate superoxide anions within the pathogen and engage in pathogen degradation.[49] NOX activity has also been recently demonstrated to be critical in efficient degradation of apoptotic cargo. Bagaitkar *et al.* demonstrated that efferocytosis of apoptotic neutrophils by murine macrophages was sufficient to induce NOX activation.[50] Using macrophages from mice with one of the NOX subunits deleted, the authors further demonstrated that superoxide generation was essential for the rapid degradation of apoptotic cargo and to prevent aberrant presentation of self-antigens to T cells.[50]

A second mechanism contributing to efficient degradation of apoptotic cargo within efferosomes is efferosome acidification. Acidification is crucial for phagosome and efferosome function.[45,51] Many proteases that serve to degrade pathogens or apoptotic cells only become active at a pH below 6.0 In the context of phagocytosis specifically, cathepsin D, which plays a crucial role in the loading of peptide onto MHC class II molecules for antigen presentation, requires a sufficiently low pH to function efficiently.[45] Acidification of phagosomes and efferosomes is mediated by the v-ATPases, which serve as pumps to move protons into the efferosome.[51] The v-ATPase is comprised of two subunits, V_1 and V_0. The V_1 subunit performs ATP hydrolysis and provides the energy for movement of protons across the efferosome membrane, while the V_0 subunit forms a membrane-spanning channel to direct movement of protons inwards.[51] V-ATPase-mediated acidification plays several important roles in efferosome maturation. The low pH environment is necessary for activation of certain degradative proteases, protons within the efferosome participate in the formation of reactive oxygen species that enhance apoptotic cell degradation, and the A1 subunit of the v-ATPase appears to be required for further fusion of efferosomes with lysosomes to complete apoptotic cargo degradation.[51,52] Recruitment of the V-ATPase to the efferosome and proper regulation ofv-ATPase activity appear to depend at least in part on the activity of the small GTPase Rab7 and its effector protein RILP.[52,53] Interestingly, under hypercholesterolemic conditions, Rab7 is recruited to the phagosomes but remains inactive, with phagosomal acidification impaired as a result.[54]

One final mechanism that is involved efferosome maturation is fusion between the efferosome and lysosomes. This delivers lysosomal enzymes to the efferosome that aid in the degradation of apoptotic cargo.[55] As we have demonstrated in **Chapter 3**, following internalization of apoptotic bodies, efferosomes ultimately go on to acquire lysosomal markers such as LAMP-1, indicating that fusion with lysosomes has taken place. Active Rab7 is again required for efferolysosomal fusion. RILP, along with another key Rab7 effector ORP1L, serve to recruit a dynein-dynactin complex and drive efferosomal migration towards the cell centre along microtubules.[53,56] This serves to bring the efferosomes into close proximity with lysosomes, which are concentrated in the perinuclear region.[53] The importance of Rab7 in the regulation of this process is underscored by the

fact that hypercholesterolemia-induced Rab7 inactivity inhibits the capacity of phagosomes to undergo migration towards the cell centre and fuse with lysosomes.[54] There is also some evidence that LC3-associated phagocytosis (LAP), which involves translocation of some components of the cellular autophagy machinery to the efferosome, is also required for efficient efferolysosomal fusion.[57]

5.1.4 Rationale and importance

As described in **Chapter 4**, gene expression profiling of macrophages isolated from early-stage human pre-atherosclerotic lesions located in the proximal aorta from patients undergoing open-heart surgery revealed profound dysregulation in both cholesterol metabolism and in efferocytosis and efferosome maturation. The challenge is now to identify potential regulatory transcription factors that could account for part of all of this unique macrophage phenotype. We found just three non-cell cycle transcription factors to be upregulated in patient macrophages, with only GATA2 being confirmed to be upregulated by RT-qPCR.

GATA2 is of interest over RARG and E4F1 since of the three, only SNPs in GATA2 are associated with increased risk for CAD.[26,27] Mutations in GATA2 are also strongly associated with immunological and hematological abnormalities, including myelodysplasia and an elevated risk of leukemia.[23,35] Intriguingly, Jaiswal *et al.* have recently shown that certain mutations associated with the development of leukemia, in particular mutations in TET—another transcription factor involved in hematopoiesis—also increase the risk of developing atherosclerosis and cardiovascular disease.[58] Gain-of-function mutations in GATA2 are associated with blast crisis in CML and increased GATA2 expression is a marker of worse outcomes in AML.[25,40] There is therefore some biological plausibility in GATA2 being a master regulator of the dysregulation observed in patient macrophages. Further connecting GATA2 and defects in efferosomal maturation, Lasbury *et al.* have shown that in the context of *Pneumocysitis carnii* infection of the airways, GATA2 upregulation suppresses the phagocytic capacity of alveolar macrophages in response to infection.[59]

In this chapter, we utilize an *in vitro* model of atherosclerotic macrophages and genetic manipulation of GATA2 to study the effect of perturbing GATA2 expression on cholesterol homeostasis, efferocytosis and efferosome maturation, and on peptide citrullination in these cells. GATA2 is an attractive candidate for a master regulatory factor that could drive some or all of the defects observed in patient macrophages. Determining to what extent perturbation of GATA2 expression affects macrophage cholesterol handling and efferocytosis would add significantly to our understanding of the mechanisms driving macrophage dysregulation in early atherosclerotic disease and development of defective efferocytosis. GATA2 and its downstream targets could also represent potential therapeutic targets for development of novel atherosclerosis treatments targeting the inflammatory component of atherosclerotic disease.

5.2 Methods

5.2.1 Generation of atherosclerotic macrophages

J744.2 and THP-1 macrophage cell lines were cultured as described in **Chapter 2.4.1**. Primary human macrophages were prepared as described in **Chapter 2.4.2**. Prior to oxLDL treatment, THP-1 cells were differentiated into adherent macrophages by treatment with 100 nM PMA for 72 hrs. Cells were incubate with human oxLDL at a concentration of 50 µg/mL for 48 hrs (J744.2 cells[13] and primary human macrophages[14]) or 100 µg/mL for 72 hrs (THP-1 cells[10]). oxLDL-treated cells were washed with PBS to remove excess oxLDL and were placed into fresh, oxLDL-free media prior to use in downstream assays.

5.2.2 Measurement of cholesterol accumulation

Cholesterol accumulation in oxLDL-treated macrophages was measured by staining with either Oil Red O or Nile Red. For Oil Red O staining, stock Oil Red O solution (1:250 w/v Oil Red O power in 100% isopropanol) was diluted 3:2 in ddH_2O to a working concentration, mixed by vortexing, allowed sit for 20 min at room temperature, and filtered through a 0.2 µm filter. The cells to be stained were washed 1× with PBS and then fixed with 4% PFA for 20 min at room temperature. Fixed cells were washed 3× 5min with PBS

to remove excess PFA. Cells were then washed briefly with a 3:2 v/v mixture of isopropanol and ddH_2O and allowed to dry completely. Cells were covered with the minimum volume of Oil Red O working solution to ensure complete coverage and allowed to incubate for 5 min at room temperature. Cells were washed 3× 5 min with PBS to remove excess Oil Red O. If desired, Oil Red O-stained cells may be prepared for imaging under white light at this point by mounting coverslips on glass slides using Permafluor. Otherwise, Oil Red O can be extracted by treating cells with 100% isopropanol for 10 min at room temperature with gentle agitation. Oil Red O concentration can be quantified by measurement of absorbance at 460 nm using an Eppendorf BioPhotometer Plus (Thomas Scientific).

For Nile Red staining, stock Nile Red solution is prepared by dissolving Nile Red power in acetone at a concentration of 1 mg/mL. Cells to be stained are washed 1× with PBS and fixed with 4% PFA for 20 min at room temperature. Fixed cells were washed 3× 5min with PBS to remove excess PFA. Stock Nile Red is diluted 1:100 in PBS to generate a working solution. Fixed cells are covered with Nile Red working solution for 5 min at room temperature. Cells are then washed 3× 5 min with PBS to remove excess PBS and prepared for imaging by mounting coverslips on a glass slide using Permafluor. For Nile Red staining of live cells, cells are prepared for live cell imaging in a Leiden chamber as described in **Chapter 2.10.2** with time-lapse images captured on white light and Nile Red channels at 630× magnification every 15 min for 8 hrs. Nile Red fluorescence is measured using a solid-state white light source in conjunction with a 550/570 nm bandpass excitation filter and a 605/52 nm bandpass emission filter. Nile Red stock solution is added 1:100 v/v directly to the culture media and live cell imaging is performed as usual. If desired, cells can be incubated for 3-5 hrs in serum-free media prior to staining to remove background lipid deposition.

5.2.3 Cholesterol efflux assay

Cholesterol efflux was measured using a high-sensitivity assay initially described by Sankaranarayanan *et al.*[60] To prepare labelling media, BODIPY-cholesterol and unlabeled cholesterol were mixed together at a ratio of 1:5 v/v in a glass bottle and dried under nitrogen away from light. The cholesterol mixture was solubilized with MEM-HEPES

(MEM media with 10 mM HEPES, pH 7.4) containing 20 mM methyl-β-cyclodextran (MβCD) at a molar ratio of 1:40 cholesterol to MβCD in MEM-HEPES. The mixture was agitated in a sonicating water bath at 37 °C for 30 min. The sonicated suspension was placed on a stirring hot plate pre-heated to 37 °C and kept stirring with a sterile stir bar for 3 hrs. This labelling media can be used immediately or stored at 4 °C away from light until ready to use. Immediately prior to use, labelling media is again sonicated in a sonicating water bath at 37 °C for 30 min and filtered through a 0.45 µm filter.

ApoB-depleted human serum is used as the cholesterol acceptor. To prepare ApoB-depleted serum, 1M $CaCl_2$ is added to whole human plasma at a ratio of 1:40 v/v. The plasma is allowed to incubate for 1 hr at room temperature to allow for clotting, after which serum is separated from the clotted plasma proteins by centrifugation for 5 min at 1,000 ×g. ApoB was precipitated from the serum through addition of PEG solution (20% PEG 8,000 in 200 mM glycine buffer, pH 7.4) to serum at a 2:5 v/v ratio. The mixture is allowed to incubate for 20 min at room temperature and then centrifuged for 30 min at 10,000 ×g and 4 °C. The supernatant, containing apoB-depleted serum, is transferred to a fresh tube.

To perform the cholesterol efflux assay, THP-1 cells were cultured in a 48-well plate to a density of 75,000 cells/well. At 24 hrs prior to starting the assay, cells are differentiated into adherent macrophages through addition of 100 nM PMA. Cells are washed 1× with PBS and incubated with 250 µL/well of labelling media for 1 hr at 37 °C and 5% CO_2. Cells are washed 2× with MEM-HEPES to remove excess labelling media. Cells are then incubated with incomplete RPMI containing 0.2% BSA for 16 hrs at 37 °C and 5% CO_2. Cells were again washed 2× with MEM-HEPES and then incubated with fresh MEM-HEPES containing 10% apoB-depleted serum for 4 hrs at 37 °C and 5% CO_2. A negative control where cells are incubated with MEM-HEPES lacking apoB-depleted serum should also be prepared at this point. Media from each well was collected, filtered through a 0.45 µm filter and fluorescence intensity (ex. 482 nm, em. 515 nm) was recorded using a Gemini Fluorescence Microplate Reader running SoftMax Pro (Molecular Devices). The cells used in the negative control were solubilized with the addition of 4% cholic acid and incubated for 4 hrs at room temperature with gentle agitation. Supernatants were collected, filtered through a 0.45 µm filter and fluorescence intensity was recorded and used as the baseline

value for total cholesterol present within the cells. The percent cholesterol efflux was calculated as fluorescence intensity of media divided by fluorescence intensity of cholic acid.

5.2.4 Nitroblue tetrazolium assay

A microscopy-based nitroblue tetrazolium (NBT) assay protocol was used to assess macrophage NADPH oxidase activity.[61] Apoptotic Jurkat cells were prepared according to **Chapter 2.8.2.2** and added at a multiplicity of infection (MOI) of 10 to PMA-differentiated THP-1 cells and briefly centrifuged for 1 min at 400 ×g to force contact between the macrophages and apoptotic cells. NBT was added to a final concentration of 100 µg/mL and the assay was allowed to incubate for 1 hr at 37 °C and 5% CO_2. Following incubation, cells were washed 3× 5 min to remove unbound apoptotic cells and excess NBT reagent. Cells were fixed with 4% PFA for 20 min at room temperature. Cells were then washed 3× 5 min with PBS and coverslips were mounted onto glass slides using Permafluor for imaging. Fluorescence of diformazan deposits formed were imaged on an epifluorescence microscope at 630× magnification using a solid-state white light source in conjunction with a 650/670 nm bandpass excitation filter and a 700/50 nm bandpass emission filter.

5.2.5 Dextran fusion assay

Dextran fusion assay to quantify phagolysosomal fusion was performed according to the protocol of Flannagan *et al.*[62] PMA-differentiated THP-1 macrophages were treated with 100 µg/mL 10,000 MW TRITC-conjugated dextran for at least 16 hrs at 37 °C and 5% CO_2. Dextran-loaded macrophages were washed 3× with PBS to remove excess dextran and then incubated in serum-free RPMI for 1.5 hrs at 37 °C and 5% CO_2 to allow for loading of the dextran onto the lysosomal compartment. IgG-coated beads prepared according to **Chapter 2.8.2.1** were added to macrophages at a MOI of 10 and the mixture was briefly centrifuged for 1 min at 400 ×g to force contact between macrophages and beads. The assay was allowed to incubate for 30 min at 37 °C and 5% CO_2. Following incubation, cells were washed 1× with PBS to remove unbound beads and labelled 1:1,000 with a Cy5-conjugated anti-human IgG secondary antibody to label bound but uninternalized beads. Cells were subsequently washed 3× 5 min with PBS and fixed with

4% PFA for 20 min at room temperature. Following fixation, cells were washed 3× 5min to remove excess PFA and coverslips were mounted onto glass slides using Permafluor. Assays were imaged under epifluorescence microscopy at 630× magnification with a 550/570 nm bandpass excitation filter and a 605/52 nm bandpass emission filter (TRITC-dextran) and a 650/670 nm bandpass excitation filter and a 700/50 nm bandpass emission filter (Cy5-conjugated anti-human IgG).

5.2.6 Phagosome acidification assay

Human IgG was labelled using a pHrodo Red Microscale Labeling Kit (Invitrogen) as per the manufacturer's instructions. 5 μm polystyrene/DVB beads were coated with a 50:1:1 ratio of unlabeled:pHrodo-conjugated:AF647-conjugated human IgG as per our published protocols.[63,64] Beads were added to PMA-differentiated THP1 macrophages at a MOI of 10 and time-lapse images on the white light, pHrodo (ex. 550/570 nm bandpass filter, em. 605/52 nm bandpass filter) and AF647 (ex. 650/670 nm bandpass filter, em. 700/50 nm bandpass filter) channels were recorded at 630× magnification, 1 frame-per-minute, for 60 min. At the end of the imaging period, the cell culture medium was replaced with calibration buffers of known pH (140 mM KCl, 1 mM $MgCl_2$, 0.2 mM EGTA, 20 mM NaCl with either 20 mM MES (pH 4 and 5) or 20 mM HEPES (pH 6 and 7)). Images were captured on the pHrodo and AF647 channels after each pH change. Using FIJI,[65,66] phagocytosed beads were identified in the DIC channel, and the intensity of the pHrodo and AF647 signal on individual beads recorded at each time point starting immediately prior to phagosome closure through to the end of the time-lapse. For each phagosome, at each time point, the pHrodo signal was normalized using the AF647 channel, and then the calibration curve for the phagosome used to determine the pH of the phagosome at each time point.

5.2.7 Anti-modified citrulline staining

Anti-modified citrulline (AMC) staining was employed to detect citrullinated peptides in patient aortic punch tissue sections, according to the protocol developed by Vossenaar *et al.*[67] From FFPE sections prepared according to **Chapter 2.2.3.2**. Sections were de-paraffinized through sequential exposure to: xylene 2× 5-10 min, 100% ethanol 2× 5-10

min, 95% ethanol 2× 5-10 min, 75% ethanol 2× 5-10 min, ddH_2O 2× 5-10 min and PBS 1× 20 min. Follow de-paraffinization, the citrulline modification step was performed using the Anti-Citrulline (Modified) Detection Kit (Sigma-Aldrich) according to the manufacturer's instructions for 3 hrs at 37 °C. Antigen retrieval was performed using the Trypsin Enzymatic Antigen Retrieval Solution (Abcam) according to the manufacturer's instructions with a 30 min room temperature incubation period. Following modification, sections were incubated for a further 30 min with 3% H_2O_2 to block endogenous peroxidases. Sections were washed 3× 5 min with PBS and blocked with 10% goat serum for 30 min at room temperature. Sections were then incubated with either 1% goat serum (negative control), 1µg/mL normal human IgG (isotype control), or 1:1,000 anti-peptidyl-citrulline antibody (Sigma-Aldrich, clone F95) overnight at room temperature. Excess antibody was removed by washing 3× 5 min with PBS and 1:2000 of 0.8mg/mL goat anti-human HRP conjugate was applied to the sections for 1 hr at room temperature. Sections were then developed with Vector DAB HRP substrate (Vector Laboratories) was applied for 2-10 min until staining reaches an appropriate level. Sections were rinsed with PBS to stop the reaction and then washed a further 2× 10 min with PBS. Sections were then counterstained with haemotoxylin for 5 min, rehydrated with increasing concentrations of ethanol followed by xylene. Sections were then mounted on glass coverslips using Cytoseal 60.

AMC staining of cultured THP-1 macrophages was performed using a modified version of the procedure outlined above. To label individual cells, 1mg/mL Cy5-conjugated wheat germ agglutinin was added 1:200 to cells for 10 min protected from light and washed 3× 5 min with PBS. Cells were then fixed in 2% PFA for 15 min at room temperature, washed 3× 5min with PBS, and then permeabilized with 0.2% Triton X-100 for 10 min at room temperature. Citrulline modification step was performed as described above. Cells were washed 3× 5 min with PBS and blocked with 5% fetal bovine serum for 3 hrs at room temperature. Thereafter, cells were incubated with 1% goat serum (negative control), 1µg/mL normal human IgG (isotype control), or 1:1,000 of 1mg/mL anti-peptidyl-citrulline antibody (Sigma-Aldrich, clone F95) for 1 hr at room temperature. Cells were again washed 3× 15 min with PBS and then incubated with 1:1,000 of 1mg/mL Cy3-

conjugated goat anti-human IgG for 30 min at room temperature. Cells were washed 3× 15 min with PBS and mounted onto glass slides using Permafluor.

5.3 Results

5.3.1 Confirmation of GATA2 expression in patient aortic punch macrophages

We observed a significant upregulation of GATA2 expression in patient aortic punch macrophages in our microarray dataset (**Chapter 4.3.4**) and subsequently verified this in a set of independent patient and control macrophage samples by RT-qPCR (**Chapter 4.3.5**). Our results from qPCR indicated that not only was GATA2 significantly upregulated in patient macrophages, it was expressed at much higher levels than detected by microarray. To confirm that GATA2 is specifically expressed in lesion-resident macrophages, we performed immunofluorescence imaging of sectioned patient aortic punch tissues stained for human GATA2 and the human pan-macrophage marker CD68 (**Figure 5.3a**).

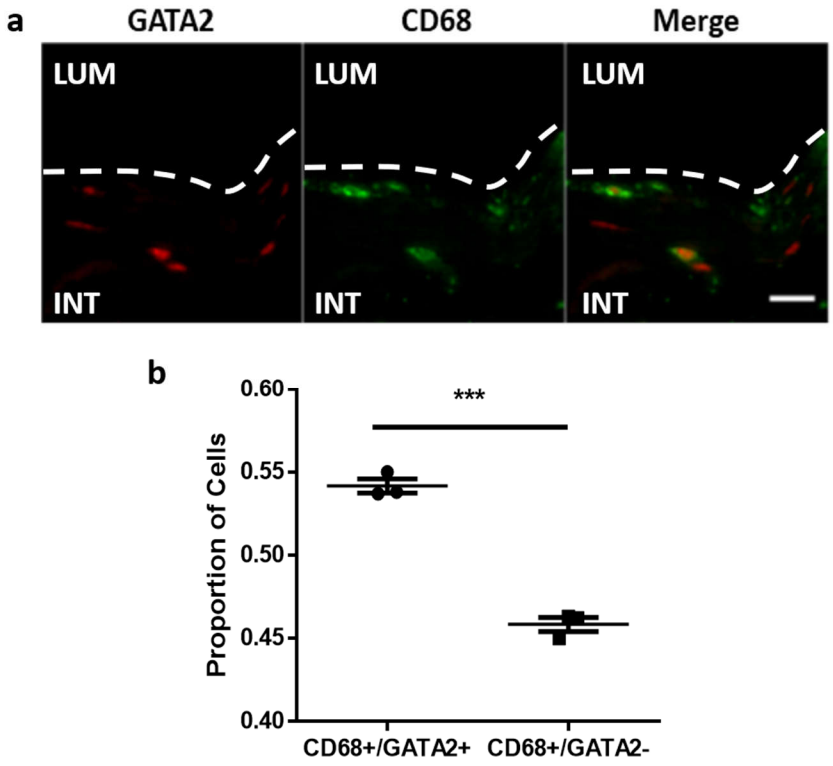

Figure 5.3 Co-localization of GATA2 expression with patient lesion-resident CD68+ macrophages.

Patient aortic punch tissue sections were stained for GATA2 and the pan-macrophage marker CD68. Sectioned were subsequently imaged using a fluorescence microscope to examine co-localization between GATA2 and $CD68^+$ cells. The image is representative of (**a**) and the graph quantifies (**b**) localization of GATA2 within $CD68^+$ across N = 3 patients shown as mean ± SEM. LUM = lumen, INT = intima. ***$p < 0.001$ by unpaired, two-tailed Student's t test. Scale bar = 20 μm.

We observed co-localization of GATA2 with approximately 50% of $CD68^+$ cells within the intima (**Figure 5.3b**), indicating that expression of GATA2 is heterogenous across the population of lesion-resident macrophages. It is also possible that a number of these $CD68^+$ cells are smooth muscle cells that have adopted a foam cell-like phenotype,[68] however this experiment was not designed to be able to discriminate between these two cell populations.

5.3.2 Generation of an *in vitro* model of atherosclerotic macrophages

To study the effects of GATA2 on macrophage function, we first generated an *in vitro* model of atherosclerotic macrophages through exposure of human monocyte-like THP-1 cells to oxLDL following PMA-differentiation based on the method of Seo *et al.*[14] Characterization of Oil Red O accumulation in THP-1 macrophages incubated with 100 µg/mL oxLDL by white light microscopy (**Figure 5.4a**) or quantification of Oil Red O content extracted from cells by measurement of absorbance at 420 nm by spectrophotometer (**Figure 5.4b**) demonstrated a linear increase in intracellular lipid content over a period of 24 hrs, resulting in cells that resemble cholesterol-laden foam cells in appearance. Due to the kinetics of GATA2 expression in THP-1 cells exposed to oxLDL, we also examined sustained exposure of THP-1 cells to oxLDL over a period of 72 hrs and again demonstrated a significant increase in intracellular lipid content in these cells as compared to cells cultured for 72 hrs without exogenous oxLDL (**Figure 5.4c**).

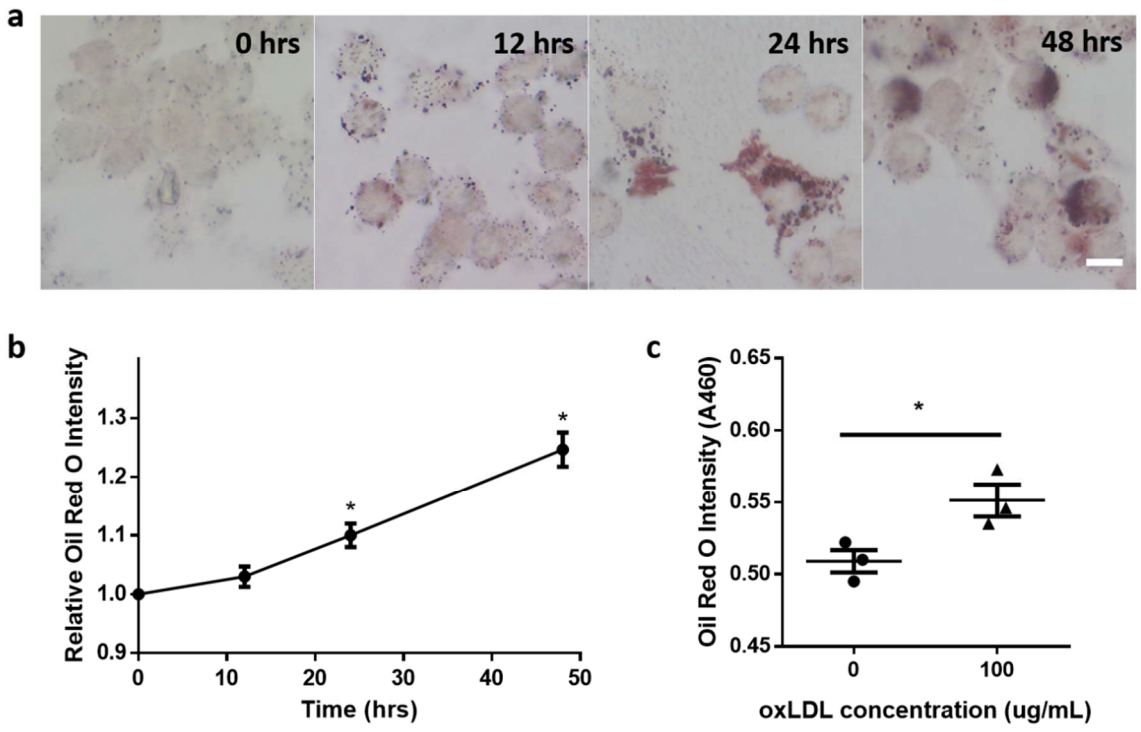

Figure 5.4 Exposure to oxLDL induces an increase in intracellular lipid content in THP-1 macrophages. (on opposite page)

THP-1 monocyte-like cells were incubated with 100 μg/mL human oxLDL over a period of 48 (**a**, **b**) or 72 hrs (**c**). (**a**) Cells were stained with Oil Red O following 0, 12, 24 and 48 hrs incubation with oxLDL and imaged under a white light microscope. (**b**) Cells were incubated with oxLDL for the time points specified previously and stained with Oil Red O. Intracellular Oil Red O was quantified at 420 nm as a proxy of total intracellular lipid content. (**c**) Cells were incubated with oxLDL for 0 or 72 hrs and intracellular Oil Red O content was quantified at 420 nm. Data are presented as mean ± SEM of N = 3 replicates. *$p < 0.05$ compared to Time = 0 hrs by 1-way ANOVA with Sidak multiple comparison test (**b**) or compared to oxLDL concentration = 0 μg/mL by unpaired, two-tailed Student's t test. Scale bar = 10 μm.

Accumulation of intracellular lipid droplets is perhaps the most important feature of lesion-resident atherosclerotic macrophages and foam cells. We demonstrate here that incubation of THP-1 macrophages with human oxLDL for at least 48 hrs is sufficient to induce significant amounts of intracellular lipid accumulation in these cells, suggesting that we are able to re-capitulate at least part of the lesion-resident atherosclerotic phenotype *in vitro*.

5.3.3 Exposure to oxLDL induces GATA2 expression in THP-1 and primary human macrophages

After confirming that exposure to oxLDL *in vitro* can induce an atherosclerosis-like phenotype in THP-1 macrophages, we went on to determine whether oxLDL exposure is sufficient to induce upregulation of GATA2 expression in both THP-1 cells and primary human macrophages. We incubated THP-1 cells with 100 μg/mL oxLDL and primary human macrophages with 50 μg/mL oxLDL (100 μg/mL oxLDL resulted in toxicity in these cells, data not shown) over 72 hrs and quantified GATA2 expression by RT-qPCR over this time period (**Figure 5.5**).

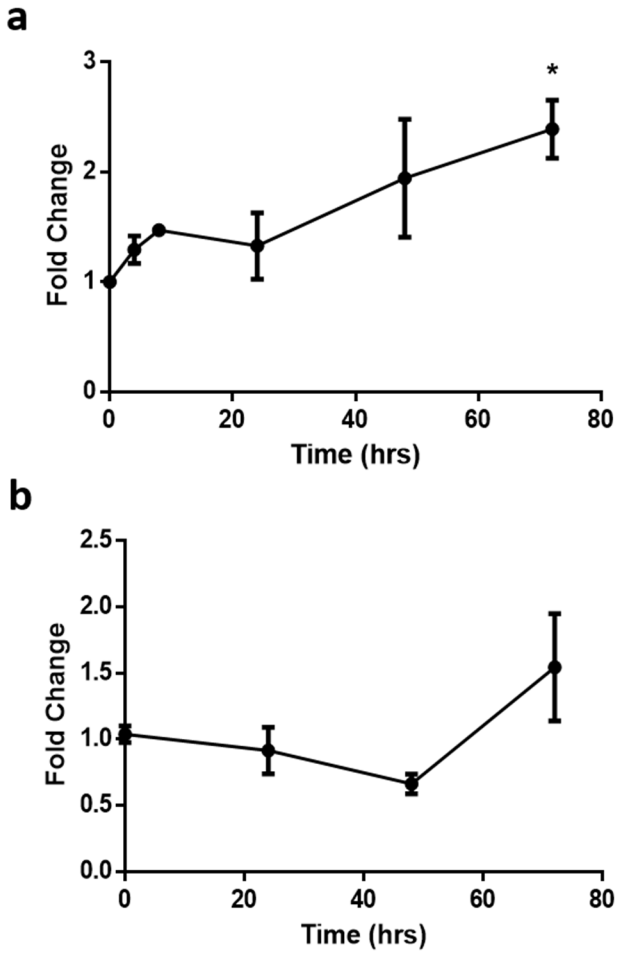

Figure 5.5 Exposure to oxLDL is sufficient to induce upregulation of GATA2 expression in macrophages.

Quantification of relative GATA2 expression in macrophage cells following exposure to oxLDL. PMA-differentiated THP-1 macrophages (**a**) or *ex vivo* monocyte-derived primary human macrophages (**b**) were incubated with 100 or 50 μg/mL human oxLDL respectively for up to 72 hrs. GATA2 expression levels were measured by RT-qPCR at various time points and normalized to GATA2 expression at Time = 0 hrs. Data are shown as mean ± SEM from N = 3 biological replicates. *$p < 0.05$ compared to Time = 0 hrs by 1-way ANOVA with Sidak multiple comparisons test.

Incubation with oxLDL resulted in a linear increase in the level of GATA2 expression in THP-1 macrophages but this increase was not significant compared to baseline until 72 hrs

post-oxLDL exposure (**Figure 5.5a**). With respect to primary human macrophages, we did not observe an increase in GATA2 until 72 hrs of incubation with oxLDL but we did not find this increase to be significantly different compared to baseline (**Figure 5.5b**). This may be a result of the lower concentration of oxLDL used in the primary human macrophage experiments or it could be that a longer incubation period is required. However, on the basis of this data and the previous section, incubation with oxLDL for a period of 72 hrs is sufficient to induce cholesterol accumulation within THP-1 macrophages accompanied by a significant increase in GATA2 expression.

5.3.4 Generation of GATA2 overexpression and knockdown cell lines

To study the effect of perturbing GATA2 expression both in the presence and absence of oxLDL, we generated stable GATA2 overexpression and knockdown THP-1 cell lines. To generate a GATA2 overexpression vector, the human GATA2 consensus coding sequence was cloned into a pLVX-IRES-ZsGreen1 backbone, a lentiviral expression vector that allows simultaneous expression of GATA2 along with the ZsGreen1 fluorophore under a CMV promoter (see **Figure 5.6a** for cloning strategy and Appendix A for sequences of). To generate a GATA2 knockdown vector, shRNA sequences targeting human GATA2 were generated using the siRNA Wizard Software 3.1 (InvivoGen). Each shRNA generated was cloned into a pGFP-C-shLenti backbone, a lentiviral shRNA expression vector that allows simultaneous expression of a GATA2 shRNA and the TurboGFP fluorophore under a SV40 promoter (see **Figure 5.6b** for cloning strategy for most effective shRNA sequence). See **Appendix A** for the sequence of the most effective shRNA sequence.

Figure 5.6 Cloning strategy for GATA2 overexpression and knockdown vectors. (on opposite page)

Cloning strategy employed to create the (**a**) GATA2 overexpression (pLVX-IRES-ZsGreen1 GATA2) and (**b**) knockdown (pGFP-C-shLenti GATA2 shRNA1) vectors. Diagrams were created using SnapGene Version 4.3 (GSL Biotech).

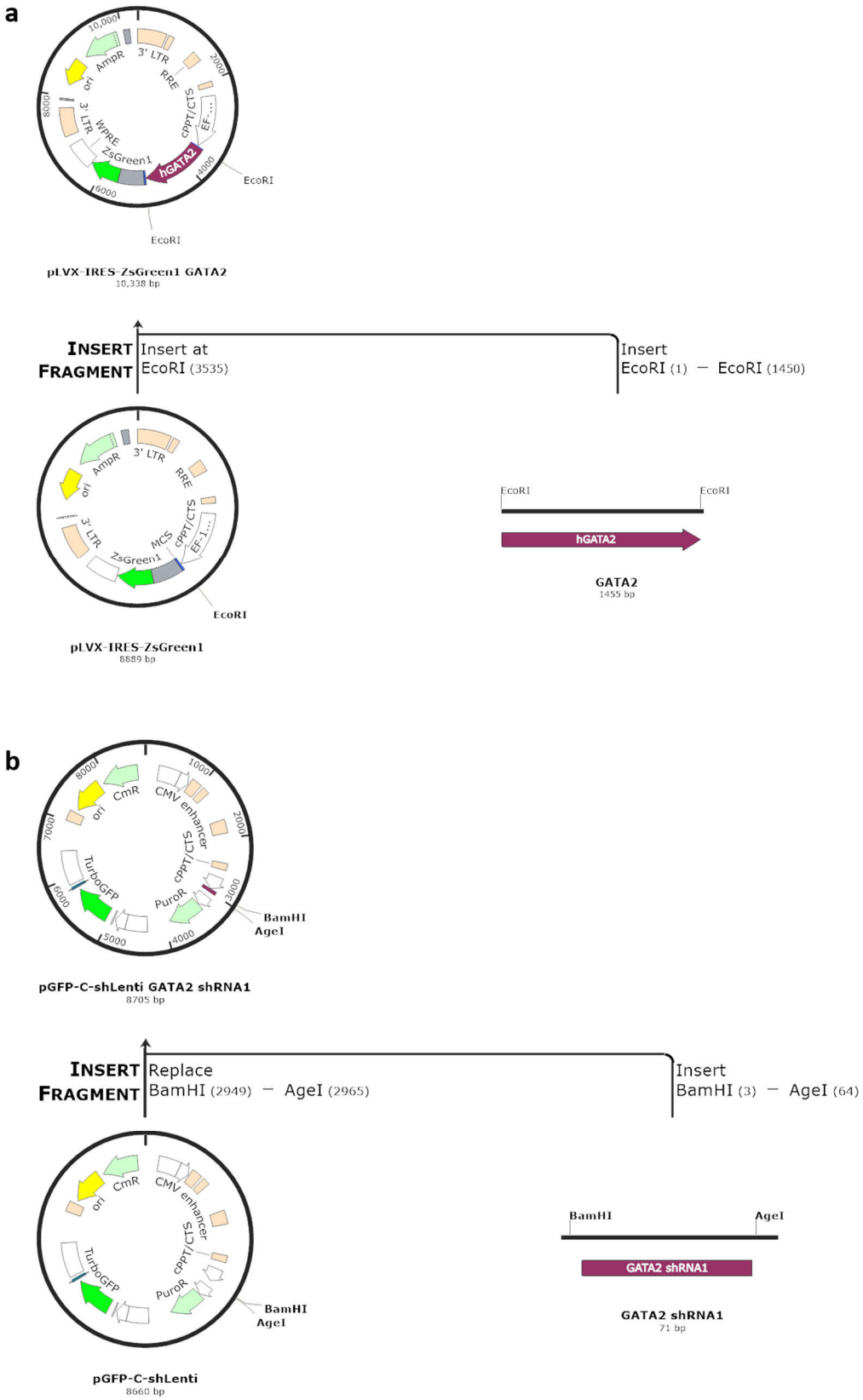
a
pLVX-IRES-ZsGreen1 GATA2
10,338 bp
INSERT FRAGMENT
Insert at EcoRI (3535)
Insert EcoRI (1) – EcoRI (1450)
pLVX-IRES-ZsGreen1
8889 bp
GATA2
1455 bp
b
pGFP-C-shLenti GATA2 shRNA1
8705 bp
INSERT FRAGMENT
Replace BamHI (2949) – AgeI (2965)
Insert BamHI (3) – AgeI (64)
pGFP-C-shLenti
8660 bp
GATA2 shRNA1
71 bp

The GATA2 overexpression vector was packaged into a lentivirus and stably transduced into THP-1 cells. Transduced cells were sorted to contain only successfully-transfected cell populations by a fluorescence-activated cell sorting strategy using a FACSAria III Flow Cytometric Cell Sorter (BD Biosciences) and gating on the 10% of live cells expressing the highest levels of green fluorescence (data not shown). Immunofluorescence imaging demonstrated that in ZsGreen1^{+} cells that were successfully transduced with the overexpression vector, GATA2 is significantly overexpressed (**Figure 5.7a**). As expected, controls transduced with an empty pLVX-IRES-ZsGreen1 vector did not show any GATA2 expression (**Figure 5.7a**). We examined this at the protein level, measuring GATA2 protein expression by Western blot in stably-transduced THP-1 cells. GATA2 protein levels were increased in the transduced THP-1 cells as compared to a untransduced control, as demonstrated by the Western blot (**Figure 5.7b**) and densitometry quantification thereof (**Figure 5.7c**). Finally, we confirmed upregulation of GATA2 expression in transduced THP-1 cells by RT-qPCR (**Figure 5.7d**).

Figure 5.7 Generation of a stably-transduced THP-1 GATA2 overexpression cell line. (on opposite page)

A stably-transduced THP-1 GATA2 overexpression cell line was generated through lentiviral transduction of the pLVX-IRES-ZsGreen1 GATA2 vector into THP-1 cells and a pure GATA2-overexpression THP-1 population was obtained through FACS sorting of ZsGreen^{bright} cells. (**a**) Stably-transduced THP-1 were immunostained for human GATA2, using THP-1 cells transduced with an empty pLVX-IRES-ZsGreen1 vector as a negative control. (**b**) Demonstration of GATA2 protein production in stably-transduced THP-1 as compared to a negative control transduced with the empty vector by Western blotting, and (**c**) quantification thereof by band densitometry analysis. (**d**) Measurement of GATA2 overexpression in stably-transduced cells by RT-qPCR compared to cells transduced with an empty vector control. Images and graph are representative of (**a-c**) or quantifies (**d**) N =3 biological replicates. Data are shown as mean (**c**) or mean ± SEM (**d**). **$p < 0.01$ by unpaired, two-tailed Student's t test. Scale bar = 10 μm.

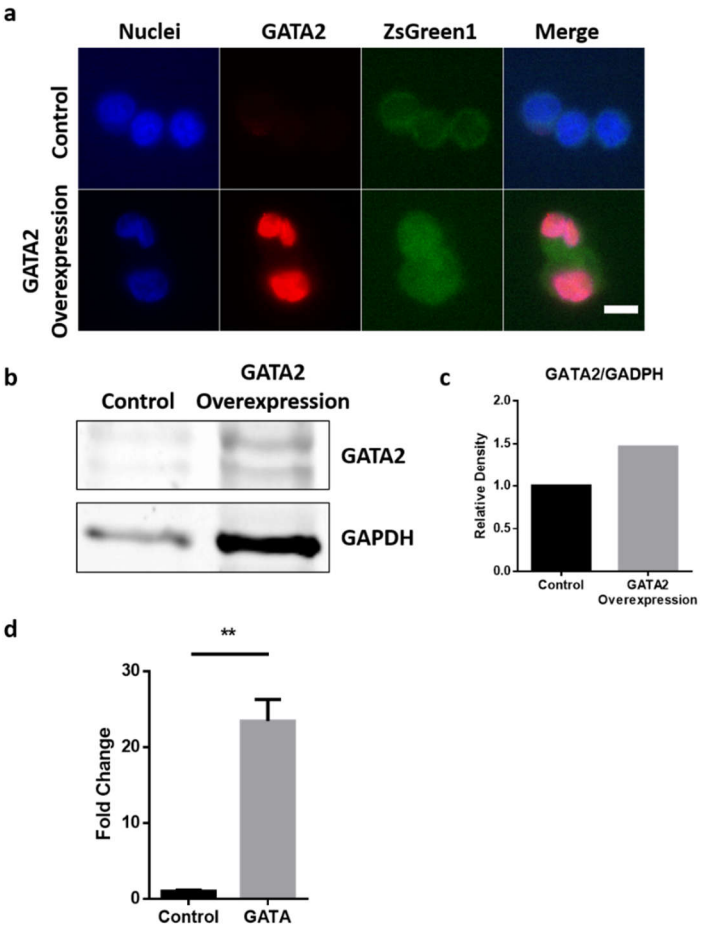

Since THP-1 cells do not produce appreciable levels of endogenous GATA2, it was not possible to test the efficiency of shRNA constructs on knocking down GATA2 expression in these cells directly. Instead, we adopted a strategy of co-transfecting the GATA2 overexpression and the shRNA vectors into HEK cells. This allowed us to determine the degree to which each shRNA construct created could inhibit GATA2 overexpression. We demonstrated that the most effective shRNA construct (hereafter referred to as shRNA1) could reduce GATA2 protein expression by approximately 50% (**Figure 5.8a**, **5.8b**). The shRNA1 sequence was used to generate the GATA2 knockdown vector, which was stably-transduced into THP-1 cells and sorted by FACS to generate a pure GATA2 knockdown THP-1 cell population (data not shown). Analysis of GATA2 mRNA levels in stably-transduced THP-1 cells following oxLDL exposure showed a significant reduction in GATA2 levels in the cells expressing the GATA2 shRNA compared to cells transduced with a scrambled shRNA control (**Figure 5.8c**).

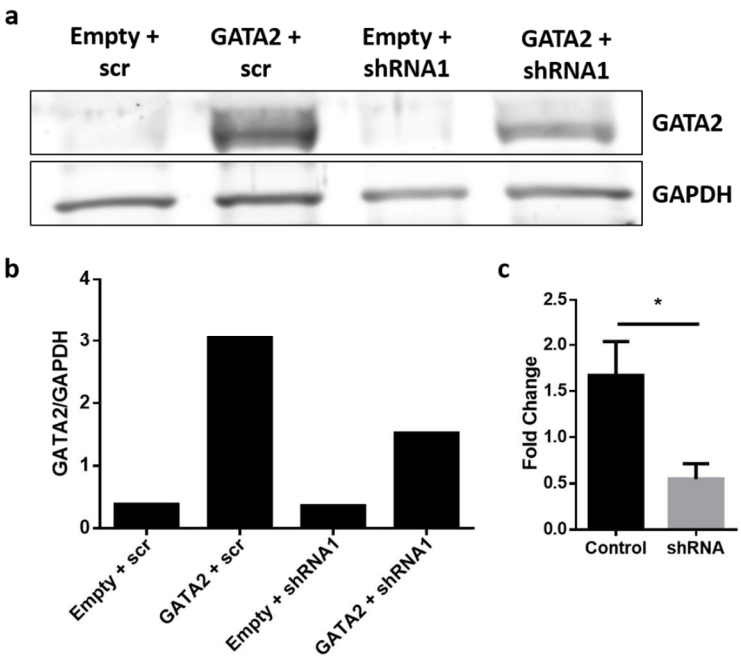

Figure 5.8 Generation of a stably-transduced THP-1 GATA2 knockdown cell line.

A stably-transduced THP-1 GATA2 knockdown cell line was generated through lentiviral transduction of the pGFP-C-shLenti GATA2 shRNA1 vector into THP-1 cells and a pure GATA2-knockdown THP-1 population was obtained through FACS sorting of TurboGFP^{bright} cells. (**a**) Demonstrating that co-transfection of HEK cells with the GATA2 overexpression and knockdown vectors results in a decrease in GATA2 protein levels compared to co-transfection of HEK cells with the overexpression vector and a scrambled shRNA control by Western blotting, and (**b**) quantification thereof by band densitometry. Empty = empty pLVX-IRES-ZsGreen1 vector, scr = scrambled shRNA vector. THP-1 GATA2 knockdown cell line was generated through lentiviral transduction of the pGFP-C-shLenti GATA2 shRNA1 vector into THP-1 cells and a pure GATA2-knockdown THP-1 population was obtained through FACS sorting of TurboGFP^{bright} cells. (**c**) Quantification of GATA2 knockdown in stably-transduced GATA2-knockdown THP-1 cells incubated with human oxLDL for 72 hrs compared to cells transduced with a scrambled shRNA control by RT-qPCR. Image and graph are representative of (**a**, **b**) or quantifies (**c**) N = 3 biological replicates. Data are shown as mean (**b**) or mean ± SEM (**c**). *$p < 0.05$ by unpaired, two-tailed Student's t test.

5.3.5 Perturbation of GATA2 expression does not alter macrophage cholesterol metabolism

Following the generation of stably-transduced GATA2 overexpression and knockdown THP-1 cell lines, we used these cells to examine the effect of perturbing GATA2 expression on macrophage cholesterol handling. Cholesterol loading in macrophages with exposure to oxLDL was measured by observing accumulation of the lipophilic dye Nile Red in THP-1 macrophages over a period of 8-12 hrs (**Figure 5.9a**). THP-1 macrophages continually accumulate cholesterol over a period of 12 hrs, with the most rapid rate of accumulation occurring between 4-8 hrs of oxLDL exposure and slowing down after 8 hrs (**Figure 5.9b**).

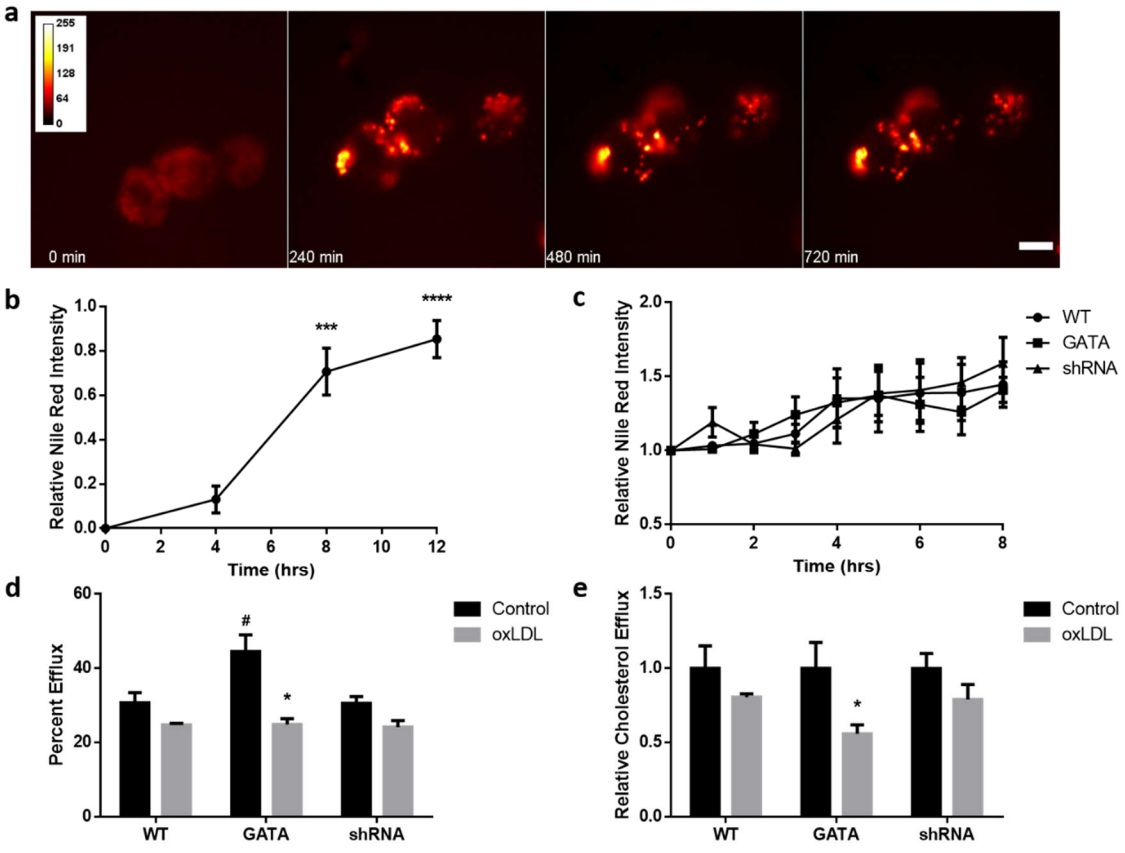

Figure 5.9 Perturbation of GATA2 expression does not have a consistent effect on macrophage cholesterol handling. (on opposite page)

Cholesterol handling was assessed in THP-1 cell lines with differing levels of GATA2 expression. (**a**) Accumulation of cholesterol in THP-1 macrophages imaged with live cell Nile Red staining over a period of 12 hrs, and (**b**) quantification of these images demonstrating intracellular cholesterol accumulation. (**c**) Accumulation of cholesterol over 8 hrs in THP-1 cells with differing levels of GATA2 expression. (**d** and **e**) Cholesterol efflux from THP-1 macrophages grown under normal (Control) or hyperlipidemic (oxLDL) conditions quantified using fluorescent BODIPY-labelled cholesterol shown as percent efflux from baseline (**d**) or relative to the degree of cholesterol efflux in cells grown in normal conditions (**e**). WT = wild type THP-1 cells, GATA = GATA2 overexpressing THP-1 cells, shRNA = GATA2 knockdown THP-1 cells. Colours in (**a**) are representative of Nile Red fluorescence intensity. Data are representative of (**a**) or quantifies (**b** - **e**) a minimum of N = 3 biological replicates. Data are shown as mean ± SEM. (**b**) ***$p < 0.001$ and ****$p < 0.0001$ compared to Time = 0 hrs by 1-way ANOVA with Sidak multiple comparisons test, (**d**, **e**) #$p < 0.05$ compared to the WT + Control condition and *$p < 0.05$ compared to Control condition in the same cell line by 2-way ANOVA with Tukey's post-hoc test. Scale bar = 10 μm.

We examined cholesterol accumulation by Nile Red staining of live wild type, GATA2 overexpressing and GATA2 knockdown THP-1 macrophages, and we did not find any difference in the rate or degree of cholesterol accumulation between these cells over a period of 8 hrs (**Figure 5.9c**), suggesting that perturbation of GATA2 expression does not significantly affect the rate of cholesterol accumulation in macrophages. We also measured the rate of cholesterol efflux in wild type, GATA2 overexpressing and GATA2 knockdown THP-1 macrophages cultured normally or in the presence of human oxLDL. GATA2 overexpression significantly increased the rate of cholesterol efflux, suggesting that GATA2 expression may be an adaptive response to elevated cholesterol stress. However, this enhanced efflux was not retained in the presence of oxLDL, and unexpectedly, GATA2

knockdown had no effect on the efflux rate (**Figures 5.9d** and **5.9e**). Regardless of the level of GATA2 expression, neither enhanced or impaired cholesterol efflux was observed under hyperlipidemic conditions, suggesting that the enhanced efflux of cholesterol observed in GATA2-overexpressing cells is suppressed by the presence of oxLDL via a non-GATA2 pathway (**Figure 5.9e**).

5.3.6 oxLDL exposure and perturbation of GATA2 expression alters macrophage phagocytic/efferocytic capacity and phagosome/ efferosome maturation

We went on to determine the effect of perturbing GATA2 expression on macrophage efferocytic capacity and efferosome maturation. We first examined the impact of GATA2 overexpression and knockdown on the capacity of macrophages to internalize IgG-coated beads (**Figure 5.10a**). GATA2 has previously been shown to regulate phagocytic activity in rat macrophages in the context of *Pneumocystis carinii* infection, where GATA2 downregulation resulted in decreased macrophage phagocytic capacity.[59] In contrast, in our hands human macrophages overexpressing GATA2 demonstrated significant impairment in their capacity to internalize the IgG-coated beads. This impairment was even more pronounced if the GATA2 overexpressing macrophages were cultured in the presence of oxLDL. Conversely, downregulation of GATA2 expression did not result in any significant impairment of phagocytic capacity and was actually sufficient to rescue the impairment in phagocytosis seen when wild type macrophages were cultured in the presence of oxLDL.

The same trend was observed when we examined the capacity of our macrophages to efferocytose PS-coated beads (**Figure 5.10b**). Culturing wild type macrophages in the presence of oxLDL resulted in a decrease in efferocytic capacity, which is consistent with previously published literature.[69,70] GATA2 overexpressing macrophages showed impaired efferocytotic capacity, regardless of whether they were cultured in the presence of oxLDL. While GATA2 overexpressing macrophages cultured with oxLDL showed slightly decreased efferocytic capacity compared to those cultured under normal conditions, this was not statistically significant. Interestingly, as with phagocytosis, GATA2 knockdown did not impair efferocytosis in macrophages cultured under normal conditions and restored efferocytic capacity in macrophages cultured in the presence of oxLDL. The same

observations held true when we used apoptotic Jurkat cells in place of PS-coated beads and quantified the fraction of individual apoptotic cells internalized by macrophages (**Figure 5.10c**). Efferocytosis of apoptotic cells was markedly reduced both when wild type macrophages were cultured in the presence of oxLDL and by GATA2 overexpression independently of oxLDL levels. Again, no impairment in efferocytosis was observed in GATA2 knockdown macrophages and critically, GATA2 knockdown protected macrophages against the oxLDL-induced loss of apoptotic cell efferocytosis.

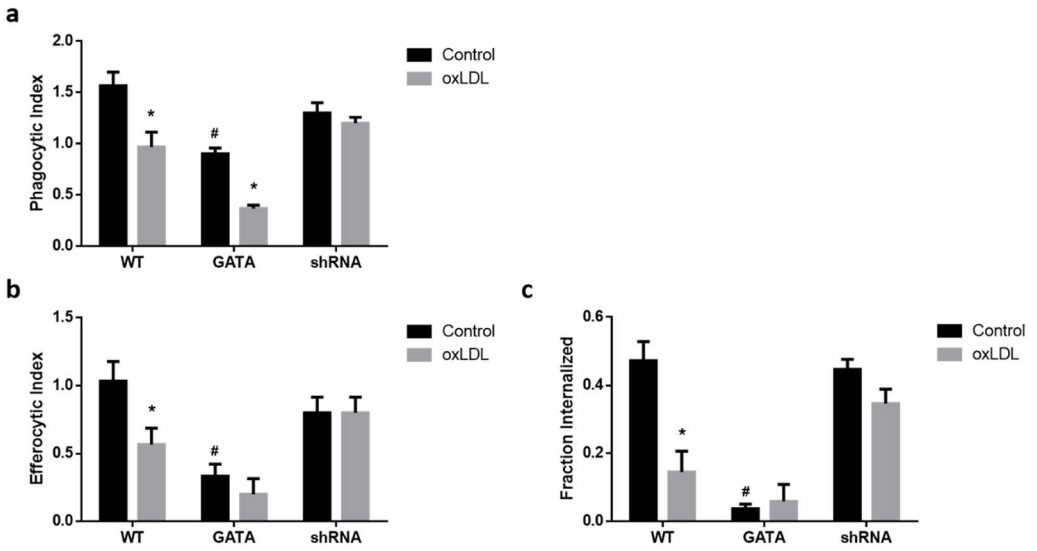

Figure 5.10 GATA2 overexpression impairs macrophage phagocytic and efferocytic capacity.

Phagocytic and efferocytic capacity in THP-1 macrophages with perturbed GATA2 expression grown under normal (Control) or in the presence of human oxLDL (oxLDL) was assessed by phagocytosis and efferocytosis assays using a variety of bead-based phagocytic/efferocytic mimics and apoptotic cells. (**a**) Phagocytic index of THP-1 macrophages incubated for 30 min with IgG-coated 5-μm polystyrene beads was assessed by fluorescence microscopy. (**b**) Efferocytic index of THP-1 macrophages incubated for 60 min with PS-coated 3-μm silica beads was assessed by fluorescence microscopy. (**c**) THP-1 macrophages were co-incubated with fluorescently-labelled apoptotic Jurkat cells for 90 min and the fraction of apoptotic materials internalized by macrophages was assessed by microscopy. WT = wild type THP-1 cells, GATA = GATA2 overexpressing

THP-1 cells, shRNA = GATA2 knockdown THP-1 cells. Data quantifies a minimum of N = 3 biological replicates. Data are shown as mean ± SEM. #$p < 0.05$ compared to the WT + Control condition and *$p < 0.05$ compared to Control condition in the same cell line by 2-way ANOVA with Tukey's post-hoc test.

In addition to efferocytic uptake, proper maturation of the efferosome is equally important for proper processing of apoptotic cells, the avoidance of self-antigen presentation, and the generation of autoimmunity.[71] Therefore, beyond simply assessing efferocytic capacity, we also sought to assess efferosome maturation in THP-1 macrophages with perturbed GATA2 expression. There are multiple mechanisms involved in proper efferosome maturation, including generation of superoxides within the efferosome through the action of NADPH oxidase, efferosome acidification driving by vacuolar ATPases and fusion between efferosomes and lysosomes (reviewed in detail in **Chapter 5.1.3**).

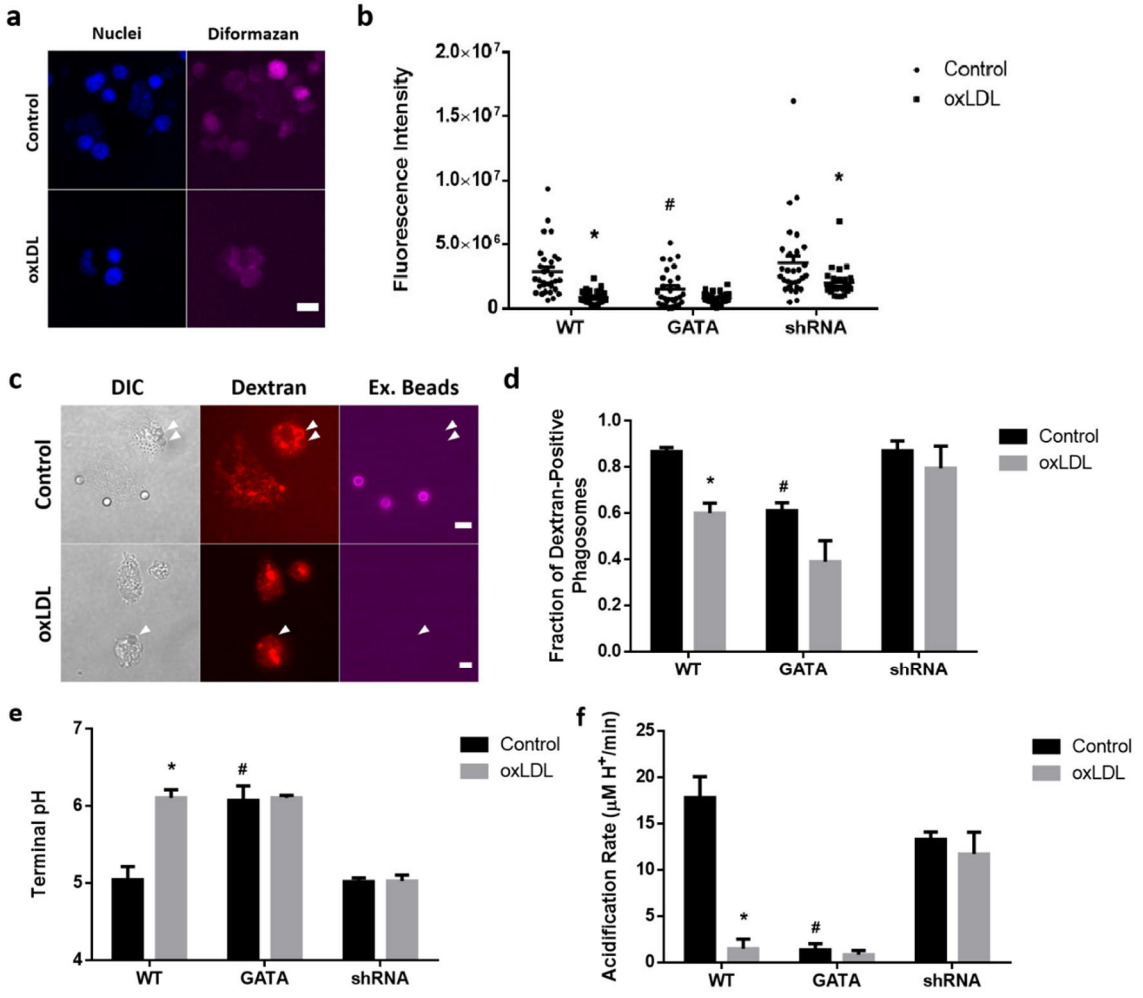

Figure 5.11 GATA2 overexpression impairs macrophage efferosome maturation.

Efferosome maturation in THP-1 macrophages with perturbed GATA2 expression grown under normal (Control) or in the presence of human oxLDL (oxLDL) was assessed using a number of functional assays. (**a**, **b**) Nitro blue tetrazolium assay was used to measure NADPH oxidase activity in THP-1 macrophages. Fluorescence intensity of diformazan deposits was quantified as a measure of superoxide production. (**c**, **d**) Macrophages were pulsed with tetramethylrhodamine-conjugated dextran to label cellular lysosomal compartments and then allowed to internalize IgG-coated beads. Phagolysosomal fusion was monitored by fluorescence microscopy as internalized beads that have accumulated dextran. (**e**, **f**) Phagocytosis assays with pHrodo- and IgG-coated beads were imaged using live cell fluorescence microscopy over a period of 60 min at 1 frame/min to determine

terminal phagosome pH and phagosomal acidification rate for the first five minutes post-complete phagosomal closure respectively. WT = wild type THP-1 cells, GATA = GATA2 overexpressing THP-1 cells, shRNA = GATA2 knockdown THP-1 cells. Images are representative of (**a**, **c**) N =3 biological replicates. Graphs quantify N = 3 biological replicates (**d**-**f**) or 30 individual cells across N = 3 biological replicates (**b**). White arrows indicate beads that have been internalized (**c**). Data are shown as mean ± SEM. #$p < 0.05$ compared to the WT + Control condition and *$p < 0.05$ compared to Control condition in the same cell line by 2-way ANOVA with Tukey's post-hoc test. Scale bar = 10 μm.

To assess NADPH oxidase activity, we allowed macrophages to efferocytose apoptotic Jurkat cells in the presence of nitro blue tetrazolium, which reacts with superoxide radicals to form a fluorescent diformazan precipitate (**Figure 5.11a** and **5.11b**). Macrophages cultured in the presence of oxLDL show reduced NADPH activity, as do GATA2 overexpressing macrophages, even in the absence of oxLDL. GATA2 knockdown does not significantly alter NADPH activity, however, in contrast to what was observed with phagocytic and efferocytic capacity, GATA2 knockdown does not completely rescue the defect in superoxide production in macrophages cultured with oxLDL.

To assess whether phagolysosomal fusion would also be impaired in our model system, we performed a pulse-chase experiment with fluorescently-labelled dextran to assess fusion between lysosomes and phagosomes containing IgG-coated beads (**Figures 5.11c** and **5.11d**). Consistent with the previous observations, we noted a slight but statistically significant decrease in phagolysosomal fusion in macrophages cultured with oxLDL and in GATA2 overexpressing macrophages. In contrast, GATA2 knockdown macrophages did not display any impairment in phagolysosomal fusion and indeed, GATA2 knockdown was sufficient to prevent impaired phagolysosomal fusion in macrophages cultured with oxLDL.

We assessed vacuolar ATPase activity by first assessing the terminal pH of maturing IgG phagosomes (**Figure 5.11e**) following internalization of IgG- and pHrodo-coated beads (as efferosome and phagosome acidification are thought to be driven by the same mechanisms). We observed both a failure to reach an appropriate terminal phagosome pH

in macrophages cultured with oxLDL. The same held true for GATA2 overexpressing macrophages, regardless of whether or not they were cultured in the presence or absence of oxLDL, and again, these impairments were rescued in GATA2 knockdown macrophages.

Since lysosome fusion was impaired (**Figure 5.11d**), it is possible this lack of phagosome acidification was due to poor lysosome fusion rather than decreased vATPase expression. To assess this possibility, we quantified the rate of acidification in the first five minutes following phagosome closure, which is prior to the time of phagosome-lysosome fusion.[72] The same trends were observed in the early acidification rate as were observed with phagosome terminal pH, confirming that oxLDL-driven GATA2 overexpression impairs phagosome acidification, at least in part, through decreased expression of the vATPase (**Figure 5.11f**).

5.3.7 oxLDL exposure but not perturbation of GATA2 expression alters peptide citrullination in macrophages

Amongst the genes found to be upregulated in patient macrophages in our microarray dataset was PADI3, a member of the peptide arginine deaminase (PAD) family of enzymes that catalyze peptide citrullination and which play a central role in the pathogenesis of rheumatoid arthritis.[67,73] There is a well-established connection between rheumatoid arthritis and increased cardiovascular disease risk, with aberrant presentation of self-antigen within the atherosclerotic plaque being a potential driver of autoimmune disease.[74,75] We therefore sought to assess whether peptide citrullination was occurring with the atherosclerotic lesions in our patient aortic punch tissue samples and whether GATA2 drives increased peptide citrullination in the context of atherosclerotic disease.

IHC staining of sectioned patient aortic punch tissue with an AMC antibody demonstrated evidence of peptide citrullination specifically within the aortic intima (**Figure 5.12a**). Experimental evidence shows that macrophages (and monocytes) in patients with rheumatoid arthritis express increased levels of PAD enzymes.[76] We therefore examined PADI3 gene expression levels in both patient and control macrophages and PADI3 levels were found to be significantly increased in patient macrophages (**Figure 5.12b**). As we

have previously demonstrated, oxLDL is a crucial environmental ligand that induces macrophages to become impaired in efferocytic uptake and efferosome maturation. Here, we show that THP-1 macrophages cultured in the presence of oxLDL also showed increased expression of PADI3 as compared to macrophages cultured under control conditions (**Figure 5.12c**). Indeed, we could further demonstrate the exposure of THP-1 macrophages to oxLDL resulted in the generation of citrullinated peptides *in vitro* (**Figure 5.12d**).

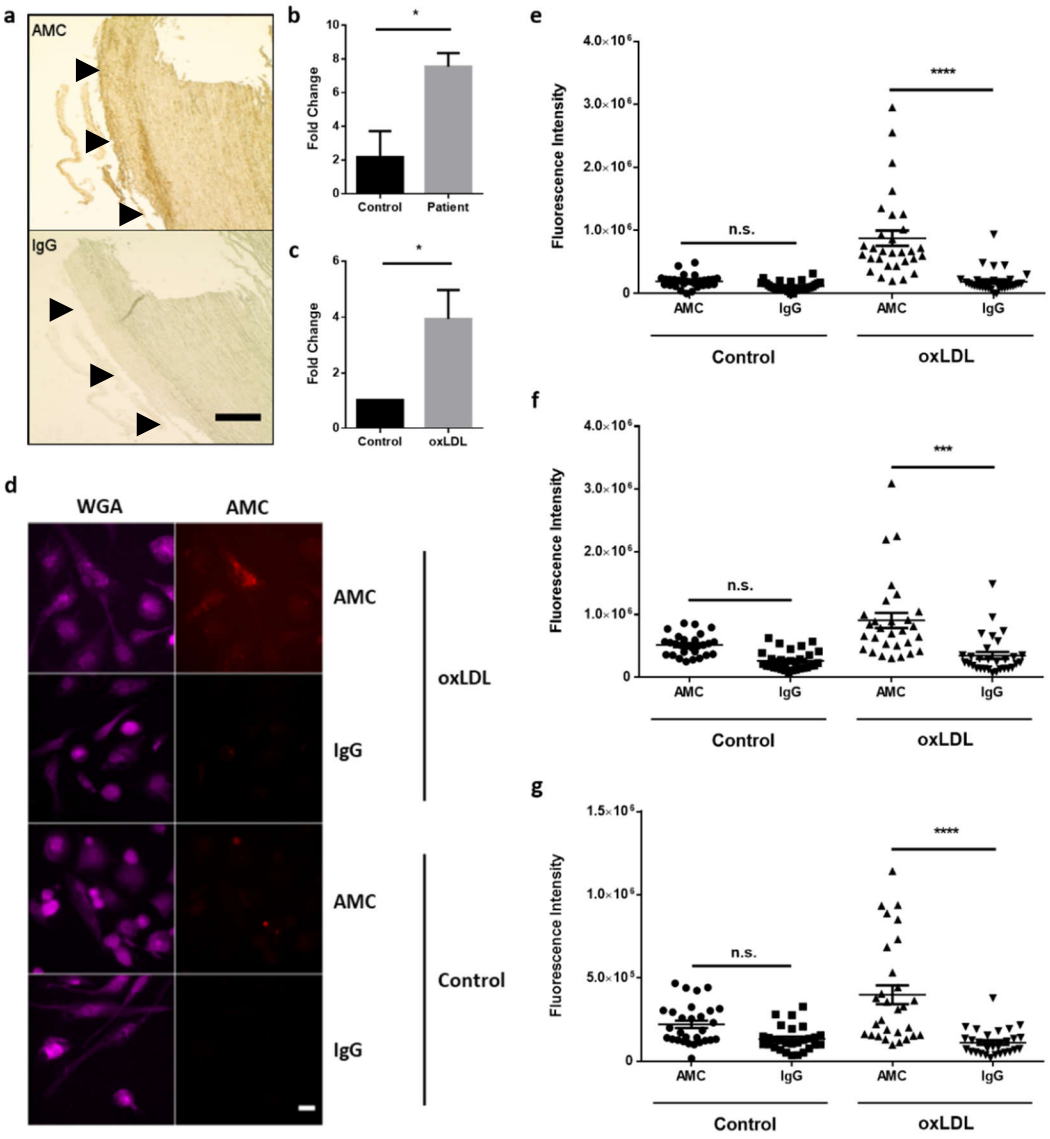

Figure 5.12 oxLDL exposure but not GATA2 expression drives PADI3 expression and peptide citrullination in atherosclerotic macrophages. (on opposite page)

The degree of peptide citrullination and PADI3 enzyme expression was assessed in both patient aortic punch tissues and atherosclerotic THP-1 macrophages. (**a**) FFPE patient aortic punch tissue sections were immunostained for modified citrulline with an AMC antibody (AMC) or an IgG isotype (IgG) as a negative control; AMC = anti-modified citrulline. (**b**, **c**) Quantification of PADI3 expression by RT-qPCR in patient and control macrophages (**b**) and THP-1 macrophages cultured under normal (Control) and hyperlipidemic (oxLDL) conditions (**c**). (**d**) Immunofluorescence staining of THP-1 macrophages cultured for 72 hrs in the presence (oxLDL) or absence (Control) of human oxLDL with an AMC antibody (AMC) or an IgG isotype (IgG) as a negative control. Individual cells are labelled using a AF647-conjugated wheat germ agglutinin (WGA). (**e** – **g**) Immunofluorescence staining of wild type THP-1 macrophages (**e**), GATA2 overexpressing THP-1 macrophages (**f**) and GATA2 knockdown THP-1 macrophages (**f**) cultured under either normal (Control) or hyperlipidemic (oxLDL) conditions using an AMC antibody (AMC) or IgG isotype (IgG) as a negative control. Images are representative of either N = 3 individual patients (**a**) or N = 3 biological replicates (**d**). Graphs are representative of N = 5 individual patients (**b**), N = 3 biological replicates (**c**) or 30 cells across N = 3 biological replicates (**e** – **g**). Data are shown as mean ± SEM. *$p < 0.05$ by unpaired, two-tailed Student's t test (**b**, **c**), ***$p < 0.001$ and ****$p < 0.0001$ by 1-way ANOVA with Tukey's post-hoc test (**e** – **g**). Black arrows indicate the vessel intima. Scale bars = 100 μm (**a**) or 10 μm (**d**).

We then sought to determine the role of perturbed GATA2 expression on oxLDL-induced peptide citrullination in THP-1 macrophages. The degree of peptide citrullination as quantified by immunofluorescence staining of macrophages with the AMC antibody was assessed in wild type THP-1 macrophages (**Figure 5.12e**), GATA2 overexpressing THP-1 macrophages (**Figure 5.12f**) and GATA2 knockdown macrophages (**Figure 5.12g**). In each case, we found that little to no peptide citrullination occurred in the absence of oxLDL regardless of the GATA2 expression level, whereas for cells cultured with oxLDL peptide citrullination was observed at comparable levels regardless of GATA2 expression.

5.3.8 GATA2 overexpression is driven by signaling through ERK and the Src family kinases

We next sought to determine the upstream signaling pathways that contribute to GATA2 upregulation in response to stimulation with oxLDL. There are a number of canonical oxLDL receptors that are expressed on the cell surface of human macrophages, including members of the class A and B scavenger receptors (in particular CD36) and TLR4. CD36 and TLR4 are able to activate a number of distinct downstream signal transduction pathways.[13] Wu *et al.* have shown that stimulation of TLR4 by LPS drives GATA2 upregulation in a MEK/ERK-dependent pathway.[32] This pathway may be specifically inhibited using the small molecule inhibitor U0126.[77] Heit *et al.* have demonstrated that CD36 internalizes ligands through engagement with Src-family kinases (SFK's) and Syk.[78] The small molecule inhibitors protein phosphatase 1 (PP1) and Syk inhibitor (SykI) are small molecule inhibitors of SFK's and Syk respectively.[78,79]

Using these small molecule inhibitors, we inhibited in turn the activity of SFK's (**Figure 5.13a**), MEK/ERK (**Figure 5.13b**) and Syk (**Figure 5.13c**) in THP-1 macrophages cultured with human oxLDL for 72 hrs. Compared to a DMSO-treated control, macrophages treated with PP1 or SykI exhibited significantly impaired GATA2 upregulation in response to oxLDL stimulation. Treatment with U0126 had no effect on GATA2 upregulation. Downstream of these signaling pathways, we did not determine experimentally which transcription factor(s) are involved in oxLDL-driven GATA2 upregulation. However, previous studies have suggested that SP1 is important in driving GATA2 expression. SP1 is phosphorylated downstream of the c-Src/Syk signaling pathway following ligand engagement by CD36.[80,81] Therefore, SP1 is a likely candidate for activating GATA2 transcription in response to oxLDL-driven signaling through the c-Src/Syk pathway downstream of CD36 (**Figure 5.13e**).

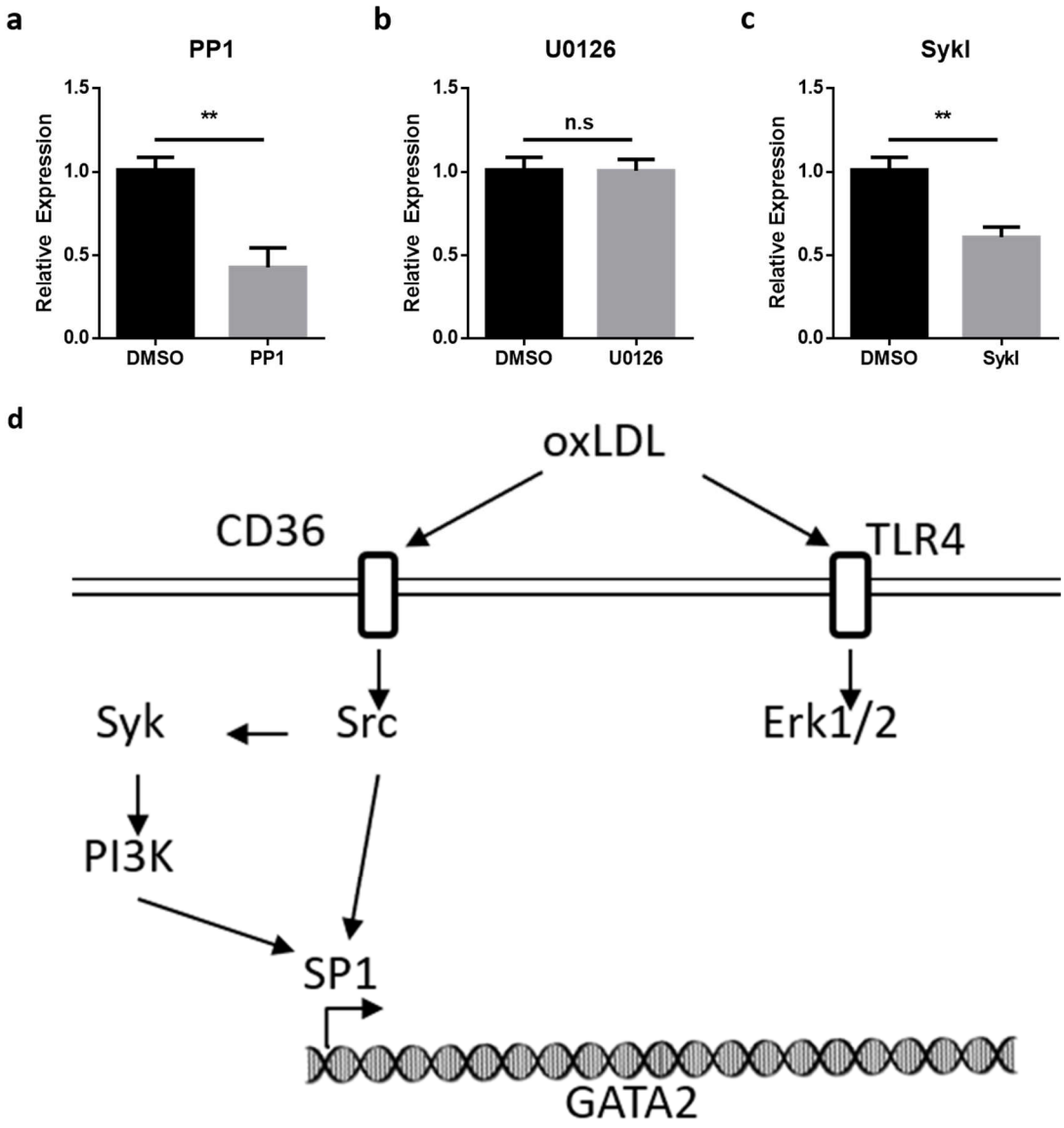

Figure 5.13 oxLDL-induced GATA2 upregulation requires signaling through the Src pathway.

THP-1 macrophages were cultured in the presence of oxLDL for 72 hrs with 200 nM PP1 (**a**), 2 nM U0126 (**b**) or 10 μM SykI (**c**). GATA2 expression in these cells were compared to THP-1 macrophages cultured for 72 hrs with oxLDL and a DMSO vehicle control (Veh). (**d**) Schematic of oxLDL-induced GATA2 upregulation in human macrophages. Data are shown as mean ± SEM and quantify N = 3 biological replicates. *$p < 0.05$ by unpaired, two-tailed Student's t test.

5.3.9 GATA2 trends toward being elevated in *Ldlr*$^{-/-}$ mice fed a high-fat diet

Finally, we examined *Gata2* expression levels in the aorta of *Ldlr*$^{-/-}$ mice fed high-fat, high-cholesterol (HFHC) or standard chow diet for 12 weeks by RT-qPCR (**Figure 5.14**). The expression of Gata2 was consistently low in the plaques of *Ldlr*$^{-/-}$ mice fed a normal diet, but underwent a highly heterogeneous response in response to a high-fat diet. These data suggest that GATA2 may be upregulated in *Ldlr*$^{-/-}$ mice in response to a high-fat diet, but this protocol requires further refinement before conclusive data can be generated.

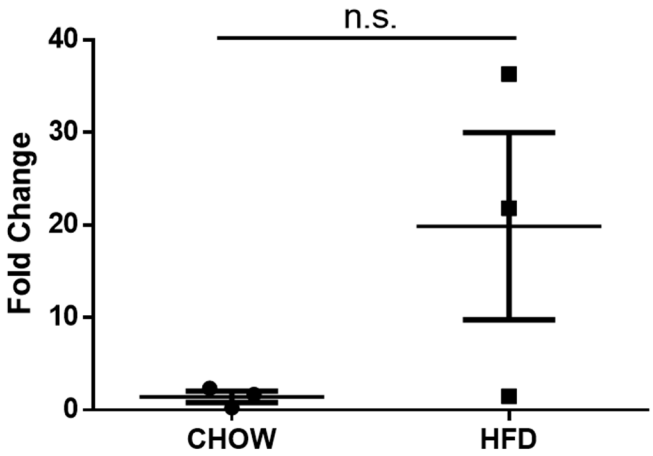

Figure 5.14 Gata2 expression trends towards being increased in high-fat diet atherosclerotic mice.

Ldlr$^{-/-}$ knockout mice were maintained for 12 weeks on a chow (CHOW) or high-fat (HDF) diet. At 12 weeks, mice were sacrificed, and their aortas dissected for use in RT-qPCR studies that measured Gata2 expression. Data summarize N = 3 mice in each group and are presented as mean ± SEM. The difference in Gata2 expression was found to not be statistically significant by a two-tailed, unpaired Student's t test.

5.4 Discussion

In this Chapter, we examined the impact of perturbing GATA2 expression on macrophage cholesterol handling, peptide citrullination and efferocytosis/efferosome maturation using an *in vitro* model of atherosclerotic macrophages. We found that GATA2 overexpression was sufficient to impair macrophage efferocytotic uptake and efferosome maturation, even in the absence of pro-atherogenic stimuli. Importantly, knockdown of GATA2 expression using an shRNA normalized efferocytosis and efferosome maturation when macrophages were exposed to oxLDL. Taken together, these data indicate that GATA2 acts as a master regulatory factor that appears to be required for oxLDL-mediated impairment of macrophage efferocytic uptake and efferosome maturation. However, we did not find any effect of GATA2 perturbation on either cholesterol handling nor peptide citrullination, suggesting that the effect of GATA2 is specific to macrophage apoptotic uptake and degradation.

Our most interesting finding is the impact of perturbing GATA2 expression on efferocytic uptake of apoptotic cells and on subsequent efferosome maturation and processing of apoptotic cargo. We are able to replicate the finding that macrophage efferocytosis is impaired following exposure to oxLDL, but our data show that this effect appears to be dependent on the upregulation of GATA2 in response to this atherogenic stimulus. Indeed, we find that when GATA2 expression is abrogated using a shRNA, macrophages retain full efferocytic capacity. To date, mechanisms underlying impaired macrophage efferocytic capacity in atherosclerosis remain poorly defined. Cai *et al.* showed that ADAM17-mediated cleavage of a key efferocytic receptor, MerTK, results in increased plaque necrotic core size in *Ldlr*$^{-/-}$ mice.[82] Our finding that oxLDL-mediated GATA2 upregulation leads to impaired efferocytic capacity may represent an alternate mechanism driving defective efferocytosis in atherosclerotic plaques. Importantly, we have also found that perturbation of GATA2 expression had profound impacts on efferosome maturation in addition to efferocytic capacity. Our data show that GATA2 upregulation drives impairment in efferosomal NADPH oxidase activity and superoxide generation, efferosomal acidification and potentially interferes with efficient efferosome-lysosome fusion. Efficient efferosomal maturation and processing of cargo is essential for

macrophages in maintaining a rapid rate of efferocytosis, and impaired efferosomal maturation may partially explain how efferocytosis becomes defective in the course of atherosclerotic disease. Impaired apoptotic cargo degradation may also result in the generation of inflammation and autoimmunity. A number of investigators have identified rapid cargo degradation as a key mechanism in limiting antigen presentation. For example, Erwig *et al.* found that efferosomal maturation following apoptotic cell uptake by macrophages proceeded much faster than following uptake of IgG-coated pathogen mimics, while Yates *et al.* observed decreased phagosome degradative capacity following macrophage activation.[83,84] Impaired efferosomal maturation, in addition to interfering with efficient apoptotic cell clearance, may also be a potential mechanism driving autoantigen presentation and autoimmunity in atherosclerosis.

Another fascinating observation from our microarray dataset was the upregulation of the PADI3 enzyme in patient macrophages. Here, we demonstrate through IHC that peptide citrullination is present within the early atherosclerotic plaque. This is in agreement with the findings of Sokolove *et al.*, who identified the presence of citrullinated fibrinogen within human atherosclerotic plaques by Western blot.[85] While Sokolove *et al.* suggested that intra-plaque citrullination is driven by PADI4,[85] our data implicates PADI3 as another player in this process. We demonstrated by RT-qPCR that PADI3 expression is upregulated within both atherosclerotic lesion-resident macrophages and in macrophages treated *in vitro* with oxLDL. While we did not find strong evidence that GATA2 affects the expression of PADI3 or the degree of peptide citrullination that occurs in atherosclerotic macrophages, exposure of macrophages to oxLDL is sufficient to induce citrullination *in vitro* regardless of the level of GATA2 expression. Increased risk of cardiovascular disease in patients with rheumatoid arthritis has been well established, thought to be the result of elevated inflammation in these patients.[75,86] However, there is some evidence that the relationship is a reciprocal one, with atherosclerosis driving the genesis and/or progression of rheumatoid arthritis and other forms of autoimmune disease.[87,88] Autoantibodies against oxLDL, HSP60 and ApoB100 (the major lipoprotein component of LDL) have been identified in patients with atherosclerosis.[87] Furthermore, various T cell subsets have been isolated from human atherosclerotic plaques, with Th1 cells being the predominant type.[88] Whether these lesion-resident T cells also recognize and respond to the presence of

citrullinated peptides remains to be shown, but such a mechanism would help explain the high degree of coincidence between rheumatoid arthritis and atherosclerosis.

There is some evidence that GATA2 could be involved in regulation of cholesterol handling in macrophages. Cheng *et al.* showed that leptin-mediated activation of GATA2 expression and DNA binding resulted in the downregulation of the transcription factor PPARγ.[89] PPARγ plays a number of important roles in the context of atherosclerosis. First, it is a major driver of anti-inflammatory activation and PPARγ agonists have been shown to demonstrate some protective effects in animal models of atherosclerosis through restraining inflammation within the atherosclerotic plaque.[90,91] Simultaneously, Lee *et al.* have demonstrated that activation of PPARγ results in upregulation of ABCA1 and increases the rate of cellular cholesterol efflux.[92] However, our data indicate that while GATA2 expression does enhance cholesterol efflux, this effect is lost in the presence of oxLDL and therefore cannot serve a protective function in the context of atherosclerosis. This could be a result of the potent activation of multiple pathways related to cholesterol metabolism as a result of oxLDL exposure that are antagonistic to either GATA2 expression or function. These results are interesting, however, in that they suggest that GATA2 may be upregulated by macrophages in order to adapt to cellular stress, and that the negative impacts on phagocytosis and efferocytosis are an unwanted side-effect of this adaptive process. However, further work remains to be done in dissecting out the specific role of GATA2 in cholesterol handling during atherogenesis in order to fully explore this possibility.

We have begun to define the signaling pathways upstream of oxLDL-induced GATA2 upregulation. Inhibition of either Src family kinases or Syk results in decreased levels of GATA2 expression in response to oxLDL. Src and Syk are recruited downstream of ligand engagement by CD36, a class B scavenger receptor that plays a crucial role in recognition and internalization of oxLDL in macrophages.[78,93] CD36 is activated as a multi-unit complex along with β_1 and β_2 integrins along with CD9 and CD81. This complex phosphorylates the signaling adaptor FcRγ, which, via its phosphorylated ITAM motifs and active SFKs, is capable of recruiting and activating Syk.[78] While less well understood, the Toll-like receptors TLR2 and TLR4 are also known to be activated by oxLDL, and to

activate a similar Src/Syk pathway. The downstream targets of Src and Syk in the context of CD36 and TLR activation are poorly understood. However, a few recent studies of novel therapeutic agents in leukemia have shed light on one potential regulatory pathway that can drive GATA2 activation.[94,95] Yang *et al.* have shown that inhibition of GATA2 by the proteasome inhibitor K-7174 results in sensitization of acute myeloid leukemia cells to chemotherapy.[94] K-7174 is known to exert its activity on GATA2 via degradation of the transcription factor Sp1, which functions as a transactivator of class I histone deacetylases and promotes transcriptional activation of GATA2.[95] Sp1 may be activated by Src family kinases or PI3K downstream of Syk signaling.[80,96] Therefore, we propose a model whereby activation of CD36 by oxLDL results in Src and Syk signaling, which activates Sp1 and drives transcriptional activation and upregulation of GATA2. Whether Sp1 is able to directly bind upstream of GATA2 and drive transcription or if it functions through its chromosomal remodeling activity to allow other transcription factors to cooperatively drive GATA2 expression remains to be determined.

To study the impact of GATA2 on efferocytosis, peptide citrullination and cholesterol handling, we established an *in vitro* cell culture model of atherosclerotic macrophages by incubating THP-1 cells with human oxLDL. We show that after 72 hrs of culture in the presence of oxLDL, THP-1 macrophages adopt a distinctive foam cell-like appearance, which is accompanied by upregulation of GATA2 expression. Culture of macrophages with oxLDL or another modified LDL is a well-established method of generating foam cells *in vitro*.[10] While the precise type and concentration of lipoprotein as well as the culture time varies between different investigators, multiple groups have shown that oxLDL-treated macrophages accumulate cholesterol and form lipid droplets in their cytoplasm.[14,97,98] Cholesterol loading of macrophage also induces production of proinflammatory cytokines, including TNFα, IL-6 and IL-1β, as well as ER stress and the unfolded protein response.[16,99] While we did not examine generation of proinflammatory cytokines and our *in vitro* system is certainly an oversimplification of the actual atherosclerotic plaque microenvironment, we were able to observe significant cholesterol accumulation and lipid droplet formation in our THP-1 macrophages. However, we are the first to report upregulation of GATA2 in response to cholesterol accumulation in both THP-1 macrophage-like cells and primary monocyte-derived human macrophages. This

suggests that within the atherosclerotic plaque microenvironment, endogenous modified lipoproteins such as oxLDL are sufficient to induce GATA2 upregulation.

In summary, we have identified the hematopoietic transcription factor GATA2 as a master regulator of defective efferocytosis in atherosclerotic macrophages. GATA2 upregulation impairs both the efferocytic uptake of apoptotic cells and multiple stages of the subsequent catabolic process which degrades the efferosomal cargo. This impairment in efferosomal maturation represents a previously unrecognized mechanism that not only drives defective apoptotic cell clearance in atherosclerosis but may also contribute to autoantigen presentation and the generation of inflammation and autoimmunity within the atherosclerotic plaque. Therefore, GATA2 could prove to be an important therapeutic target for enhancing efferocytosis within the atherosclerotic plaque, promoting inflammation resolution, and limiting the development of the necrotic core of the plaque to reduce plaque vulnerability in the setting of advanced atherosclerotic disease. In the aftermath of the CANTOS trial demonstrating a role for therapies targeting the inflammatory component of atherosclerotic disease,[100] targeting inflammation through improving efferocytosis within the plaque could hold the potential to address the unmet residual inflammatory risk of atherosclerotic disease.

5.5 References

1. Moore KJ, Tabas I. Macrophages in the pathogenesis of atherosclerosis. *Cell*. 2011;145(3):341-355. doi:10.1016/j.cell.2011.04.005

2. Tabas I. 2016 Russell Ross Memorial Lecture in Vascular Biology. *Arterioscler Thromb Vasc Biol*. 2016:ATVBAHA.116.308036. doi:10.1161/ATVBAHA.116.308036

3. Moore KJ, Sheedy FJ, Fisher E a. Macrophages in atherosclerosis: a dynamic balance. *Nat Rev Immunol*. 2013;13(10):709-721. doi:10.1038/nri3520

4. Wada Y, Sugiyama A, Kohro T, et al. In vitro model of atherosclerosis using

coculture of arterial wall cells and macrophage. *Yonsei Med J*. 2000;41(6):740-755.

5. Dorweiler B, Torzewski M, Dahm M, et al. A novel in vitro model for the study of plaque development in atherosclerosis. *Thromb Haemost*. 2006;95:182-189. doi:10.1160/TH05

6. Zuniga MC, White SLP, Zhou W. Design and utilization of macrophage and vascular smooth muscle cell co-culture systems in atherosclerotic cardiovascular disease investigation. *Vasc Med (United Kingdom)*. 2014;19(5):394-406. doi:10.1177/1358863X14550542

7. Yu P, Xiong T, Tenedero CB, et al. Rosuvastatin Reduces Aortic Sinus and Coronary Artery Atherosclerosis in SR-B1 (Scavenger Receptor Class B Type 1)/ApoE (Apolipoprotein E) Double Knockout Mice Independently of Plasma Cholesterol Lowering. *Arterioscler Thromb Vasc Biol*. 2017;1:ATVBAHA.117.305140. doi:10.1161/ATVBAHA.117.305140

8. Kanters E, Hofker MH, De MPJ, et al. Inhibition of NF- k B activation in macrophages increases atherosclerosis in LDL receptor – deficient mice Find the latest version : Inhibition of NF- κ B activation in macrophages increases atherosclerosis in LDL receptor – deficient mice. *J Clin Invest*. 2003;112(8):1176-1185. doi:10.1172/JCI200318580.Introduction

9. Libby P, Ridker PM, Hansson GK. Progress and challenges in translating the biology of atherosclerosis. *Nature*. 2011;473(7347):317-325. doi:10.1038/nature10146

10. Lara-Guzmán OJ, Gil-Izquierdo Á, Medina S, et al. Oxidized LDL triggers changes in oxidative stress and inflammatory biomarkers in human macrophages. *Redox Biol*. 2018;15(September 2017):1-11. doi:10.1016/j.redox.2017.11.017

11. Chistiakov DA, Bobryshev Y V., Orekhov AN. Macrophage-mediated cholesterol handling in atherosclerosis. *J Cell Mol Med*. 2015;XX(X):n/a-n/a.

doi:10.1111/jcmm.12689

12. Li Y, Seitz H, Cui D, et al. Cholesterol-induced Apoptotic Macrophages Elicit an Inflammatory Response in Phagocytes , Which Is Partially Attenuated by the Mer Receptor *. *J Bacteriol*. 2006;281(10):6707-6717. doi:10.1074/jbc.M510579200

13. Miller YI, Viriyakosol S, Binder CJ, Feramisco JR, Kirkland TN, Witztum JL. Minimally modified LDL binds to CD14, induces macrophage spreading via TLR4/MD-2, and inhibits phagocytosis of apoptotic cells. *J Biol Chem*. 2003;278(3):1561-1568. doi:10.1074/jbc.M209634200

14. Seo J-W, Yang E-J, Yoo K-H, Choi I-H. Macrophage Differentiation from Monocytes Is Influenced by the Lipid Oxidation Degree of Low Density Lipoprotein. *Mediators Inflamm*. 2015;2015:1-10. doi:10.1155/2015/235797

15. Kim K, Shim D, Lee JS, et al. Transcriptome Analysis Reveals Nonfoamy Rather Than Foamy Plaque Macrophages Are Proinflammatory in Atherosclerotic Murine Models. *Circ Res*. 2018;123(10):1127-1142. doi:10.1161/CIRCRESAHA.118.312804

16. Li Y, Schwabe RF, DeVries-Seimon T, et al. Free cholesterol-loaded macrophages are an abundant source of tumor necrosis factor-α and interleukin-6: Model of NF-κB- and map kinase-dependent inflammation in advanced atherosclerosis. *J Biol Chem*. 2005;280(23):21763-21772. doi:10.1074/jbc.M501759200

17. Doran AC, Ozcan L, Cai B, et al. CAMKIIγ suppresses an efferocytosis pathway in macrophages and promotes atherosclerotic plaque necrosis. *J Clin Invest*. 2017;(16):1-15. doi:10.1172/JCI94735

18. Duewell P, Kono H, Rayner KJ, et al. NLRP3 inflammasomes are required for atherogenesis and activated by cholesterol crystals. *Nature*. 2010;464(7293):1357-1361. doi:10.1038/nature08938

19. Roshan M, Tambo A, Pace N. The role of TLR2, TLR4, and TLR9 in the pathogenesis of atherosclerosis. *Int J Inflam*. 2016:1-11.

doi:10.1056/NEJM197608192950805

20. Tremblay M, Sanchez-ferras O, Bouchard M. GATA transcription factors in development and disease. *Development*. 2018;145:1-20. doi:10.1242/dev.164384

21. Lentjes MH, Niessen HE, Akiyama Y, de Bruïne AP, Melotte V, van Engeland M. The emerging role of GATA transcription factors in development and disease. *Expert Rev Mol Med*. 2016;18(May):1-15. doi:10.1017/erm.2016.2

22. Trainor CD, Ghirlando R, Simpson MA. GATA zinc finger interactions modulate DNA binding and transactivation. *J Biol Chem*. 2000;275(36):28157-28166. doi:10.1074/jbc.M000020200

23. Bresnick EH, Katsumura KR, Lee HY, Johnson KD, Perkins AS. Master regulatory GATA transcription factors: Mechanistic principles and emerging links to hematologic malignancies. *Nucleic Acids Res*. 2012;40(13):5819-5831. doi:10.1093/nar/gks281

24. Campanella JJ, Bitincka L, Smalley J. MatGAT: An application that generates similarity/identity matrices using protein or DNA sequences. *BMC Bioinformatics*. 2003;4:1-4. doi:10.1186/1471-2105-4-29

25. Zhang S-J, Ma L-Y, Huang Q-H, et al. Gain-of-function mutation of GATA-2 in acute myeloid transformation of chronic myeloid leukemia. *Proc Natl Acad Sci*. 2008;105(6):2076-2081. doi:10.1073/pnas.0711824105

26. Connelly JJ, Wang T, Cox JE, et al. GATA2 is associated with familial early-onset coronary artery disease. *PLoS Genet*. 2006;2(8):1265-1273. doi:10.1371/journal.pgen.0020139

27. Muiya NP, Wakil S, Al-Najai M, et al. A study of the role of GATA2 gene polymorphism in coronary artery disease risk traits. *Gene*. 2014;544(2):152-158. doi:10.1016/j.gene.2014.04.064

28. Cheng M, An S, Li J. CDKN2B-AS may indirectly regulate coronary artery

disease-associated genes via targeting miR-92a. *Gene*. 2017;629(February):101-107. doi:10.1016/j.gene.2017.07.070

29. Schober A, Weber C. Mechanisms of MicroRNAs in Atherosclerosis. *Annu Rev Pathol Mech Dis*. 2016;11(1):583-616. doi:10.1146/annurev-pathol-012615-044135

30. Qiu C, Wang Y, Zhao H, et al. The critical role of SENP1-mediated GATA2 deSUMOylation in promoting endothelial activation in graft arteriosclerosis. *Nat Commun*. 2017;8:1-15. doi:10.1038/ncomms15426

31. Yang Y, Sun D, Zhou J, et al. LPS expands MDSCs by inhibiting apoptosis through the regulation of the GATA2/let-7e axis. *Immunol Cell Biol*. 2018. doi:10.1111/imcb.12204

32. Wu T, Tai Y, Cherng Y, et al. GATA-2 Transduces LPS-Induced il-1β Gene Expression in Macrophages via a Toll-Like Receptor 4 / MD88 / MAPK-Dependent Mechanism. *PLoS One*. 2013;8(8):1-10. doi:10.1371/journal.pone.0072404

33. Lim KC, Hosoya T, Brandt W, et al. Conditional Gata2 inactivation results in HSC loss and lymphatic mispatterning. *J Clin Invest*. 2012;122(10):3705-3717. doi:10.1172/JCI61619

34. Kazenwadel J, Scott HS, Harvey NL, et al. GATA2 is required for lymphatic vessel valve development and maintenance. *J Clin Invest*. 2015;125(8):2979-2994. doi:10.1172/JCI78888.prior

35. Shih AH, Jiang Y, Meydan C, et al. Mutational cooperativity linked to combinatorial epigenetic gain of function in acute myeloid leukemia. *Cancer Cell*. 2015;27(4):502-515. doi:10.1016/j.ccell.2015.03.009

36. Rae W, Ward D, Mattocks CJ, et al. Autoimmunity/inflammation in a monogenic primary immunodeficiency cohort. *Clin Transl Immunol*. 2017;6(9):e155. doi:10.1038/cti.2017.38

37. Spinner MA, Sanchez LA, Hsu AP, et al. GATA2 deficiency: A protean disorder of hematopoiesis, lymphatics, and immunity. *Blood*. 2014;123(6):809-821. doi:10.1182/blood-2013-07-515528

38. Walsh JC, DeKoter RP, Lee HJ, et al. Cooperative and antagonistic interplay between PU.1 and GATA-2 in the specification of myeloid cell fates. *Immunity*. 2002;17(5):665-676. doi:10.1016/S1074-7613(02)00452-1

39. Katsumura KR, Ong IM, DeVilbiss AW, Sanalkumar R, Bresnick EH. GATA factor-dependent positive-feedbak circuit in acute myeloid leukemia cells. *Cell Rep*. 2016;16(9):2428-2441. doi:10.1016/j.cogdev.2010.08.003.Personal

40. Luesink M, Hollink IHIM, van der Velden VHJ, et al. High GATA2 expression is a poor prognostic marker in pediatric acute myeloid leukemia. *Blood*. 2012;120(10):2064-2075.

41. Tabas I. Macrophage death and defective inflammation resolution in atherosclerosis. *Nat Rev Immunol*. 2009;10(1):36-46. doi:10.1038/nri2675

42. Henson PM. Cell Removal : Efferocytosis. *Annu Rev Cell Dev Biol*. 2017;33:1-18.

43. Cai B, Kasikara C, Doran AC, Ramakrishnan R, Birge RB, Tabas I. MerTK signaling in macrophages promotes the synthesis of inflammation resolution mediators by suppressing CaMKII activity. 2018;3721(September).

44. Thorp E, Cui D, Schrijvers DM, Kuriakose G, Tabas I. Mertk receptor mutation reduces efferocytosis efficiency and promotes apoptotic cell accumulation and plaque necrosis in atherosclerotic lesions of apoe-/- mice. *Arterioscler Thromb Vasc Biol*. 2008;28(8):1421-1428. doi:10.1161/ATVBAHA.108.167197

45. Kinchen JM, Ravichandran KS. Phagosome maturation: going through the acid test. *Nat Rev Mol Cell Biol*. 2008;9(10):781-795. doi:10.1038/nrm2515

46. Schlam D, Bohdanowicz M, Chatilialoglu A, et al. Diacylglycerol kinases terminate diacylglycerol signaling during the respiratory burst leading to

heterogeneous phagosomal NADPH oxidase activation. *J Biol Chem*. 2013;288(32):23090-23104. doi:10.1074/jbc.M113.457606

47. Nunes P, Demaurex N, Dinauer MC. Regulation of the NADPH oxidase and associated ion fluxes during phagocytosis. *Traffic*. 2013;14(11):1118-1131. doi:10.1111/tra.12115

48. Canton J, Khezri R, Glogauer M, Grinstein S. Contrasting phagosome pH regulation and maturation in human M1 and M2 macrophages. *Mol Biol Cell*. 2014;25(21):3330-3341. doi:10.1091/mbc.E14-05-0967

49. Panday A, Sahoo MK, Osorio D, Batra S. NADPH oxidases: An overview from structure to innate immunity-associated pathologies. *Cell Mol Immunol*. 2015;12(1):5-23. doi:10.1038/cmi.2014.89

50. Bagaitkar J, Huang J, Zeng MY, et al. NADPH oxidase activation regulates apoptotic neutrophil clearance by murine macrophages. *Blood*. 2018. doi:10.1104/pp.111.188953

51. Flannagan RS, Jaumouillé V, Grinstein S. The Cell Biology of Phagocytosis. *Annu Rev Pathol Mech Dis*. 2011;7(1):61-98. doi:10.1146/annurev-pathol-011811-132445

52. Rupper A, Grove B, Cardelli J. Rab7 regulates phagosome maturation in Dictyostelium. *J Cell Sci*. 2001;114(13):2449-2460.

53. Johnson DE, Ostrowski P, Jaumouillé V, Grinstein S. The position of lysosomes within the cell determines their luminal pH. *J Cell Biol*. 2016;212(6):677-692. doi:10.1083/jcb.201507112

54. Huynh KK, Gershenzon E, Grinstein S. Cholesterol accumulation by macrophages impairs phagosome maturation. *J Biol Chem*. 2008;283(51):35745-35755. doi:10.1074/jbc.M806232200

55. Fairn GD, Grinstein S. How nascent phagosomes mature to become

phagolysosomes. *Trends Immunol*. 2012;33(8):397-405. doi:10.1016/j.it.2012.03.003

56. Harrison RE, Bucci C, Vieira O V, Schroer T a, Grinstein S. Phagosomes fuse with late endosomes and/or lysosomes by extension of membrane protrusions along microtubules: role of Rab7 and RILP. *Mol Cell Biol*. 2003;23(18):6494-6506. doi:10.1128/MCB.23.18.6494

57. Green DR, Oguin TH, Martinez J. The clearance of dying cells: table for two. *Cell Death Differ*. 2016;23(6):915-926. doi:10.1038/cdd.2015.172

58. Jaiswal S, Natarajan P, Silver AJ, et al. Clonal Hematopoiesis and Risk of Atherosclerotic Cardiovascular Disease. *N Engl J Med*. 2017;377(2):111-121. doi:10.1056/NEJMoa1701719

59. Lasbury ME, Tang X, Durant PJ, Lee C. Effect of Transcription Factor GATA-2 on Phagocytic Activity of Alveolar Macrophages from. *Infect Immun*. 2003;71(9):4943-4952. doi:10.1128/IAI.71.9.4943

60. Sankaranarayanan S, Kellner-Weibel G, de la Llera-Moya M, et al. A sensitive assay for ABCA1-mediated cholesterol efflux using BODIPY-cholesterol. *J Lipid Res*. 2011;52(12):2332-2340. doi:10.1194/jlr.D018051

61. Trinh LA, McCutchen MD, Bonner-Fraser M, Fraser SE, Bumm LA, McCauley DW. Fluorescent in situ hybridization employing the conventional NBT/BCIP chromogenic stain. *Biotechniques*. 2007;42(6):756-759. doi:10.2144/000112476

62. Flannagan RS, Heit B, Heinrichs DE. Intracellular replication of Staphylococcus aureus in mature phagolysosomes in macrophages precedes host cell death, and bacterial escape and dissemination. *Cell Microbiol*. 2016;18(4):514-535. doi:10.1111/cmi.12527

63. Taruc K, Yin C, Wootton DG, Heit B. Quantification of Efferocytosis by Single-cell Fluorescence Microscopy. *J Vis Exp*. 2018;(138):1-12. doi:10.3791/58149

64. Evans AL, Blackburn JWD, Yin C, Heit B. Quantitative efferocytosis assays. *Methods Mol Biol*. 2017;1519:25-41. doi:10.1007/978-1-4939-6581-6

65. Schneider CA, Rasband WS, Eliceiri KW. NIH Image to ImageJ: 25 years of image analysis. *Nat Methods*. 2012;9(7):671-675. doi:10.1038/nmeth.2089

66. Schindelin J, Arganda-Carreras I, Frise E, et al. Fiji: an open-source platform for biological-image analysis. *Nat Methods*. 2012;9(7):676-682. doi:10.1038/nmeth.2019

67. Vossenaar ER, Nijenhuis S, Helsen MMA, et al. Citrullination of synovial proteins in murine models of rheumatoid arthritis. *Arthritis Rheum*. 2003;48(9):2489-2500. doi:10.1002/art.11229

68. Allahverdian S, Chehroudi AC, McManus BM, Abraham T, Francis GA. Contribution of intimal smooth muscle cells to cholesterol accumulation and macrophage-like cells in human atherosclerosis. *Circulation*. 2014;129(15):1551-1559. doi:10.1161/CIRCULATIONAHA.113.005015

69. Yurdagul A, Doran AC, Cai B, Fredman G, Tabas IA. Mechanisms and Consequences of Defective Efferocytosis in Atherosclerosis. 2017;4(January):1-10. doi:10.3389/fcvm.2017.00086

70. Cai B, Thorp EB, Doran AC, et al. MerTK receptor cleavage promotes plaque necrosis and defective resolution in atherosclerosis. *J Clin Invest*. 2017:1-5. doi:10.1172/JCI90520

71. Blander JM, Medzhitov R. On regulation of phagosome maturation and antigen presentation. *Nat Immunol*. 2006;7(10):1029-1035. doi:10.1038/ni1006-1029

72. Yin C, Kim Y, Argintaru D, Heit B. Rab17 mediates differential antigen sorting following efferocytosis and phagocytosis. *Cell Death Dis*. 2016;7(12):e2529-12. doi:10.1038/cddis.2016.431

73. Olivares-Martínez E, Hernández-Ramírez DF, Núñez-Álvarez CA, Cabral AR,

Llorente L. The amount of citrullinated proteins in synovial tissue is related to serum anti-cyclic citrullinated peptide (anti-CCP) antibody levels. *Clin Rheumatol*. 2016;35(1):55-61. doi:10.1007/s10067-015-3047-2

74. Wade NS, Major AS. The problem of accelerated atherosclerosis in systemic lupus erythematosus: insights into a complex co-morbidity. *Thromb Haemost*. 2011;106(5):849-857. doi:10.1016/j.biotechadv.2011.08.021.Secreted

75. Crowson CS, Liao KP, Davis JM, et al. Rheumatoid arthritis and cardiovascular risk. *Am Heart J*. 2013;166:622-628. doi:10.1016/j.ahj.2013.07.010

76. Vossenaar ER, Radstake TRD, Van Der Heijden A, et al. Expression and activity of citrullinating peptidylarginine deiminase enzymes in monocytes and macrophages. *Ann Rheum Dis*. 2004;63(4):373-381. doi:10.1136/ard.2003.012211

77. An D, Hao F, Hu C, Kong W, Xu X, Cui M-Z. JNK1 Mediates Lipopolysaccharide-Induced CD14 and SR-AI Expression and Macrophage Foam Cell Formation. *Front Physiol*. 2017;8(January):1075. doi:10.3389/fphys.2017.01075

78. Heit B, Kim H, Cosío G, et al. Multimolecular signaling complexes enable syk-mediated signaling of CD36 internalization. *Dev Cell*. 2013;24(4):372-383. doi:10.1016/j.devcel.2013.01.007

79. Mócsai A, Ligeti E, Lowell CA, Berton G. Adhesion-dependent degranulation of neutrophils requires the Src family kinases Fgr and Hck. *J Immunol*. 1999;162(2):1120-1126.

80. Liu ZM, Huang HS. As2O3-induced c-Src/EGFR/ERK signaling is via Sp1 binding sites to stimulate p21WAF1/CIP1 expression in human epidermoid carcinoma A431 cells. *Cell Signal*. 2006;18(2):244-255. doi:10.1016/j.cellsig.2005.04.006

81. Merchant JL, Du M, Todisco A. Sp1 phosphorylation by Erk 2 stimulates DNA binding. *Biochem Biophys Res Commun*. 1999;254(2):454-461.

doi:10.1006/bbrc.1998.9964

82. Cai B, Thorp EB, Doran AC, et al. MerTK receptor cleavage promotes plaque necrosis and defective resolution in atherosclerosis. *J Clini*. 2017;127(2):564-568. doi:10.1172/JCI90520.We

83. Erwig L-P, McPhilips KA, Wynes MW, Ivetic A, Ridley AJ, Henson PM. Differential regulation of phagosome maturation in macrophages and dendritic cells mediated by Rho GTPases and ezrin–radixin–moesin (ERM) proteins. *Proc Natl Acad Sci USA*. 2006;103(34):12825-12830. doi:10.1155/2015/359153

84. Yates RM, Hermetter A, Taylor GA, Russell DG. Macrophage activation downregulates the degradative capacity of the phagosome. *Traffic*. 2007;8(3):241-250. doi:10.1111/j.1600-0854.2006.00528.x

85. Sokolove J, Sharpe O, Brennan M, et al. Citrullination within the atherosclerotic plaque: A potential target for the anti-citrullinated protein antibody response in rheumatoid arthritis. *Arthritis Rheum*. 2013;65(7):1719-1724. doi:10.1002/art.37961

86. Legge A, Hanly JG. Managing premature atherosclerosis in patients with chronic inflammatory diseases. *CMAJ*. 2018;190(14):E430-E439. doi:10.1503/cmaj.170776

87. Koltsova EK, Ley K. How dendritic cells shape atherosclerosis. *Trends Immunol*. 2011;32(11):540-547. doi:10.1016/j.it.2011.07.001

88. Tse K, Tse H, Sidney J, Sette A, Ley K. T cells in atherosclerosis. *Int Immunol*. 2013;25(11):615-622. doi:10.1093/intimm/dxt043

89. Cheng Y, Zhu X, Cheng F, Ji L, Zhou Y. Delta-like homolog1/GATA binding protein 2 axis mediates leptin inhibition of PPARγ2 expression in hepatic stellate cells in vitro. *Life Sci*. 2018;192(November 2017):183-189. doi:10.1016/j.lfs.2017.11.050

90. Croasdell A, Duffney PF, Kim N, Lacy SH, Sime PJ, Phipps RP. PPAR ?? and the Innate Immune System Mediate the Resolution of Inflammation. *PPAR Res*. 2015;2015(Figure 1):1-20. doi:10.1155/2015/549691

91. Chistiakov DA, Melnichenko AA, Myasoedova VA, Grechko A V., Orekhov AN. Mechanisms of foam cell formation in atherosclerosis. *J Mol Med*. 2017;95(11):1153-1165. doi:10.1007/s00109-017-1575-8

92. Lee SM, Moon J, Cho Y, Chung JH, Shin MJ. Quercetin up-regulates expressions of peroxisome proliferator-activated receptor γ, liver X receptor α, and ATP binding cassette transporter A1 genes and increases cholesterol efflux in human macrophage cell line. *Nutr Res*. 2013;33(2):136-143. doi:10.1016/j.nutres.2012.11.010

93. Freeman SA, Grinstein S. Phagocytosis: Receptors, signal integration, and the cytoskeleton. *Immunol Rev*. 2014;262(1):193-215. doi:10.1111/imr.12212

94. Yang L, Sun H, Cao Y, et al. GATA2 inhibition sensitizes acute myeloid leukemia cells to chemotherapy. *PLoS One*. 2017;12(1):1-12. doi:10.1371/journal.pone.0170630

95. Kikuchi J, Yamada S, Koyama D, et al. The novel orally active proteasome inhibitor K-7174 exerts anti-myeloma activity in vitro and in vivo by down-regulating the expression of class i histone deacetylases. *J Biol Chem*. 2013;288(35):25593-25602. doi:10.1074/jbc.M113.480574

96. Liu Y, Liao R, Qiang Z, Zhang C. Pro-inflammatory cytokine-driven PI3K/Akt/Sp1 signalling and H 2 S production facilitates the pathogenesis of severe acute pancreatitis . *Biosci Rep*. 2017;37(2):BSR20160483. doi:10.1042/bsr20160483

97. Chan L, Hong J, Pan J, et al. Role of Rab5 in the formation of macrophage-derived foam cell. *Lipids Health Dis*. 2017;16(1):170. doi:10.1186/s12944-017-0559-6

98. Pulanco MC, Cosman J, Ho M, et al. Complement Protein C1q Enhances

Macrophage Foam Cell Survival and Efferocytosis. *J Immunol*. 2016;198. doi:10.4049/jimmunol.1601445

99. Tabas I. Apoptosis and plaque destabilization in atherosclerosis: the role of macrophage apoptosis induced by cholesterol. *Cell Death Differ*. 2004;11 Suppl 1:S12-S16. doi:10.1038/sj.cdd.4401444

100. Ridker PM, Dellborg M, Kastelein JJP, et al. Antiinflammatory Therapy with Canakinumab for Atherosclerotic Disease. *N Engl J Med*. 2017;377(12):1119-1131. doi:10.1056/nejmoa1707914

Chapter 6

6 Summary, Discussion and Future Directions

6.1 Summary of major findings

The clearance of apoptotic cells by efferocytosis is an essential mechanism of limiting inflammation and maintaining tissue homeostasis.[1] In contrast to the phagocytosis and clearance of pathogens, efferocytosis is immunologically silent and may promote the generation of anti-inflammatory and pro-tolerogenic factors by professional efferocytes such as macrophages.[2,3] When efferocytosis becomes impaired, apoptotic cells are not cleared and instead undergo secondary necrosis—resulting in the release of pro-inflammatory danger signals and self-antigens that are normally confined within the cytoplasm of apoptotic bodies.[4] In the context of atherosclerosis, efferocytic removal of apoptotic cells and debris within the atherosclerotic plaque by lesion-infiltrating macrophages is an important mechanism of limiting plaque growth and the development of the necrotic core that is a pathological feature of late-stage disease.[5,6] In this thesis, we identified a Rab17-dependant vesicular trafficking pathway responsible for the immunologically silent degradation of efferocytosed materials, and identified a GATA2-driven transcriptional profile that drives efferocytic defects in early-stage atheroma formation. This work provides new insights into the cellular mechanisms regulating efferocytosis, and on how atherogenic conditions can drive defects in these processes.

In **Chapter 3** of this thesis, we made use of an unbiased mass spectrometry approach to identify proteins that differentially localize to the surface of efferosomes versus phagosomes. Through this approach, we discovered several proteins that appeared to be selectively recruited to the surface of the maturing efferosome. In particular, we identified the small GTPase Rab17 as one of these efferosome-specific proteins. Rab GTPases act as master regulators of intracellular trafficking, marking specific intracellular organelles and compartments and recruiting effector molecules that mediate vesicular docking and fusion in a highly-regulated fashion.[7,8] We therefore examined whether Rab17 functioned as a regulator of differentially cargo processing between efferosomes and phagosomes. First, we saw that while Rab17 is transiently recruited to the surface of nascent phagosome and

then quickly displaced, it is maintained on the surface of efferosomes throughout efferosome maturation. Following fusion with lysosomes, the efferosome undergoes a fission process, generating several smaller EDVs. Rab17-labelled EDVs subsequently migrate to the cell periphery and fuse with the recycling endosome, presumably resulting in exocytosis or recycling of degraded efferosomal cargo. Knockdown of Rab17 activity using a dominant negative mutant disrupted this process. Efferosomes did not undergo fission to the same degree but instead remained sequestered within the perinuclear region of the cell, where they acquired MHC class II molecules and presumably matured into MHC class II loading compartments. We therefore concluded that Rab17 is a central regulator of immunologically silent efferosome maturation and is required to direct efferosomal cargo to the recycling endosome in order to avoid the loading of apoptotic cell-derived self-antigens onto MHC class II.

The onset of defective macrophage efferocytosis greatly accelerates plaque growth and the development of large necrotic cores that are characteristic of unstable plaques.[9,10] In **Chapter 4**, we sought to perform gene expression profiling of lesion-resident macrophages isolated from human atherosclerotic plaques to better characterize the molecule mechanisms that drive the development of defective efferocytosis. We obtained tissue samples from the ascending aorta of patients undergoing coronary artery bypass graft surgery. Plaques identified in these tissue samples we found to have the histological features of pre-atherosclerotic lesions. Macrophages from these early-stage lesions were selectively isolated by laser capture microdissection using the scavenger receptor CD163 as a macrophage-specific marker. Purified patient macrophages were compared to *in vitro* differentiated peripheral monocyte-derived macrophages from healthy individuals used as controls by microarray. This revealed dramatic dysregulation in patient macrophage gene expression, with approximately 3,000 protein-coding transcripts found to be differentially expressed in these cells. Significantly, these genes clustered in pathways involved in cellular lipid metabolism, cell stress responses, and intracellular trafficking. Gene set enrichment analysis revealed specific defects in cholesterol handling, efferocytosis and efferosome maturation. Of note, we identified three non-cell cycle transcription factors genes to be significantly upregulated in patient macrophages: RARG, GATA2 and E4F1. Amongst these, only GATA2 was previously associated with cardiovascular disease, is not

normally expressed by mature myeloid cells, and is a known regulator of myeloid cell development.[11–13] We confirmed that GATA2 was upregulated nearly 50-fold in patient macrophages by RT-qPCR. Together, these results suggest that lesion-resident macrophages in early-stage human plaques possess a distinctive and previous unappreciated phenotype characterized by impaired cholesterol handling and efferosome maturation that may be driven by aberrant GATA2 expression.

As we had identified the hematopoietic transcription factor GATA2 as being significantly upregulated in patient macrophages, we proceeded to determine in **Chapter 5** whether GATA2 was a master regulator of the unique macrophage phenotype we had previously described. We confirmed that GATA2 was present in a significant proportion of $CD68^{+}$ foam cells within patient aortic intima and that *in vitro* exposure of macrophages to the pro-atherogenic molecule oxLDL resulted in GATA2 upregulation. Using stable GATA2-overexpressing and -knockdown THP-1 macrophage cell lines we performed a number of functional assays to assess the impact of perturbing GATA2 function on a variety of macrophage functions, including efferocytosis and efferosome maturation. As expected, both exposure to oxLDL and GATA2 overexpression independently resulted in markedly impaired macrophage efferocytosis and efferosome maturation, but neither GATA2 overexpression or depletion had any effect on cholesterol influx or efflux. Critically, shRNA-mediated knockdown of GATA2 expression was sufficient to prevent impaired efferocytic uptake and efferosome maturation in macrophages cultured in the presence of oxLDL, with GATA2 upregulation by oxLDL dependent on signaling pathways known to be downstream of oxLDL signaling. Therefore, we concluded that GATA2 is a novel transcription factor induced by exposure to modified lipoproteins, that is involved in the pathogenesis of atherosclerosis through driving impaired apoptotic cell uptake and degradation. GATA2 upregulation in response to oxLDL exposure drives both impaired efferocytic internalization of apoptotic cells and the efficient degradation of apoptotic cargo through efferosome maturation.

6.2 Discussion

6.2.1 A novel mechanism of apoptotic cargo sorting following efferocytosis

Despite the critical role of efferocytosis in restraining pathologic inflammation and autoimmunity, there are many open questions on how professional efferocytes like macrophages recognize and internalize apoptotic cells, and how these efferocytes then process the apoptotic cargo to avoid an inflammatory response and self-antigen presentation.[4,14] We are beginning to develop a comprehensive understanding of the first question, with researchers uncovering a host of apoptotic cell-derived signals and corresponding efferocyte receptors that mediate the localization, recognition and internalization of apoptotic cells by professional efferocytes.[15] However, comparatively less is known about how efferocytes then process efferosomal cargo following internalization of the apoptotic cell. Much of what is currently known about the process of efferosomal maturation has been inferred from studies on the maturation of phagosome.[8,16,17] Although these processes undoubtedly share many similarities, degradation of pathogens within the phagosome ultimately leads to antigen presentation and activation of an adaptive immune response.[18] However, the same is not true of efferocytosis and the molecular mechanisms that distinguish the ultimate fate of phagosomal versus efferosomal cargo remain largely unknown.

Some previous studies have suggested that signaling from pattern recognition receptors such as TLRs on the surface of phagosomes is responsible for discrimination between self- and non-self-antigens.[19] Blander & Medzhitov describe a “phagosome-autonomous” model whereby phagosomes containing TLR ligands undergo rapid maturation in order to generate the hydrolytic environment necessary to successfully process the MHC class II-associated invariant chain (Ii).[20,21] Processing of Ii is required for generation of the class II-associated invariant chain-associated peptide (CLIP) and proper binding of antigenic peptides to MHC class II.[22] Under this framework, efferosomes containing apoptotic cells undergo terminal cargo degradation without creating the conditions necessary for antigenic loading of MHC class II.[20] However, these findings have been called into questions by

Yates & Russell, who found that phagosome maturation proceeds at similar rates regardless of whether TLR2 or TLR4 ligands were present.[23]

In this thesis, we have described a novel mechanism of sorting apoptotic versus pathogen-derived cargo following internalization. In macrophages, we found that Rab17 is recruited to the surface of nascent efferosomes and directs apoptotic cargo away from the MHC class II loading compartment and towards the recycling endosome. Rab17^{+} efferosomes undergo fission to form EDVs, which traffic to the cell periphery in process which is likely dependent on the activity of kinesins. Importantly, when Rab17 function is disrupted, apoptotic cargo is instead directed to the MHC class II loading compartment, presumably without any TLR signaling from the efferosome. Whether TLR signaling from phagosomes prevents Rab17 recruitment or actively removes Rab17 from the surface of pathogen-containing phagosomes remains to be seen, but our findings suggest that it is the presence of Rab17 that prevents efferosomes from maturing into MHC class II loading compartments and present apoptotic cell-derived self-antigens.

6.2.2 Defects in macrophage function develop early in atherosclerotic disease

Altered macrophage function in atherosclerosis has been well-documented.[24,25] Within the plaque microenvironment, macrophages are exposed to hypercholesterolemic conditions that reprogram their behaviour.[26] Uptake of cholesterol by macrophages has several important consequences. The accumulation of free cholesterol in the cytoplasm can activate the unfolded protein response and drive the production of pro-inflammatory cytokines, including IL-1β, TNFα and IL-6.[27,28] Exposure to pro-inflammatory cytokines polarizes lesion-resident macrophages to a M1-like phenotype, which drives the further production of cytokines and a decrease in efferocytic capacity.[29] Excess cholesterol is also thought to inhibit the ability of macrophages to efficiently clear apoptotic cells, although the mechanisms that underlie this phenomenon remain unclear.[30]

While the ontology of human aortic and cardiac macrophages are not as well understood, macrophages with markers of M1-polarization (iNOS, CD86), M2-polarization (MR, dectin-1), and TREM2^{+}-polarization (TREM2, CD9^{hi}) have been identified in human

plaque[31,32]. Later in disease other macrophage sub-types may emerge. For example, intraplaque hemorrhage gives rise to atheroprotective HA-mac and Mhem macrophages in mice, which scavenge hemoglobin and are resistant to oxidative stress[33,34]. While multiple macrophage polarization states have been identified in mouse models and in human atheroma samples, very little is known of the transcription factors or the tissue- and environment-specific cues which regulate their transcriptional programs. One of the best characterized atheroma-resident macrophage populations is the Mox sub-type, which in mice accounts for 30% of atheroma-resident macrophages[35]. Mox cells are characterized by a transcriptional profile mediated by the transcription factor Nrf2 which, when knocked out, delays atheroma formation[36]. Nrf2 upregulates several genes not normally expressed in M1 or M2 polarized cells, including genes for processing heme, angiogenic factors, and anti-oxidant mechanisms[35].

In general, it has previously been thought that defects in apoptotic cell clearance only occurs in advanced atherosclerotic plaques.[4,10] Indeed, the accumulation of uncleared apoptotic cells is a marker of late-stage disease and forced induction of macrophage apoptosis during early stages of disease actually slows progression and promotes plaque stabilization, at least in murine models of atherosclerosis.[37,38] In human studies, accumulation of $TUNEL^+$ secondary necrotic cells have been documented in carotid plaque samples obtained from endarterectomy.[37] This stands in contrast to tissues where there is a high rate of cell turnover but efferocytic capacity remains preserved, such as the tonsils. In these tissues, $TUNEL^+$ cells are almost undetectable.[37] However, the carotid samples commonly used in human atherosclerosis studies consist almost exclusively of late-stage plaques where uncleared apoptotic and secondarily necrotic cells are known to accumulate. To date, there have been very few studies that have studied early-stage atherosclerotic plaques in humans.[39,40] Furthermore, to the best of our knowledge none of these studies have examined apoptotic cell clearance or macrophage function. Although animal studies of plaque progression including early-stage plaque have been more comprehensive, studies that have shown a benefit of macrophage apoptosis early in atherosclerosis have used knockout mice lacking proteins involved in the intrinsic apoptotic pathways (Bax and Bcl2).[41] Deletion of these critical proteins may have resulted in off target effects that complicates the interpretation of the experimental results.

In our study, we studied primarily early-stage human atherosclerotic plaques as a result of our use of aortic punch samples, which typically are excised from regions of the aorta that have a comparatively lower degree of plaque burden. Although initially somewhat discouraging, this strategy ultimately provided us with the rare opportunity to study early-stage human atherosclerosis lesions. Consistent with previous reports, we observed diffuse intimal thickening along with sub-intimal lipid accumulation along with macrophage accumulation in our patient samples.[40] Surprisingly, we found that even in an early stage of disease, macrophage gene expression was severely dysregulated in lesion-resident macrophages. Genes involved in cellular cholesterol efflux, efferocytic uptake and efferosome maturation were significantly downregulated in patient macrophages compared to controls. However, despite the apparent downregulation of the core efferocytic machinery in lesion-resident macrophages, we found very few necrotic $TUNEL^+$ cells in our patient tissue samples. One interpretation of these results is that the ability of macrophages to clear apoptotic cells begins to decline early in atherosclerosis, but this defect does not become severe enough for macrophage efferocytic capacity to be unable to keep up with apoptotic cell turnover in the plaque until later on during disease progression. These results could also mean that there is heterogeneity in macrophage function early in atherosclerosis, with some macrophages developing impaired efferocytosis while others remain fully functional. Unfortunately, our study was not designed to assess these possibilities, but our data suggest that there is greater complexity in macrophage behaviour in early atherosclerosis than has been previously appreciated.

6.2.3 Impaired efferosome maturation contributes to defective efferocytosis in atherosclerosis

While defective efferocytic clearance of apoptotic cell is widely recognized as an important driver of atherosclerotic disease progression through accelerating the growth of plaque necrotic cores and increasing intra-lesion inflammation, how efferocytosis becomes impaired in the context of atherosclerosis remains poorly understood.[4] Several recent studies have implicated decreased expression of key efferocytic receptors or their cleavage from the macrophage cell surface within the inflammatory plaque microenvironment, while other studies have shown that alleviation of “don’t eat me” signals in the plaque can

delay disease progression.[9,42,43] Other studies have found that excessive oxidation of phosphatidylserine can actually inhibit CD36-mediated apoptotic cell clearance.[44] A recent seminal study from Cai *et al.* showed that ADAM17-mediated cleavage of the efferocytic receptor MerTK leads to increased necrotic core size and plaque progression.[9] Significantly, the authors of this study also demonstrated the presence of cleaved MerTK in human carotid plaques, suggesting that this is a *bona fide* mechanism of impaired efferocytosis in human atherosclerotic disease.[9]

Beyond the engagement between efferocytic receptor and target required for binding and uptake of apoptotic cells, we now understand that efficient processing of internalized apoptotic cargo is required to maintain efficient efferocytosis. Wang *et al.* have shown that defects in Drp1, a protein involved in mitochondrial fission, leads to impaired apoptotic cargo degradation and recycling.[45] This in turn drove defective apoptotic cell clearance and promoted the accumulation of necrotic cells in *Drp1*$^{-/-}$/*Ldlr*$^{-/-}$ double-knockout mice.[45]

In this thesis, we uncovered evidence suggesting that macrophage efferosome maturation and apoptotic cargo degradation are impaired in human atherosclerotic disease. We found that several genes involved in efferosome maturation to be downregulated in patient macrophages compared to controls. These included RAB7, which coordinates both phagosome and efferosome maturation through regulating fusion with late endosome and driving phagosome/efferosome fusion with lysosomes,[46] and genes encoding the NADPH oxidase and the vacuolar ATPase, both of which function to permit efficient degradation of apoptotic cell cargo.[8,47] We further determined that culturing macrophages in the presence of a pro-atherogenic stimulus results in impairment of several key mechanisms that are required for efficient apoptotic cargo degradation, including generation of superoxides, efferosome acidification and efferolysosomal fusion. Therefore, our data suggest that in addition to cleavage of efferocytic receptors, impaired efferosome maturation in macrophages is an additional mechanism that drives defective efferocytosis in human atherosclerotic disease.

6.2.4 GATA2 is involved in driving macrophage dysfunction in atherosclerosis

Our previous findings collectively support the conclusion that we have identified a previously unappreciated macrophage phenotype that is unique to early-stage human atherosclerosis. These macrophages are characterized by impaired cholesterol handling and efferocytic capacity without demonstrating the features classically associated with M1-like macrophages or other known atherosclerosis-associated subsets such as increased production of proinflammatory cytokines.[48,49] We sought to identify transcription factors that were responsible for the induction of this phenotype. Only a few transcription factors have been identified to be associated with atherosclerotic macrophages. These include the PPARs, liver X receptor (LXR), retinoic acid receptor (RAR) and retinoid X receptor (RXR).[50–52] These receptors tend to be activated in respond to macrophage cholesterol loading and function to modulate macrophage cholesterol metabolism and drive expression of both proteins involved in cholesterol efflux such as ABCA1 and efferocytic receptors such as CD36.[53]

In this thesis, we identified just three non-cell cycle transcription factors as being upregulated in patient macrophages in our microarray dataset. Initially, we were excited to see a member of the RAR family of transcription factors RARγ amongst these. However, we could not confirm RARγ upregulation in an independent set of patient and control macrophage samples. Therefore, we turned our focus to GATA2, a zinc finger transcription factor best studied for its role in maintenance of the hematopoietic stem cell population and in myeloid lineage specification during hematopoiesis.[54] Interestingly, SNPs in GATA2 have been implicated in previous genome-wide association studies to be involved in coronary artery disease.[11] We found that GATA2 overexpression in the absence of a pro-atherogenic trigger was sufficient to induce defects in efferocytotic uptake and in multiple steps of efferosome maturation. Furthermore, knockdown of GATA2 could protect macrophages against oxLDL-induced impairments in efferocytic uptake and efferosome maturation. These data suggest that aberrant GATA2 expression drives efferocytic defects in macrophages during the early stages of human atherosclerotic disease.

Germline mutations in GATA2 in humans are exceedingly rare but when they do occur result in a spectrum of diseases connected by aberrant development of the myeloid cell lineage (macrophages and neutrophils) and a propensity for developing acute myeloid leukemia (AML).[55,56] Indeed, *de novo* mutations in GATA2 within the bone marrow have been recognized as contributing to the development of AML.[56] Recent work from Jaiswal *et al.* demonstrated that mutations in genes that pre-dispose individuals to developing AML also contributes to increased risk of atherosclerosis and coronary artery disease in a process termed "clonal hematopoiesis of indeterminant potential" (CHIP).[57] AML driver mutations increase the rate of myeloid cell proliferation and accelerate the development of atherosclerosis.[58,59] In particular, work from Fuster *et al.* on the same phenomenon found that in Ldlr-knockout mice lacking Tet2, an enzyme that regulates epigenetic modification of DNA, atherosclerotic plaques were larger and lesion-resident macrophages produced greater levels of IL-1β.[58] Interestingly, GATA2 is recognized as another gene that is often found to be mutated in AML.[56,60] Although to date there have been no reported cases of GATA2 mutations contributing to CHIP in humans, it is possible that *de novo* mutations in GATA2 may increase the risk of coronary artery disease.

6.3 Limitations

6.3.1 Alteration in Rab17 expression or function in atherosclerotic macrophages

Given the importance of Rab17 as a regulator of efferosomal maturation in macrophages, and the broad array of maturation defects present in oxLDL-treated macrophages, we were surprised to find that it was not differentially expressed in our patient macrophages. Instead, impaired efferosome maturation in our patient atherosclerotic macrophages was found to be mediated primarily through a downregulation of Rab7—which mediates efferosome-lysosome fusion[61]—as well as efferosomal acidification, NADPH oxidase activation, and efferolysosomal fusion. We did not initially examine Rab17 expression or localization in our GATA2 overexpression and knockdown macrophage cell lines here because its expression was not significantly altered in our microarray dataset. However,

further investigation in this direction is warranted. Consequently, it is unclear at this point whether Rab17 plays a role in macrophage dysfunction in atherosclerosis. While Rab17 expression may not be affected in atherosclerosis, its function or localization may well be. Unfortunately, we do not currently have a clear picture of how Rab17 is recruited to the surface of efferosomes, nor have we identified any potential downstream Rab17 effectors. This makes studying Rab17 function in atherosclerotic macrophages challenging. Further work is required in defining how Rab17 directs efferosomal cargo trafficking before we will be able to unravel whether it plays a role in defective efferocytosis in atherosclerosis.

6.3.2 Sampling of patient atherosclerotic plaques

The choice to utilize aortic punch tissue as our source of atherosclerotic plaque presents both advantages and drawbacks. Since plaque burden in the ascending aorta in humans is relatively low and surgeons will select a region of the aorta that is macroscopically free from plaque when performing the aortic punch biopsy, we were able to obtain early-stage atherosclerotic plaque for our studies. Early stage plaque is understudied in the human context because investigators to date have focused on the late-stage lesions that are readily available from carotid endarterectomy procedures, while mouse studies into early plaque are limited by the accelerated disease progression in these models.[62,63] Moreover, while our aortic biopsy samples contain plaque that is histologically classified as early plaque, this material is recovered from patients with advanced disease. Consequently, while we propose that this thesis has explored early-stage plaque, it is possible that some of the observed gene expression patterns are a product of late-stage disease. Concordantly, we are in the process of starting a new study to perform comparative gene expression studies of monocytes and aortic plaque macrophages from the same patients, in order to trace the ontology of the defects we have observed. Ideally, we would also liked to have accessed advanced lesions in our original study as well. These plaques have been better studied and are arguably more clinically-relevant to study because of they tend to be more vulnerable and have an increased risk of rupture.[64] Access to both early-stage and advanced plaque from the same patient would have also offered us the possibility of comparing gene expression changes between different stages of disease progression. Unfortunately, limitations in current clinical practice (i.e. the same patient is unlikely to require both a

CABG operation and a carotid endarterectomy within a reasonable timeframe) make it difficult to access both early and advanced lesions from the same patient and precludes us from doing these studies.

6.3.3 Utilization of CD163 as a macrophage-specific marker

The use of CD163 as our macrophage-specific marker is an undoubtedly controversial choice. We selected this marker because the most commonly-utilized macrophage markers in human studies, CD68, is abundantly expressed within the atherosclerotic plaque by smooth muscle cells.[66] In fact, recent studies suggest that more than half of the $CD68^+$ cells in atherosclerotic plaques are derived from smooth muscle cells rather than macrophages.[67] CD163 is a hemoglobin/haptoglobin scavenger receptor that is typically thought of as a marker of alternatively-activated M2-like macrophages.[33,68] However, there is abundant evidence that in humans CD163 expression is not restricted to M2 macrophages. CD163 expression has been detected in several populations in tissue-resident macrophages, including Kupffer cells and splenic red pulp macrophages.[68] Significantly, a study of 1,105 pathology specimens at Stanford University Medical Center found CD163 to be restricted to cells of the monocyte/macrophage lineage, making it a highly specific marker of macrophages.[69] Furthermore, our own data showed that CD163 was detectable on the surface of primary monocyte-derived macrophages *in vitro* regardless of whether these macrophages were polarized to M0, M1 or M2 states (**Figure 4.4a**). We also observed that CD163 was often co-expressed with CD68 expression in patient aortic intima (**Figure 4.4b**), suggesting that we were able to capture a majority of macrophages by CD163 staining. However, our approach did sacrifice sensitivity for specificity and it is unknown whether this led to any bias in our microarray dataset. An alternative approach that could be taken in future studies is to stain for CD45 along with CD68. CD45 expression is restricted to leukocytes and therefore we can be reasonably certain that any CD68/CD45 double-positive cells within the plaque would be macrophages or macrophage-derived foam cells.[70]

6.3.4 Use of peripheral monocyte-derived macrophages as a control in gene expression profiling

Finally, the most significant limitation of this thesis was the use of peripheral monocyte-derived macrophages from age- and sex-matched healthy individuals as the control for our microarray study. This approach made it difficult to distinguish gene expression changes specific to atherosclerotic macrophages from those arising from the *in vitro* differentiation of monocytes into macrophages. Our rational for using these cells are four-fold. Firstly, macrophages are present at extremely low density in non-diseased vascular intima – in our samples, aortic biopsies lacking early-stage plaque had fewer than 1-2 intimal macrophages per low-power field. Assuming those numbers are typical of what would be observed in non-diseased individuals, the density of macrophages in healthy intima would be too low to allow for recovery of enough cells for microarray analysis. Secondly, the resident cardiac macrophages found in the healthy heart and adventitial macrophages found in healthy arteries are largely of embryonic origin and therefore are of a completely different ontology than plaque macrophages, the majority of which are hematopoietic in origin.[71–73] Thirdly, low-level atherosclerosis is near-ubiquitous in the North American adult population, making it questionable whether truly non-diseased tissue is available.[74] Finally, it is established that myeloid cells undergo significant changes in their gene expression profiles as individuals age.[75] As such, the choice to use monocyte-derived macrophages recapitulates the correct ontology and age of the cells, in sufficient numbers to enable experimentation, while allowing us to compare our patient samples to macrophages from an environment free of atherogenic cues. That said, the lack of aortic intima-specific developmental cues will have contributed some of the differentially-expressed genes we observed in our microarray dataset. While we took pains to verify through functional assays *in vitro* of GATA2-mediated impairment of efferocytosis and efferosome maturation, an alternative source of control macrophages would have added to our confidence in the macrophage phenotype we have described. Unfortunately, an appropriate population of macrophages to serve as a control is lacking. An alternative approach would have been to compare gene expression in macrophages isolated from early-stage and late-stage plaques, or to compare the expression of genes between monocytes and lesion-resident macrophages from the same patient. In our case this was not possible because of a lack of late-stage

plaque from our aortic punch tissue samples and the inability to specifically identify the patients from which each aortic punch sample was obtained due to the nature of our ethics approval, which was limited to use discarded tissue.

6.4 Future Directions

6.4.1 Understanding the role of Rab17 in antigen presentation and atherosclerosis

In this thesis, we have demonstrated that Rab17 is a crucial mediator of cargo trafficking in efferocytosis. However, while we have demonstrated that interfering with Rab17 function results in mis-trafficking of apoptotic cargo to the MHC class II loading compartment, whether this results in presentation of apoptotic cell-derived antigens remains to be seen. Moving forwards, we will utilize model pathogens and apoptotic cells expressing a fusion protein consisting of ovalbumin and the Eα peptide to study antigen presentation in a Rab17 knockdown model. Ovalbumin-derived antigens are presented on both MHC class I (SIINFEKL; H-2Kb) and MHC class II (OVA 323-339; I-A[d]), whereas Eα peptide is presented exclusively on MHC class II (Eα 52-68; I-A[b]). Presentation of ovalbumin-derived SIINFEKL peptide on MHC class I H-2Kb is readily detectable by the 25-D1.16 mouse monoclonal antibody whereas presentation of Eα 52-68 on MHC class II I-A[b] can be detected using the Y-Ae mouse monoclonal antibody. Presentation of ovalbumin-derived antigens on MHC class I and MHC class II may also be assessed by T cell proliferation assays with naïve lymphocytes from OTI and OTII transgenic mice, which express a limited T cell repertoire such that they are only responsive to ovalbumin-derived antigens. Using these methods, we will be able to assess the impact on antigen presentation following either phagocytosis of a pathogen or efferocytosis of an apoptotic cell under normal conditions and with Rab17 functionally knocked down.

It will also be interesting to determine whether Rab17 has any biological role in atherosclerosis. Our microarray and functional data show that efferosome maturation and apoptotic cargo processing are dysregulated in atherosclerotic macrophages. Whether Rab17 plays a role in this process remains unknown. It is well established that the

development of plaque-reactive antibodies and T cells accelerates atherosclerosis disease. This raises the interesting hypothesis that impaired or altered apoptotic cell processing in atherosclerosis, potentially due to altered Rab17 activity, may drive the pro-atherogenic presentation of atheroma-derived antigens–self-antigens which normally be restricted from presentation by Rab17-mediated trafficking.[76] We will seek to use live-cell fluorescence imaging to assess the recruitment of Rab17 to efferosome under atherosclerotic conditions and also to determine whether functional knockdown of Rab17 gives rise to any deleterious effect in atherosclerotic macrophages.

6.4.2 Further elucidation of the biological role of GATA2 in atherosclerosis

We have demonstrated thus far that GATA2 is upregulated in atherosclerotic macrophages in early-stage lesions and that GATA2 upregulation appears to be required for oxLDL-mediated impairment of efferocytic uptake and efferosome maturation in these macrophages. We further demonstrated that signaling through the Src/Syk pathway downstream of the oxLDL receptors CD36, TLR2 and TLR4 is required for GATA2 upregulation in response to oxLDL stimulus. However, there are still many unanswered questions about the role of GATA2 in atherosclerosis.

First, there is a need to identify the mechanism(s) driving GATA2 upregulation. This could be through oxLDL signaling via CD36 or other receptors, or in response to ER-stress pathways activated in these cells—neither of which were explored in this thesis. This may be achieved using receptor-specific shRNA and inhibitors of TLR and ER-stress signaling. Second, it is still unclear how GATA2 upregulation results in impairment of efferocytosis and efferosome maturation. Data from our microarray analysis suggests that this may be through downregulation of signal transduction molecules required for efferocytic receptor-mediated apoptotic cell internalization (e.g. ILK, ITGAX) and downregulation of specific genes required for efficient efferosome maturation (e.g. RAB7A, ATP6V1B1). However, this remains to be demonstrated experimentally. One immediate first step is to perform a ChIP-Seq assay in patient aortic punch macrophages or oxLDL-treated macrophages to determine which genes GATA2 regulates in these cells. It may also be of interest to directly compare gene expression in wild type macrophages compared to GATA2 overexpressing

macrophages to identify the complete set of genes for which expression levels change with increased levels of GATA2.

Fundamentally, it will also be necessary to directly demonstrate that GATA2 has a biological role in atherosclerosis by studying the effect of GATA2 deletion on atherosclerotic plaque development. This will require generating a monocyte/macrophage-specific *Gata2* knockout mouse and either back-crossing this mouse onto a *Ldlr*$^{-/-}$ background or performing bone marrow transplantation from the *Gata2* knockout into *Ldlr*$^{-/-}$ mice. It is unclear at this time whether GATA2 is regulated the same in mice as in humans, with preliminary experiments in *Ldlr*$^{-/-}$ mice fed a high-fat diet for 12 weeks compared to chow diet-fed animals showing variable upregulation of GATA2 in the plaque. A myeloid-specific approach is necessary because whole body *Gata2* knockout is embryonically lethal due to hematopoietic and lymphatic collapse.[54] Additionally, since GATA2 is required for maintenance of the hematopoietic stem cell population and for myeloid-lineage specification, it may be necessary create a floxed mouse where target gene recombination is under the transcriptional control of a gene that is only expressed in terminally-differentiated monocytes (e.g. CD11b), or where GATA2 excision is controlled by a mature myeloid-restricted inducible knockout.[54] We would then look at plaque size and surface area, necrotic core size, macrophage numbers and phenotype within the plaque as well as characterize plasma lipid levels and levels of circulating immune cells. Studying myeloid-specific *Gata2* knockout will be critical in establishing a biological role for this transcription factor in atherosclerosis.

6.4.3 Characterizing changes in macrophage and monocyte gene expression with atherosclerotic disease progression

A limitation in the present study is a lack of an appropriate population of control macrophages to which atherosclerotic macrophage gene expression can be compared. One way to circumvent this difficulty is to compare the gene expression profiles of macrophages isolated from the plaques and monocytes isolated from the blood of patients with differing atherosclerotic disease severities. There are many clinical scores that assess atherosclerotic disease severity, including the Gensini score and the SYNTAX score.[77,78] These scores may be used to stratify patients into differing categories of disease severity. The gene

expression profiles of macrophages and monocytes from patients from different categories may then be compared against one another. This approach will allow us to identify genes involved in atherosclerosis disease progression, at least within the latter stages of disease in humans.

Another approach is to compare gene expression between lesion-resident macrophages and circulating monocytes within the same patient. This would allow us to determine the changes that occur in gene expression as monocytes migrate into the atherosclerotic plaque and differentiate into macrophages. Such an approach has the potential to answer important questions on the effect of the plaque microenvironment on macrophage function following migration into the plaque.

6.4.4 Utilizing macrophage and monocyte gene expression profiling to predict clinical outcomes in patients with coronary artery disease

Understanding gene expression changes in macrophages and monocytes with progressive atherosclerotic disease severity has the potential to allow us to identify important genes and pathways involved in the underlying biology of plaque macrophages. This information may then serve as a basis for determining whether differences in monocyte and macrophage gene expression can be used to predict clinical outcomes in patients with significant atherosclerotic disease (i.e. those patients who have experienced at least one cardiac or cerebrovascular event as a result of atherosclerosis).

From a cohort of patients undergoing coronary artery bypass graft surgery for any reason, the expression of a few genes of interest (e.g. GATA2), as determined on the basis of characterizing the genes and pathways important for disease progression as outlined in the previous section, will be quantified. These patients will then be followed for a period of two years for cases of major adverse cardiovascular and cerebrovascular events (MACCE; defined as a composite of myocardial infarction, ischemic stroke, need for repeat bypass surgery and death).[79] We will then determine whether gene expression in monocytes and/or macrophages correlate with the incidence of MACCE. This will allow us to determine whether the expression of certain genes in macrophages and/or monocytes can be used as

a biomarker of adverse clinical outcomes in patients with high existing atherosclerotic disease burden.

6.5 Concluding Remarks

In conclusion, the work presented in this doctoral thesis advances our understanding of efferocytosis and the mechanisms by which efferocytosis becomes impaired in the setting of atherosclerotic disease. We present three major findings: 1) the small GTPase Rab17 traffics degraded apoptotic cell contents from the phagolysosome to the recycling endosome, likely preventing the presentation of apoptotic cell-derived antigens, 2) macrophages isolated from early-stage plaque down-regulate many of the genes required for efficient uptake and processing of apoptotic cells, and 3) upregulation of the hematopoietic transcription factor GATA2 is required for the onset of impaired efferocytosis and efferosome maturation in macrophages in response to oxLDL loading.

The findings presented here advance our fundamental knowledge of how apoptotic cells are processed and degraded following internalization by an efferocyte. To date, how macrophages discriminate between pathogens and apoptotic cells during cargo processing is poorly understood. Previous studies have suggested that differences in TLR signaling from the phagosome or in the inherent differences in kinetics between phagosome and efferosome maturation are responsible for the divergent outcomes observed following efferocytosis and phagocytosis.[21,80] Our observation that Rab17 is required for efferosomal cargo trafficking to the recycling endosome and that impaired Rab17 activity leads to mis-trafficking of cargo to the MHC class II loading compartment (**Chapter 3**) suggests that there is a phagocyte-intrinsic, TLR-independent pathway that plays a role in discrimination between pathogens and apoptotic cell cargo.

Our findings also challenge some widely-held notions in the field about the development of efferocytic defects in the setting of atherosclerosis. Our observation that lesion-resident macrophages from early-stage human plaques already have dysregulated expression of genes involved in efferocytosis (**Chapter 4**) suggest that the onset of impaired

efferocytosis may be occurring much earlier than previously thought. We are also the first to identify a potential defect in efferosome maturation in human lesion-resident macrophages (**Chapter 4**), suggesting that defects in how macrophages process apoptotic cargo, in addition to defects in recognition and efferocytic uptake of apoptotic cells, plays a role in the development of defective efferocytosis. Finally, we are also the first to identify a potential role for the hematopoietic transcription factor GATA2 in driving macrophage dysfunction in human atherosclerotic disease. We observed that GATA2 is required for oxLDL-mediated impairments in both efferocytic uptake and efferosome maturation (**Chapter 5**), implicating this transcription factor as a major driver of dysregulated macrophage function under atherosclerotic conditions.

Much work remains to be done in furthering our understanding of the role of macrophages, defective apoptotic cell clearance and inflammation in atherosclerosis. Following decades of clinical interest and success in treating the dyslipidemia component of atherosclerosis, the results of the recent CANTOS trial have brought the inflammatory component of this disease back into the primetime.[81] The results presented in this thesis represent a just small step forward in unraveling our understanding of the underlying mechanisms of how apoptotic cell clearance becomes impaired in human atherosclerotic disease. Importantly, our discovery of GATA2 as a potential master regulator of defective efferocytosis in early-stage human atherosclerotic macrophages merits further investigation. GATA2 and its downstream targets may represent viable therapeutic targets in the development of novel anti-inflammatory agents for the treatment of the residual inflammatory risk in atherosclerosis.

6.6 References

1. Nagata S. Apoptosis and Clearance of Apoptotic Cells. *Annu Rev Immunol*. 2018;361829(1):1-18. doi:10.1146/annurev-immunol

2. Green DR, Oguin TH, Martinez J. The clearance of dying cells: table for two. *Cell Death Differ*. 2016;23(6):915-926. doi:10.1038/cdd.2015.172

3. Trahtemberg U, Mevorach D. Apoptotic Cells Induced Signaling for Immune Homeostasis in Macrophages and Dendritic Cells. *Front Immunol*. 2017;8(October). doi:10.3389/fimmu.2017.01356

4. Tabas I. Macrophage death and defective inflammation resolution in atherosclerosis. *Nat Rev Immunol*. 2009;10(1):36-46. doi:10.1038/nri2675

5. Van Vré E a., Ait-Oufella H, Tedgui A, Mallat Z. Apoptotic cell death and efferocytosis in atherosclerosis. *Arterioscler Thromb Vasc Biol*. 2012;32(4):887-893. doi:10.1161/ATVBAHA.111.224873

6. Kojima Y, Weissman IL, Leeper NJ. The Role of Efferocytosis in Atherosclerosis. *Circulation*. 2017;135(5):476-489. doi:10.1161/CIRCULATIONAHA.116.025684

7. Stenmark H, Olkkonen VM. The Rab GTPase family. *Genome Biol*. 2001;2(5):REVIEWS3007. doi:10.1186/gb-2001-2-5-reviews3007

8. Kinchen JM, Ravichandran KS. Phagosome maturation: going through the acid test. *Nat Rev Mol Cell Biol*. 2008;9(10):781-795. doi:10.1038/nrm2515

9. Cai B, Thorp EB, Doran AC, et al. MerTK receptor cleavage promotes plaque necrosis and defective resolution in atherosclerosis. *J Clini*. 2017;127(2):564-568. doi:10.1172/JCI90520.We

10. Tabas I. 2016 Russell Ross Memorial Lecture in Vascular Biology. *Arterioscler Thromb Vasc Biol*. 2016:ATVBAHA.116.308036. doi:10.1161/ATVBAHA.116.308036

11. Muiya NP, Wakil S, Al-Najai M, et al. A study of the role of GATA2 gene polymorphism in coronary artery disease risk traits. *Gene*. 2014;544(2):152-158. doi:10.1016/j.gene.2014.04.064

12. Connelly JJ, Wang T, Cox JE, et al. GATA2 is associated with familial early-onset coronary artery disease. *PLoS Genet*. 2006;2(8):1265-1273. doi:10.1371/journal.pgen.0020139

13. Bresnick EH, Katsumura KR, Lee HY, Johnson KD, Perkins AS. Master regulatory GATA transcription factors: Mechanistic principles and emerging links to hematologic malignancies. *Nucleic Acids Res*. 2012;40(13):5819-5831. doi:10.1093/nar/gks281

14. Ariel A, Ravichandran KS. 'This way please': Apoptotic cells regulate phagocyte migration before and after engulfment. *Eur J Immunol*. 2016:1-4. doi:10.1002/eji.201646505

15. Henson PM. Cell Removal : Efferocytosis. *Annu Rev Cell Dev Biol*. 2017;33:1-18.

16. Cui Y, Zhao Q, Gao C, et al. Activation of the Rab7 GTPase by the MON1-CCZ1 complex is essential for PVC-to-vacuole trafficking and plant growth in Arabidopsis. *Plant Cell*. 2014;26(5):2080-2097. doi:10.1105/tpc.114.123141

17. Rupper A, Grove B, Cardelli J. Rab7 regulates phagosome maturation in Dictyostelium. *J Cell Sci*. 2001;114(13):2449-2460.

18. Flannagan RS, Jaumouillé V, Grinstein S. The Cell Biology of Phagocytosis. *Annu Rev Pathol Mech Dis*. 2011;7(1):61-98. doi:10.1146/annurev-pathol-011811-132445

19. Blander JM. Regulation of Phagosome Maturation by Signals from Toll-Like Receptors. *Science*. 2011;1014(2004):1014-1018. doi:10.1126/science.1096158

20. Blander JM, Medzhitov R. On regulation of phagosome maturation and antigen presentation. *Nat Immunol*. 2006;7(10):1029-1035. doi:10.1038/ni1006-1029

21. Magarian Blander J, Medzhitov R. Toll-dependent selection of microbial antigens for presentation by dendritic cells. *Nature*. 2006;440(7085):808-812. doi:10.1038/nature04596

22. Schröder B. The multifaceted roles of the invariant chain CD74 - More than just a chaperone. *Biochim Biophys Acta - Mol Cell Res*. 2016;1863(6):1269-1281. doi:10.1016/j.bbamcr.2016.03.026

23. Yates RM, Russell DG. Phagosome maturation proceeds independently of stimulation of toll-like receptors 2 and 4. *Immunity*. 2005;23(4):409-417. doi:10.1016/j.immuni.2005.09.007

24. Moore KJ, Sheedy FJ, Fisher E a. Macrophages in atherosclerosis: a dynamic balance. *Nat Rev Immunol*. 2013;13(10):709-721. doi:10.1038/nri3520

25. Rojas J, Salazar J, Martínez MS, et al. Macrophage Heterogeneity and Plasticity: Impact of Macrophage Biomarkers on Atherosclerosis. *Scientifica (Cairo)*. 2015;2015:1-17. doi:10.1155/2015/851252

26. Westover E. Cholesterol in Health and Disease. *J Clin Invest*. 2002;110(5):583-590. doi:10.1172/JCI200216381.Imagine

27. Li Y, Gerbod-Giannone MC, Seitz H, et al. Cholesterol-induced apoptotic macrophages elicit an inflammatory response in phagocytes, which is partially attenuated by the Mer receptor. *J Biol Chem*. 2006;281(10):6707-6717. doi:10.1074/jbc.M510579200

28. Li Y, Seitz H, Cui D, et al. Cholesterol-induced Apoptotic Macrophages Elicit an Inflammatory Response in Phagocytes , Which Is Partially Attenuated by the Mer Receptor *. *J Bacteriol*. 2006;281(10):6707-6717. doi:10.1074/jbc.M510579200

29. Seo J-W, Yang E-J, Yoo K-H, Choi I-H. Macrophage Differentiation from Monocytes Is Influenced by the Lipid Oxidation Degree of Low Density Lipoprotein. *Mediators Inflamm*. 2015;2015:1-10. doi:10.1155/2015/235797

30. Cui D, Thorp E, Li Y, et al. Pivotal advance: macrophages become resistant to cholesterol-induced death after phagocytosis of apoptotic cells. *J Leukoc Biol*. 2007;82(5):1040-1050. doi:10.1189/jlb.0307192

31. Stöger JL, Gijbels MJJ, van der Velden S, et al. Distribution of macrophage polarization markers in human atherosclerosis. *Atherosclerosis*. 2012;225(2):461-468. doi:10.1016/j.atherosclerosis.2012.09.013

32. Cochain C, Vafadarnejad E, Arampatzi P, et al. Single-Cell RNA-Seq Reveals the Transcriptional Landscape and Heterogeneity of Aortic Macrophages in Murine Atherosclerosis. *Circ Res*. 2018;122(12):1661-1674. doi:10.1161/CIRCRESAHA.117.312509

33. Boyle JJ, Harrington H a, Piper E, et al. Coronary intraplaque hemorrhage evokes a novel atheroprotective macrophage phenotype. *Am J Pathol*. 2009;174(3):1097-1108. doi:10.2353/ajpath.2009.080431

34. Boyle JJ, Johns M, Kampfer T, et al. Activating transcription factor 1 directs Mhem atheroprotective macrophages through coordinated iron handling and foam cell protection. *Circ Res*. 2012;110(1):20-33. doi:10.1161/CIRCRESAHA.111.247577

35. Kadl A, Meher AK, Sharma PR, et al. Identification of a novel macrophage phenotype that develops in response to atherogenic phospholipids via Nrf2. *Circ Res*. 2010;107(6):737-746. doi:10.1161/CIRCRESAHA.109.215715

36. Sussan TE, Jun J, Thimmulappa R, et al. Disruption of Nrf2, a key inducer of antioxidant defenses, attenuates ApoE-mediated atherosclerosis in mice. *PLoS One*. 2008;3(11):e3791. doi:10.1371/journal.pone.0003791

37. Schrijvers DM, De Meyer GRY, Kockx MM, Herman AG, Martinet W. Phagocytosis of apoptotic cells by macrophages is impaired in atherosclerosis. *Arterioscler Thromb Vasc Biol*. 2005;25(6):1256-1261. doi:10.1161/01.ATV.0000166517.18801.a7

38. Gautier EL, Huby T, Witztum JL, et al. Macrophage apoptosis exerts divergent effects on atherogenesis as a function of lesion stage. *Circulation*. 2009;119(13):1795-1804. doi:10.1161/CIRCULATIONAHA.108.806158

39. Pulanco MC, Cosman J, Ho M, et al. Complement Protein C1q Enhances Macrophage Foam Cell Survival and Efferocytosis. *J Immunol*. 2016;198. doi:10.4049/jimmunol.1601445

40. Nakashima Y, Chen YX, Kinukawa N, Sueishi K. Distributions of diffuse intimal thickening in human arteries: Preferential expression in atherosclerosis-prone arteries from an early age. *Virchows Arch*. 2002;441(3):279-288. doi:10.1007/s00428-002-0605-1

41. Liu J, Thewke DP, Su YR, Linton MF, Fazio S, Sinensky MS. Reduced macrophage apoptosis is associated with accelerated atherosclerosis in low-density lipoprotein receptor-null mice. *Arterioscler Thromb Vasc Biol*. 2005;25(1):174-179. doi:10.1161/01.ATV.0000148548.47755.22

42. Zhang S, Yeap XY, Grigoryeva L, et al. Cardiomyocytes induce macrophage receptor shedding to suppress phagocytosis. *J Mol Cell Cardiol*. 2015;87:171-179. doi:10.1016/j.yjmcc.2015.08.009

43. Kojima Y, Volkmer J-P, McKenna K, et al. CD47-blocking antibodies restore phagocytosis and prevent atherosclerosis. *Nature*. 2016;536(7614):86-90. doi:10.1038/nature18935

44. Kimani SG, Geng K, Kasikara C, et al. Contribution of defective PS recognition and efferocytosis to chronic inflammation and autoimmunity. *Front Immunol*. 2014;5(NOV):1-9. doi:10.3389/fimmu.2014.00566

45. Wang Y, Subramanian M, Yurdagul A, et al. Mitochondrial Fission Promotes the Continued Clearance of Apoptotic Cells by Macrophages. *Cell*. 2017;171(2):331-345.e22. doi:10.1016/j.cell.2017.08.041

46. Kinchen JM, Ravichandran KS. Identification of two evolutionarily conserved genes regulating processing of engulfed apoptotic cells. *Nature*. 2010;464(7289):778-782. doi:10.1038/nature08853

47. Bagaitkar J, Huang J, Zeng MY, et al. NADPH oxidase activation regulates apoptotic neutrophil clearance by murine macrophages. *Blood*. 2018. doi:10.1104/pp.111.188953

48. de Gaetano M, Crean D, Barry M, Belton O. M1- and M2-Type Macrophage

Responses Are Predictive of Adverse Outcomes in Human Atherosclerosis. *Front Immunol*. 2016;7(July). doi:10.3389/fimmu.2016.00275

49. Mills CD, Lenz LL, Ley K. Macrophages at the fork in the road to health or disease. *Front Immunol*. 2015;6(February):1-6. doi:10.3389/fimmu.2015.00059

50. Röszer T. Transcriptional control of apoptotic cell clearance by macrophage nuclear receptors. *Apoptosis*. 2016;0(0):0. doi:10.1007/s10495-016-1310-x

51. Doran AC, Ozcan L, Cai B, et al. CAMKIIγ suppresses an efferocytosis pathway in macrophages and promotes atherosclerotic plaque necrosis. *J Clin Invest*. 2017;(16):1-15. doi:10.1172/JCI94735

52. Costet P, Lalanne F, Gerbod-Giannone MC, et al. Retinoic Acid Receptor-Mediated Induction of ABCA1 in Macrophages. *Mol Cell Biol*. 2003;23(21):7756-7766. doi:10.1128/mcb.23.21.7756-7766.2003

53. Chistiakov DA, Melnichenko AA, Myasoedova VA, Grechko A V., Orekhov AN. Mechanisms of foam cell formation in atherosclerosis. *J Mol Med*. 2017;95(11):1153-1165. doi:10.1007/s00109-017-1575-8

54. Lim KC, Hosoya T, Brandt W, et al. Conditional Gata2 inactivation results in HSC loss and lymphatic mispatterning. *J Clin Invest*. 2012;122(10):3705-3717. doi:10.1172/JCI61619

55. Shih AH, Jiang Y, Meydan C, et al. Mutational cooperativity linked to combinatorial epigenetic gain of function in acute myeloid leukemia. *Cancer Cell*. 2015;27(4):502-515. doi:10.1016/j.ccell.2015.03.009

56. Luesink M, Hollink IHIM, van der Velden VHJ, et al. High GATA2 expression is a poor prognostic marker in pediatric acute myeloid leukemia. *Blood*. 2012;120(10):2064-2075. doi:10.1182/blood-2011-12-397083 LK - http://sfx.library.uu.nl/utrecht?sid=EMBASE&issn=00064971&id=doi:10.1182%2Fblood-2011-12-397083&atitle=High+GATA2+expression+is+a+poor+prognostic+marker+in+ped

iatric+acute+myeloid+leukemia&stitle=Blood&title=Blood&volume=120&issue=10&spage=2064&epage=2075&aulast=Luesink&aufirst=Maaike&auinit=M.&aufull=Luesink+M.&coden=BLOOA&isbn=&pages=2064-2075&date=2012&auinit1=M&auinitm=

57. Jaiswal S, Natarajan P, Silver AJ, et al. Clonal Hematopoiesis and Risk of Atherosclerotic Cardiovascular Disease. *N Engl J Med*. 2017;377(2):111-121. doi:10.1056/NEJMoa1701719

58. Fuster JJ, MacLauchlan S, Zuriaga MA, et al. Clonal hematopoiesis associated with Tet2 deficiency accelerates atherosclerosis development in mice. *Science (80-)*. 2017;1381(January).

59. Xie M, Lu C, Wang J, et al. Age-related cancer mutations associated with clonal hematopoietic expansion. *Nat Med*. 2015;20(12):1472-1478. doi:10.1038/nm.3733.Age-related

60. Zhang S-J, Ma L-Y, Huang Q-H, et al. Gain-of-function mutation of GATA-2 in acute myeloid transformation of chronic myeloid leukemia. *Proc Natl Acad Sci*. 2008;105(6):2076-2081. doi:10.1073/pnas.0711824105

61. Harrison RE, Bucci C, Vieira O V, Schroer TA, Grinstein S. Phagosomes fuse with late endosomes and/or lysosomes by extension of membrane protrusions along microtubules: role of Rab7 and RILP. *Mol Cell Biol*. 2003;23(18):6494-6506. doi:10.1128/MCB.23.18.6494

62. Chai JT, Ruparelia N, Goel A, et al. Differential Gene Expression in Macrophages From Human Atherosclerotic Plaques Shows Convergence on Pathways Implicated by Genome-Wide Association Study Risk Variants. *Arterioscler Thromb Vasc Biol*. 2018;38(11):2718-2730. doi:10.1161/ATVBAHA.118.311209

63. Getz GS, Reardon C a. Animal models of Atherosclerosis. *Arterioscler Thromb Vasc Biol*. 2012;32(5):1104-1115. doi:10.1161/ATVBAHA.111.237693

64. Yahagi K, Kolodgie FD, Otsuka F, et al. Pathophysiology of native coronary, vein

graft, and in-stent atherosclerosis. *Nat Rev Cardiol*. 2015;advance on. doi:10.1038/nrcardio.2015.164

65. Trogan E, Choudhury RP, Dansky HM, Rong JX, Breslow JL, Fisher E a. Laser capture microdissection analysis of gene expression in macrophages from atherosclerotic lesions of apolipoprotein E-deficient mice. *Proc Natl Acad Sci U S A*. 2002;99(4):2234-2239. doi:10.1073/pnas.042683999

66. Allahverdian S, Chehroudi AC, McManus BM, Abraham T, Francis GA. Contribution of intimal smooth muscle cells to cholesterol accumulation and macrophage-like cells in human atherosclerosis. *Circulation*. 2014;129(15):1551-1559. doi:10.1161/CIRCULATIONAHA.113.005015

67. Wang Y, Dubland JA, Allahverdian S, et al. Smooth Muscle Cells Contribute the Majority of Foam Cells in ApoE (Apolipoprotein E)-Deficient Mouse Atherosclerosis. *Arterioscler Thromb Vasc Biol*. 2019;39(5):876-887. doi:10.1161/ATVBAHA.119.312434

68. Etzerodt A, Moestrup SK. CD163 and inflammation: biological, diagnostic, and therapeutic aspects. *Antioxid Redox Signal*. 2013;18(17):2352-2363. doi:10.1089/ars.2012.4834

69. Nguyen TT, Schwartz EJ, West RB, Warnke RA, Arber DA, Natkunam Y. Expression of CD163 (hemoglobin scavenger receptor) in normal tissues, lymphomas, carcinomas, and sarcomas is largely restricted to the monocyte/macrophage lineage. *Am J Surg Pathol*. 2005;29(5):617-624. doi:10.1097/01.pas.0000157940.80538.ec

70. Nakano A, Harada T, Morikawa S, Kato Y. Expression of Leukocyte Common Antigen (CD45) on Various Human Leukemia/Lymphoma Cell Lines. *Pathol Int*. 1990;40(2):107-115. doi:10.1111/j.1440-1827.1990.tb01549.x

71. Epelman S, Lavine KJ, Beaudin AE, et al. Embryonic and adult-derived resident cardiac macrophages are maintained through distinct mechanisms at steady state

and during inflammation. *Immunity*. 2014;40(1):91-104. doi:10.1016/j.immuni.2013.11.019

72. Ensan S, Li A, Besla R, et al. Self-renewing resident arterial macrophages arise from embryonic CX3CR1+ precursors and circulating monocytes immediately after birth. *Nat Immunol*. 2015;17(2):159-168. doi:10.1038/ni.3343

73. Rahman K, Vengrenyuk Y, Ramsey SA, et al. Inflammatory Ly6Chimonocytes and their conversion to M2 macrophages drive atherosclerosis regression. *J Clin Invest*. 2017;127(8):2904-2915. doi:10.1172/JCI75005

74. Herrington W, Lacey B, Sherliker P, Armitage J, Lewington S. Epidemiology of Atherosclerosis and the Potential to Reduce the Global Burden of Atherothrombotic Disease. *Circ Res*. 2016;118(4):535-546. doi:10.1161/CIRCRESAHA.115.307611

75. Lissner MM, Thomas BJ, Wee K, Tong AJ, Kollmann TR, Smale ST. Age-related gene expression differences in monocytes from Human Neonates, Young Adults, and Older Adults. *PLoS One*. 2015;10(7):1-18. doi:10.1371/journal.pone.0132061

76. Abdolmaleki F, Farahani N, Hayat SMG, et al. The role of efferocytosis in autoimmune diseases. *Front Immunol*. 2018;9(JUL):1-13. doi:10.3389/fimmu.2018.01645

77. Sianos G, Morel M-A, Kappetein AP, et al. The SYNTAX Score: an angiographic tool grading the complexity of coronary artery disease. *EuroIntervention*. 2005;1(2):219-227. doi:EIJV1I2A36 [pii]

78. Kashani H, Zeraati H, Mohammad K, et al. Analyzing gensini score as a semi-continuous outcome. *J Tehran Univ Hear Cent*. 2016;11(2):55-61.

79. Serruys PW, Ong ATL, van Herwerden LA, et al. Five-Year Outcomes After Coronary Stenting Versus Bypass Surgery for the Treatment of Multivessel Disease. *J Am Coll Cardiol*. 2005;46(4):575-581. doi:http://dx.doi.org/10.1016/j.jacc.2004.12.082

80. Erwig L-P, McPhilips KA, Wynes MW, Ivetic A, Ridley AJ, Henson PM. Differential regulation of phagosome maturation in macrophages and dendritic cells mediated by Rho GTPases and ezrin–radixin–moesin (ERM) proteins. *Proc Natl Acad Sci USA*. 2006;103(34):12825-12830. doi:10.1155/2015/359153

81. Ridker PM, Dellborg M, Kastelein JJP, et al. Antiinflammatory Therapy with Canakinumab for Atherosclerotic Disease. *N Engl J Med*. 2017;377(12):1119-1131. doi:10.1056/nejmoa1707914

Appendices

Appendix A List of all constructs used in this thesis

Gene	Sequence
	qPCR primers
18S	5'-GAGGGAGCCTGAGAAACGG-3' 5'-GTCGGGAGTGGGTAATTTGC-3'
CD14	5'-AGCCAAGGCAGTTTGAGTCC-3' 5'-TAAAGGACTGCCAGCCAAGC-3'
SMA	5'-CCGACCGAATGCAGAAGGA-3' 5'-ACAGAGTATTTGCGCTCCG-3'
GATA2	5'-GTCACTGACGGAGAGCATGA-3' 5'-GGCACATAGGAGGGGTAGGT-3'
E4F1	5'-ACACCACACAGGCGAGA-3' 5'-TCCTCAGACACCAGCAAC-3'
RARG	5'-CTGCCAGTACTGCCGGCTAC-3' 5'-TCTGCACTGGAGTTCGTGGTATACT-3'
ABCA1	5'-GCACTGAGGAAGATGCTGAAA-3' 5'-AGTTCCTGGAAGGTCTTGTTCAC-3'
NPC1	5'-AGCCAGTAATGTCACCGAAAC-3' 5'-CCGAGGTTGAAGATAGTGTCG-3'
NPC2	5'-TATCCCTCTATAAAACTGGTGGTG-3' 5'-CCAGATGCACCGAACTCAAT-3'
RAB7A	5'-CATCCTGGGAGATTCTGGAGTC-3' 5'-TGTGTCCCATATCTGCATTGTG-3'
ITGAX	5'-GCTGAAGGCACACTGTGAAA-3' 5'-AGGGAGGCCGTGAAGTATCT-3'
CD44	5'-TGGCACCCGCTATGTCCAG-3' 5'-GTAGCAGGGATTCTGTCTG-3'
ILK	5'-ATGTACTACATGAAGGCACCAATTTC-3' 5'-CCCCTTGCCATGTCCAAAG-3'
PADI3	5'-GGAGACCCTCGTGGACATTT-3' 5'-CTCCAAAGTCGCGTCAAAGC-3'
mGata2	5'-GCAGAGAAGCAAGGCTCGC-3' 5'-CAGTTGACACACTCCCGGC-3'
mGapdh	5'-CTCCCACTCTTCCACCTTCG-3' 5'-GCCTCTCTTGCTCAGTGTCC-3'
	PCR primers
GATA2	5'-TATTTCCGGTGAATTCATGGAGGTGGCGGCCGAGCA-3' 5'-CGGGATCCGCGGCCGCTAGCCCATGGCGGTCACCATGCT-3'
Rab17	5'- AAAAAAAAAGAATTCGATGGCACAGGCACACAGGACCCC-3' 5'-TTTTTTTTTGGATCCCTAGTGGGCGCAGCATTTGGCCT-3'
DN-Rab17	5'-GCCCACCAGCATCACCAGGACTTC-3' 5'-ATCAAGACGGACCTCAGCCAGGAGCGG-3'

	shRNA sequences
GATA2	5'-AAGGATCCAGCAAGGCTCGTTCCTGTTCATCAAG AGTGAACAGGAACGAGCCTTGCTTTTTTACCGGTAA-3'

Appendix B List of all primers and oligos used in this thesis.

Construct	Backbone	Enzyme Cut Sites	Sequencing Primer(s)
PM-RFP	pcDNA3	HindIII; XbaI	CMV; SV40pA-R
PM-GFP	pcDNA3	HindIII; XbaI	CMV; SV40pA-R
Rab5-GFP	pEGFP-C1	EcoRI; BamHI	EGFP-C; SV40pA-R
Rab7-RFP	pmCherry-C1	EcoRI; BamHI	SV40pA-R
Rab17-GFP	pEGFP-C1	EcoRI; BamHI	EGFP-C; SV40pA-R
Rab17-RFP	pmCherry-C1	EcoRI; BamHI	SV40pA-R
DN-Rab17-RFP	pmCherry-C1	EcoRI; BamHI	SV40pA-R
Rab6b-GFP	pEGFP-C1	EcoRI; BamHI	EGFP-C; SV40pA-R
Rab45-GFP	pEGFP-C1	EcoRI; BamHI	EGFP-C; SV40pA-R
pLVX-IRES-ZsGreen1 GATA2	pLVX-IRES-ZsGreen1	EcoRI	CMV
pGFP-C-shLenti GATA2 shRNA1	pGFP-C-shLenti	BamHI; AgeI	CMV

Appendix C List of the 100 most up-regulated genes from the patient macrophage microarray

Number	Gene Symbol	Fold Change
1	OR2T12	9.62722
2	LRRC3C	6.74565
3	ZNF705E	4.42287
4	LOC646743	3.85502
5	CLEC18A	3.84465
6	TCEA2	3.78658
7	GPRC5D	3.78366
8	OR52I1	3.7386
9	OR2A42	3.50104
10	KRTAP12-4	3.42346
11	LINC01562	3.33314
12	CHFR	3.22888
13	OR51S1	3.20428
14	PGM5	3.16232
15	C10orf53	3.12336
16	BAGE4	3.07173
17	CAMK2N2	3.05843
18	C7orf65	3.05369
19	OR2T3	3.02501
20	OR51B4	2.93111
21	ZNF648	2.92935
22	ZNF675	2.86593
23	NBPF4	2.86195
24	KRTAP4-8	2.73692
25	TMEM200C	2.73062
26	TPBGL	2.66528
27	PRAMEF8	2.66506
28	AVP	2.66329
29	LOC101930023	2.65457
30	RAB44	2.63632
31	KCNK18	2.61918
32	CNTNAP3	2.60335
33	CHST3	2.55363
34	C3orf18	2.54441
35	OR10H4	2.53899
36	FOXF2	2.53369
37	CACNG5	2.52677
38	OR5F1	2.50943
39	C9orf62	2.48851
40	FAM26E	2.48581

41	ZACN	2.48312
42	HPCA	2.47082
43	OLFM1	2.4674
44	LGALS14	2.46699
45	YAP1	2.45382
46	MSX2	2.45281
47	KRT81	2.43951
48	CHST5	2.43565
49	GATA2	2.42342
50	ANKRD63	2.42284
51	TMEM98	2.42282
52	C5orf60	2.41695
53	MYH7	2.40692
54	KIR3DL2	2.37758
55	CFAP77	2.37248
56	LOC162137	2.37207
57	NANOS3	2.36682
58	S100A7A	2.36563
59	ARID3C	2.36417
60	GOLGA7B	2.3582
61	LINC00355	2.34773
62	SNORA78	2.3349
63	TMEM74B	2.32943
64	E4F1	2.32076
65	SPRN	2.3178
66	RARG	2.30969
67	LOC101929469	2.30961
68	PADI3	2.30731
69	FOXD4L5	2.30638
70	MTRNR2L10	2.2982
71	LDB3	2.29628
72	MAGIX	2.2868
73	PNMA5	2.2776
74	FKRP	2.27714
75	LAGE3	2.27668
76	ANKRD60	2.27227
77	HOXA7	2.25975
78	SBK3	2.25707
79	MOSPD3	2.24509
80	PSKH2	2.24342
81	ANTXRL	2.23942
82	LMX1B	2.23414
83	LOC101927503	2.22992
84	C1orf116	2.22789

85	CGN	2.22447
86	HSFX1	2.21322
87	TRPC7	2.21214
88	HNF4A-AS1	2.2089
89	ST6GALNAC5	2.20807
90	KCNJ14	2.20672
91	HCRTR1	2.20412
92	BHLHB9	2.19662
93	CYP2A13	2.19164
94	TCEAL3	2.18544
95	DRD3	2.184
96	MMRN1	2.18251
97	LOC100287477	2.18245
98	KDM4D	2.18208
99	DNAJB7	2.17999
100	RUNX1T1	2.17761

Appendix D List of the 100 most down-regulated genes from the patient macrophage microarray

Number	Gene Symbol	Fold Change
1	TXN	-411.775
2	C15orf48	-304.907
3	FTL	-273.736
4	SUMO2	-251.54
5	HLA-DRA	-249.226
6	PLAUR	-213.088
7	RAB7A	-181.069
8	CTSS	-175.483
9	OAZ1	-161.761
10	TMSB10	-155.19
11	CYBB	-142.868
12	FCER1G	-125.149
13	POMP	-117.743
14	PRDX1	-117.17
15	LAPTM5	-114.969
16	CCL4	-112.871
17	CXCL16	-111.563
18	SLC7A11	-106.723
19	NPC2	-103.934
20	RPL27	-99.386
21	MMP9	-94.4103
22	PSAP	-90.8828
23	SQRDL	-88.5736
24	ATP6V0E1	-87.0824
25	IGSF6	-86.649
26	IFI30	-86.0078
27	CD68	-85.0816
28	COX4I1	-84.5514
29	SRGN	-84.234
30	SLAMF7	-81.9502
31	LYZ	-81.1264
32	RPL41	-81.035
33	CHI3L1	-80.5382
34	RPS2	-79.1202
35	CBWD2	-77.2671
36	ATP6V1F	-76.9367

37	BCL2A1	-70.9492
38	PLA2G7	-70.2001
39	PSMA3	-69.3309
40	ARPC5	-68.7327
41	RPS2	-68.2021
42	COX8A	-67.5268
43	AQP9	-66.065
44	ACTG1	-65.3203
45	RAB31	-64.7101
46	ATP5B	-61.2968
47	GMFG	-60.7423
48	TNFAIP6	-58.9338
49	ANXA5	-57.8008
50	NBEAL1	-57.4835
51	UBA52	-56.6651
52	SEP15	-56.6403
53	SPP1	-56.5101
54	DAD1	-56.3629
55	CD44	-55.613
56	LAPTM4A	-55.4191
57	SOD1	-53.6316
58	EIF4G2	-53.1141
59	ADAMDEC1	-52.9579
60	AHR	-52.8631
61	CES1P1	-51.9996
62	ITGAX	-51.7944
63	WSB1	-51.2909
64	ACTR3	-50.372
65	FDX1	-50.1473
66	NDUFA1	-49.7039
67	UBE2K	-48.7071
68	PSMB3	-48.5966
69	KYNU	-48.1175
70	RPS2	-47.79
71	MSN	-47.2697
72	SERINC3	-46.8628
73	ANXA1	-46.2265
74	RPS28	-45.5
75	CYB5A	-45.3311
76	GLIPR1	-44.9408
77	CALR	-44.1832
78	TIMM23	-43.4285
79	ITM2B	-42.5918
80	RAB1A	-42.1434

81	RPS11	-42.0848
82	GRN	-41.6052
83	CCL2	-41.4591
84	VAMP8	-41.3574
85	APLP2	-41.1694
86	MMP7	-40.7584
87	HIST1H2AC	-38.9235
88	IL1A	-38.9067
89	VMP1	-38.8178
90	DRG1	-38.6188
91	ATP6AP2	-38.5816
92	IL1B	-37.4948
93	ATP6V1C1	-37.2856
94	YBX1	-37.2772
95	CSGALNACT2	-36.9458
96	ERP44	-36.484
97	NOP10	-36.1277
98	CXCR4	-35.7405
99	CCL3L3	-35.4365
100	ELF1	-35.0605

Appendix E Patient aortic punch collection protocol ethics permission

Western Research

Research Ethics

Western University Health Science Research Ethics Board
HSREB Delegated Initial Approval Notice

Principal Investigator: Dr. Dave Nagpal
Department & Institution: Schulich School of Medicine and Dentistry\Critical Care, London Health Sciences Centre

Review Type: Delegated
HSREB File Number: 107566
Study Title: Role of Defective Efferocytosis in Atherosclerosis

HSREB Initial Approval Date: January 14, 2016
HSREB Expiry Date: January 14, 2017

Documents Approved and/or Received for Information:

Document Name	Comments	Version Date
Letter of Information & Consent	LHSC standard consent to collect samples- Received Jan 14, 2016	
Data Collection Form/Case Report Form	Received Jan 14, 2016	

The Western University Health Science Research Ethics Board (HSREB) has reviewed and approved the above named study, as of the HSREB Initial Approval Date noted above.

HSREB approval for this study remains valid until the HSREB Expiry Date noted above, conditional to timely submission and acceptance of HSREB Continuing Ethics Review.

The Western University HSREB operates in compliance with the Tri-Council Policy Statement Ethical Conduct for Research Involving Humans (TCPS2), the International Conference on Harmonization of Technical Requirements for Registration of Pharmaceuticals for Human Use Guideline for Good Clinical Practice Practices (ICH E6 R1), the Ontario Personal Health Information Protection Act (PHIPA, 2004), Part 4 of the Natural Health Product Regulations, Health Canada Medical Device Regulations and Part C, Division 5, of the Food and Drug Regulations of Health Canada.

Members of the HSREB who are named as Investigators in research studies do not participate in discussions related to, nor vote on such studies when they are presented to the REB.

The HSREB is registered with the U.S. Department of Health & Human Services under the IRB [redacted]n number IRB 00000940.

[redacted]

Ethics Officer, on behalf of Dr. Marcelo Kremenchutzky, HSREB Vice Chair

Ethics Officer to Contact for Further Information: Erika Basile ✓ Nicole Kaniki ___ Grace Kelly ___ Katelyn Harris ___ Vikki Tran ___

[redacted]

London, ON, Canada N6G 1G9 t. 519.661.3036 f. 519.850.2466 www.uwo.ca/research/ethics

Appendix F Human whole blood collection protocol ethics permission

Western Research

Research Ethics

Use of Human Participants - Initial Ethics Approval Notice

Principal Investigator: Prof. Bryan Heit
File Number:104010
Review Level: Delegated
Protocol Title: Venipuncture for Immune Cell Purification
Department & Institution: Schulich School of Medicine and Dentistry\Microbiology & Immunology,Western University
Sponsor:
Ethics Approval Date: October 09, 2013 **Expiry Date:**July 31, 2016
Documents Reviewed & Approved & Documents Received for Information:

Document Name	Comments	Version Date
Protocol	Microscopy & analysis protocols	2013/07/02
Letter of Information & Consent	Consent Statement	2013/07/02
Protocol	Preparation of phagocytic/efferocytic targets	2013/07/02
Protocol	Western blotting protocol	2013/07/02
Protocol	Mass spectometry protocols	2013/07/02
Protocol	Macrophage & neutrophil isolation and differntiation methods.	2013/07/02
Western University Protocol		2013/07/03
Other	Reply to Reviewer Request #4 - attach data collection forms.	2013/08/13
Letter of Information & Consent	Consent form	2013/08/22
Advertisement	Advertisement poster	2013/08/22

This is to notify you that The University of Western Ontario Research Ethics Board for Health Sciences Research Involving Human Subjects (HSREB) which is organized and operates according to the Tri-Council Policy Statement: Ethical Conduct of Research Involving Humans and the Health Canada/ICH Good Clinical Practice Practices: Consolidated Guidelines; and the applicable laws and regulations of Ontario has reviewed and granted approval to the above referenced revision(s) or amendment(s) on the approval date noted above. The membership of this REB also complies with the membership requirements for REB's as defined in Division 5 of the Food and Drug Regulations.

The ethics approval for this study shall remain valid until the expiry date noted above assuming timely and acceptable responses to the HSREB's periodic requests for surveillance and monitoring information. If you require an updated approval notice prior to that time you must request it using the University of Western Ontario Updated Approval Request Form.

Members of the HSREB who are named as investigators in research studies, or declare a conflict of interest, do not participate in discussion related to, nor vote on, such studies when they are presented to the HSREB.

The Chair of the HSREB is Dr. Joseph Gilbert. The HSREB is registered with the U.S. Department of Health & Human Services under the IRB

[redacted]

This is an official document. Please retain the original in your files.

[redacted]

London, ON, Canada N6A 3K7 t. 519.661.3036 f. 519.850.2466 www.uwo.ca/research/services/ethics

Appendix G Animal use protocol ethics permission

eSirius3G Notification -- 2018-131 New Protocol Approved

eSirius3GWebServer [redacted]
Mon 2018-11-19 12:15 PM
To: [redacted]
Cc:

Western

AUP Number: 2018-131
PI Name: Barra, Lillian
AUP Title: The Role of Citrullination and the Shared Epitope in the accelerated atherosclerosis of Rheumatoid Arthritis
Approval Date: 11/01/2018

Official Notice of Animal Care Committee (ACC) Approval:
Your new Animal Use Protocol (AUP) 2018-131:1: entitled " The Role of Citrullination and the Shared Epitope in the accelerated atherosclerosis of Rheumatoid Arthritis"
has been APPROVED by the Animal Care Committee of the University Council on Animal Care. This approval, although valid for up to four years, is subject to annual Protocol Renewal.

Prior to commencing animal work, please review your AUP with your research team to ensure full understanding by everyone listed within this AUP.

As per your declaration within this approved AUP, you are obligated to ensure that:

1) Animals used in this research project will be cared for in alignment with:

a) Western's Senate MAPPs 7.12, 7.10, and 7.15
http://www.uwo.ca/univsec/policies_procedures/research.html

b) University Council on Animal Care Policies and related Animal Care Committee procedures

http://uwo.ca/research/services/animalethics/animal_care_and_use_policies.htm

2) As per UCAC's Animal Use Protocols Policy,

a) this AUP accurately represents intended animal use;

b) external approvals associated with this AUP, including permits and scientific/departmental peer approvals, are complete and accurate;

c) any divergence from this AUP will not be undertaken until the related Protocol Modification is approved by the ACC; and

d) AUP form submissions - Annual Protocol Renewals and Full AUP Renewals - will be submitted and attended to within timeframes outlined by the ACC.

e)

http://uwo.ca/research/services/animalethics/animal_use_protocols.html

3) As per MAPP 7.10 all individuals listed within this AUP as having any hands-on animal contact will

a) be made familiar with and have direct access to this AUP;

b) complete all required CCAC mandatory training (training@uwo.ca); and

c) be overseen by me to ensure appropriate care and use of animals.

4) As per MAPP 7.15,

a) Practice will align with approved AUP elements;

b) Unrestricted access to all animal areas will be given to ACVS Veterinarians and ACC Leaders;

c) UCAC policies and related ACC procedures will be followed, including but not limited to:

i) Research Animal Procurement
ii) Animal Care and Use Records
iii) Sick Animal Response
iv) Continuing Care Visits

5) As per institutional OH&S policies, all individuals listed within this AUP who will be using or potentially exposed to

hazardous materials will have completed in advance the appropriate institutional OH&S training, facility-level training, and reviewed related (M)SDS Sheets,

http://www.uwo.ca/hr/learning/required/index.html

Submitted by: Copeman, Laura
on behalf of the Animal Care Committee
University Council on Animal Care

Dr.Timothy Regnault,
Animal Care Committee Chair

The University of
Western Ontario
Animal Care Committee / University
Council [redacted]

Appendix H Permission to use published manuscript from Springer Nature

Gmail

Charles Yin [redacted]

RE: Permission to Use Copyrighted Material in a Doctoral Thesis

1 message

Journalpermissions [redacted] 16 April 2019 at 07:11

To: Charles Yin [redacted]

Dear Charles,

Thank you for your recent Springer Nature permissions request. This work is licensed under the Creative Commons Attribution 4.0 International License, which permits unrestricted use, distribution, modification, and reproduction in any medium, provided you:

1) give appropriate acknowledgment to the original author(s) including the publication source,

2) provide a link to the Creative Commons license, and indicate if changes were made.

You are not required to obtain permission to reuse this article, but you must follow the above two requirements.

Images or other third party material included in the article are encompassed under the Creative Commons license, unless indicated otherwise in the credit line. If the material is not included under the Creative Commons license, users will need to obtain permission from the license holder to reproduce the material.

To view a copy of the Creative Commons license, please visit http://creativecommons.org/licenses/by/4.0/

Best wishes,

Oda

Oda Siqveland

Rights Executive

SpringerNature

[redacted]

From: Charles Yin [redacted]
Sent: 15 April 2019 21:42
To: Journalpermissions
Subject: Permission to Use Copyrighted Material in a Doctoral Thesis

Dear Springer Nature,

I am a Western University (London, Ontario) PhD Candidate currently completing my doctoral thesis.

I would like permission to allow inclusion of the contents of the paper "Rab17 mediates differential antigen sorting following efferocytosis and phagocytosis" by Yin et al. (2016), published in Cell Death and Disease Vol 7 Iss 12 in my thesis.

Please see: https://grad.uwo.ca/academics/thesis/publication.html for an overview of Western University's copyright policies for graduate theses. These policies will in no way restrict republication of the material in any other form by you or by others authorized by you. The material will also be attributed through a citation and a co-authorship statement in the thesis document.

Please confirm in writing whether this will be possible. Thank you!

Cheers,

Charles

Charles Yin

[redacted]

Appendix I Permission to use published manuscript from Taylor & Francis

Taylor & Francis
Taylor & Francis Group

Our Ref: AF/KSGT/P19/1142

19 June 2019

Dear Charles Yin,

Material requested: 'Charles Yin, Dean Argintaru & Bryan Heit (2019) Rab17 mediates intermixing of phagocytosed apoptotic cells with recycling endosomes, Small GTPases, 10:3, 218-226, DOI: 10.1080/21541248.2017.1308852'

(Please gain permission from Authors/Co-Authors before adapting Figures)

Thank you for your correspondence requesting permission to reproduce the above mentioned material from our Journal in your printed Thesis and to be posted in the university's repository.

We will be pleased to grant permission on the sole condition that you acknowledge the original source of publication and insert a reference to the article on the Journals website:

"This is the authors accepted manuscript of an article published as the version of record in ©2019 Taylor & Francis - https://doi.org/10.1080/21541248.2017.1308852 ".

This permission does not cover any third party copyrighted work which may appear in the material requested.

Please note that this licence does not allow you to post our content on any third party websites or repositories.

This licence does not allow the use of the Publishers version/PDF (this is the version of record that is published on the publisher's website) to be posted online.

Thank you for your interest in our Journal.

Yours sincerely,

Annabel Flude – Permissions Administrator, Journals
Taylor & Francis Group

[redacted]

Taylor & Francis Group
an informa business

Taylor & Francis is a trading name of Informa UK Limited, registered in England under no. 1072954

[redacted]

Curriculum Vitae

Name: Charles Yin

Post-secondary Education and Degrees:

McMaster University
Hamilton, Ontario, Canada
2010-2014 B.Sc. (Hons.) Integrated Science

The University of Western Ontario
London, Ontario, Canada
2016-2019 Ph.D. Microbiology and Immunology

The University of Western Ontario
London, Ontario, Canada
2014-2021 M.D. (expected)

Honours and Awards:

The University of Western Ontario
Hargreaves MD Award
2014-2016, 2019-2021

Canadian Institutes of Health Research (CIHR)
MD/PhD Studentship
2015-2020

Canadian Institutes of Health Research (CIHR)
Frederick Banting and Charles Best Canada Graduate Scholarship
2016-2017

The University of Western Ontario
Western Graduate Research Scholarship
2016-2019

Department of Microbiology and Immunology
Dr. Frederick W. Luney Graduate Travel Award
2017

Canadian Institutes of Health Research (CIHR)
Vanier Canada Graduate Scholarship
2017-2019

The University of Western Ontario
Inductee to School of Graduate and Postdoctoral Studies Wall of Fame
2017

Society for Leukocyte Biology (SLB)
Travel Award
2017

Department of Microbiology and Immunology
Infection and Immunity Research Forum 1st Place Oral Presentation Award
2017

International Atherosclerosis Society (IAS)
Young Investigator Fellowship
2018

Department of Microbiology and Immunology
Dr. Frederick W. Luney Graduate Travel Award
2018

The University of Western Ontario
London Health Research Day Feature Platform Presentation Award
2018

The University of Western Ontario
Nellie Farthing Fellowship in Medical Sciences
2018

Public Service Alliance of Canada, Local 610
Scholarship for Outstanding Research Contributions
2018

Department of Microbiology and Immunology
Infection and Immunity Research Forum Poster Award
2018

Society for Leukocyte Biology (SLB)
Presidential Award
2018

Network of Immunology Frontier Winter School on Advanced Immunology
Travel Fellowship
2019

Canadian Society for Immunology (CSI)
Travel Award
2019

Department of Microbiology and Immunology
Dr. Frederick W. Luney Graduate Travel Award
2019

Department of Microbiology and Immunology
John A. Thomas Award
2019

Canadian Resident Matching Service (CaRMS)
Sandra Banner Award for Leadership
2019

The University of Western Ontario
London Health Research Day Feature Platform Presentation Award
2019

Canadian Institutes of Health Research (CIHR)
Canadian Student Health Research Forum Travel Award
2019

Related Work Experience

Teaching Assistant – Microbiology Laboratory 3610F
The University of Western Ontario
2016-2017

Publications:

Law, J. and **C. Yin**. (2015). A day with an orthoptist. University of Western Ontario Medical Journal. 84(1):23-24.

Armstrong, S.M., Sugiyama, M.G., Fung, K.Y.Y., Gao, Y., Wang, C., Levy, A.S., Azizi, P., Roufaiel, M., Zhu, S.-N., Neculai, D., **Yin, C.**, Bolz, S.-S., Seidah, N.G., Cybulsky, M.I., Heit, B. and W.L. Lee. (2015). A novel assay uncovers an unexpected role for SR-BI in LDL transcytosis. Cardiovascular Research. 108(2):268-277.

Yin, C. and J. Law. (2015). Community-acquired pneumonia and pneumococcal vaccination in the elderly. University of Western Ontario Medical Journal. 84(2):23-25.

Novakowski, K.E., Huynh, A., Han, S., Dorrington, M.G., **Yin, C.**, Pelka, P., Whyte, P., Guarne, A., Sakamoto, K. and D.M.E. Bowdish. (2016). Naturally occurring transcript variants of macrophage receptor with collagenous structure (MARCO) reveal that the scavenger receptor cysteine rich (SRCR) domain is critical for ligand binding and uptake. Immunology & Cell Biology. 94(7):646-55.

Yin, C. and S. Danby. (2016). A review of housing-first strategies in reducing rates of substance use amongst people experiencing homelessness. University of Western Ontario Medical Journal. 85(1):35-37.

Danby, S. and **C. Yin**. (2016). A review of issues concerning implementation of cardiac rehabilitation programs. University of Western Ontario Medical Journal. 85(2):66-68.

Yin, C., Kim, Y., Argintaru, D. and B. Heit. (2016). Rab17 mediates differential antigen sorting following efferocytosis and phagocytosis. Cell Death and Disease. 7(12):e2529.

Yin, C., Daoust, K., Young, A., Tebbs, E.J. and D.M. Harper. (2017). Tackling community undernutrition at Lake Bogoria, Kenya: the potential of Spirulina (Arthrospira fusiformis) as a food supplement. African Journal of Food, Agriculture, Nutrition and Development. 17(1):11603-11615.

Yin, C., Steadman, P.E., Apramian, T., Zhou, T.E., Ishaque, A., Wang, X., Kuzyk, A. and N. Warsi. (2017). Training the next generation of Canadian clinician-scientists: charting a path to success. Clinical and Investigative Medicine. 40(2):E95-E101.

Novakowski, K.E., Yap, N.V.L., **Yin, C.**, Sakamoto, K., Heit, B., Golding, G.B. and D.M.E. Bowdish. (2017). Human-specific mutations and positively-selected sites in the macrophage receptor with collagenous structure (MARCO) confers functional changes. Molecular Biology & Evolution. 35(2):440-450.

Yin, C. and B. Heit. (2017). Armed for destruction: formation, function and trafficking of neutrophil granules. Cell & Tissue Research. 371(3):455-471.

Evans, A.L., Blackburn, J.W.D., **Yin, C.** and B. Heit. Quantitative efferocytosis assays. In: Botelho, R., ed. Phagocytosis and Phagosomes. New York: Springer. 2017. p25-41.

Yin, C., Blom, J.N. and J.F. Lewis. (2018). The 2nd annual clinician scientist trainee symposium, August 22, 2017, London, Canada. Clinical and Investigative Medicine. 41(1):E34-E36.

Taruc, K., **Yin, C.**, Wootton, D.G. and B. Heit. (2018). Quantification of efferocytosis by fluorescence microscopy. Journal of Visualized Experiments. 138:e58149.

Yin, C., Barra, L., Nagpal, D. and B. Heit (2018). Gene expression profiling of lesion-resident macrophages in human atherosclerosis. Atherosclerosis. 32:106.

Yin, C., Argintaru, D. and B. Heit. (2019). Rab17 mediates intermixing of phagocytosed apoptotic cells with recycling endosomes. Small GTPases. 10(3):218-226.

Wavell, C., Sokolowski, A. **Yin, C.**, Klingel, M. and A.D. Nagpal. (2019). Clinical effectiveness of durable continuous-flow left ventricular assist device (LVAD) therapy in

non-ischemic versus ischemic cardiomyopathy: a systematic review and meta-analysis. Canadian Journal of Surgery. Accepted.

Yin, C., Moszcyznski, A.J., Blom, J.N., Johnson, T.P.E. and D.L. Jones. (2019). Advancing the understanding of research in medical education through collaborative learning: the Collaboration of Practitioners and Researchers Seminar Series. BMC Medical Education. In Review.

Yin, C., Vrieze, A.M., Akingbasote, J., Pawlak, E.N., Jacob, R.A., Hu, J., Sharma, N., Blackler, G., Dikeakos, J.D., Barra, L., Nagpal, A.D. and B. Heit. GATA2 Expression by Intima-Infiltrating Macrophages Drives Early Atheroma Formation. bioRxiv 715565.

Levit**,** A., **Yin, C.** and J.F. Lewis. (2019). The 4th annual clinician scientist trainee symposium at the Schulich School of Medicine & Dentistry. Clinical and Investigative Medicine. Submitted.